IN VIVO AND *IN VITRO* DEVELOPMENTAL STUDY OF PORCINE TESTIS CELLS AND TISSUE

A Thesis Submitted to the
College of Graduate and Postdoctoral Studies
In Partial Fulfillment of the Requirements
For the Degree of Doctor of Philosophy
In the Department of Veterinary Biomedical Sciences
University of Saskatchewan
Saskatoon

By

MOHAMMAD AMIN FAYAZ

PERMISSION TO USE

In presenting this thesis/dissertation in partial fulfillment of the requirements for a Postgraduate degree from the University of Saskatchewan, I agree that the Libraries of this University may make it freely available for inspection. I further agree that permission for copying of this thesis/dissertation in any manner, in whole or in part, for scholarly purposes may be granted by the professor or professors who supervised my thesis/dissertation work or, in their absence, by the Head of the Department or the Dean of the College in which my thesis work was done. It is understood that any copying or publication or use of this thesis/dissertation or parts thereof for financial gain shall not be allowed without my written permission. It is also understood that due recognition shall be given to me and to the University of Saskatchewan in any scholarly use which may be made of any material in my thesis/dissertation.

Requests for permission to copy or to make other uses of materials in this thesis/dissertation in whole or part should be addressed to:

Head of Department of Veterinary Biomedical Sciences
Western College of Veterinary Medicine
52 Campus Drive
University of Saskatchewan
Saskatoon, Saskatchewan S7N 5B4 Canada

OR

Dean
College of Graduate and Postdoctoral Studies
University of Saskatchewan
116 Thorvaldson Building, 110 Science Place
Saskatoon, Saskatchewan S7N 5C9 Canada

ABSTRACT

Testis development and function involve multiple cell types and require complex cellular interactions and signaling cascades; hence, the study of these processes necessitates improvement of *ex situ* models of testicular cells or tissue. Accordingly, objectives of the first and second studies in this thesis were to improve *in vitro* culture of testis cells by testing the effects of various culture components on proliferation, colony-formation, and potency of germline stem cells. The examined components included different media, serum types, and several key growth factors, tested in sequential experiments using a factorial design. The third study focused on assessment of pluripotency of cultured neonatal porcine gonocytes and their potential to trans-differentiae into somatic cells of different cell lineages. The goal of our fourth study was to investigate the feasibility of applying ultrasound biomicroscopy (UBM) for the assessment of testis tissue grafts and cell implants by initially validating its use in a short-term study. In the fifth study, we examined repeated application of UBM in a longitudinal manner to test its reliability and accuracy in representing the developmental changes in grafts and implants. As a result, we showed increased proliferation of porcine gonocytes with a given culture condition combination (DMEM+15% FBS), followed by attainment of pluripotency markers by cultured gonocytes and their colonies, indicative of their spontaneous transformation into a pluripotent state. Supplementation of certain growth factors at a given concentration to the base media also led to further increases in gonocyte numbers and colony diameters, while maintaining their expression of pluripotency and germ cell markers. We also observed successful derivation of somatic cells of different lineages from germ cell originated-pluripotent stem cells. Furthermore, application of UBM for non-invasive *in vivo* developmental study of testicular grafts and implants was shown to be accurate and reliable, thereby reducing the number of animals needed in future similar experiments. Taken together, the studies describe improved germ cell culture conditions, transformation of gonocytes into a pluripotent state, as well as validating and using UBM as an accurate and reliable tool for *in vivo* developmental study of testis grafts and implants.

ACKNOWLEDGEMENTS

First and foremost, I would like to thank my supervisor and mentor, Dr. Ali Honaramooz for giving me the opportunity to learn under his guidance and supporting me continuously throughout my PhD program with brilliant insights. I am forever thankful to him for being always available to help me patiently and support me with encouragement and inspiration.

I am grateful to my advisory committee members, Drs. Suraj Unniappan, Carlos Carvalho, Daniel MacPhee, and Jaswant Singh for their insightful comments and constructive feedback throughout the development of the present work. I am also thankful to my external examiner Dr. Kent Hamra for reading the present thesis and providing helpful feedback.

I also would like to sincerely thank the faculty, Drs. Muhammad Anzar, Gregg Adams, Lynn Weber, Maud Ferrari, Ahmad Al-Dissi, and Janet Hill for their intellectual or technical help during my PhD projects. Also, I would like to express my deep gratitude to Dr. Eiko Kawamura and LaRhonda Sobchishin for technical support in imaging, Champika Fernando and Samantha Ekanayake for invaluable assistance in gene expression analyses, Tatjana Ometlic and her staff at Prairie Swine Center and Monique Burmester at Animal Care Unit of WCVM for assistance in animal studies.

I also acknowledge the University of Saskatchewan, government of Saskatchewan, and Natural Sciences and Engineering Research Council of Canada for financial support of my projects.

Also, my special thanks to former graduate students Drs. Awang Hazmi Awang Junaidi and Rodrigo Carrasco for their generous support and sharing their expertise and knowledge whenever I needed. I also thank all VBMS researchers, staff, graduate students, and lab-mates for their mental and intellectual support as well as a lot of good memories that we made together, especially the coffee trips.

Finally, my deepest thank you to my family for always believing in me. This journey would not have been possible without their unconditional love and support.

DEDICATION

To my family, for their encouragement, patience, and immeasurable love.

TABLE OF CONTENTS

PERMISSION TO USE ..... **i**
ABSTRACT ..... **ii**
ACKNOWLEDGEMENTS ..... **iii**
DEDICATION ..... **iv**
TABLE OF CONTENTS ..... **v**
LIST OF TABLES ..... **x**
LIST OF FIGURES ..... **xi**
LIST OF ABBREVIATIONS ..... **xv**
CHAPTER 1: INTRODUCTION **1**
CHAPTER 2: LITERATURE REVIEW AND OBJECTIVES **6**
2.1. PHYSIOLOGY AND FUNCTION OF THE TESTIS 6
2.1.1. Prenatal Testis Development 6
2.1.2. Postnatal Testis Development 13
2.1.3. Testis Structure 16
2.1.4. Spermatogenesis, Steroidogenesis, and their Regulation 18
2.2. ORIGIN, DEVELOPMENT, AND SPECIALIZATION OF MALE GERMLINE STEM CELLS 22
2.2.1. Primordial Germ Cells 22
2.2.2. Gonocytes 25
2.2.3. Spermatogonial Stem Cells 27
2.3. *IN VIVO* MODELS TO STUDY TESTIS DEVELOPMENT AND FUNCTION 28
2.3.1. Germ Cell Transplantation 28
2.3.2. Testis Tissue Xenografting 31
2.3.3. Testis Cell Aggregate Implantation 34
2.3.4. Factors Affecting the Development of Grafts and Implants 39
2.4. *IN VITRO* MODELS FOR THE STUDY AND MANIPULATION OF TESTIS CELLS 43
2.4.1. Identification, Isolation, and Enrichment of Gonocytes 43
2.4.2. Maintenance and Propagation of Germline Stem Cells in Culture Systems 49
2.4.3. *In Vitro* Generation of Pluripotent Cells from Male Germline Stem Cells 51
2.4.4. *In Vitro* Trans-Differentiation of Male Germline Stem Cells 53
2.4.5. *In Vitro* Spermatogenesis 54
2.5. GROWTH FACTORS AND TESTIS DEVELOPMENT 57
2.5.1. Basic Fibroblast Growth Factor 57
2.5.2. Glial Cell-derived Neurotrophic Factor 59
2.5.3. Leukemia Inhibitory Factor 60
2.6. APPLICATIONS OF ULTRASOUND BIOMICROSCOPY IN REPRODUCTIVE SCIENCES 64

2.7. APPLICATIONS OF MALE GERMLINE STEM CELLS IN RESEARCH AND CLINICAL SETTINGS 65
2.8. CONCLUSIONS 68
2.9. OBJECTIVES AND HYPOTHESES 69
CHAPTER 3: EFFECTS OF DIFFERENT CULTURE CONDITIONS ON PROLIFERATION, COLONY-FORMATION, AND PLURIPOTENCY STATE OF PORCINE MALE GERM CELLS 71
3.1. ABSTRACT 71
3.2. INTRODUCTION 71
3.3. MATERIALS AND METHODS 74
3.3.1. Study Design 74
3.3.2. Castration of Animals, Cell Isolation, and Culture 75
3.3.4. Evaluation of Cultured Gonocytes and Gonocyte Colonies 76
3.3.5. Sampling and Immunocytochemistry 76
3.3.6. RNA Extraction and RT-PCR Analysis 76
3.3.7. Transmission Electron Microscopy 77
3.3.8. Statistical Analyses 77
3.4. RESULTS 78
3.4.1. Morphometrical and Developmental Assessment 78
3.4.1.1. Experiment 3.1: Effects of Individual Concentrations of FBS and KSR 78
3.4.1.2. Experiment 3.2: Effects of Combined Concentrations of FBS and KSR 79
3.4.2. Immunocytochemistry 80
3.4.3. Gene Expression Analyses 80
3.4.4. Ultrastructural Assessment of Cultured Gonocytes and EBLCs in Selected Media 80
3.5. DISCUSSION 95
TRANSITION 100
CHAPTER 4: CULTURE SUPPLEMENTATION OF BFGF, GDNF, AND LIF ALTERS *IN VITRO* PROLIFERATION, COLONY-FORMATION, AND PLURIPOTENCY OF NEONATAL PORCINE GERM CELLS 101
4.1. ABSTRACT 101
4.2. INTRODUCTION 102
4.3. MATERIALS AND METHODS 105
4.3.1. Study Design 105
4.3.2. Collection of Testes and Isolation of Testis Cells 106
4.3.3 Evaluation of Viability and Number of Isolated Cells 107
4.3.4. Cell Culture 108
4.3.5. Imaging and Assessment of Cultured Cells 109
4.3.6. Immunocytochemistry 109
4.3.7. Extraction of RNA and RT-PCR 111
4.3.8. Statistical Analyses 111

4.4. RESULTS 111
4.4.1. Testis Cell Count and Viability Assessment 111
4.4.2. Cell Development and Morphology 112
4.4.2.1. Experiment 4.1: Effects of Individual Growth Factors 112
4.4.2.2. Experiment 4.2: Effects of Combined Concentrations of Growth Factors 113
4.4.3. Double Immunocytochemistry against Pluripotency-determining and Gonocyte-specific Markers 114
4.4.4. Gene Expression of Pluripotency-determining Factors 114
4.5. DISCUSSION 126
TRANSITION 135
CHAPTER 5: NEONATAL PORCINE GERM CELLS DEDIFFERENTIATE AND DISPLAY OSTEOGENIC AND PLURIPOTENCY PROPERTIES *IN VITRO* 136
5.1. ABSTRACT 136
5.2. INTRODUCTION 136
5.3. MATERIALS AND METHODS 139
5.3.1. General Experimental Design 139
5.3.2. Castration of Donors, Testis Cell Isolation, and Culture in Regular Media 139
5.3.3. *In Vitro* Osteogenic Trans-Differentiation of Porcine Germ Cells 140
5.3.4. *In Vitro* Tri-lineage Differentiation of Porcine Germ Cells 140
5.3.5. Imaging and Morphometrical Assessment 141
5.3.6. Staining and Immunocytochemistry for Evaluation of Dedifferentiation and Trans-Differentiation 141
5.3.6.1. Alizarin Red S Staining 141
5.3.6.2. Immunofluorescence Assay 141
5.3.7. Gene Expression Analyses for Confirmation of Dedifferentiation and Trans-Differentiation 142
5.3.8. Subcutaneous Implantation of Cultured Cells and Colonies 142
5.3.9. Retrieval of the Subcutaneous Implants and (Immuno)histochemistry 143
5.3.10. Statistical Analyses 143
5.4. RESULTS 143
5.4.1. Viability and Morphometric Assessments 143
5.4.2. Alizarin Red S Staining and Immunofluorescence Assay 144
5.4.2.1. Osteogenic Differentiation 144
5.4.2.2. Pluripotency of Germ Cells and their Differentiation into Derivatives of Three Germinal Layers 145
5.4.3. Gene Expression Analyses 145
5.4.4. Characterization of Dedifferentiated Cell Implants 146
5.4.4.1. H&E Staining 146
5.4.4.2. Immunohistochemistry 146
5.5. DISCUSSION 158

TRANSITION 164
CHAPTER 6: VALIDATION OF ULTRASOUND BIOMICROSCOPY FOR THE ASSESSMENT OF XENOGENEIC TESTIS TISSUE GRAFTS AND CELL IMPLANTS IN RECIPIENT MICE 165
6.1. ABSTRACT 165
6.2. INTRODUCTION 166
6.3. MATERIALS AND METHODS 168
6.3.1. Study Design 168
6.3.2. Preparation of Testis Tissue Fragments and Testis Cell Aggregates 168
6.3.3. Recipient Mice and Grafting/Implantation Procedures 169
6.3.4. UBM Examination 169
6.3.5. Graft and Implant Sample Recovery, and Physical Evaluation 171
6.3.6. Histological Analyses 171
6.3.7. Statistical Analyses 172
6.4. RESULTS 172
6.4.1. UBM Assessment 172
6.4.2. Physical and Morphometric Assessment 173
6.4.3. Histological Assessment 174
6.4.4. Comparative Analysis 174
6.5. DISCUSSION 187
TRANSITION 192
CHAPTER 7: LONG-TERM MONITORING OF DONOR XENOGENEIC TESTIS TISSUE GRAFTS AND CELL IMPLANTS IN RECIPIENT MICE USING ULTRASOUND BIOMICROSCOPY 193
7.1. ABSTRACT 193
7.2. INTRODUCTION 193
7.3. MATERIALS AND METHODS 195
7.3.1. Preparation of Testis Tissue Fragments and Cells 195
7.3.2. Procedures for TTX and TCAI 196
7.3.3. UBM of the Grafts and Implants 196
7.3.4. Sample Retrieval and Histological Evaluations 197
7.3.5. Immunohistochemistry and Trichrome Staining 198
7.3.6. Histomorphometric Analyses 199
7.3.7. Statistical Analyses 200
7.4. RESULTS 200
7.4.1. UBM Evaluations 200
7.4.2. (Immuno)histological Evaluations 201
7.4.3. UBM *vs.* Histological Findings 203
7.5. DISCUSSION 217
CHAPTER 8: GENERAL DISCUSSION AND FUTURE DIRECTIONS 223

8.1. GENERAL DISCUSSION 223
8.1.1. *In Vitro* Effects of Different Media and Serum Types on Porcine Germ Cell Proliferation, Colony-Formation, Ultrastructure, and Potency 223
8.1.2. Effects of Individual and Combined Growth Factor Concentrations on Porcine Germ Cell Proliferation, Colony-Formation, and Potency 224
8.1.3. Dedifferentiation and Trans-Differentiation Potential of Porcine Germ Cells 225
8.1.4. Validation of UBM for *In Vivo* Examination of Testis Tissue Grafts and Cell Implants 226
8.1.5. Long-term Examination of Tissue Grafts and Cell Implants Using UBM 227
8.2. FUTURE DIRECTIONS 228
8.2.1. Manipulation of Culture Conditions to Enhance Proliferation of Gonocytes 228
8.2.2. Assessment of Pluripotency State of Cultured Germ Cells Following Injection into Immunodeficient Recipients using UBM 229
8.2.3. Non-invasive Examination of Gonad and Accessory Sex Gland Development in Mice using UBM 229
REFERENCES **231**
APPENDIX A **277**

LIST OF TABLES

Table 3.1. Name and specification of media used in treatment groups **82**

Table 3.2. Summary of primary and secondary antibodies used for immunofluorescence assay **82**

Table 3.3. Primers used for RT-PCR analysis **83**

Table 4.1. X- and Y-axis average diameter (mean ± SEM) of EBLCs on Day 28 in culture wells treated with basic media (DMEM+15% FBS) supplemented with individual concentrations of bFGF, GDNF, or LIF and without growth factor supplementation (DMEM+15% FBS or DMEM+5% FBS+10% KSR)..... **116**

Table 4.2. X- and Y- axis average diameter (mean ± SEM) of EBLCs on Day 28 in culture wells treated with basic media (DMEM+15% FBS) supplemented with 10 ng/mL bFGF, combined concentrations of bFGF, GDNF and LIF or without growth factor supplementation (DMEM+15% FBS or DMEM+5% FBS+10% KSR)..... **116**

Table 5.1. Antibodies used for immunofluorescence and immunocytochemistry..... **147**

Table 5.2. RT-PCR primer sequences for gene expression analyses..... **147**

Table 6.1. Percentage difference (% of increases/decreases, mean ± SEM) in biomicroscopy (UBM) and physical measurements of the length, width, height, and volume of grafts and implants..... **176**

Table 7.1. Histomorphometric analysis of cell implants and tissue grafts at different retrieval time points showing the percentage (mean ± SEM) of cords/tubules with the most advanced germ cells **205**

LIST OF FIGURES

Fig. 2.1. Overview of procedures in testis tissue xenografting (TTX) and testis cell aggregate implantation (TCAI). **38**

Fig. 2.2. Overview of testis structure and its potential paracrine signaling map **63**

Fig. 3.1. Schematic overview of the experimental design **84**

Fig. 3.2. Representative images demonstrating varying developmental status of cultured testis cells in different media and serum/serum replacement combinations **85**

Fig. 3.3. Effects of different media supplemented with various serum concentrations on gonocyte numbers after 28 days of *in vitro* culture **86**

Fig. 3.4. Representative images of testis cells cultured in DMEM+10% KSR **87**

Fig. 3.5. Effects of DMEM combined with serum or serum replacement on EBLC numbers (mean ± SEM) (A) and diameters (mean ± SEM) (B) **88**

Fig. 3.6. Average number of gonocytes (mean ± SEM) (A) and EBLCs (mean ± SEM) (B) as well as the diameter of EBLCs (mean ± SEM) (C) in DMEM supplemented with combined concentrations of FBS and KSR on Day 28 of culture **89**

Fig. 3.7. Double immunocytochemistry of freshly-isolated and 28-day cultured porcine testis cells for gonocyte-specific and pluripotency-determining markers **91**

Fig. 3.8. Expression of pluripotency-determining gene transcripts in samples of freshly-isolated testis cells from neonatal piglets and those cultured for 7, 14, 21, or 28 days **93**

Fig. 3.9. Transmission electron microscopy of cultured porcine testis cells in the selected media and serum combination (DMEM+5% FBS+10% KSR) **94**

Fig. 4.1. Schematic overview of the experimental design **117**

Fig. 4.2. Representative photomicrographs of cultured cells in groups treated with 10 ng/mL bFGF **118**

Fig. 4.3. Number of gonocytes (mean ± SEM) in different treatment groups on (A) Day 28 and (B) over time changes in the number of gonocytes in cultures supplemented with 10 ng/mL bFGF **119**

Fig. 4.4. Number of gonocytes (mean ± SEM) in cultures supplemented with combined concentrations of growth factors **121**

Fig. 4.5. Double-immunostaining of the freshly isolated and cultured testis cells against gonocyte- and pluripotency-specific markers **123**

Fig. 4.6. RT-PCR analysis for detection of pluripotency-determining gene transcripts in fresh testis cell isolate and 28-day cultured testis cells **125**

Fig. 5.1. Schematic representation of the experimental design **148**

Fig. 5.2. Representative photomicrographs of culture wells in regular media and osteogenic differentiation media, as well as the average diameter of EBLCs in different groups **149**

Fig. 5.3. Representative photomicrographs obtained from culture wells before (day 0) and 7 days after incubation with the tri-lineage differentiation media **151**

Fig. 5.4. Evaluation of POU5F1 expression as a pluripotency marker and DBA as a gonocyte-specific marker by freshly-isolated and cultured porcine testis cells in regular media **152**

Fig. 5.5. Expression of a gonocyte-specific marker (DBA) and markers of endoderm (SOX17 and AFP), mesoderm (Brachyury and ASM), and ectoderm (OTX2 and GFAP) by cultured gonocytes and their colonies in regular and differentiation media **153**

Fig. 5.6. Gene expression analyses of germinal layer-specific markers using RT-PCR **155**

Fig. 5.7. Representative photomicrographs captured from (immuno)histological sections of dedifferentiated cell implants **156**

Fig. 6.1. Schematic representation of the experimental design **177**

Fig. 6.2. Representative ultrasound biomicroscopy (UBM) images used for segmentation volume measurement of testis cell implants **178**

Fig. 6.3. Representative two-dimensional (2-D) ultrasound biomicroscopic (UBM) images of cell implants at 2 wk (A and C) and 4 wk (B) post-implantation, or tissue graft at 2 wk (D) **179**

Fig. 6.4. Ultrasound biomicroscopic (UBM) and physical measurements (mean±SEM) of tissue grafts and cell implants **180**

Fig. 6.5. Representative three-dimensional (3-D) reconstructed images from ultrasound biomicroscopy (UBM) of testis tissue grafts and cell implants. 3-D volumetric mesh and reconstructed 3-D image of a cell implant examined at 2 wk (A-C) or 8 wk (D-F)..... **181**

Fig. 6.6. Representative macrophotographs of testis tissue grafts and cell implants recovered after 2 or 8 wk post-grafting/implantation **182**

Fig. 6.7. Representative images of testis cell implants obtained using ultrasound biomicroscopy (UBM) and histology at different time points..... **183**

Fig. 6.8. The percentage (mean±SEM) of cordal, non-cordal and fluid-filled cavity areas delineated on histological cross-sections and 2-D UBM images of implants (A-F and I), as well as the UBM pixel intensity and pixel heterogeneity (mean±SEM) (G and H) in recovered implants at 2 and 6 wk **185**

Fig. 6.9. Comparison between physical and UBM attributes of the grafts and implants. Correlations between the UBM *vs.* physical measurements of length (A), height (B), and volume (C) of the grafts and implants **186**

Fig. 7.1. Experimental design of the study **206**

Fig. 7.2. Three-dimensional (3-D) reconstruction of a representative subcutaneous tissue graft and its contralateral cell implant from wk 1 to 24 ..... **207**

Fig. 7.3. Representative 2-D UBM images and largest histological sections of grafts (A-I) and implants (J-R)..... **208**

Fig. 7.4. Histological sections and their corresponding 2-D UBM images of representative cell implants at the largest section and at different time points..... **210**

Fig. 7.5. UBM measurements (mean ± SEM) of tissue grafts and cell implants **211**

Fig. 7.6. Histological measurements (mean ± SEM) of retrieved samples **212**

Fig. 7.7. Immunolocalization of UCH-L1 (PGP9.5) in germ cells of cell implants (a and b) and tissue grafts (C, D, E, and F)..... **213**

Fig. 7.8. Representative photomicrographs of grafts (A and B) and implants (C and D) at wk 2 (A and C) and 24 (B and D) as well as representative 2-D UBM images of implants at the largest section in colour Doppler mode at wk 2 (E) and 24 (F) **214**

Fig. 7.9. Correlation analysis between UBM and histological attributes of retrieved samples **216**

LIST OF ABBREVIATIONS

2-D	Two-dimensional
3-D	Three-dimensional
ABP	Androgen Binding Protein
ACTA2	Actin Alpha 2
ADAM	A-Disintegrin and A-Metalloproteinase domain
AFP	Alpha-Fetoprotein
ALC	Adult Leydig Cell
AMH	Anti-Müllerian hormone
ANOVA	Analysis of Variance
AR	Androgen Receptor
ASM	Alpha-Smooth Muscle Actin
bFGF	basic Fibroblast Growth Factor
BLIMP1	B-lymphocyte-induced Maturation Protein 1
BMP	Bone Morphogenetic Protein
c-kit	Tyrosine-protein Kinase Kit
cDNA	complementary DNA
DAPI	4′,6-diamidino-2-phenylindole
DAZL	Deleted in Azoospermia-like
DBA	*Dolichos biflorus* agglutinin
DDX4	DEAD-box helicase 4
DHEA	Dehydroepiandrosterone
DHH	Desert Hedgehog
DHT	Dihydrotestosterone
DMEM	Dulbecco's Modified Eagle’s Medium
DMEM/F12	Dulbecco's Modified Eagle’s Medium and Ham’s F12
DNA	Deoxyribonucleic Acid
DPBS	Dulbecco’s Phosphate-Buffered Saline
dpc	days post-coitum
dpp	days post-partum
EBLC	Embryoid Body-Like Colony
ECM	Extra Cellular Matrix

EDTA	Ethylenediaminetetraacetic Acid
EGF	Epidermal Growth Factor
EMX2	Empty Spiracles Homeobox gene 2
ES cell	Embryonic Stem cell
ETV5	ETS variant gene 5
FBS	Fetal Bovine Serum
FGF	Fibroblast Growth Factor
FITC	Fluorescein Isothiocyanate
FLC	Fetal Leydig Cell
FSH	Follicle Stimulating Hormone
FUT4	Fucosyltransferase 4
g	Relative Centrifugal Force (RCF)
GAPDH	Glyceraldehyde 3-phosphate dehydrogenase
GATA4	GATA-binding protein 4
GCC	Gametogenesis-competent Cells
GCT	Germ Cell Transplantation
GDNF	Glial Cell-derived Neurotrophic Factor
GFAP	Glial Fibrillary Acidic Protein
GFP	Green Fluorescent Protein
GFRα-1	GDNF Family Receptor α-1
GMEM	Glasgow Minimum Essential Medium
GnRH	Gonadotropin-Releasing Hormone
H&E	Hematoxylin and Eosin
hCG	human Chorionic Gonadotropin
HEPES	(4-(2-hydroxyethyl)-1-piperazineethanesulfonic acid
HPG axis	Hypothalamic Pituitary Gonadal Axis
i.v.	intravenous
ICM	Inner Cell Mass
ICSI	Intracytoplasmic Sperm Injection
IFITM	Interferon-induced Transmembrane protein
IGF	Insulin-like Growth Factor
INSL3	Insulin-like Peptide 3
iPS cell	induced Pluripotent Stem cell

IVF	*In Vitro* Fertilization
IVS	*In Vitro* Spermatogenesis
kg	kilogram
KITLG	KIT Ligand
KSR	Knock-out Serum Replacement
LH	Luteinizing Hormone
LHX9	LIM homeobox gene 9
LIF	Leukemia Inhibitory Factor
LIFR	Leukemia Inhibitory Factor Receptor
MEF	Mouse Embryonic Fibroblast
MEM	Minimum Essential Medium
mg	milligram
MGSC	Male Germline Stem Cell
min	minute(s)
mL	millilitre
mo	month(s)
mRNA	messenger RNA
NANOG	NANOG homeobox
NGN3	Neurogenin 3
OCT4	Octamer-binding Transcription Protein 4
OTX2	Orthodenticle Homeobox 2
PBS	Phosphate-Buffered Saline
PDGF	Platelet-derived Growth Factor
PDGFR-β	Platelet-derived Growth Factor Receptor-β
PGP9.5	Protein Gene Product 9.5
PMC	Peritubular Myoid Cell
pMGSC	pig Male Germline Stem Cells
POU5F1	POU Domain Class 5 Transcription Factor 1
RA	Retinoic Acid
RAR	Retinoic Acid Receptor
RET	Receptor Tyrosine Kinase
ROSI	Round Spermatid Injection
RPMI	Roswell Park Memorial Institute medium

RT-PCR	Reverse Transcription-Polymerase Chain Reaction
s.c.	subcutaneous
SCF	Stem Cell Factor
SCID	Severe Combined Immunodeficient
SEM	Standard Error of Mean
SF1	Steroidogenic Factor 1
SFM	Serum Free Medium
SHO	SCID Hairless Outbred
SOHLH	Spermatogenesis and Oogenesis Specific Basic Helix-Loop-Helix
SOX17	SRY-Box Transcription Factor 17
SOX2	Sex Determining Region-Y (SRY)-Box 2
SPSS	Statistical Package for Social Sciences
SRY	Sex Determining Region-Y
SSC	Spermatogonial Stem Cell
SSEA-1	Stage Specific Embryonic Antigen-1
StAR	Steroid Acute Regulatory protein
STO	Sandos Inbred Mice (SIM)-Embryo-Derived Thioguanine and Ouabain-Resistant
TBXT	T-Box Transcription Factor T
TCAI	Testis Cell Aggregate Implantation
TEM	Transmission Electron Microscopy
TGF-β	Transforming Growth Factor-β
TTX	Testis Tissue Xenografting
UBM	Ultrasound Biomicroscopy
UCH-L1	Ubiquitin Carboxy-Terminal Hydrolase-L1
VEGF	Vascular Endothelial Growth Factor
vs.	versus
wk	week(s)
WT1	Wilms' Tumor suppressor 1
µg	microgram
µL	microlitre

CHAPTER 1

INTRODUCTION

Male germline stem cells (MGSCs) are a unique germ cell population owing to their dual potential for self-renewal and differentiation into specialized germ cells (Culty 2009). Primordial germ cells (PGCs) are the primitive MGSC population that migrate to the undifferentiated gonads and undergo spermatogenic pathway in the male embryo (Saitou and Yamaji 2012). Following colonization, PGCs give rise to a new germ cell population, known as gonocytes, which correspond to the fetal and neonatal germ cells between PGCs and spermatogonial stem cells (SSCs). Despite their importance in the continuity of species and a wide range of potential applications, our knowledge of factors affecting the proliferation or differentiation of MGSCs is far from complete. This is mainly due to the complexity of their microenvironment and inaccessibility to MGSCs *in situ*. Therefore, reliable new or improved *in vivo* and *in vitro* models are required to overcome the limitations associated with the study and manipulation of MGSCs.

Once gonocytes develop from PGCs, their lifespan extends into early postnatal period. In rodents, being the frequently-used animal models for the studies on germ cells, gonocytes can be identified up to 2 weeks after birth, while in primates this period is extended up to several months (Markert 1979). These cells are progenitors of spermatogonial stem cells (SSCs), known as the life-long reservoir of germline stem cells (Culty 2013). Gonocytes in the neonatal testis are the preferred source for use in the study and manipulation of MGSCs because of their greater proportion to other germ cells, unique morphological features, and specific markers, making them easily identifiable (Jiang and Short 1998; Jiang 2001; Goel *et al.* 2007; Culty 2009; Honaramooz and Yang 2011; Awang-Junaidi and Honaramooz 2018; Sahare *et al.* 2018). However, in rodents and pigs gonocytes still make up only ~2% and ~7% of the testis cell populations, respectively (Honaramooz *et al.* 2005; Lee *et al.* 2013) and as such, utilization of highly efficient methods for their isolation and enrichment is necessary prior to their application. As such, thus far, a diverse range of methods have been developed for enrichment of germ cells including culturing, differential plating, magnetic activated cell soring (MACS), and fluorescence activated cell sorting (FACS), combined with utilizing cell-specific markers (Nagano *et al.* 1998; Goel *et al.* 2007; Hamra *et al.* 2008; Kim *et al.* 2010; Younan *et al.* 2010). A testis cell isolation method has also been introduced in our laboratory leading to enriched populations of testis cells composed of ~40%

gonocytes and 60% somatic cells. Isolated testis cells can even undergo further enrichment to yield to a cell population consisting of ~90% gonocytes using density gradient centrifugation and differential plating (Yang *et al.* 2010; Honaramooz and Yang 2011).

In vitro culture is one of the feasible approaches to increase the gonocyte numbers prior to their application. It also provides a means to study the underlying factors involved in gonocyte proliferation and differentiation (Park *et al.* 2017; Sakib *et al.* 2019). Being the primitive/early germ cells, both gonocytes and spermatogonia have been the focus of many *in vitro* studies in rodents. In piglets, however, gonocytes are the main germ cells in the neonatal testes (Goel *et al.* 2007), while little is known about the exact timing of their transformation into spermatogonia (Kanatsu-Shinohara *et al.* 2014; Almunia *et al.* 2018). Furthermore, due to similarities between human and porcine testicular structure and pathophysiology, pigs have been used as suitable models for *in vitro* studies targeting germ cells (Piquet-Pellorce *et al.* 2000; Kubota *et al.* 2004, 2011; Goel *et al.* 2007; Kim and Belmonte 2011; Sato *et al.* 2011; Kanatsu-Shinohara and Shinohara 2013; Sahare *et al.* 2016, 2018). However, there are still challenges associated with *in vitro* propagation of porcine gonocytes. These cells are largely affected by their milieu and thereby, their successful culture depends on establishment of a supportive microenvironment in which they ideally maintain their germ- and stem cell potential (Nagano *et al.* 2001; Hamra *et al.* 2002; Kanatsu-Shinohara, Toyokuni *et al.* 2004a; Goel *et al.* 2007).

Two main components of most culture conditions are media and serum which can directly affect the survival and proliferation of germ cells. Therefore, to find the best media composition which can optimally support gonocyte survival and propagation and to improve our previously-established culture conditions, in Chapter 3 of the present thesis we tested the effects of 6 different media combined with two sources of serum supplements, fetal bovine serum (FBS) and/or knock-out serum replacement (KSR) (Awang-Junaidi and Honaramooz 2018). We then used our optimized conditions as a base to further enhance gonocyte proliferation and colony-formation by testing the effects of 24 groups of growth factor supplementation (Chapter 4).

When cultured, gonocytes form clusters and large 3-D colonies, which resemble embryonic stem (ES) cell colonies (Kuijk *et al.* 2009; Mirzapour *et al.* 2012; Awang-Junaidi *et al.* 2020). Some reports have also shown expression of pluripotency-determining factors by cultured germ cells of different species including mice and humans (Kim and Belmonte 2011). This is indicative of

spontaneous reprogramming of cultured MGSCs into a pluripotent state (Kanatsu-Shinohara, Inoue *et al.* 2004; Goel *et al.* 2007; Ko *et al.* 2009; Kim and Belmonte 2011). As such, cultured germ cells can potentially be used as alternatives for existing pluripotent stem cells for *in vitro* differentiation into various cell types (Kim and Belmonte 2011; Wang *et al.* 2015). This is especially important due to ethical issues and general concerns regarding the use of ES cells or induced pluripotent stem (iPS) cells as a source for cell-based therapy and regenerative medicine. We also showed expression of pluripotency-determining factors by cultured gonocytes in our refined culture conditions in Chapter 3 and 4 and concluded that these cells undergo spontaneous reprogramming into more primitive developmental stages *in vitro*. As such, we designed and carried out additional experiments in Chapter 5 to confirm the pluripotency of cultured gonocytes using an *in vivo* implantation assay and directed their trans-differentiation towards cell derivatives from all three germinal layers (*i.e*., endoderm, mesoderm, and ectoderm).

Beside *in vitro* culture systems, several *in vivo* models have been developed and improved over time to gain a deeper understating of testis development and function (Dufour *et al.* 2002; Honaramooz *et al.* 2002; Honaramooz *et al.* 2007; Awang-Junaidi *et al.* 2020). Among different models, testis tissue xenografting (TTX) and testis cell aggregate implantation (TCAI) have offered alternative *in vivo* strategies for the study of male gonadal development, spermatogenesis, steroidogenesis, and cell-cell interactions within an *ex situ* testis model from a wide range of animals species (Honaramooz *et al.* 2002; Dobrinski 2007; Ibtisham and Honaramooz 2020).

In TTX, small pieces of testis tissue from immature donor species, grafted into immunodeficient recipient mice developed into functional tissue and produced fertilization competent sperm (Honaramooz *et al.* 2002). Porcine testis tissue was used in the first attempts of TTX (Honaramooz *et al.* 2002), and thereafter, a range of species were used as donors showing that this regeneration potential is retained among donor species (Honaramooz 2014). As such, TTX provided an invaluable approach for fundamental study of testis development and function in diverse mammalian species and opened new windows of opportunity for conservation of endangered species as well as preservation of fertility potential of testis cancer patients whose survival depends upon gonadotoxic treatments (Ibtisham and Honaramooz 2020; Ibtisham *et al.* 2020). TCAI has been another invaluable approach to study testicular development and potential factors affecting it. TCAI was first established in 2007 by implantation of dissociated testis cells obtained from

donor piglets into the subcutaneous tissue of recipient mice. The cell aggregates were prepared by enzymatic digestion of testis parenchyma, underwent extensive rearrangements following implantation and developed into a functional testis tissue (Honaramooz *et al.* 2007). Formation of testis tissue has been also observed using immature donor mouse, rat, pig, sheep, cattle, peccary, and marmoset testis cells (Gassei *et al.* 2006; Honaramooz *et al.* 2007; Kita *et al.* 2007; Arregui *et al.* 2008; Aeckerle *et al.* 2013; Sharma *et al.* 2018). This model allowed manipulation of testis development and can be used to gain a better understanding of testis morphogenesis (Honaramooz *et al.* 2007).

An important aspect of TTX and TCAI studies is evaluation of the grafts and implants, which has been dependent upon surgical retrieval of samples followed by (immuno)histological analysis. As such, in initial TTX and TCAI experiments, sample assessment was limited to the time of euthanasia of the recipients (Honaramooz, *et al.* 2002; Honaramooz *et al.* 2007). Later, recipients underwent multiple surgical sampling, allowing the same recipient to be used for obtaining several samples over time. Even though the latter approach provided a longitudinal assessment strategy, it was still invasive, required a large quantity of recipients, and could pose a high risk of infection (Abbasi and Honaramooz 2011a,b, 2012; Fayaz *et al.* 2020a,b). Additionally, obtained samples had to be processed for (immuno)histological evaluation, leading to inaccurate measurements. Another limitation of surgical sampling for evaluation purposes is limited number of grafts and implants per recipients (Honaramooz 2014). Therefore, we decided to establish a non-invasive approach to be able to visualize sample development without the need for surgical retrieval and histological evaluation by taking advantage from an ultrasound imaging system, known as ultrasound biomicroscopy (UBM), which offers high-definition images of the tissues at microscopic resolutions.

Among different imaging modalities, UBM is a non-invasive approach for real-time assessment of organs and tissues at high magnifications (Greco *et al.* 2012). This imaging system has been widely used with great precision in various clinical and research fields, including reproductive biology (Baerwald *et al.* 2009; Jaiswal *et al.* 2009; Mircea *et al.* 2009; Pfeifer *et al.* 2012, 2014). In the present work, we designed the first UBM experiment aimed at its validation using a short-term assessment of grafts and implants (Chapter 5). Given the accuracy of this method in providing reliable and precise information on echotexture of implants, sample dimensions, and volume, we

utilized this monitoring approach for long-term evaluation of grafts and implants in a second UBM experiment (Chapter 6). In the latter longitudinal evaluation, we also compared *de novo* testis morphogenesis among craniocaudal implantation locations and compared graft *vs.* implant development mainly by using UBM.

Rodents are traditional animal models in biomedicine which allow basic genetic manipulations with high reproducibility and are easily manageable in research facilities; however, they lack pathophysiological complexities of human body (Bassols *et al.* 2014). Pigs are considered as an alternative and well-suited animal model in translational research due to anatomical, physiological, genetic, and metabolic similarities to humans (Swindle *et al.* 2012). More specifically, similar physiology, protein distribution, structure and development of reproductive organs make them a suitable animal model for the study and manipulation of the testes (Swindle *et al.* 2012). Moreover, porcine gonocytes can be identified up to ~2 months after birth while in rodents these cells differentiate into spermatogonia in the first few days post-partum (dpp) (Russell 1980). Availability of gonocytes in the neonatal porcine testis for a longer period of time, their unique morphological features, and specific biomarkers for their identification make them a well-suited option among MGSCs to study physiology and manipulation of germline stem cells (de Rooij and Russell 2000; Meng *et al.* 2000a; Culty 2009; Awang-Junaidi and Honaramooz 2018).

Overall, there are unravelled biological aspects in physiology of germ cells as well as numerous potential applications. However, complexities associated with *in situ* studies and manipulations of germ cells necessitate reliable development of refined alternative *ex situ* models. In the present thesis we set out to use novel optimized approaches to gain in-depth understanding of testis biology, morphogenesis, and cellular interplay. Thus, the overall objective of the present thesis was to gain a better understanding of the developmental potential of porcine testis cells and tissue and especially gonocytes.

CHAPTER 2

LITERATURE REVIEW AND OBJECTIVES

2.1. Physiology and Function of the Testis

2.1.1. Prenatal Testis Development

Sexual development in mammals is comprised of two separate processes known as sex determination and sexual differentiation. Sex determination is the process that establishes the sexual fate of an organism, which may be driven by a number of genetic and/or environmental cues, leading to structural changes and formation of either ovaries or testes from undifferentiated gonads (Luckenbach and Yamamoto 2018). Sexual differentiation is the period when gender-specific structures such as gonads become established (Greenfield 2015; Capel 2017; Yang *et al.* 2019). Among different species, the mouse is a well-studied animal model of mammalian gonadal development due to extensive work conducted on its embryos. Development of the gonads in other mammalian species is expected to follow the same pattern with small timing and anatomical differences (Wilhelm *et al.* 2007). Testis development is typically divided into two phases. The first phase culminates in formation of bipotential gonads, also known as the genital ridges and during the second phase, triggering of the testis-determining gene *Sry* leads to extensive cellular rearrangements and differentiation of the bipotential gonads into testes (Yang *et al.* 2019). During embryonic development, genital ridges arise from the intermediate mesoderm as a pair in the coelomic cavity and on either side of the dorsal mesentery at ~10.5 days post-coitum (dpc). These structures are formed by increased coelomic epithelial cell divisions on the ventromedial surface of the mesonephroi. Each mesonephros contains a mesonephric duct (Wolffian duct) which further develops into epididymis, vas deferens, and seminal vesicles in the male embryo. The female equivalent of mesonephric ducts known as the paramesonephric duct is also present in each mesonephros, and develops into oviduct, uterus, and vagina in the female embryo (Hannema and Hughes 2007; Shaw and Renfree 2014; Yang *et al.* 2019). Coelomic epithelial cell divisions on the ventromedial surface of the mesonephros create a dense, pseudostratified epithelial cell layer (Gropp and Ohno 1966; Pelliniemi 1974; Wartenberg *et al.* 1991). Gradually, the basement membrane of epithelial cells undergo fragmentation, allowing them to move dorsally towards the mesonephroi (Karl and Capel 1998; Kusaka *et al.* 2010). Along with fragmentation, these cells

undergo epithelial to mesenchymal transition and later differentiate into somatic and stromal cells in the gonads (Karl and Capel 1998; Ito *et al.* 2006; Kusaka *et al.* 2010; Mork *et al.* 2012). Epithelial cells are present in early gonads and continue to delaminate from the coelomic epithelium up to ~11.5 dpc, forming the precursors of the supporting cells and steroid-secreting cells (Merchant-Larios *et al.* 1993; Karl and Capel 1998).

In the developing gonads, PGCs can potentially produce both male and female germline (Yang *et al.* 2019). In response to chemoattractants released by somatic cells, this population of alkaline phosphatase-positive cells migrate from yolk sac to the base of allantois and colonize the gonads by ~7 dpc in mice or week 3-4 of gestation in humans (Lawson *et al.* 1999). About 45 PGCs initiate their migration to the gonads and establish the population of germline stem cells in the mouse (Lefebvre *et al.* 1997). During their migration, PGCs undergo extensive cell divisions and reach a population of ~3,000 cells by the time they arrive at the genital ridges. When located at the genital ridges, PGCs lose their motility while sustaining their self-renewal divisions. Colonization of PGCs in the indifferent gonads takes up to ~8.5-13.5 dpc in mice and week ~4.5 of gestation in humans (Wilhelm *et al.* 2007). PGCs express gene transcripts that are associated with the undifferentiated pluripotent state such as POU domain class 5 transcription factor 1 (POU5F1), also known as octamer-binding transcription factor 4 (OCT4) and alkaline-phosphatase (Wilhelm *et al.* 2007). These markers are also expressed in the inner cell mass (ICM) during initial stages of embryonic development. The cells of ICM are an established source of ES cells which can undergo infinite rounds of proliferation and are capable of differentiation into all tissues (Wilhelm *et al.* 2007). Typically, once established from ES cells, primary germ layers lose their ability to express pluripotency-associated markers such as POU5F1 and alkaline-phosphatase (Lawson and Hage 1994). However, expression of these markers is maintained in PGCs, thereby they can potentially be used for derivation of embryonic germ cell lines with similar properties to ES cells (McLaren *et al.* 1984; Wilhelm *et al.* 2007). Once in gonads, PGCs upregulate the genes required for gametogenesis and concurrently downregulate the expression of pluripotency-related gene transcripts. The regulation of gene expression in PGCs during their specialization is known as licensing (Stebler *et al.* 2004; Gill *et al.* 2011; Rolland *et al.* 2011; Seisenberger *et al.* 2012; Fayomi and Orwig 2018). Licensing of PGCs results in formation of a cell population known as gametogenesis-competent cells (GCCs) which can differentiate into male or female specialized germ cells (McLaren *et al.* 1984; Adams and McLaren 2002; Gill *et al.* 2011).

During male embryonic development, sex-determining region Y (SRY) protein also known as testis determining factor (TDF), encoded by *SRY* gene, induces the production of regulatory proteins which direct the transformation of bipotential gonads towards testis formation, while absence of SRY results in formation of the female embryo (Gubbay *et al.* 1990; Sinclair *et al.* 1990; Karl and Capel 1998). SRY triggers a cascade of gene expressions which ultimately lead to testis differentiation, first by encoding a transcription factor that can activate production of testis-specific enhancer SRY-Box Transcription Factor 9 (SOX9) (Koopman *et al.* 1991; Vidal *et al.* 2001; Wilhelm *et al.* 2007). Activation of SOX9 is essential for differentiation of somatic cell precursors to Sertoli cells (Koopman *et al.* 1990). Sertoli cells regulate differentiation of all other cell types in the gonad and organize gonadal structures during differentiation process (Karl and Capel 1998). Precursors of Sertoli cells originate from the pluripotent coelomic epithelial cells and are the first to differentiate in the gonad from bipotential precursor cells and as such, can be considered as early indicators of sexual differentiation during embryonic development (Wilhelm *et al.* 2007). In mice, SRY-positive cells first appear in the middle third or central regions of the indifferent gonads and gradually expand towards the poles (Albrecht and Eicher 2001; Bullejos and Koopman 2001; Wilhelm *et al.* 2007). SRY expression reaches a threshold at ~11 dpc, activates SOX9 expression, which in turn leads to pre-Sertoli cell differentiation and cord formation (Svingen and Koopman 2013). However, Sertoli cell differentiation does not happen synchronously in all parts of the developing gonad, which can explain ovotestis formation in abnormal conditions (Svingen and Koopman 2013). In the absence of SOX9, the precursor cells transform into specialized follicle cells, which normally happens during development of a female embryo (Albrecht and Eicher 2001). In response to SRY, high expression of SOX9 is maintained within Sertoli cells. Reaching a sufficient population of SOX9-positive cells triggers morphological changes of the indifferent gonad into testis (Warr and Greenfield 2012). These morphological changes include generation of interstitial cell lineages such as peritubular myoid cells (PMCs) and Leydig cells, mitotic arrest of germ cells, and formation of testis cords (Larney *et al.* 2014). SRY expression also results in formation of intercellular membrane connections and generation of gonadal cords around PGCs in the medulla (Patni *et al.* 2017). Peritubular myoid cells gradually appear on the outer side of the testis cords (Patni *et al.* 2017). SRY also activates FGF-9 expression, which is pivotal for increasing the SOX9-positive cell divisions. This in turn maximizes the ratio of SOX9-positive cells relative to SOX9-negative cells in the genital ridges

(Schmahl *et al.* 2000). FGF-9 is also crucial for development of testis cords as its absence interferes with *in vitro* testis cord formation (Hiramatsu *et al.* 2010). This is also shown by *Fgf9*-null mice displaying male to female sex reversal (Colvin *et al.* 2001; Kim *et al.* 2007; Bagheri-Fam *et al.* 2008). FGF-9 suppresses the expression of pro-ovary genes such as Wnt family 4 (*Wnt4*) (Jameson *et al.* 2012). Formation of the gonadal ridges and differentiation of the bipotential gonads also involve extensive gene expression, including Wilms' tumor suppressor 1 (*WT1*) (Kreidberg *et al.* 1993; Hammes *et al.* 2001), LIM homeobox gene 9 (*LHX9*) (Birk *et al.* 2000), GATA-binding protein 4 (*GATA4*) (Hu *et al.* 2013), and empty spiracles homeobox gene 2 (*EMX2*) (Miyamoto *et al.* 1997). Homozygous null mutation of any of the above-mentioned genes show gonadal agenesis. Embryonic development of other organ systems is also dependent on these genes, thereby their mutation leads to a range of abnormal phenotypes beyond the reproductive system (Ingraham *et al.* 1994; Klamt *et al.* 1998; Hammes *et al.* 2001; Tevosian *et al.* 2015).

SOX9 activation triggers both somatic cell specialization and their aggregation around clusters of germ cells, leading to *de novo* formation of testis cords (Svingen and Koopman 2013). At this time, somatic cells in close contact with the PGCs are called Sertoli cells. Once the population of PGCs arrive at the genital ridge and become surrounded by Sertoli cells they undergo morphological transformation and convert into a cell population known as M-prospermatogonia or more generally as gonocytes (Wilhelm *et al.* 2007). M-prospermatogonia retain their mitotic activity but before birth become mitotically inactive and are then called T1-prospermatogonia. The process of normal cord formation has been also shown to occur in gonads devoid of germ cells (Merchant 1975; Escalante-Alcalde and Merchant-Larios 1992; Merchant-Larios *et al.* 1993), indicating that cord formation depends on Sertoli cell interactions but not germ cell aggregation (Svingen and Koopman 2013). This process also requires changes to Sertoli cell surface molecules, enabling them to recognize each other, form aggregates and 3-D cordal tubes (Svingen and Koopman 2013). Formation of PGC-containing cords is a defining event in differentiation of the testis. These cords provide the basis for two important functions of the testis, namely spermatogenesis and steroidogenesis. Cords also prevent early exposure of gonocytes to retinoic acid (RA) which is present in the interstitium, and which otherwise can induce immature initiation of meiosis (McCoshen 1982, 1983; Escalante-Alcalde and Merchant-Larios 1992; Merchant-Larios *et al.* 1993; Griswold and Behringer 2009). Sertoli cells play a pivotal role in survival and differentiation of germ cell lineage by producing several molecules and releasing paracrine factors

that influence the germline. For instance, Sertoli cells produce CYP26B1 which restricts entry of germ cells into early meiosis by catabolizing RA (Bowles *et al.* 2006; Koubova *et al.* 2006). Similarly, these cells release FGF-9 which also prevents the effects of RA on germ cells (Bowles and Koopman 2010) and triggers expression of Nodal coreceptor Cripto, which leads to maintenance of germ cell pluripotency and increases spermatogenic fate (Bowles and Koopman 2010; Spiller *et al.* 2012). Activin A, transforming growth factor β (TGF-β), platelet-derived growth factor (PDGF), and estrogen are among other important supporting factors produced by Sertoli cells and are essential for pre- and post-natal survival as well as quiescence regulation of germ cell (Moreno *et al.* 2010; Mendis *et al.* 2011).

About 13 cords are initially formed in the mouse gonads at ~12 dpc. These cords appear as a stack of circular cell organizations which later join to form 3-D tube-shaped structures (Svingen and Koopman 2013). Vascular endothelial cells which originate from the mesonephros are also crucial in formation of the gonadal cords since disruption of their migration interferes with normal cord formation (Coveney *et al.* 2008; Combes *et al.* 2009; Cool *et al.* 2011). Over time, Sertoli cells proliferate and establish stronger contacts with germ cells, which together, lead to cord elongation (Nel-Themaat *et al.* 2011). By ~13 dpc, cords are shaped into toroid structures. At this stage, the appearance of Sertoli cells changes from fibroblast-like to epithelial-like cells, PMCs form an outer layer on the cords, and the somatic cells develop an extracellular matrix (ECM) (Nel-Themaat *et al.* 2011).

PMCs develop shortly after formation of testis cords and can be identified as early as ~13.5 dpc in mice and week ~12 of gestation in humans (Ostrer *et al.* 2007). PMCs were believed to originate from the migrating cells of the mesonephros, while more recent studies revealed that mesonephric cells can transform to endothelial cells but not PMCs in the differentiating gonads, and as such the origin of PMCs remains unknown (Buehr *et al.* 1993; Combes *et al.* 2009; Cool *et al.* 2011; Nurmio *et al.* 2012). Due to lack of cell-specific markers early identification of PMC remains a challenge. However, it is speculated that they arise from the intragonadal cells or coelomic epithelium (Campagnolo *et al.* 2001; Combes *et al.* 2009). PMCs form a single cell monolayer in smaller rodents, while in larger mammals they generate multiple cell layers separated by connective tissue (Maekawa *et al.* 1996). ECM and PMCs together form the lamina propria which acts as a boundary, separating the cords from testis interstitium and helps in movements of sperm towards

the rete testis. In humans, this layer also contains myofibroblasts (Davidoff *et al.* 1990; Dym 1994; Holstein *et al.* 1996).

The steroidogenic function of the testis depends on Leydig cells, making them crucial for the drive and maintenance of secondary sexual features. Due to their endocrine features, Leydig cells typically are seen in clusters close to the blood vessels of the testis interstitium (Bowles and Koopman 2010). Interestingly, Leydig cells which appear during the embryonic stage do not simply develop into those found in the post-pubertal testis. Rather, two separate populations of Leydig cells have been identified with distinct functions (Roosen-Runge and Anderson 1959; Lording and De Kretser 1972; Vergouwen *et al.* 1991; Chen *et al.* 2009; O'Shaughnessy and Fowler 2011). The fetal Leydig cells (FLCs) partially arise from the mesonephros at ~12.5 dpc and are responsible for androgen synthesis and development of male characteristics during this period. Differentiation of FLCs is regulated by anti-Müllerian hormone (AMH) and Sertoli cell signals. FLCs maintain a small cell population after birth (O'Shaughnessy and Fowler 2011). These cells release androgens required for secondary sexual development during embryonic stage, including maintenance of Wolffian ducts, external genitalia, and testicular descent (Svingen and Koopman 2013). Hence, masculinization process in the embryo happens independently, as a result of androgen production by FLCs, and prior to the establishment of the hypothalamus-pituitary-gonadal axis (Huhtaniemi 1989; O'Shaughnessy and Fowler 2011). As such, unlike adult Leydig cells (ALCs) differentiation of FLCs is not luteinizing-hormone (LH) dependent (O'Shaughnessy *et al.* 2000; Shima 2019). Also, in contrast to ALCs, FLCs lack hydroxysteroid 17-beta dehydrogenase 3 (HSD17B3) which is an enzymatic component required for conversion of cholesterol to testosterone. Therefore, FLCs produce androstenedione which is subsequently converted to testosterone by fetal Sertoli cells (O'Shaughnessy and Fowler 2011; Shima *et al.* 2013). Testosterone is also converted to dihydrotestosterone (DHT) by 5α-reductase, which is a more effective androgen. DHT induces formation of prostate and external genitalia and transforms the cranial and caudal portions of the mesonephric duct to epididymis and ductus deferens, respectively (Mäkelä *et al.* 2019). Production of fetal androgens by FLCs not only results in differentiation of male gonads and genitalia, but also drives subtle differences in the brain patterning which is normally followed by development of male-specific behaviors (Barker 1990; Vilain and McCabe 1998; Robinson 2006). FLCs also produce insulin-like peptide 3 (INSL3), which is necessary in development of the gubernaculum testis. This ligament controls the

transabdominal descent of the testes and regulates their migration towards scrotum, and as such absence of INSL3 leads to failure of testicular descent and results in cryptorchidism (Nef and Parada 1999; Zimmermann *et al.* 1999; Adham *et al.* 2000; Emmen *et al.* 2000; Bogatcheva *et al.* 2003; Tomiyama *et al.* 2003; Hutson and Hasthorpe 2005). ALCs differentiate shortly after birth from mesenchymal precursor cells located in the interstitium (Bowles and Koopman 2010). The main trigger for differentiation of these cells is not clear but desert hedgehog (DHH) or PDGF are suggested to be involved in this process (Clark *et al.* 2000; Gnessi *et al.* 2000). DHH is released by Sertoli cells, which attaches to the receptor patched (*Ptc1*), expressed on the Leydig cell precursors (Yao *et al.* 2002). In Leydig cells, steroidogenic factor-1 (*Sf1*) regulates the enzymes required for testosterone production. These enzymes include steroid acute regulatory protein (StAR), cytochrome P450 family 11 subfamily A member 1 (CYP11A1), cytochrome P450 hydroxylase (CYP17), and 3β-hydroxysteroid dehydrogenase (3βHSD) (Yao *et al.* 2002). Produced androgens exert their effects through androgen receptors (AR) on Sertoli cells, Leydig cells, and PMCs (Ketelslegers *et al.* 1978; Corbier *et al.* 1992; Bremner *et al.* 1994; Sharpe 1994).

Further structural development of the testis includes formation of septa between the convoluted seminiferous cords by mesenchymal cells, giving lobulated appearance to the testis parenchyma. The mesenchyme also produces a connective tissue between the testis cords and tunica albuginea (Patni *et al.* 2017). Furthermore, while in the male embryo AMH produced by Sertoli cells results in regression of the Müllerian ducts, the absence of AMH in female embryos leads to regression of Wolffian ducts and differentiation of Müllerian ducts into female reproductive tract (Shima *et al.* 2015).

During the final stages of prenatal development, testes migrate from their embryonic intraabdominal position into the scrotum. This process can be divided into two phases of transabdominal and inguinoscrotal (Gier and Marion 1969; Puri 1986). Transabdominal phase occurs between week 10-15 of gestation in humans, 14.5-16.5 dpc in mice, and ~55 dpc in pigs (Klonisch *et al.* 2004). During the transabdominal phase, testes descend from their pararenal location into a lower abdominal location. This phase is androgen independent and controlled by INSL3. The inguinoscrotal phase, however, is androgen dependent and is characterized by the movement of testes through inguinal canal and into the scrotum. This phase happens just before

birth in humans, within the first 2 weeks of neonatal development in mice and ~90 dpc in pigs (Hadziselimovic and Herzog 1993; Klonisch *et al.* 2004; Hutson *et al.* 2010).

2.1.2. Postnatal Testis Development

Gonocytes and more specifically T1-prospermatogonia in the neonatal testis are located in the center of seminiferous cords and are in mitotic arrest (Hutson *et al.* 2013). During the postnatal testis development, these cells form cytoplasmic processes enabling them to migrate between Sertoli cells and towards the basement membrane of the cords. T1-prospermatogonia become T2-prosperamognia when they are released from mitotic arrest and start their migration (Phillips *et al.* 2010). The migratory phase of gonocytes happens between 3-9 months of age in humans and 2-6 days after birth in mice (Huff *et al.* 2001; Drumond *et al.* 2011). Once they arrive at the cordal basement membrane, gonocytes establish the pool of spermatogonia. Gonocytes which fail to travel from the center to periphery of the cords undergo degeneration (Kluin and de Rooij 1981), indicating the important role of basement membrane environment for progression of germ cell development (Vergouwen *et al.* 1991; Nagano *et al.* 2000). Gonocytes continue proliferating even after they complete their migration. The exact trigger and regulatory mechanism for this migration are not fully understood but PDGF B and D and PDGF receptor-β (PDGFR-β) are suggested to be involved in this process (Basciani *et al.* 2008, 2010). Also, expression of c-KIT has been shown to be critical in formation of the pseudopodia by gonocytes and activation of their migratory behavior (Orth *et al.* 1997). Since gonocytes are in immediate contact with Sertoli cells, their migration is also dependent upon the physical support and paracrine secretions from neighboring Sertoli cells (Orth *et al.* 1997).

Following their migration, gonocytes give rise to a pool of undifferentiated spermatogonia (Vergouwen *et al.* 1991; Drumond *et al.* 2011). Establishment of the SSC pool is essential to sustain continuous supply of undifferentiated spermatogonia throughout life (Culty 2009). A fraction of gonocytes also produces differentiating type A spermatogonia which has the potential of differentiation towards spermatozoa (de Rooij 1998; Phillips *et al.* 2010). Type A spermatogonia are early germ cells and are subdivided into A single (A_s), A paired (A_{pr}), and A aligned (A_{al}), depending on their differentiation stage and incomplete cytokinesis. Type A spermatogonia express a range of markers such as integrin β-1 and integrin α-6 (Kanatsu-Shinohara *et al.* 1999), receptors of glial cell-derived neurotrophic factor (GDNF) known as GDNF

family receptor (GFRα-1), and receptor tyrosine kinase (RET) (de Rooij and Russell 2000). Differentiating spermatogonia are also immunopositive for SOHLH1, SOHLH2, neurogenin 3 (NGN3), and c-KIT which is a receptor for stem cell factor (SCF) (Besmer *et al.* 1993; Ballow *et al.* 2006; Yoshida *et al.* 2006; Filipponi *et al.* 2007; Hao *et al.* 2008). Close to puberty, A spermatogonia give rise to intermediate and B spermatogonia. B spermatogonia are more specialized germ cells which can differentiate into spermatocytes and progress into meiosis (Phillips *et al.* 2010). The number of germ cells slightly decreases during the first 3 years of life in humans, possibly because of apoptosis, but then it increases by 7 years of age at which time it reaches a plateau. This increase in germ cell numbers is mainly due to the proliferation of type A spermatogonia and their differentiating version, type B spermatogonia. After the prepubertal period and during puberty, spermatogonial population increases exponentially along with the testis volume (Mäkelä *et al.*). Although fetal germ- and pluripotent stem cells have the potential to differentiate to any cell types, postnatal germ cells retain the differentiation potential after birth but only into more specialized germ cells (Hofmann *et al.* 2005). SSCs undergo self-renewal divisions throughout life and their mitotic activity is dependent on the extrinsic factors of their niche similar to other adult stem cells in the body. These extrinsic factors mainly originate from their surrounding Sertoli cells which dictate the intracellular signalling pathways, gene expression, and regulation of cell cycles (Yang and Oatley 2014).

Between birth and puberty, Sertoli cells play key roles in regulation of testis development. These cells increase in numbers by about four-fold during the first five months after birth in humans along with increased length of the testis cords, leading to an overall increase in the size of the testes (Rey *et al.* 1993; Marshall and Plant 1996; Berensztein *et al.* 2002). Between 2-4 months of age in humans, secretion of gonadotropin-releasing hormone (GnRH) increases testosterone production in prepubertal testes. Thereafter, testosterone levels decrease and become negligible until the onset of puberty. The sudden increase in GnRH during prepubertal period is called “mini-puberty”. While androgen levels fall in the prepubertal period, AMH secretion by Sertoli cells increases and remains high until puberty (Job *et al.* 1988; Hadziselimovic and Zivkovic 2007; Hutson *et al.* 2013). Between the mini-puberty and puberty, the hypothalamic-pituitary-gonadal (HPG) axis remains inactive, resulting in limited testosterone production, and the HPG axis increases its pulsatile activity only closer to puberty (Mäkelä *et al.*). Between birth and onset of puberty, seminiferous cords lack the lumen and Sertoli cells possess immature morphological

features including limited cytoplasm and small nucleoli (Rey 1999). Immature Sertoli cells gradually become elongated and develop tight junctions. The proliferative activity of these cells diminishes and finally stops at puberty, which happens at 15 and 20 days of age in mice (Orth 1982) and rats (Vergouwen *et al.* 1991), respectively. Since testicular function during adulthood is largely dependent upon the number of Sertoli cells, factors affecting Sertoli cell proliferation during prepubertal period indirectly affects the spermatogenic activity later in life (Sharpe *et al.* 2003; Meroni *et al.* 2019). Among these factors are hormones such as follicle stimulating hormone (FSH) and androgens which stimulate Sertoli cell proliferation during both fetal and early postnatal life. Similarly, insulin family of growth factors such as insulin-like growth factor 1 and 2 (IGF-1 and IGF-2), and relaxin have proliferative effects on immature Sertoli cells (Borland *et al.* 1984; Saez *et al.* 1988; Khan *et al.* 2002; Meroni *et al.* 2019). Also, activin and inhibin belong to the transforming growth factor-β (TGF-β) family with significant effects on proliferation of immature Sertoli cells prior to puberty. Activin A which is mainly produced by PMCs, induces Sertoli cell division, and its levels drop at puberty which marks the Sertoli cell maturation. Inhibin is synthetized by Sertoli cells, and its increasing levels counteract activin effects at puberty (Meroni *et al.* 2019).

Reactivation of the HPG axis, release of LH and FSH, and their effects on gonads mark the initiation of puberty. FSH upregulates AR expression on Sertoli cells, PMCs, and Leydig cells and boosts germ cell proliferation, leading to increased testicular volume (Rey 2014; Koskenniemi *et al.* 2017). Knock-out mice lacking FSH receptor have shown reduced Sertoli cell proliferation and declined testicular growth, which indicates the crucial role of this hormone in testicular development during puberty (Koskenniemi *et al.* 2017). LH-release induces maturation of Leydig cells which in turn, initiates secretion of androgens (Rey 2014). Sertoli cells undergo maturation process when exposed to increased levels of intratesticular androgens at about 3 months and 7 years of age in pigs and humans, respectively. Sertoli cell maturation entails formation of blood-testis barrier, loss of Sertoli cell mitotic activity, and downregulation of AMH synthesis (Rey *et al.* 2009). At this stage, morphology of Sertoli cells also changes to provide sufficient room for embracing germ cells. Also, AR expression by Sertoli cells and testosterone levels increase, while AMH levels decrease (Koskenniemi *et al.* 2017). FSH during prepubertal and pubertal periods promotes both spermatogonial and Sertoli cell proliferation whereas androgens are required for

spermatogenesis and their release marks the culmination of testicular growth (Koskenniemi *et al.* 2017).

After birth, germ- and Sertoli cells continuously proliferate in the seminiferous cords but at different growth rates. Proliferative activity of Sertoli cells during this period is twice as much as that of germ cells and as such, prepubertal increase in the size of the cords is mainly owing to the Sertoli cell expansion (Van Straaten and Wensing 1977). At puberty, however, Sertoli cells reduce their proliferative activity and thereby germ cell expansion becomes the main factor responsible for enlargement of tubules both in diameter and length (Hilscher *et al.* 1974; Iczkowski *et al.* 1991; Des Jardins 1993; França *et al.* 2000). Attachment of androgens to AR at puberty results in Sertoli cell secretion of paracrine factors and development of cell surface receptors required for initiation of germ cell differentiation (Emmen *et al.* 2000; Hutson *et al.* 2010; Mäkelä *et al.* 2019). Tight junctions between Sertoli cells are further developed to form the blood-testis barrier. This barrier defines a border where undifferentiated germ cells such as germline stem cells reside near the basement membrane. Conversely, germ cells undergoing differentiation and haploid cells develop above this barrier (O'Donnell *et al.* 2015). Also, LH release at puberty triggers differentiation of ALCs and production of testosterone (Shima 2019). PMC and Sertoli cell secretions are also essential for Leydig cell maturation and production of steroids. Release of androgens from Leydig cells in turn triggers initiation of spermatogenesis and SSC differentiation into spermatocytes and more specialized germ cells (Koskenniemi *et al.* 2017). Spermatogenesis starts at about 9 years of age in humans, takes up to 64 days, leading to first produced sperm at ~14 years of age (O'Donnell *et al.* 2015). This process requires precise spatial organization in testis structure (Sharpe 1994; O'Donnell *et al.* 2015).

2.1.3. Testis Structure

Testes have dual functions of spermatogenesis and steroidogenesis which necessitates a complex structural foundation and are located within the scrotum. Two testes are separated by scrotal septum, and covered by visceral and parietal vaginal tunics (Tiwana and Leslie 2017). During testicular descent, gubernaculum testis steers the testes into the scrotum. This ligamentous structure originates from undifferentiated mesenchymal cells attached to the genital swelling and testes. Testicular enlargement during regression of the mesonephros as well as the swelling reaction in gubernaculum testis results in relocation of the testes closer to the inguinal canal. Cell

divisions and production of extracellular matrix in gubernaculum increase, leading to its enlargement while its proximal portion remains short. The enlargement of gubernaculum in its distal portion will pull the testes along with the peritoneal layers covering the abdominal cavity into the scrotum (Hutson *et al.* 2013). Thereafter, the testes will be attached to the body via the spermatic cord from one side and to the scrotum by scrotal ligament which is the remnant of the gubernaculum testis (Burgos and Fawcett 1955). The cremaster muscle covering the spermatic cord is involved in thermoregulation of the testes by controlling their movement towards or against the body (Kayalioglu *et al.* 2008). Following the testicular descent, tunica vaginalis forms a double layer around the testes which is essentially the extensions of visceral and parietal peritoneum. Between the two layers of tunica vaginalis resides a fluid-filled space (*i.e.*, tunica vaginalis cavity), which facilitates the free movement of the testes within the scrotum (Schumacher 2012; Hutson *et al.* 2013). Layers of tunica vaginalis surround the deepest attached testicular layer, tunica albuginea. Tunica albuginea is a fibrous tissue which directly covers the testes and branches inward, forms septa within the testes, and divides the parenchyma into lobes and lobules. Each lobule contains two main compartments known as interstitial tissue and seminiferous tubules (Sprengel *et al.* 1990).

The seminiferous tubule compartment contains Sertoli cells and developing germ cells. During the prepubertal period, these tubules initially lack the lumen and are hence known as seminiferous cords (Lara *et al.* 2018; de Lima e Martins Lara *et al.* 2019). The tubules are U-shaped continuous channels lined with Sertoli cells, embracing germ cells. At the onset of spermatogenesis, the cords undergo enlargement as they become hollow and filled with fluid (Hess and Hermo 2018). The cords/tubules open into a chamber of anastomosing channels known as the rete testis. The seminal fluid is then transported into the efferent ductules, which emerge from the rete. The efferent ductules connect the rete to the epididymis, a convoluted tubular structure (Robaire *et al.* 2006; Robaire and Hinton 2015). Within the seminiferous tubules, Sertoli cells envelop the germ cells and provide them with physical and functional support (Russell and de França 1995). The interstitial (intertubular) compartment of the testis is a highly vascularized structure containing fibroblasts, mast cells, vasculature, macrophages, and Leydig cells which especially surround the vessels. This compartment is mainly colonized by Leydig cells which possess large smooth endoplasmic reticulum and mitochondria, enabling them to produce testosterone in response to LH stimulation. As such, Leydig cells are responsible for high testosterone concentrations observed

within the interstitium and seminiferous tubules (Jones and Fuller 2009; Schumacher 2012). PMCs are a type of smooth muscle cells which surround the seminiferous tubules and are in the peritubular region. These cells possess abundant actin filaments in their cytoplasm as well as other cytoskeletal proteins including myosin, desmin/vimentin, and alpha-actin. Being contractile in nature, PMCs play a key role in transport of spermatozoa and testicular fluid in the tubules (Maekawa *et al.* 1996; Zhou *et al.* 2019).

Products of the seminiferous tubules, known as seminal fluid, are transferred into the epididymis via the rete testis and efferent ductules. Epididymis is a small, highly convoluted, and tube-like structure. This highly compressed canal consists of three parts including the head, body, and tail (Hutson *et al.* 2013; Tiwana and Leslie 2017). The head of the epididymis receives the seminal fluid from efferent ductules and allows the passage of sperm to more distal parts. Convoluted structure of the epididymis provides the space required for storage and maturation of sperm (Robaire *et al.* 2006; Tiwana and Leslie 2017).

2.1.4. Spermatogenesis, Steroidogenesis, and their Regulation

Spermatogenesis is a chronological process of sperm production from immature germ cells which takes ~35 days in mice, ~54 days in rats, and ~72 days in humans (Sikka and Gurbuz 2006). This highly organized process can be divided into three phases of proliferation of spermatogonia, meiosis, and spermiogenesis (O'Donnell 2014). During the proliferation phase, spermatogonia undergo multiple mitotic divisions to form a large population of germ cells for further development. As such, this phase of spermatogenesis is also known as spermatocytogenesis. Among the population of spermatogonia, A_s spermatogonia are relatively quiescent and are unique in that they possess the ability of self-renewal divisions and differentiation into more specialized spermatogonia (de Rooij and Russell 2000). Division of A_s spermatogonia leads to formation of either two new A_s spermatogonia or two attached spermatogonia with incomplete cytokinesis, namely paired. A_{pr} spermatogonia can further divide to generate attached spermatogonia known as aligned A_{al} comprised of chains of 4-16 cells. All three types of spermatogonia are considered undifferentiated; however, attached cells are more committed to undergo transition into A1 differentiating spermatogonia without cell divisions. A1 spermatogonia will produce more differentiating (A2, A3, A4) and differentiated (intermediate, B type) spermatogonia. The transition (without cell division) from A_{al} to A1 spermatogonia marks the initiation of

differentiation in germ cells which is involved with major changes in their morphological features (Hess and Moore 1993; Russell and de França 1995; Phillips *et al.* 2010).

In the second phase of spermatogenesis, B spermatogonia must migrate through the blood-testis barrier, enter the adluminal compartment, and give rise to primary spermatocytes by undergoing another mitotic division. The primary spermatocytes go through two stages of meiotic divisions and produce haploid round spermatids (Sharpe 1994; de Rooij and Russell 2000). Round spermatids produced from meiosis do not have proliferative activity and will undergo a complex series of cytodifferentiation to form spermatozoa over a period of 2-3 weeks in mice and rats (Oakberg 1956; Clouthier *et al.* 1996; Sikka and Gurbuz 2006). The process by which round spermatids transform into elongated spermatids and spermatozoa is known as spermiogenesis. During spermatid maturation these cells undergo nuclear elongation and chromatin condensation, which involves replacement of histones by arginine and cysteine-rich protamine (O'Donnell 2014; Zirkin and Goldberg 2018). The chromatin becomes tightly packed and transcriptionally inactive once it undergoes condensation. Also, during maturation, the Golgi apparatus produces acrosomal granules containing hydrolytic enzymes required later for penetration of sperm during fertilization. Following production of acrosomal granules, acrosome and nucleus polarize to one side of the head, signalling initiation of elongation phase. At this stage, spermatids establish junctions with Sertoli cells (Wong *et al.* 2008). Another major event during maturation of spermatids is formation and development of flagellum. Following completion of meiosis, the central component of the flagellum is assembled from microtubules. During elongation of spermatids, additional structures involved in normal function of flagellum, such as dense fibers, fibrous sheath, and mitochondrial sheath are assembled on top of the central axoneme (Escalier 2006; Hermo *et al.* 2010). Following elongation, spermatids are translocated to the luminal edge by Sertoli cells. The spermatid head and flagella are gradually extended into the lumen while the cytoplasm remains anchored to the Sertoli cells (McLean *et al.* 2003; O'Donnell 2014; Zirkin and Goldberg 2018).

The last step of spermiogenesis is spermiation, which is a critical determinant of the sperm number in epididymis and as such, it defines sperm content in ejaculate (O'Donnell *et al.* 2011). During spermiation, elongated spermatids undergo multi-step remodelling and are released from the seminiferous epithelium. This step happens over several days (~82 hours in rats) at the apical border of the seminiferous epithelium and is marked by alignment of elongated spermatids along

the luminal edge of the seminiferous tubules (O'Donnell *et al.* 2011). The process encompasses removal of intercellular adhesion junctions and remodeling of the cytoplasm. During spermiation, tubulobulbar complexes (TBCs), a form of endocytic machinery, are formed between spermatids and Sertoli cells. These complexes contain a tubular region surrounded by actin filaments, and a bulbous portion. Clathrin is suggested to be involved in organizing actin filaments for TBC formation. TBC formation is initiated when a small portion of spermatid cytoplasm protrudes into the Sertoli cell membrane (Russell and Clermont 1976; Russell 1979). Internalization and degradation of spermatid-Sertoli cell cytoplasmic membrane depends on TBCs (Young *et al.* 2009; O'Donnell 2014). The cytoplasm of the spermatid undergoes repositioning until it is separated from the spermatid and remains as a residual body on Sertoli cells (Russell and Griswold 1993). Failure in normal formation of TBCs has been associated with spermiation failure, indicative of their important role in release of mature spermatozoa into the seminiferous tubules (D'Souza *et al.* 2009). Overall, during spermiation, TBCs are involved in reduction of spermatid cytoplasmic volume, endocytosis of junctional molecules, modeling of the spermatid acrosome and finally detachment of spermatozoa from the luminal edge. Once spermatozoa are released into the tubule, spermiation is completed (Saito *et al.* 2000; O'Donnell *et al.* 2011).

Spermatogenesis is largely affected by hormonal fluctuations in the testis environment and is highly dependent on hormonal regulation (Miller and Auchus 2011). Notably, testosterone, which is an anabolic steroid, plays a key role in initiation and progression of spermatogenesis (Toor and Sikka 2017). In general, steroid hormones regulate a variety of processes during fetal life and adulthood. These hormones are derived from cholesterol and have relatively similar structural basis. In humans, cholesterol is supplied from two sources; *de novo* synthesis from acetate and circulating low-density lipoproteins (LDL) derived from diet. In rodents, however, cholesterol is mainly produced by adrenal gland and from high-density lipoproteins through the activity of scavenger receptor B1. Cholesterol is then transferred to mitochondria, the known hub for steroid production. Within the mitochondria, StAR facilitates movement of cholesterol from the outer to the inner mitochondrial membrane (Brown *et al.* 1979; Horton *et al.* 2002; Flück and Pandey 2017).

Production of high frequency GnRH signals the initiation of spermatogenesis and leads to enhanced biosynthesis of testosterone. GnRH is a peptide hormone synthetized and released from

GnRH neurons of the hypothalamus. During pubertal period, upon release, GnRH travels to the pituitary gland and stimulates production of FSH and LH (Millar 2005; Flanagan and Manilall 2017). In the testis, LH binds to its receptor on Leydig cells and enhances biosynthesis of testosterone, which happens shortly after birth in mice and about 5-8 months of age in pigs (Almeida *et al.* 2006; Bowles and Koopman 2010; Montoto *et al.* 2012). Similar to other androgens, testosterone is produced from cholesterol in mitochondria. The main source of circulating testosterone in the body is the testes; however, a small amount is also secreted by the adrenal cortex and peripheral organs by converting precursor steroids (Shima *et al.* 2013; Flück and Pandey 2017). ALCs are specialized cells for production of testosterone since they can express all required factors common to testosterone producing cells (Hansson *et al.* 1976). StAR activity is upregulated following attachment of LH to its receptor on the surface of ALCs, resulting in increased cholesterol uptake and transport into the inner mitochondrial membrane (Sharpe 1994; Clark *et al.* 1995). Within the mitochondria, cholesterol is converted into pregnenolone by activity of CYP11A1, ferredoxin (FDX1), and ferredoxin-reductase (FDXR) (Miller and Auchus 2011). Pregnenolone is then converted into 17α-hydroxy pregnenolone (17OHPreg) and dehydroepiandrosterone (DHEA) by delta 5 pathway, which is supported by CYP17A1 (Flück *et al.* 2003). DHEA is turned into testosterone by the activity of groups of enzymes that belong to the hydroxysteroid dehydrogenase family. Germ cells lack functional receptor for androgens, thereby the released testosterone diffuses into the Sertoli cells, attaches to AR, and induces functional responses essential for regulation of spermatogenesis. Testosterone is locally and mainly produced by Leydig cells, thereby its concentration is typically 25-125 folds higher within the testis compared to the serum (Smith and Walker 2014). Although testosterone plays a key role in maintaining the population of spermatogonia, its main function has been associated with development of post-meiotic germ cells (O'shaughnessy *et al.* 2012). As is the case for FSH, effects of testosterone on germ cells are indirectly mediated through somatic cells since germ cells lack AR (Abel *et al.* 2008).

FSH increases the production of androgen binding protein (ABP) by Sertoli cells and triggers the establishment of the blood-testis barrier. ABP binds to testosterone, transports it to the epididymis, and once released from ABP, testosterone is converted into DHT by epithelial 5α-reductase in genital skin and prostate (Creasy and Chapin 2013). DHT has about 10 times more affinity for androgen receptor and leads to development of the secondary male characteristics. FSH also

stimulates production of inhibin, a dimeric glycoprotein, by Sertoli cells. Inhibin reduces FSH release from the pituitary gland through a negative feedback loop (Meachem *et al.* 2001; Toor and Sikka 2017). Mice lacking FSH or its receptor have been shown to develop reduced number of germ cells (McLachlan *et al.* 1995; Matthiesson *et al.* 2005). Also, administration of FSH to rats lacking functional GnRH has been associated with increased germ cell numbers, both indicative of FSH roles in survival of germ cells (McLachlan *et al.* 1995). In contrast, small amounts of androstenedione and testosterone are transformed into estradiol and estrone via the activity of CYP19A1. Produced steroid hormones not only affect the reproductive function but also regulate general homeostasis in the body (Flück and Pandey 2017; Miller *et al.* 2021).

2.2. Origin, Development, and Specialization of Male Germline Stem Cells

2.2.1. Primordial Germ Cells

PGCs are precursors of sperm and oocytes, derived from a population of pluripotent cells in the proximal epiblast and next to extraembryonic ectoderm. Therefore, these cells originate far from their site of function during gastrulation (de Rooij and van Dissel-Emiliani 1997; Achermann and Hughes 2011). PGCs are alkaline-phosphate positive cells which migrate through the hindgut to reach and colonize the genital ridges. During their migration, PGCs divide to form a large population (de Rooij and van Dissel-Emiliani 1997; De Felici *et al.* 2004; Chuma *et al.* 2005). By day ~13 of development in mice, PGCs are mostly confined to the genital ridges. Colonization of the genital ridges by PGCs is regulated by influences from molecules, receptors, and matrix proteins including KIT, KIT ligand (KITLG), integrin β-1, E-cadherin, interferon-induced transmembrane protein 1 (IFITM1), IFITM3, CXCL12, and its receptor (Achermann and Hughes 2011). The undifferentiated state of PGCs is maintained by factors such as POU5F1. However, these cells are committed to differentiation as a result of specific signaling molecules. Once arrived at the genital ridges, PGCs enter mitotic arrest (Kispert and Gossler 2004).

Different transcription factors have been suggested to determine PGC identity prior to colonization of the genital ridges. For instance, derivation of PGCs from epiblast has been shown to largely depend upon bone morphogenetic protein (BMP) signaling. *Bmp4* and *Bmp8b* are expressed in the extraembryonic ectoderm and their knock-out results in loss of PGCs (Ying *et al.* 2000; Ying and Zhao 2001). *Bmp* heterozygous mice also show reduced functional PGCs (Ying and Zhao 2001). Similarly, heterozygous, homozygous mutant, or knock-out mice for BMP type 1 receptor, *Alk2,*

and intracellular BMP-transducer *Smad5* and *Smad1* all demonstrate reduced number of PGCs. As such, BMP production by extraembryonic ectoderm is essential for PGC induction (Leitch *et al.* 2013). In addition to BMP, PR-domain-containing protein 1 (PRDM1) also known as B-lymphocyte-induced maturation protein 1 (BLIMP1) is involved in derivation of PGCs from epiblast. BMP triggers expression of BLIMP1 by activating specific genes such as *Stella* and *Fragilis* and reducing the activity of somatic genes (*e.g.*, *Hox*). As such, PGCs develop from the epiblast cells and obtain cytoplasmic extensions enabling them to migrate towards the genital ridges where they transform into gonocytes (Leitch *et al.* 2013).

At ~7 dpc, PGCs develop pseudopodia and start their migration towards the gonadal ridges (Grimaldi and Raz 2020). The migratory behavior of PGCs through hindgut appears to be highly conserved among mammalian species (Tanaka *et al.* 2005; Lange *et al.* 2008; Sasaki *et al.* 2016). When PGCs enter the embryonal endodermal layers, they attach to the basolateral region of endodermal epithelial cells. Next, PGCs become incorporated into the ventral hindgut, which is facilitated through the process of gastrulation. These cells actively move towards the genital ridges in a random manner. The migratory potential of PGCs is retained *in vitro*, which further confirms the active process of their translocation during embryonic development (Donovan *et al.* 1986; Kanamori *et al.* 2019). Attachment of PGCs to the basement membrane has been shown to be essential for initiation of their active movement. Particularly, the dorsal mesentery forms a complex matrix composed of laminin, fibronectin, type IV collagen, perlecan, and heparin sulphate to provide a scaffold upon which PGC movement is facilitated in the coelomic epithelium (Kanamori *et al.* 2019). PGCs then become distributed from the ventral side to the entire circumference of the endodermal tube. Overall, successful migration of PGCs seems to be the result of their passive translocation from epiblast to the hindgut followed by active and random movements towards the left and right gonads. During their migration and divisions, these cells maintain the expression of STELLA and other gene transcripts associated with pluripotency such as OCT4, NANOG, SOX2, and stage-specific embryonic antigen-1 (SSEA-1) (Tilgner *et al.* 2008; Wolf *et al.* 2011; Saitou and Yamaji 2012).

While undergoing multiple mitotic divisions along their movement, PGCs navigate through the hindgut via chemotaxis mechanisms (Molyneaux *et al.* 2001). Stromal-derived factor-1 (SDF-1) also known as CXCL12 is expressed by the genital ridges and attaches to its receptor on the surface

of PGCs. Knock-out studies have shown that SDF-1 or its G-protein coupled receptor chemokine (CXCR4) leads to failure in normal colonization of the genital ridges by PGCs. This indicates that CXCL12 and CXCR4 are both essential for directing PGCs towards their destination and are important chemokine-receptor complexes for PGC migration (Ara *et al.* 2003; Molyneaux, Zinszner *et al.* 2003). Other important factors for migration of PGCs are c-KIT and its ligand Steel factor (Runyan *et al.* 2006; Gu *et al.* 2009), WNT5A (Chawengsaksophak *et al.* 2012), and E-cadherin (Bendel-Stenzel *et al.* 2000). Once they arrive at the genital ridges, PGCs lose their cytoplasmic extensions and become immobile possibly as a result of CXCR4 downregulation. PGCs which fail to migrate and relocate completely to the genital ridges remain in the midline and undergo apoptosis (Kanamori *et al.* 2019; Grimaldi and Raz 2020). While migrating, PGCs retain their genomic properties associated with pluripotency by expressing core pluripotency genes (Tilgner *et al.* 2008; Wolf *et al.* 2011; Saitou and Yamaji 2012). At this stage, these cells are even able to produce teratoma when injected into the mouse testes (Chuma *et al.* 2005). When arrived at the genital ridges, PGCs start expressing a set of gene transcripts essential for sexual differentiation and gametogenesis, and turn off the expression of pluripotency program (Gill *et al.* 2011). PGCs are then referred to as GCCs, can undergo male or female differentiation, and initiate meiosis (Gill *et al.* 2011; Hu *et al.* 2015). GCCs receive signals from their surrounding somatic cells to enter either spermatogenesis or oogenesis pathways once the indifferent gonads undergo transition into testis or ovary at ~12.5 dpc in mice. Entrance of GCCs into one of these pathways, known as licensing, is a major step in faith determination of germ cells (McLaren and Southee 1997). Transition of PGCs into GCCs and their subsequent specialization is suggested to be dependent upon their localization into the genital ridges since it has been shown that loss of somatic transcription factor *Gata4* leads to failure in development of genital ridges, subsequent PGC to GCC transition, and lack of GCC competence to enter spermatogenic pathway (Hu *et al.* 2015). PGCs do not autonomously choose to undergo spermatogenesis or oogenesis pathways and sexual differentiation. Instead, this process depends on the somatic gonad. Sustained specialization of ectopic germ cells in male adrenal glands towards oocyte production further support the role of neighboring somatic cells of the genital ridge in fate determination of PGCs (Upadhyay and Zamboni 1982). Since genital ridges and adrenal glands both originate from adrenogonadal primordium, these two organs possibly produce mutual transcription factors such as deleted in

azoospermia-like (DAZL) and DEAD-box helicase 4 (DDX4), essential for licensing process and induction of differentiation in PGCs (Hatano *et al.* 1996; Gill *et al.* 2011; Laufer *et al.* 2012).

2.2.2. Gonocytes

Gonocytes, also known as prospermatogonia, are a finite population of germ cells derived from PGCs (Culty 2009). PGCs become resident in the gonads and once surrounded by gonadal somatic cells, they start expressing germ cell nuclear antigen (GCNA1). This is the time that PGCs are usually referred to as gonocytes (Enders and May; Richards *et al.* 1999; Culty 2009). At around birth, gonocytes appear as round in shape, are located at the center of the seminiferous cords while being embraced by the Sertoli cell cytoplasm. These cells are considered as functional SSC precursors that ensure the life-long generation of spermatozoa (Culty 2009, 2013; McGuinness and Orth 1992). Developmental phases of gonocytes can be classified into quiescence, proliferation, migration, and differentiation (Manku and Culty 2015). In mice, however, the developmental stages of gonocytes are not completely synchronized, leading to coexistence of two different categories of quiescent and proliferative gonocytes during the neonatal period (Culty 2013). After birth, gonocytes are released from their fetal-early neonatal quiescence state, re-initiate their proliferative phase, and move towards the basement membrane (Huff *et al.* 2001; Culty 2009, 2013; Drumond *et al.* 2011), leading to their translocation and differentiation into SSCs (Manku and Culty 2015). Generally, gonocytes are comprised of a heterogenous cell population including successive stages of mitotic (M) and transitional (T) prospermatogonia, which itself is subdivided into T1 and T2-prospermatogonia (Hilscher *et al.* 1974; Fukuda *et al.* 1975; Hilscher 1991; Vergouwen *et al.* 1991). Gonocytes at each developmental stage express different subsets of gene transcript combinations in varying levels including melanoma antigen-A4 (MAGE-A4) (Aubry *et al.* 2001) and guanylate cyclase-activating protein (GCAP) (Pauls *et al.* 2006; Culty 2009). The presence of these germ cells is not necessarily synchronized within the seminiferous cords/tubules, generating an overlap of different cell populations. For instance, quiescent, mitotic, and differentiating prospermatogonia which are at different developmental stages can be simultaneously present (Culty 2009). M-prospermatogonia appear during the prenatal period, are mitotically active, located far from the basement membrane, and can be found in the center of the cords (McLaren 2003). This type of prospermatogonia has the same morphological features as that of oogonia at the equivalent developmental stage. It has been

suggested that the first identifiable distinction between male and female germ cells can be observed at the T1-prospermatogonia stage, where germ cells enter mitotic arrest (McCarrey 2013). M-prospermatogonia become T1-prospermatogonia and enter G0 of the cell cycle at ~16.5 dpc in mice (Yoshida *et al.* 2007; Culty 2009, 2013). These cells remain mitotically inactive until a few days after birth when they transform into T2-prospermatogonia and re-start their cell division while migrating towards the basement membrane (Yoshida *et al.* 2007; Culty 2009). Following their migration and once located in the basement membrane niche, these cells give rise to type A spermatogonia which later establish the life-long process of spermatogenesis. Transformation of prospermatogonia into SSCs starts at birth and takes up to ~6 days in rodents (Wu *et al.* 2009).

The proliferation *vs.* quiescent state of prospermatogonia during the fetal and neonatal periods is regulated through paracrine and endocrine release of hormones and cytokines (Busada and Geyer 2016). Several studies support the role of RA in determining the prospermatogonia fate. During the fetal period, these cells are normally protected from RA exposure which otherwise would induce their premature differentiation and activate their apoptosis program. Protection of these cells against RA is partly achieved through the action of cytochrome P450 enzyme CYP16B1 (MacLean *et al.* 2007; Li *et al.* 2009). Another study showed that RA increases the proliferative activity of prospermatogonia but induces apoptosis at greater rates, which overall points at the loss of fetal germ cells following exposure to RA (Livera *et al.* 2000). Also, activin A and androgens are suggested to negatively regulate fetal germ cell proliferation (Li *et al.* 2009; Mendis *et al.* 2011). In addition, aberrations of normal temporal sequences in cytokine release can lead to abnormal behavior of germ cells such as premature initiation of their proliferation or differentiation (Manku and Culty 2015). For instance, improper initiation of germ cell differentiation can result in development of carcinoma *in situ*, known as a cause of testicular germ cell tumor (TGCT), which has been especially prevalent in young adults in the past few decades. The underlying triggers for TGCT are yet to be fully understood but abnormal exposure to endocrine-disrupting compounds is often held responsible (Skakkebaek *et al.* 1987; Sonne *et al.* 2009).

Depending on the species, translocation of the prospermatogonia happens before or shortly after birth (de Rooji 1998; Nel-Themaat *et al.* 2011). These cells develop pseudopodia and pass through the cytoplasm of the Sertoli cells by ameboid movements (Nagano *et al.* 2000). Failure in proper migration will ultimately lead to germ cell degeneration, while complete migration and interaction

of germ cells with the basement membrane results in continuation of their development into spermatogonia and establishment of SSC pool (Orwig *et al.* 2002). The migratory behavior of gonocytes also depends upon expression of molecular cues from germ and somatic cells as well as germ-somatic cell interactions (Orth *et al.* 1997). KIT is one of the transcription factors expressed by germ cells undergoing translocation towards the basal compartment. Blocking this factor can result in reduced numbers of gonocytes *in vitro* and failure of their migration *in vivo* (Besmer *et al.* 1993; Lamb 1993; Orth *et al.* 1997). PDGF is another factor produced by Sertoli cells which promotes germ cell migration to the periphery of the cords (Marziali *et al.* 1993; Basciani *et al.* 2008). Also, deletion of *Aip1* in Sertoli cells was shown to impair the migration of germ cells, suggestive of involvement of actin interacting protein 1 (AIP1) in translocation of germ cells from the center to the cordal periphery (Xu *et al.* 2015). In addition, several members of A-Disintegrin and A-Metalloproteinase domain (ADAM), a surface receptor, are expressed in the fetal, neonatal, and prepubertal testis and have been proposed to be involved in migration of gonocytes (Rosselot *et al.* 2003). Once located on the basement membrane, gonocytes become engulfed in a microenvironment composed of vasculature, somatic cells, growth factor milieu, and physical architecture which all contribute to their fate determination. This unique microenvironment is referred to as the germ cell 'niche'.

2.2.3. Spermatogonial Stem Cells

SSCs are adult stem cells in the testis which arise from T2-prospermatogonia. T2-prospermatgonia continue their mitotic divisions even after sitting on the basement membrane. A subset of these cells give rise to A spermatogonia (Kubota and Brinster 2018). SSCs first appear at ~5 days after birth in rodents, 1-2 months after birth in pigs, and ~3 months of age in humans (Goel *et al.* 2007; Jan *et al.* 2012; Hutson *et al.* 2013). These cells constitute a very rare population of germ cells in the testis and ensure the life-long maintenance of spermatogenesis (Tagelenbosch and de Rooij 1993). SSCs are also unique germ cells owing to their ability to both undergo mitotic divisions to repopulate and produce daughter cells committed to generate terminally differentiated haploid cells (Aponte 2015; Kubota and Brinster 2018). As discussed earlier, different types of A spermatogonia include A_s, A_{pr}, and A_{al} (Nagano and Yeh 2013; Kubota and Brinster 2018). While A_s spermatogonia are only ~0.03% of total adult testis cells in rodents, they are the only source of both diploid and haploid germ cell population in the testis (Aponte 2015; Ibtisham and

Honaramooz 2020). A_{al} to A1 transition marks the initiation of differentiation and major morphological changes in germ cells. Clones of A_{al} spermatogonia differentiate to A1 to A4, intermediate and B spermatogonia. (de Rooij and Russell 2000; Griswold 2016; Kubota and Brinster 2018).

In primates, A spermatogonia are further classified as A_{dark} and A_{pale}, depending on the intensity of their nuclear staining. Although both spermatogonia types reside on the basement membrane A_{dark} spermatogonia possess smaller and round shape, darker nucleus, are considered as reserve stem cells, and have relatively limited mitotic activity. In contrast, A_{pale} spermatogonia are larger and oval shape, and show lighter nuclear staining (Clermont 1969). A_{pale} and A_{dark} spermatogonia in primates correspond to the undifferentiated spermatogonia composed of A_s, A_{pr}, and A_{al}, whereas primate type B spermatogonia are counterparts of rodent differentiating spermatogonia (Boitani *et al.* 2016). Self-renewal and differentiation of the spermatogonia relies on paracrine factors and cytokines released in the niche. Notably, GDNF released by Sertoli cells promotes self-renewal divisions through attachment to the GDNF receptors, RET and GFRα1 on the surface of clustered spermatogonia. This has been supported by knock-out studies showing depletion of seminiferous tubules in $GDNF^{+/-}$ mice (de Rooij 2001; Kanamori *et al.* 2019). However, progression of spermatogonia differentiation depends on RA and PDGF signaling (Wang and Culty 2007; Manku *et al.* 2015).

2.3. *In Vivo* Models to Study Testis Development and Function

2.3.1. Germ Cell Transplantation

Germ cell transplantation (GCT), also known as SSC transplantation, is a process where isolated germ cells from a donor male are transplanted into the testis of a recipient, leading to their colonization, and even donor-derived spermatogenesis (Honaramooz and Yang 2011). GCT was first introduced by Brinster and colleagues in 1994 by isolating testis cells from ZFlacZ mice, expressing the *Escherichia coli* β-galactosidase, and transferring them to the tubules of busulfan-treated recipient mice which lacked endogenous germ cells. Following transplantation, donor germ cells colonized the recipient seminiferous tubules visualized by exposure to X-Gal and produced donor-derived spermatozoa (Brinster and Avarbock 1994). In this method, donor germ cells that are initially localized in the center of the seminiferous tubules, gradually pass between Sertoli cells using their cytoplasmic projections to relocate to the basolateral compartment, proliferate, and

generate a new spermatogenic colony. These colonies further develop and can potentially initiate spermatogenesis (Nagano *et al.* 1999; Ohta *et al.* 2000). Although this technique was first introduced in mice (Brinster and Zimmermann 1994), it was also successfully applied in rats (Jiang and Short 1995). GCT from different laboratory animals such as mouse, hamster, and rat into mice can successfully lead to establishment of spermatogenesis. However, spermatogenesis cannot be achieved when donors and recipients are phylogenetically more distant; for instance, when germ cells from rabbit or farm animals are microinjected into recipient mice, donor cells only colonize the testes and do not undergo complete spermatogenesis (Dobrinski *et al.* 1999, 2000; Kim *et al.* 2006). This is believed to be the result of limited support from recipient Sertoli cells (Honaramooz and Yang 2011). Nevertheless, this technique remains as the only reliable bioassay to detect the stemness potential of donor germ cells from any donor species (Hermann *et al.* 2012).

GCT has important potential applications in fertility restoration of cancer patients for instance by auto-transplantation of the cryopreserved germ cells back into their testes following cytotoxic cancer treatments. Other potential applications include preservation of genetic potential of endangered species/prized animals, correction of spermatogenic defects, elucidation of the mechanisms regulating MGSCs and their niche, and production of transgenic animals (Dobrinski 2005; Hamra *et al.* 2017; Uchida and Dobrinski 2018). Notably, this method represents a unique functional bioassay to test the functionality of 'true' SSCs (Honaramooz and Yang 2011). Production of transgenic animals by GCT involves transplantation of genetically modified germ cells from a donor to the recipients, leading to production of spermatozoa carrying a transgene. Transgenesis through MGSCs has great potential especially in large domestic species such as goats and pigs where available methods for transgene transmission are inefficient, expensive, and complex (Dobrinski 2008; Kim *et al.* 2008; Zeng *et al.* 2013). Especially, transduction of the transgene through germline stem cells circumvents the complexities associated with traditional methods such as pronucleus microinjection or somatic cell nuclear transfer where manipulation of embryos and can cause subsequent developmental abnormalities (Honaramooz and Yang 2011; Zeng *et al.* 2013). In addition, utilization of recently developed molecular tools for manipulation of the genome such as clustered regularly interspaced short palindromic repeat/CRISPR-associated protein 9 (CRISPR/Cas9) combined with GCT may provide tremendous advantages over the conventional methods of germline transfection and viral transduction. In this method, transplanted

MGSCs can act as vehicles for the transgene, colonize the recipient seminiferous tubules, and produce transgenic sperm over the life of the recipient (Honaramooz *et al.* 2003; Zeng *et al.* 2013).

GCT in laboratory animals usually requires inherently immunodeficient recipients or cytoablative treatments to prevent from rejection of the transplanted cells and facilitate their migration and colonization. In contrast, large animal recipients do not typically reject germ cells from genetically unrelated donors of the same species (Dobrinski *et al.* 2000; Nagano *et al.* 2001; Dobrinski 2005; Honaramooz and Yang 2011). Also, the success rate of GCT increases when endogenous germ cells are reduced. In laboratory animals, different approaches have been utilized to remove or reduce the recipient germ cells prior to GCT. These include utilization of mouse recipients with white-spotting (*W*) mutations, resulting in defective c-kit proto-oncogene or Steel (*Sl*) mutant mice, which lack functional KITLG (*Kitl*), application of hyperthermal or cytoablative treatments, cold ischemia, or irradiation to deplete germ cells (Brinster and Zimmermann 1994; Kim *et al.* 2006; Honaramooz and Yang 2011). In large animals, unlike laboratory animal models, recipients with genetically impaired spermatogenesis are not available and as such, different approaches have been developed for preparation of the testes prior to GCT. These include busulfan treatment in pregnant sows to remove the germ cells in their progeny, and irradiation of the testes in recipient goats (Honaramooz *et al.* 2003; Honaramooz *et al.* 2005). Also, using immature recipients has been shown to facilitate the migration process of donor germ cells from lumen to the periphery of the tubules since immature animals lack multiple cellular layers in the seminiferous tubules. Nevertheless, the efficiency of GCT in farm animals is still low with ~7% donor-derived progeny in goats, which has been only improved by ~1-3% following preparation by irradiation (Honaramooz *et al.* 2002; Honaramooz *et al.* 2003; Honaramooz and Yang 2011).

The efficiency of GCT is also dependent on preparation or choice of donors. SSCs form only ~0.02 to 0.2% of testis cells in rodents at post-pubertal stage while only ~7-20% of the transplanted SSCs colonize the tubules following transplantation (Huckins 1971; Tagelenbosch and de Rooij 1993; Kanatsu-Shinohara 2005). Expectedly, transplantation of increased numbers of SSCs will enhance their colonization and establishment of spermatogenesis. Different strategies have been used to increase germ cell proportion among transplanted cells such as using cryptorchid, vitamin-A deficient or Steel mutant mice, which possess greater number of undifferentiated spermatogonia (van Pelt *et al.* 1996; Ogawa *et al.* 2000; Shinohara and Brinster 2000). In larger animals, however,

the practicality of these methods is low due to added complication to the procedure and instead, immature animals can serve as donors, which naturally offer greater proportion of undifferentiated SSCs (Honaramooz and Yang 2011). Another approach to increase germ cell numbers is application of efficient isolation and enrichment techniques which enhance the removal of somatic cells while increasing isolated germ cells (Yang *et al.* 2010). Frequently-used enrichment methods for increasing germ cell populations include density gradient centrifugation such as Nycodenz density centrifugation, leading to a testis cell population with ~80% gonocytes (Yang *et al.* 2010), differential plating, magnetic activated cell sorting (MACS) (Buageaw *et al.* 2005), and fluorescent-activated cell soring (FACS) (Shinohara *et al.* 2000). Combination of Nycodenz density gradient and differential plating has been shown to offer enriched testis cell populations containing ~90% gonocytes (Honaramooz and Yang 2011).

To evaluate the success rate of GCT and track the transplanted cells, several approaches has been used. For instance, donor cells are tagged with a dye such as trypan blue or a fluorochrome (*e.g*., carboxyfluorescein diacetate succinyl diester-CFDA-SE or PKH26) prior to transplantation (Honaramooz *et al.* 2002; Hill *et al.* 2005; Rodriguez-Sosa *et al.* 2006, 2009; Zhang *et al.* 2008). Alternatively, a particular transcript can be integrated into the germ cell genome by viral transduction (*e.g*., adeno-associated virus; rAAV) which leads to production of a fluorescent signal (*e.g*., green fluorescent protein-GFP) or expression of the transcript leads to production of an enzyme which can generate a visible color following incubation with a substrate (*e.g.*, *lacZ*) (Brinster and Avarbock 1994; Brinster *et al.* 2003). Using rAAV vectors, transgenic goats have been produced with long-term expression of GFP and presence of transgenic sperm in ~35% of the ejaculates (Honaramooz *et al.* 2008).

2.3.2. Testis Tissue Xenografting

Grafting of testis tissue was first experimented in 18th century to understand the role of testis in development of the secondary sexual characteristics, mechanism of androgen production, and spermatogenesis. The initial experiments of testis grafting were limited to allografting, where donor and recipient of the tissue were different individuals of the same species, or even more scarce reports of autografting, where obtained tissues of an individual were grafted back into the body (reviewed in Setchell 1990; Honaramooz 2014). Allografting and xenografting studies were limited especially owing to the immunorejection of the tissue by the host body. This limitation was

overcome later by introduction of different strains of immunodeficient mice which are unable to initiate immune response towards the grafted tissue (Honaramooz 2014). The first grafting of testis into immunodeficient mice with the aim of tissue preservation was performed in the 20th century, where fetal human testis tissue was embedded into subcutis of nude mice. Xenografted tissue was accepted by the recipient mice and its histological architecture was preserved (Povlsen *et al.* 1974; Skakkebaek *et al.* 1974). The same group also reported formation of pachytene spermatocytes in the grafts following xenotransplantation of rat testis tissue into nude mice (Setchell 1990; Arregui and Dobrinski 2014).

In 2002, testis tissue from newborn mice, pigs and goats were shown to develop up to full spermatogenesis following xenografting into nude mice (Honaramooz *et al.* 2002; Dobrinski 2005). In the later study, fragments of ~1 mm^3 in size were obtained from donor testis and grafted under the back skin of castrated immunocompromised nude mice. Dorsal subcutaneous skin normally provides appropriate temperature, corresponding to that of *in situ* requirements for spermatogenesis (~36.5° C) in most domestic animals and is an accessible and observable location for grafting, harvesting, and visualization of the tissues (Honaramooz 2014). The grafts from all donor species increased in size and underwent complete structural and functional development to complete spermatogenesis. This report was the first to show initiation of spermatogenesis in testis tissue xenografts and production of haploid sperm. Surprisingly, the sequence and kinetics of tissue development, testicular cell differentiation, and spermatogenic efficiency were comparable to those of intact testis tissue. However, spermatogenesis happened slightly faster in the porcine xenografts compared to *in situ* tissue. Interestingly, retrieved spermatozoa from xenografts were fertilization-competent, shown by intracytoplasmic sperm injections (ICSI) (Honaramooz *et al.* 2002). Following the initial reports of TTX using murine, caprine, and porcine species, multiple research groups utilized the same approach to test the feasibility of sperm production in xenografts of different species such as hamsters (Schlatt *et al.* 2002), monkeys (Honaramooz *et al.* 2004), rabbits (Shinohara 2002), bulls (Oatley *et al.* 2004; Rathi *et al.* 2005), dogs (Abrishami *et al.* 2010), and cats (Rathi *et al.* 2006). To date, a wide range of species have been used as donors in TTX studies contributing to its establishment as an applicable and reliable model especially for developmental study of the testis (Arregui and Dobrinski 2014; Honaramooz 2014) (Fig. 2.1).

TTX can be considered as an *in vivo* tissue culture system where the host provides structural, nutritional, and hormonal support for the grafted tissue. Xenografts are typically placed under the back skin of immunocompromised mice, triggering a functional circulatory connection between the host subcutaneous tissue and the grafted testis fragment (Schlatt *et al.* 2010a). Using rat testis xenografts, outgrowth of endogenous endothelial cells within the grafts and simultaneous development of blood vessels from the host was shown to establish an interconnecting vasculature, ensuring an active blood supply to the xenograft (Schlatt *et al.* 2010b). Followed by establishment of blood circulation within the grafts, endogenous functional feedback loop from pituitary hormones of the host mouse stimulates the expansion and development of the grafted tissue to fulfill spermatogenesis and steroidogenesis. Although harvested spermatozoa at this time lack epididymal maturation, they can successfully be used for ICSI (Honaramooz 2014). Sperm from xenografts have also been used for production of rabbit and pig embryos via ICSI, with normal development after being transferred into the uterus of recipient females (Shinohara 2002; Nakai *et al.* 2010; Kaneko *et al.* 2012).

TTX have a variety of applications in several research and experimental settings. Grafted tissues can be used to study testis development and function where no *in vitro* or *in vivo* alternative models are available or *in situ* studies are inherently complicated (*e.g.*, humans or endangered/rare species) (Honaramooz 2014). Importantly, TTX is an advantageous approach for the study of gonadal development in that it provides greater accessibility and ease of manipulation of the xenografts and their milieu in the host species compared to *in situ* tissues (Arregui and Dobrinski 2014; Honaramooz 2014). In addition, since preserved testis tissue has shown similar developmental potential as fresh samples, it is feasible to save testis fragments by hypothermic treatments or cryopreservation in situations where immediate grafting is not possible or desired (Abrishami *et al.* 2010; Honaramooz 2014). Moreover, given that xenografts develop up to complete spermatogenesis and produce fertilization competent sperm, TTX offers the opportunity to even produce embryos to be cryopreserved when combined with ICSI and other assisted reproductive technologies. Combination of testis tissue preservation, TTX, and ICSI opens up new windows of opportunity to possibly rescue the genetic potential of endangered species or prized farm animals, or even preserve the fertility potential of immature boys undergoing cytotoxic cancer therapies (Honaramooz *et al.* 2002; Arregui *et al.* 2008; Honaramooz 2014).

2.3.3. Testis Cell Aggregate Implantation

TCAI is the next model developed following the introduction of GCT and TTX. In TCAI, testis cells are first dissociated using enzymatic digestion, leading to formation of a tightly packed single-cell aggregate. This aggregate is then transferred into the subcutaneous tissue of immunodeficient recipient mice, which act as a bioincubator to ensure proper supply of blood, nutrients, and temperature to the implant (Dufour *et al.* 2002; Gassei *et al.* 2006; Honaramooz *et al.* 2007; Kita *et al.* 2007; Arregui *et al.* 2008; Zhang *et al.* 2008). Following implantation, testis cells undergo spontaneous reorganization and *de novo* formation of testis cords. TCAI has been experimented using diverse donor species with subcutaneous tissue of immunodeficient recipient mice being the frequently-used site for the implantation procedure (Gassei *et al.* 2006; Honaramooz *et al.* 2007; Kita *et al.* 2007; Arregui *et al.* 2008; Dores *et al.* 2012; Campos-Junior *et al.* 2014).

When using neonatal piglets as donors of implants, testis cells start to align themselves at ~4 days post-implantation, form cord-like structures after ~7 days post-implantation, and by the end of the second week, immature cords are transformed into structures resembling complete seminiferous cords of the neonatal pig testis (Honaramooz *et al.* 2007). Cellular arrangements following TCAI include polarisation of Sertoli cells to the basal compartment, translocation of gonocytes to the center of the newly-formed cords, and re-formation of the interstitial compartment consisting of Leydig cells and supporting cells of the connective tissue. Over time, regenerated testis cords develop into seminiferous tubules with complete maturation of germ cells and sequential rounds of spermatogenesis, resulting in fertilization-competent sperm (Honaramooz *et al.* 2007; Awang-Junaidi *et al.* 2020). Judging from the vesicular gland weight in castrated recipients, regenerated testis tissue developed from ectopic testis cells were also capable of producing androgens to the same level as *in situ* testis tissue (Honaramooz *et al.* 2007).

TCAI has been experimented using a diverse range of donors including the pig (Honaramooz *et al.* 2007; Awang-Junaidi *et al.* 2020), mouse (Kita *et al.* 2007), sheep (Arregui *et al.* 2008), cattle (Zhang *et al.* 2008), horse (Zeng *et al.* 2017) and monkey (Aeckerle *et al.* 2013; Shetty *et al.* 2018) (Fig. 2.1). Although there are numerous potential applications for TCAI, studies on this model have been rather limited. Spontaneous *de novo* morphogenesis of testis tissue from dissociated testis cells demonstrates a remarkable feature in that cells in this model can autonomously

reorganize themselves to form a tissue that is structurally and functionally identical to that *in situ* (Kita *et al.* 2007; Arregui *et al.* 2008; Zhang *et al.* 2008). Therefore, TCAI provides a unique opportunity to study male gonadal development in an *ex situ* environment, which is especially important where *in situ* studies are inherently difficult, for instance in endangered or rare species, or impossible in case of humans (Dores and Dobrinski 2014). TCAI can also provide a means to preserve the fertility potential of immature boys whose life relies on cytotoxic cancer therapies, by isolating unaffected testicular cells from samples obtained through biopsies, preserving them, followed by implanting them to regenerate testis tissue at later time points. Notably, TCAI is a suitable model to study the effects of environmental factors or novel pharmaceutical compounds such as experimental drugs, potential toxicants, and various growth factors on testis development (Honaramooz *et al.* 2007; Dores and Dobrinski 2014; Awang-Junaidi *et al.* 2020).

Dissociated testis cells from different donor species retain their re-organization potential once implanted into the recipient mice (Dufour *et al.* 2002; Gassei *et al.* 2006; Kawasaki *et al.* 2006, 2010; Honaramooz *et al.* 2007; Kita *et al.* 2007; Arregui *et al.* 2008; Zhang *et al.* 2008; Aeckerle *et al.* 2013; Campos-Junior *et al.* 2014). However, establishment of complete spermatogenic rounds has been reported in mouse- (Kita *et al.* 2007) and haploid germ cells in pig- and sheep implants (Honaramooz *et al.* 2007; Arregui *et al.* 2008; Campos-Junior *et al.* 2014). Cattle were used as donors only in one report with successful regeneration of cords containing Sertoli cells, while no spermatogenesis was observed since the implants were only maintained for 3 months (Zhang *et al.* 2008).

Timing in development of the grafts and implants in TTX and TCAI also appears to be different. While developmental sequence is delayed in testis cell implants, time required for full development of the grafts to achieve spermatogenesis is relatively closer to that in intact testis tissue (Berger *et al.* 1980; Honaramooz *et al.* 2002; Honaramooz *et al.* 2007). Testis tissue xenografts from neonatal porcine donors grafted into nude mice showed complete tubular formation containing spermatozoa at ~28 weeks post grafting (Honaramooz *et al.* 2002). In a comparable TCAI study, dissociated porcine testis cells formed seminiferous tubules at ~14 days post implantation and formed elongated spermatids at ~30 weeks (Honaramooz *et al.* 2007). Since sexual maturity and initiation of spermatogenesis in intact boars happen at ~6-7 months of age, it can be concluded that the temporal features of the developing grafts and implants are both fairly

accurate representatives of *in situ* testis tissue (Berger *et al.* 1980; Honaramooz *et al.* 2002). Using sheep as a donor, complete spermatogenic cycle was first observed at ~12 weeks following grafting which was comparable with intact tissue, while spermatogenesis in sheep cell implants happened at ~40 weeks post implantation (Arregui *et al.* 2008). Similarly, in TTX and TCAI studies of collard peccary, spermatogenesis was reported to occur at 6 and 8 months, respectively (Campos-Junior *et al.* 2014).

Although implanted testis cells form a testis tissue with comparable architecture to the intact tissue, some studies reported scarcity or total absence of germ cells within seminiferous tubules (Gassei *et al.* 2006; Honaramooz *et al.* 2007; Kita *et al.* 2007; Arregui *et al.* 2008). This phenomenon may be due to a low germ cell proportion among the donor cells and/or a loss of germ cells following isolation and implantation processes; in either case, this results in a reduced number of spermatids and spermatozoa produced by implants (Rathi *et al.* 2006; Arregui *et al.* 2008; Campos-Junior *et al.* 2014). Interestingly, regeneration of testicular cords can occur even in the absence of germ cells and when implanted cell aggregates were only comprised of somatic cells. This observation points to the important role of somatic cells in reorganization of testis architecture and its maintenance even in intact testis tissue (Dufour *et al.* 2002). Also, among all TCAI studies, there has been a notable lack of a consistent approach for isolation and delivery of testis cells to the implantation site. Each report used a different number of testis cells containing various germ cell proportions for implantation (Gassei *et al.* 2006; Honaramooz *et al.* 2007; Arregui *et al.* 2008; Watanabe *et al.* 2009). These factors can in turn affect the reliability of the TCAI outcomes. A recent study has optimised the method for delivery of the cell aggregates by systematically comparing different extracellular matrices as carriers of the aggregates, as well as injection *vs.* conventional surgical delivery method. In the latter study it was concluded that injection of the aggregates leads to reduced cell loss compared to conventional surgical embedding the aggerates into the subcutaneous fascia (Awang-Junaidi *et al.* 2020). In addition, TTX and TCAI studies mostly rely on surgical removal of the samples in anesthetized or euthanized animals for evaluation of the grafted or implanted tissues. Repeated retrieval of implant samples from immunodeficient mice can pose a risk of infection and other complications. Also, post-retrieval processing of the samples prior to their (immuno)histological examination expectedly leads to tissue distortion or shrinkage and biased post-retrieval assessment. As an alternative, establishment of a non-invasive examination method for live mice with comparable accuracy such as ultrasound can greatly benefit

prospective TTX and TCAI studies as it will reduce the number of required recipients and allows longitudinal examination of the subcutaneous samples.

Overall, TCAI has provided an unprecedented approach to study the unexplored aspects of male gonadal development, and to elucidate potential factors involved in the regulation of testis morphogenesis (Fig. 2.1). TCAI has also offered a unique *in vivo* culture system to gain a deeper understanding of spermatogenesis, steroidogenesis, and factors affecting them via manipulation of the testis microenvironment especially where *in situ* studies are not feasible.

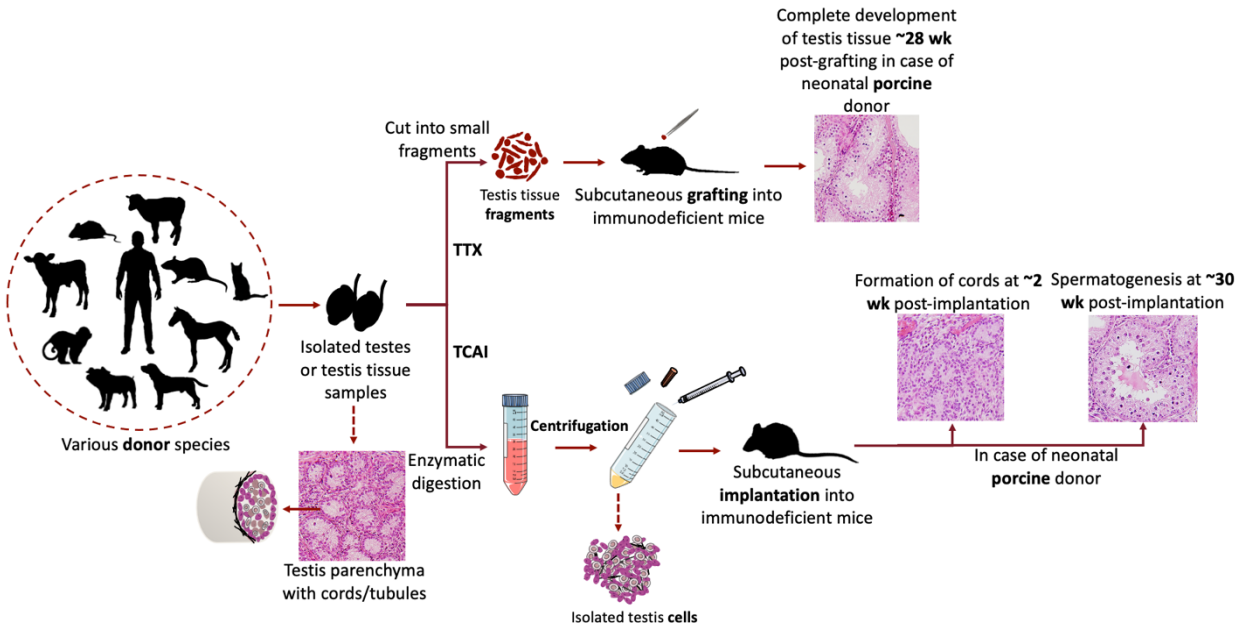

Fig. 2.1. Overview of procedures in testis tissue xenografting (TTX) and testis cell aggregate implantation (TCAI). Experimentations with TTX and TCAI have utilized a wide range of donor species. In TTX, small fragments of testis parenchyma (usually 1 mm^3 in size) are isolated following castration or surgical biopsy of a mature/immature donor. Testis fragments are then embedded under the back skin of immunodeficient recipient mice through aseptic surgical procedure. Subcutaneous tissue acts as a bioincubator leading to complete development of the testis tissue with production of fertilization-competent sperm (after ~28 wk of incubation in case of neonatal donor piglets). In TCAI, testis parenchyma is isolated and digested using a step-wise enzymatic protocol, which is a combination of physical dissociation and enzymatic digestion, leading to a highly concentrated cell aggregate. The aggregate is then embedded/injected into the subcutaneous tissue of an immunodeficient recipient mouse (usually 0.1 mL per injection site). Testis cells in the implants reorganize to form small cords (at ~2 wk after implantation in case of neonatal donor piglets), and completely regenerate functional seminiferous tubules with production of sperm (following ~30 wk in case of neonatal porcine donor).

2.3.4. Factors Affecting the Development of Grafts and Implants

Following the initial experiments, TTX and TCAI were extensively applied to different donor species with varying outcomes. Expectedly, the time required for maturation of the tissue in TTX, complete development of the implants to fulfill spermatogenesis in TCAI, and rate of spermatogenesis in both sample types rely on factors from the donors and the recipients. Therefore, the main sources of variation in results of TTX and TCAI are usually classified into the factors associated with the donors and recipient animals (Abbasi and Honaramooz 2010; Abrishami *et al.* 2010; Dores *et al.* 2012; Arregui and Dobrinski 2014).

Thus far, a wide range of species have been used as donors in TTX and TCAI studies. Grafts and implants in nearly all studies developed into a mature tissue and contained advanced germ cells (Paris and Schlatt 2007; Honaramooz 2014). While in the majority of TTX studies the maturation timing of the ectopically grafted tissue corresponded to that of *in situ* testis, cells in implants initially required some time to reorient themselves and undergo reorganization to form cord-like structures (Honaramooz *et al.* 2002; Honaramooz *et al.* 2007; Paris and Schlatt 2007; Arregui and Dobrinski 2014). As such, development of cords and more advanced germ cells appear to be delayed in cell implants compared to the age-matched tissues. Grafts from the lamb, beef calf, deer fawn, and bison turn into fully mature tissues after ~3, ~7, ~12, and more than ~16 months, respectively, which is approximately the same amount of time required for *in situ* maturation of testis tissue (Rodriguez-Sosa and Dobrinski 2009; Abrishami *et al.* 2010; Abbasi and Honaramooz 2011c, 2012). However, this is not the case in human grafts/implants, where their development is limited regardless of their developmental stage at the time of grafting/implantation (Schlatt *et al.* 2006; Yu *et al.* 2006; Geens *et al.* 2008). Similarly, grafts from banteng calves showed a long pause in meiotic development (Honaramooz *et al.* 2004). Grafts from pig, rhesus monkey, and collared peccary start to produce spermatozoa in shorter periods of time compared to *in situ* tissue (Honaramooz *et al.* 2004; Sato *et al.* 2010; Campos-Junior *et al.* 2014), while initiation of spermatogenesis takes longer in cat xenografts (Kim *et al.* 2007). Also, it is speculated that exposure of immature testis tissue to post-pubertal hormonal environment in the host mouse can lead to accelerated maturation of the xenografts from rhesus monkeys, although this has not been the case for grafts from other donor species (Honaramooz *et al.* 2004).

In addition to timing of spermatogenesis, donor species also determines the efficiency of spermatogenesis, usually reported as the percentage of seminiferous tubules with sperm or elongated spermatids. In grafts from sheep or goat, spermatogenic efficiency appeared to be high compared with that of dairy or beef cattle, buffalo, bison, and deer (Honaramooz *et al.* 2002; Oatley *et al.* 2004; Rathi *et al.* 2005b, 2006; Zeng *et al.* 2006). This can be due to greater compatibility of the grafts with the host HPG axis. The overall structure of gonadotropins shows a conserved sequence of homology among species (Bousfield *et al.* 2006); however, slight differences in amino acid sequences results in diversity in gonadotropin binding affinity to their receptors of various species (Arregui and Dobrinski 2014). Another hormonal regulator for development of the ectopic graft is testosterone. Although testosterone is also structurally conserved among vertebrates, some grafts, especially from bovine species, inherently produce large amounts of androgens, which in turn affects spermatogenic efficiency of the xenografts through the established feedback loop (Rathi *et al.* 2005; Rodriguez-Sosa *et al.* 2012). Taken together, both timing and efficiency of spermatogenesis varies between xenografts from different species (Arregui and Dobrinski 2014).

Age of donors is also an important determinant in success of spermatogenesis following grafting or implantation. Overall, grafts from immature donors seem to have a considerably greater developmental potential compared to those from mature donors (Honaramooz *et al.* 2002; Shinohara 2002; Schlatt *et al.* 2002; Kim *et al.* 2007; Arregui and Dobrinski 2014). Degeneration of the testis tissue is frequently reported following grafting from mature donors. Grafts which contain high percentage of complete spermatogenic cycles at the time of grafting demonstrated faster degeneration compared to grafts from young and immature donors (Schlatt *et al.* 2006; Arregui *et al.* 2008; Turner *et al.* 2010). Also, the extent of degeneration has been greater in grafts from donors with naturally greater spermatogenic efficiency (*e.g.,* pigs and goats) or with more advanced stages of spermatogenesis at the time of grafting (Arregui *et al.* 2008). Post-grafting degeneration may be the result of susceptibility of differentiated germ cells to hypoxia, limited blood supply, limited angiogenic potential of the mature tissues, inhospitable microenvironment immediately after ectopic grafting/implantation, and/or loss of proliferative potential of mature Sertoli cells, which in turn limits the overall regeneration of grafts following TTX (Schlatt *et al.* 2002; Rathi *et al.* 2006; Kim *et al.* 2007; Arregui *et al.* 2008; Abrishami *et al.* 2010). Treatment of the grafts with vascular endothelial growth factor (VEGF) was shown to promote angiogenesis within grafts, increase in graft size, and development of more elongated spermatids. Hence,

application of VEGF was suggested to enhance survival of grafts or implants and offset the negative effects of initial hypoxia by triggering neovascularization (Schmidt *et al.* 2006). Also, xenografts from immature donors present greater responsiveness towards the recipient's gonadotropins (Rathi *et al.* 2008). Donor age also plays a role in germ cell loss following TTX (Sato *et al.* 2010; Campos-Junior *et al.* 2014). Germ cells typically undergo apoptosis immediately after grafting and this loss is not limited to mature donor tissue but also appears to be as great in fetal tissues since spermatogonia comprise a smaller population in the testis during prenatal period compared to that of neonates (Arregui *et al.* 2014). In addition, different patterns of gene expression between mature and immature testicular cells affect cell survival, somatic cell function, and proliferation *vs.* differentiation fate of germ cells (Honaramooz 2014). However, in some species, spermatogenic efficiency is greater when grafts are in more advanced developmental stages at the time of grafting. For instance, in some species such as bovine or feline, relatively enhanced spermatogenic efficiency has been reported in grafts from young donors compared to neonatal. This observation has been attributed to increased number of SSCs in grafts because of their proliferation prior to grafting (Oatley 2005; Kim *et al.* 2007).

Grafting or implantation are not always applicable immediately following collection of testis samples, for instance when the tissue is to be transferred to the laboratory where procedures for TTX or TCAI are feasible. As such, several studies have been conducted on viability and regeneration potential of grafted tissues or implanted cells after experiencing a period of cold treatment or cryopreservation (Abrishami *et al.* 2010; Honaramooz 2012). In fact, a period of cold storage or cryopreservation of tissues has been shown to reduce hypoxic damage by lowering tissue/cell metabolism and increase cell adaptability with new ectopic environment. This has been shown by advanced development of cold-treated or cryopreserved tissues grafted into recipients (Honaramooz *et al.* 2002; Shinohara 2002; Jahnukainen *et al.* 2007; Zeng *et al.* 2009; Abrishami *et al.* 2010; Campos-Junior *et al.* 2014).

Generally, mice are the species of choice when it comes to grafting studies, since they have been genetically manipulated and offer variety of options such as hairless and immunodeficient phenotypes (Geens *et al.* 2006; Hirenallur-Shanthappa *et al.* 2017). Ease of manipulation, accessibly to large areas of loose skin for grafting/implantation purposes, and cost-effective maintenance make mice a suitable choice for such studies. Since immunodeficient mice are unable

to develop immune response against the grafted tissues or implanted cells, they have been used frequently in TTX and TCAI studies. The two frequently used strains of mice in TTX and TCAI are SCID and nude (Honaramooz *et al.* 2002; Honaramooz *et al.* 2007; Abbasi and Honaramooz 2010; Arregui and Dobrinski 2014; Dores and Dobrinski 2014; Hirenallur-Shanthappa *et al.* 2017). Systematic studies point at superior support of SCID strain for graft development and its spermatogenic efficiency when compared to nude mice (Abbasi and Honaramooz 2010; Honaramooz 2014; Awang-Junaidi *et al.* 2020). Also, reduced degeneration of human testis grafts, greater spermatogenic output in porcine grafts, and greater morphogenesis potential in implants have been reported in SCID recipients (Schlatt *et al.* 2006; Abbasi and Honaramooz 2010).

Gonadal status of the recipients also determines the outcome of TTX/TCAI. Expectedly, castration of recipients reduces androgens, obliterates the endogenous feedback loop, and as such increases release of gonadotropins from the pituitary gland. This, in turn will initially lead to stimulation of the grafts and implants by the recipients' pituitary gonadotropins and enhances steroidogenesis in grafts/implants (Schlatt *et al.* 2002). Castration of recipients also leads to elimination of stimulatory effects of testosterone on vesicular glands, making the size of this gland a reliable indicator of androgenic competence of grafts/implants. Nevertheless, the overall effects of gonadal status on TTX/TCAI are also donor-dependent since intact male recipients sufficiently supported the development of grafts from pigs, rabbits, hamsters, cattle, and buffalo (Shinohara 2002; Huang *et al.* 2008; Abbasi and Honaramooz 2010; Schlatt *et al.* 2010a; Honaramooz 2014) but grafts from immature testis of horse and rhesus monkey experienced degeneration (Honaramooz *et al.* 2004; Rathi *et al.* 2006). Sex of the recipients also seems to have some effect on the outcome of TTX (Abbasi and Honaramooz 2010). Although even female recipient mice with intact ovaries could support neonatal porcine testis grafts to full spermatogenesis, similar grafts in male recipients were slightly larger in size and showed greater recovery with more developed seminiferous tubules (Abbasi and Honaramooz 2010). Age of recipients also appears to be an important factor for graft development, since Sertoli cell-only tubules were increased in hamster testis tissue grafts developed in young mouse recipients compared to those developed in more mature recipients (Ehmcke *et al.* 2008; Honaramooz 2014). Also, greater number of grafts per recipients (*i.e.*, 16 grafts per mouse) led to greater overall weight, spermatogenic efficiency, and androgen release compared to lower number of grafts in recipience (*i.e.*, 2 grafts per mouse). Effects of recipient factors discussed above can be donor-specific, meaning that the same TTX and TCAI outcomes

cannot necessarily be extrapolated when using different donor species. For instance, no significant effect of castration was observed on the status of grafts when dairy calves were used as donors (Huang *et al.* 2008). Conversely, in case of water buffalo donors, application of non-castrated recipients seemed to be crucial for development of the ectopic tissue grafts (Reddy *et al.* 2011).

Social interactions between male mice correlates with production of androgens in the body, which in turn can potentially affect the development of grafted tissues. However, the results of a study on group *vs.* individual housing of male nude mice showed that graft recovery rate, spermatogenic efficiency, as well as graft and vesicular gland weight were not affected when housing mice individually or together (Arregui *et al.* 2008). Finally, the life span of immunodeficient mice is ~1.5 years, which is shorter than the onset of spermatogenesis in many species such as rhesus monkeys. As such, TTX or TCAI are not always applicable to represent *in situ* testis development (Honaramooz *et al.* 2004; Sato *et al.* 2010). However, in some cases, the onset of sperm production in grafts can be possibly shortened by application of exogenous hormones, which warrants further investigation (Honaramooz *et al.* 2004; Rathi *et al.* 2008).

Majority of studies have been focused on the effects of multiple factors from donors or recipients on tissue graft survival and development, which cannot necessarily represent the same outcomes for the cell implants (Dores *et al.* 2012; Arregui and Dobrinski 2014; Honaramooz 2014). Therefore, establishment of a systematic study on both donors and recipients of implants or exogenous supplementation of growth factors or hormones to implants would greatly benefit prospective TCAI studies and their downstream applications.

2.4. In Vitro Models for the Study and Manipulation of Testis Cells

2.4.1. Identification, Isolation, and Enrichment of Gonocytes

Gonocytes are the dominant germ cells in the neonatal testis (Culty 2013). Depending on the species, these cells exist up to several days, months, or even years in the seminiferous tubules (Goel *et al.* 2007; Culty 2009, 2013). In neonatal rodents, gonocytes along with undifferentiated spermatogonia are present in the testis, while in neonatal pigs, gonocytes are the primary germ cells which transform into spermatogonia at ~2 months of age (Goel *et al.* 2007; Drumond *et al.* 2011). However, the exact time point for the transition from gonocytes to spermatogonia is not yet clear. It is speculated that this transition happens around 3-6 days after birth in mice, 5-8 days in

rats, and between 3 to 12 months after birth in humans (Roosen-Runge and Leik 1968; Bellve *et al.* 1977; Zogbi *et al.* 2012; Su *et al.* 2014). This variability in duration of gonocyte-to-spermatogonia transition is predominantly the result of differences in the the quiescent stage (Tiptanavattana *et al.* 2015). Gonocytes have unique characteristics such as unique morphology which makes them easily identifiable. In addition, these cells are the progenitors of SSCs which establish the foundation of spermatogenesis. The unique features of gonocytes make them an attractive tool with multiple downstream applications (Culty 2009). However, the scarcity of gonocytes in the testis (~2% and 7% of testis cells in neonatal rats and pigs, respectively) limits their applications (Orwig *et al.* 2002; Honaramooz *et al.* 2005). Thus, different methods have been developed and carried out for enrichment of gonocytes.

Gonocytes possess a unique morphology with a large nucleus and a ring-like cytosol. These cells appear as large round cells in the center of the seminiferous cords with prominent nucleoli and low complexity of cytoplasmic organelles (Orwig *et al.* 2002). After birth, these cells develop cytoplasmic extensions which help them migrate through the Sertoli cell cytoplasmic membrane towards the basal compartment (Culty 2009, 2013). Development of pseudopodia by gonocytes has also been shown when they are propagated *in vitro* (Awang-Junaidi *et al.* 2020). Gonocyte is a general term which encompasses M-, T1-, and T2-prospermatogonia depending on their developmental stage. These stages, however, are morphologically indistinguishable using light microscopy (Culty 2009; Tiptanavattana *et al.* 2015). This has been especially shown in rats where general morphological appearance of gonocytes from 16 dpc to 3 dpp were similar (Culty 2009). Once sitting on the basement membrane, gonocytes initiate their transformation into a new germ cell population with distinct morphology, known as spermatogonia. Unlike different subtypes of gonocytes, spermatogonia possess different morphologies depending on their developmental stage, including A_s, A_{pr}, A_{al}, A1-A4, intermediate, and B spermatogonia (Culty 2009; Phillips *et al.* 2010). In humans, on the other hand, only three stages of spermatogonia have been identified including A_{pale}, A_{dark}, and B spermatogonia based on the heterochromatic contents of the cells (Phillips *et al.* 2010). There are limited studies about different categories of gonocytes and their detailed morphological features, making it challenging to identify them based on their appearance (Culty 2009).

Neonatal gonocytes in mice are divided into three categories, namely I, II, and III based on slight morphological differences. All types show the same nuclear size and one to three nucleoli. From subtype I to III there is a gradual transition in shape from round to oval. Subtype I cells are usually located in the center of the cords, and show regular cytoplasmic membrane with no extensions, while the nucleoli of subtype II are less condensed with more reticulated morphology and irregular shape. Subtype II gonocytes are also located closer to the center of the cords but usually possess cytoplasmic extensions, indicative of their migratory ability. This subtype shows a peculiar structure resembling acrosomal vesicles proximal to the nuclear envelope. Nucleoli of type III are the least condensed and reticulated. The later subtype lacks the cytoplasmic extensions and are usually found on the basement membrane. Subtype III ultimately gives rise to type A spermatogonia, which in contrast to gonocytes have smaller nuclear diameter, are more oval, and possess more condensed nucleoli. More advanced stages of spermatogonia, on the other hand, demonstrate larger diameters, lighter staining, and increasing heterochromatin (Clermont and Perey 1957; Chiarini-Garcia and Russell 2001; Drumond *et al.* 2011). In mice, the number of gonocytes is reported to stay constant in the first 24 hours due to an established balance between their proliferation and apoptosis (Drumond *et al.* 2011). After that, gonocyte numbers sharply decreases by ~3 dpp in mice since a fraction of these cells undergo mitosis, while a considerable number go through degeneration (Roosen-Runge and Leik 1968; Kluin and de Rooij 1981). As gonocyte numbers decrease in seminiferous cords, the population of A spermatogonia increases up to 37 days after birth (Drumond *et al.* 2011).

Based on *in vitro* studies, rat gonocytes capable of developing pseudopodia are destined to migrate and differentiate while gonocytes which lack cytoplasmic extensions and are unable to migrate undergo apoptosis (Manku and Culty 2015). Development of pseudopodia has been also reported in a fraction of transplanted gonocytes and is believed to be crucial in their translocation towards the basal compartment, survival, and establishment of donor-derived spermatogenesis (Orwig *et al.* 2002). As such, gonocytes can alternatively be classified based on their ability to develop cytoplasmic extensions. Another classification method for gonocytes has been suggested based on their size, where they can be distinguished as very large cells (~12 µm or larger in diameter) and medium cells (10-12 µm in diameter), both being larger than somatic cells (Culty 2009; Manku and Culty 2015). Relative size of gonocytes compared to somatic cells is even more evident following digestion of testis parenchyma (Goel *et al.* 2007). Overall, gonocytes possess

identifiable morphological features, which provide valuable means to distinguish them; however, availability of cell-specific molecular markers which are exclusively expressed by gonocytes is still crucial for their efficient identification and isolation.

Since there has been no established marker that is exclusively expressed in gonocytes, these cells are usually identified using generic early germ cell markers (*e.g.*, VASA, DAZL) (Goel *et al.* 2007; Culty 2009). Gonocytes also express a number of makers which are associated with pluripotency such as NANOG and OCT4 (Ohbo *et al.* 2003; Goel *et al.* 2007; Culty 2009). Since these cells arise between the two intermediary stages of ES cells and adult MGSCs, they are expected to express stem cell-specific markers (Culty 2009). OCT4 is present in cells of the ICM and is known as a biomarker for ES cells. Using GFP under *Oct4* promoter, mouse germ cells were also positive for OCT4 and as such, it has been accepted as a marker for PGCs, gonocytes, and spermatogonia (Zhao and Garbers 2002; Ohbo *et al.* 2003; Ohmura *et al.* 2004). Another possible marker for gonocytes is c-KIT. The proto-oncogene c-kit was first introduced as a hematopoietic stem cell marker (Ashman *et al.* 1991). c-KIT was later shown to be present on the surface of PGCs, which acts as a regulator of PGC migration towards the genital ridges (Koshimizu *et al.* 1992). Co-expression of c-KIT and OCT4 was observed in PGCs during 11.5-13.5 dpc, while PGCs at 16.5 dpp were c-KIT^{-} and OCT4^{+} (Ohbo *et al.* 2003). Expression of c-kit becomes positive for differentiating spermatogonia, while it is absent in more primitive SSCs and is present in a limited number of gonocytes (Culty 2009, 2013). OCT4 expression correlates with stemness features of gonocytes since the majority of OCT4^{+} gonocytes show high levels of proliferative and repopulation activity (Ohmura *et al.* 2004). At ~7 dpp in mice, almost half of the gonocyte population also express GDNF receptors, indicative of different gonocyte sub-populations (Ohmura *et al.* 2008; Culty 2009). Thy-1 is another marker for identification of germline stem cells. This marker was initially found on hematopoietic, mesenchymal, and embryonic stem cells (Ling and Neben 1997; Izadpanah *et al.* 2006). Thy-1 is present on neonatal gonocytes, as well as a mixed population of spermatogonia (Culty 2009, 2013). Another stem cell pluripotency marker associated with identification of germline stem cells is NANOG. This marker is a homeodomain transcription factor originally explored while investigating the stem cell self-renewal (Chambers *et al.* 2003). NANOG is expressed by cells of pre-implantation embryos and post-implantation ES cells and regulates self-renewal while restricting transition into a differentiating stage (Chambers *et al.* 2003). The inhibition from differentiation is suggested to be regulated by NANOG together

with OCT4 (Yoshida *et al.* 1994). NANOG expression diminishes after birth, with only 1% of gonocytes being positive at ~16.5 dpc and almost no positive cells in adult mouse testis (Kerr *et al.* 2008). In humans, NANOG expression is present until 20 weeks of gestation, is retained only in a small group of gonocytes until 3 months after birth and is absent in childhood and adult testes (Hoei-Hansen *et al.* 2005; Rajpert-De Meyts 2006; Culty 2009). Another set of markers for gonocyte identification includes ZBTB16 (PLZF) and SALL4 (Culty 2009; Ibtisham and Honaramooz 2020). PLZF is involved in the proliferation of gonocytes and its knock-out leads to failure in establishing the SSC pool (Costoya *et al.* 2004). Also, members of *Sall* gene family, such as *Sall4* are highly conserved among species and play key roles both in formation of germ cell pool and axis development in the embryo. SALL4 directly interacts with PLZF in regulating mitotic divisions of germ cells (Gassei and Orwig 2013). Gonocytes also show alkaline phosphatase activity, express surface molecules such as CD9 and ubiquitin carboxyl-terminal hydrolase-L1 (UCH-L1; also known as PGP9.5) (Kubota *et al.* 2003; Kanatsu-Shinohara *et al.* 2004b; Luo *et al.* 2006; Goel *et al.* 2007; Kim *et al.* 2013; Zheng *et al.* 2014). Although not a transcription factor, *Dolichos biflorus* agglutinin (DBA) is an alternative surface marker for gonocytes which has a high affinity for N-acetyl galactosamine of the cytoplasmic membrane, and as such can be used with high specificity to identify gonocytes (Goel *et al.* 2007; Yang *et al.* 2010). Overall, expression of surface markers in gonocytes is highly dependent on their developmental stage and displays different patterns with varying combinations at each stage (Goel *et al.* 2007; Culty 2009, 2013).

Dissociation of testis cells from parenchyma is the first step to obtain a mixed cell population, including germ cells, for downstream applications including *in vitro* propagation, GCT, or even TCAI (Khaira *et al.* 2005; Dobrinski and Travis 2007; de Rooij and Mizrak 2008; Oatley and Brinster 2008). Since the population of gonocytes diminishes over time from prepubertal to pubertal period, testis from neonatal donors is expectedly a superior source to obtain greater gonocyte proportion. As mentioned above, duration of gonocyte-to-spermatogonia transition is species-specific, which in rodents takes about a few days, leaving a small window during which these cells can be efficiently isolated after birth. Different strategies have been developed so far to obtain a single cell suspension from testis, yielding various proportions of germ cells (Goel *et al.* 2007; Culty 2009; Yang *et al.* 2010). Predictably, one of the major drawbacks in cell isolation is the efficiency of cell recovery, meaning that the cell viability diminishes as they experience

multiple steps of cell extraction from the parenchyma. The initial strategies for isolation of MGSCs from testis were consisted of two-step enzymatic digestions, where the parenchyma was first physically dissociated and the resultant fragments were exposed to an enzymatic solution, usually consisting of trypsin combined with other enzymes (*e.g*., DNase). However, conventional approaches of cell isolation were inefficient, yielding very limited percentages of gonocytes (~5-10%) (van Dissel-Emiliani *et al.* 1989; Orth and Bohem 1990; Li *et al.* 1997a; Honaramooz *et al.* 2002; Orwig *et al.* 2002; Honaramooz *et al.* 2003). To overcome this limitation, a three-step enzymatic digestion method was developed, resulting in noticeably improved cell recovery and gonocyte yield (~40% gonocytes). The later method was composed of a brief physical dissociation step by mincing and vortexing the parenchyma, followed by enzymatic treatment of the resultant suspension with a cocktail of digestive enzymes composed of hyaluronidase, DNases, and collagenase with final exposure of the cell isolates to an erythrolysis solution. Although intact porcine testis tissue prior to digestion contains ~7% gonocytes, this percentage reached ~40% with >90% viability following application of the latter method for germ cell isolation (Honaramooz *et al.* 2005; Yang *et al.* 2010).

Since gonocytes are a rare germ cell population in the neonatal testis, additional enrichment strategies have been developed to increase their numbers prior to their downstream applications. This is mainly because such applications (*e.g*., GCT, *in vitro* propagation, or transgenesis) will expectedly improve when the cell isolates contain a high proportion of germ cells (Goel *et al.* 2007; Yang *et al.* 2010; Honaramooz and Yang 2011). One of the main techniques for enrichment of germ cells is based on utilization of fluorophore-labelled antibodies. Fluorescent activated cell sorting (FACS) (Moudgal *et al.* 1997; Shinohara *et al.* 2000; Lo *et al.* 2005; Herrid *et al.* 2009), magnetic activated cell sorting, (MACS) (Kubota *et al.* 2004a; Buageaw *et al.* 2005; Herrid *et al.* 2009), density gradient centrifugation (Izadyar *et al.* 2002; Luo *et al.* 2006; Herrid *et al.* 2009), or differential plating (Izadyar *et al.* 2002; Luo *et al.* 2006; Herrid *et al.* 2009; Honaramooz and Yang 2011) can lead to enrichment of SSCs up to ~75% in testis cell isolates of farm animals. For gonocyte enrichment, a number of strategies have been applied in rodents and pigs, leading to improved gonocyte percentage up to ~70-90% in rats (van Dissel-Emiliani *et al.* 1989; van Den Ham *et al.* 1997; Moore *et al.* 2002) and 70% in pigs (Goel *et al.* 2007). A study in our lab showed that porcine gonocytes can be enriched up to ~80% by application of Nycodenz density gradient

or differential poly-D-lysine coated plating and even up to ~90% if the two methods are combined (Yang *et al.* 2010; Honaramooz and Yang 2011).

2.4.2. Maintenance and Propagation of Germline Stem Cells in Culture Systems

The first few reports of successful development of a culture system for germ cells in rodents attracted many researchers to explore germ cell biology and underlying factors involved in their proliferation and differentiation (Sahare *et al.* 2018). Culture of MGSCs can be used to increase their numbers from limited sources including biopsies to achieve larger cell populations for downstream applications. These applications can include GCT aimed at preserving fertility, understanding the biology of MGSCs, or producing transgenic animals with enhanced productivity traits through genetic manipulation of germ cells prior to GCT. Germ cell culture is also a valuable tool in investigating the factors involved in their proliferation and differentiation, especially given that *in situ* study of MGSCs is difficult or not feasible. Cultured MGSCs may also serve as pluripotent stem cells given that limited available studies have demonstrated MGSCs ability to spontaneously transform into pluripotent/multipotent stem cells *in vitro* (Jiang and Short 1998a; Jiang 2001; Bai *et al.* 2018). Therefore, *in vitro* propagated MGSCs offer a promising alternative source of stem cells for regenerative therapy since the application of induced pluripotent stem (iPS) cells and ES cells usually entails safety or ethical concerns (Seandel *et al.* 2007; Zheng *et al.* 2013).

Elucidating the essential factors in maintenance and proliferation of germ cells in the testis is key in their successful expansion *in vitro*. For instance, GDNF was one of the initial cytokines shown to be crucial for self-renewal as well as differentiation of mouse MGSCs (Meng *et al.* 2000b). GDNF exerts its effects through a multicomponent receptor complex composed of GFRα-1 and RET tyrosine kinases in many cell types (Jing *et al.* 1996). These two components of the receptor complex have been recognized as markers for MGSCs (Widenfalk *et al.* 2000). Given the important role of GDNF in proliferation of germ cells, short-term culture systems were developed with GDNF supplementation to improve germ cell survival, while retaining their ability to colonize the recipients' seminiferous tubules following GCT (Nagano *et al.* 2003; Kanatsu-Shinohara 2005; Naughton *et al.* 2006). However, a similar response cannot be expected from germ cells of different sources following growth factor supplementation since it has been shown that growth factor requirements for MGSC propagation largely depend on the mouse strains and the same concept

can be possibly applied to germ cells of different species (Kubota *et al.* 2004a). This in turn may suggest that MGSCs in the testis of different species require a species- or strain-specific growth factor combinations with different concentrations. To date, species-specific growth factor requirements for *in vitro* propagation of germ cells have been studied in rats (Ryu *et al.* 2005; Hamra *et al.* 2005), hamsters (Kanatsu-Shinohara *et al.* 2008), and rabbits (Kubota *et al.* 2011). Several growth factors have been suggested to play important roles in self-renewal regulation of germ cells. These include PDGF, leukemia inhibitory factor (LIF), SCF, basic fibroblast growth factor (bFGF) (also known as FGF-2), FGF-9, and RA (Tu *et al.*; Jaillard *et al.* 1987; Wang and Culty 2007; Mirzapour *et al.* 2012; Sahare *et al.* 2016, 2018).

Unlike many other cell types, MGSCs in culture are normally non-adherent, requiring a supportive feeder layer for survival. Therefore, MGSCs have been co-cultured with endogenous somatic cells of the testis, which gradually form an attached flat monolayer at the bottom of the culture dish (Orth and Rosemarie 1990; McGuinness and Orth 1992; van Dissel-Emiliani *et al.* 1993; Awang-Junaidi and Honaramooz 2018; Awang-Junaidi *et al.* 2020). Survival of gonocytes depends on their ability to establish connections with the monolayer while floating gonocytes undergo apoptosis and are removed with media (van Dissel-Emiliani *et al.* 1993). The somatic cell monolayer is also involved in regulation of germ cell metabolism and self-renewal *vs.* differentiation by producing cytokines and molecular signals. It is speculated that these molecular cues from Sertoli cells especially direct cultured germ cells towards differentiation pathways (Griswold *et al.* 1989). Other types of feeder layers used for culture of MGSCs include mitotically-inactivated cells including SIM mouse embryo-derived thioguanine and ouabain resistant fibroblast cell lines (STO) as well as mouse embryonic fibroblast cell lines (MEF) (van Dissel-Emiliani *et al.* 1993; Nagano *et al.* 1998; Hasthorpe *et al.* 1999; Kubota *et al.* 2004a; Han *et al.* 2009; Wu *et al.* 2009; Nasiri *et al.* 2012). Notably, STO has been the most supportive feeder layer for the culture of spermatogonia of various species such as rodents, livestock, and humans. Although required, application of a feeder layer is usually associated with reduced proliferative activity of germ cells and may introduce a confounding factor due to variation in its source, batches, and treatments applied during its development. Cellular biproducts in the feeder layer also potentially exert negative effects on germ cells. Therefore, co-culture of germ cells with endogenous Sertoli cells can be advantageous as they provide a relatively similar microenvironment as *in situ* conditions (He *et al.* 2015).

MGSC culture has also been experimented using livestock donors, including pigs, leading to mainly successful establishment of short-term cultures (Goel *et al.* 2007; Sahare *et al.* 2018; Ibtisham and Honaramooz 2020; Ibtisham *et al.* 2020). In such studies, a range of media (*e.g*., DMEM, DMEM/F12, MEM, and StemPro) has been used with DMEM being the most prevalent medium (van Dissel-Emiliani *et al.* 1993; Goel *et al.* 2007; Awang-Junaidi and Honaramooz 2018). Typically, culture media is supplemented with serum substitutes containing a pool of growth factors, cytokines, and hormones. Unknown serum contents might not necessarily benefit germ cell survival (Kubota *et al.* 2004b; Zheng *et al.* 2013; Sahare *et al.* 2016, 2018; Suyatno *et al.* 2018). For instance, fetal bovine serum (FBS) supplemented at 5% has been shown to maintain porcine gonocytes up to 9 days (Marret and Durand 2000), while its deleterious effects were observed when supplemented at 2-8% (van Dissel-Emiliani *et al.* 1993). Also, increased FBS concentrations led to reduced colony formation of porcine gonocytes (Zheng *et al.* 2013). Synthetic serum replacements, such as KSR, have been developed as alternatives to FBS and are used extensively in cell culture research (Kanatsu-Shinohara *et al.* 2011, 2014; Sadri-Ardekani *et al.* 2011; Sahare *et al.* 2018). Serum replacements have more consistent components and defined formulation, and were developed primarily to culture undifferentiated stem cells such as ES cells (Hua *et al.* 2009). SSCs from rats and mice have also been cultured using media supplemented with serum replacement (Kubota *et al.* 2004a; Ryu *et al.* 2005). However, there is no established protocol or culture media formulation for long-term maintenance and propagation of MGSCs from large animal species including pigs, which can provide a practical and suitable model for human germ cells (Kim *et al.* 2014; Sahare *et al.* 2016). Particularly, a systematic study on long-term culture requirements for porcine MGSCs is of great importance since, as shown in rodents, cultured MGSCs can potentially offer an alternative source for undifferentiated pluripotent stem cells for numerous downstream applications and will provide a stronger proof-of-concept for similar potential in human MGSCs.

2.4.3. In Vitro Generation of Pluripotent Cells from Male Germline Stem Cells

Pluripotent stem cells can undergo self-renewal and differentiation into specialized cell types from three germinal layers (*i.e*., ectoderm, mesoderm, and endoderm) (Wobus and Boheler 2005). Mainly, there are two types of pluripotent stem cells: ES cells and iPS cells. ES cells are derived from ICM of the preimplantation embryos and can undergo indefinite divisions while maintaining

their pluripotent state *in vitro* (Evans and Kaufman 1981; Thomson *et al.* 1998). Pluripotent stem cells can be also generated by inducing dedifferentiation of adult somatic cells through insertion of pluripotency transcription factors into the somatic cell genome which directs them through 'reprogramming' pathways into more primitive developmental stages (Takahashi and Yamanaka 2006; Takahashi *et al.* 2007). Similar to ES cells, iPS cells can self-renew indefinitely and have the potential to give rise to derivatives of three germinal layers (Romito and Cobellis 2016). These cells are produced by suppression of somatic cell gene program and increased expression of pluripotency-associated transcription factors. Given that pluripotent stem cells, including ES and iPS cells, can differentiate into all specialized cell types, they are considered as promising sources for cell-based therapies (Romito and Cobellis 2016). So far, preclinical cell therapy experiments in animal models have shown beneficial effects of pluripotent stem cells, such as restoration of locomotion following spinal cord injuries (Kriks *et al.* 2011), improved vision in blindness models using ES cell derived retinal pigment epithelium (Lund *et al.* 2006), and treatment of cardiac ischemia in a porcine model using iPS cell-derived cardiomyocytes (Kawamura *et al.* 2012). However, application of iPS cells and ES cells usually entails ethical issues regarding manipulation of embryos to obtain ES cells, biosafety risks associated with gene delivery into the somatic cells, and/or tumorigenicity. As such, more extensive research is required to find alternative sources for pluripotent stem cells, which can be utilized safely and efficiently (Golestaneh *et al.* 2009; Chen *et al.* 2020).

So far, several reports have shown derivation of ES-like cells from cultured germline stem cells (Kim and Belmonte 2011). Mouse MGSCs were first documented to obtain characteristics of ES cells *in vitro*. MGSCs of mice showed very similar morphological features and gene expression pattern as mouse ES cells, developed into all three germinal layers *in vitro*, formed teratoma upon implantation into nude mice, and contributed to formation of chimera. Interestingly, dedifferentiation process of MGSCs was carried out without addition of reprogramming factors, or introduction of pluripotency transcription factor to the germline stem cells (Kanatsu-Shinohara *et al.* 2004). Pluripotent germline stem cells were also produced from adult mice with various genetic backgrounds (Guan *et al.* 2006; Seandel *et al.* 2007). Further work resulted in introduction of multipotent human germline stem cells by utilizing ES cell culture conditions (Sadri-Ardekani 2009). Later, it was shown that acquisition of pluripotency by MGSCs is age-dependent meaning that this potential gradually decreases when mice reach more advanced developmental stages

(Guan *et al.* 2006; Seandel *et al.* 2007; Azizi *et al.* 2016). The overall mechanism of germ cell conversion into more primitive stages *in vitro* is not yet clearly understood, but it is proposed that testis microenvironment restricts the MGSC potential to both express pluripotency gene transcripts (*e.g.*, *Oct4*, *Nanog*, and *c-Myc*), and produce somatic cell derivatives. Conversely, *in vitro* environment lacks the *in situ* factors and as such, induces pluripotency by modulating the MGSC gene expression, and triggers the fate conversion under *in vitro* conditions (Kanatsu-Shinohara *et al.* 2004; Seandel *et al.* 2007). In addition to rodents, germline-derived ES-like cells were produced using human, porcine, bovine, and caprine MGSCs *in vitro* (Goel *et al.* 2007; Fagoonee *et al.* 2011; Awang-Junaidi *et al.* 2020; Kumar *et al.* 2021). Taken together, this conversion potential in MGSCs is especially important for production of multipotent germline stem cells from autologous sources with possible applications in fertility restoration and tissue regeneration, without associated risks of immunorejection and tumorigenicity as well as biosafety concerns (Struijk *et al.* 2013; Sahare *et al.* 2018).

2.4.4. In Vitro Trans-Differentiation of Male Germline Stem Cells

Several studies have been conducted so far to optimize the conversion of MGSCs to ES-like cells following the initial reports using a mouse model (Kanatsu-Shinohara *et al.* 2004; Chen *et al.* 2020). Studies on dedifferentiation of MGSCs were all suggestive of their unique potential in different species to spontaneously transform into a pluripotent state in culture conditions without addition of exogenous transcription factors or enforcing genetic manipulation (Golestaneh *et al.* 2009; Azizi *et al.* 2016, 2019; Sahare *et al.* 2018; Chen *et al.* 2020). Given that MGSCs display the morphological and biomolecular features of ES cells in culture conditions, they were subsequently directed to differentiate into different somatic cell lineages (Kanatsu-Shinohara *et al.* 2004; Azizi *et al.* 2016, 2017; Conrad *et al.* 2016). So far, pluripotent MGSCs have been differentiated into somatic cells of neuronal origin, cardiomyocytes, gastrointestinal cells, adipocytes, hepatocytes, and striated myofibroblasts in different species (Guan *et al.* 2006; Glaser *et al.* 2008; Streckfuss-Bömeke *et al.* 2009; Li *et al.* 2010; Cheng *et al.* 2012; Zhang *et al.* 2013; Luan *et al.* 2014; Wang *et al.* 2015; Kim *et al.* 2015; Chen *et al.* 2016; Javanmardy *et al.* 2016; Liu *et al.* 2016; Yang *et al.* 2017). The unique differentiation features of MGSCs are attributed to their intrinsic and extrinsic factors which collectively have made them an attractive potential source of pluripotent stem cells (Chinta *et al.* 2007). MGSCs also have the advantage of rapid

proliferation and higher adaptability to the extrinsic environment (Kubota *et al.* 2004b, 2011; Yang *et al.* 2015).

Since MGSCs have more similarity to ES cells than stem cells of other somatic tissues, recently, it was suggested that they can directly trans-differentiate when recombined with fetal or neonatal mesenchyme from various organs. This idea was experimented using an *in vivo* grafting approach in a mouse model where the mesenchyme acted as an instructive inducer, leading to direct differentiation of murine germ cells into tissues of all germ layers including prostatic, uterine, and skin epithelium (Simon *et al.* 2009, 2010). Similarly, a recent study showed trans-differentiation of human germline stem cells into hepatocytes by extracting liver mesenchymal cells, recombining them with germ cells, and grafting them under the renal capsule of nude mice (Chen *et al.* 2017). However, this approach has its own challenges, including isolation of tissue-specific mesenchymal cells, recombining them with germ cells, and *in vivo* grafting. Expectedly, even slight changes at genetic or epigenetic levels to the resultant stem cells following multiple steps of this approach as well as exposure of MGSCs to exogenous mesenchyme, and *in vivo* culture conditions can limit their applications.

Although MGSCs can potentially serve as a stem cell source, generation of germ cell-derived pluripotent stem cells *in vitro* is still challenging and complicated since based on established protocols, it requires multiple passaging, addition of multiple proteins, growth factors/cytokines, and/or co-culturing with exogenous feeder layers. These can introduce unwanted changes in their gene regulation or generate unknown epigenetic changes and as such limit their downstream applications (Golestaneh *et al.* 2009; Chen *et al.* 2020). Therefore, developing alternative simple strategies for derivation of pluripotent germline stem cells and straight-forward trans-differentiation approaches, which eliminate any possible exogenous confounding factors or concerns regarding their use will be of great value. Overall, compared to other stem cell types, the potential application of MGSCs in clinical settings can bypass immunorejection, safety and ethical concerns and as such, they are a promising source of stem cells for regenerative medicine and cell-based therapy.

2.4.5. In Vitro Spermatogenesis

In vitro spermatogenesis (IVS) is the process of producing haploid germ cells from spermatogonia in a controlled *ex situ* environment (Dissanayake 2018). *In vitro* models make it possible to better

understand the complex biological interactions between testicular cells, cellular interactions, epigenetic processes, gene regulation, genetic disorders, or pathological conditions in the testis, as well as the effects of exogenous factors on spermatogenesis. These models can include culturing testis organ/tissue or cells either using two dimensional (2-D) or three dimensional (3-D) systems (Izadyar *et al.* 2003; Ibtisham and Honaramooz 2020). Using germ cells from infertile donors in this system can for instance help the investigations on the causes of infertility and as such, paves the way for experimentations that are not otherwise feasible to be conducted *in vivo* including genetic manipulation of germ cells to resolve potential causes of infertility. In addition to advantages of *in vitro* spermatogenesis models in clinical fields, their use is also consistent with ethical principles since multiple replications can be prepared and studied at a time from a limited testis sample and/or testicular samples from animals can potentially represent human models (Stukenborg *et al.* 2009).

The first successful *in vitro* differentiation of male germ cells was reported in 1920 (Champy 1920; Song and Wilkinson 2012). Over time, progress has been made to develop a more consistent and efficient microenvironment with close resemblance to that of *in situ* testis conditions. Major components of the *in vitro* environment, which predictably affect the fate of germ cells and their survival, proliferation, and differentiation include culture media composition and serum additives. FBS has been one of the widely used media supplements which stimulates germ cells to enter differentiation. Serum alternatives such as KSR have been associated with more inconsistencies in the results and controversial outcomes; this includes improvement of germ cell differentiation in some studies (Sato *et al.* 2011; Riboldi *et al.* 2012), while preventing germ cells from undergoing specialization in others (Hogg and Western 2015). Direct application of hormones and growth factors has also been experimented with the aim of improving the efficiency of IVS. For instance, supplementation of the culture media with testosterone and FSH together or individually enhanced differentiation of germ cells. Similarly, RA has been shown to trigger differentiation of murine germ cells and induce initial steps of spermatogenesis (Wang *et al.* 2016).

Given the importance of the testicular architecture in germ cell survival and progression of germ cell proliferation and differentiation, organ/tissue culture is deemed as a feasible approach to achieve IVS. The 3-D architecture is retained in testis tissue fragments, offering an endogenous scaffold for the cells to develop, mature, and interact with each other in a relatively more hospitable

environment (Roulet *et al.* 2006; Edmonds and Woodruff 2020; Ibtisham and Honaramooz 2020). One of the major challenges in organ/tissue culture is the limited diffusion of media through the cultured tissues, leading to reduced tissue viability compared to other culture methods. Organ/tissue culture was established by introduction of a gas-liquid interface system, where testis tissue fragments were in contact with the culture media at a constant temperature and CO_2 concentration (Trowell 1959). Over time, this system was improved by adjusting the temperature and pH as well as addition of different supplements including vitamins, hormones, sera, and tissue extracts (Trowell 1959). A study in 2011 showed that utilization of agarose gel in minimum essential medium (α-MEM) supplemented with KSR for culture of mouse testis fragments can lead to successful production of fertilization-competent sperm (Sato *et al.* 2011). Subsequent modifications to this system such as application of microfluidic technology allowed consistent supply of nutrients and removal of metabolites which resulted in increased length of tissue viability up to ~6 months (Komeya *et al.* 2016).

Another approach used for *in vitro* differentiation of spermatogonia into haploid germ cells is 2-D culture systems, in which a cell suspension of enzymatically-dissociated testis cells is prepared from testis parenchyma and propagated in culture wells. This approach is especially advantageous when the aim is to expand germ cells for applications in auto-transplantation following cytoablative cancer treatments as well as in investigation of cell-specific roles or underlying genetic factors in proliferation or differentiation of germ cells (Zhang *et al.* 2017; Dissanayake 2018; Kapałczyńska *et al.* 2018). However, since this system does not provide the 3-D structural architecture, it does not replicate the *in situ* spatial properties of the seminiferous tubules. A 2-D culture system also makes morphological identification of cell types cumbersome, where identification of various cell types would only be feasible via application of molecular markers or cell sorting techniques (Jiang and Short 1998a; Jiang 2001; Bai *et al.* 2018; Kapałczyńska *et al.* 2018). This system has also been improved over time to provide a platform for IVS. The first offspring resulting from mouse haploid germ cells developed in 2-D spermatogonia culture systems were produced in 2003 (Marh *et al.* 2003). Overall, this system can also provide the basis for IVS, where the continuous interactions between germ cells and somatic cells in 2-D culture systems appear to play a substantial role in survival and progression of spermatogenesis (van Dissel-Emiliani *et al.* 1993; Awang-Junaidi and Honaramooz 2018; Awang-Junaidi *et al.* 2020).

3-D culture of testis cell aggregates is another approach for *in vitro* study of testicular cell interactions and testis organogenesis. Artificially constructed 3-D testis cell aggregates were first cultured in 2006 using 18-day old rat testis cells (Lee *et al.* 2006). Testis cell aggregates were placed on collagen gel matrices to represent the basement membrane. This 3-D culture system supported survival of the germ cells and even resulted in their differentiation. This system was further improved by application of a soft agar, which consisted of a gel phase containing spermatogonia and a solid phase comprised of somatic cells. Using this system differentiated germ cells from rhesus monkeys have been produced (Stukenborg *et al.* 2008; Huleihel *et al.* 2015). Later, a 3-D model was described using a three-layer gradient system which allowed reorganization of testicular cells obtained from 20-day old rats. Cells in organoids were consisted of germ- and somatic cells along with the first report of establishment of blood-testis barrier (Alves-Lopes *et al.* 2017; Sakib *et al.* 2019).

2.5. Growth Factors and Testis Development

2.5.1. Basic Fibroblast Growth Factor

Normal development of the testis results from complex processes of coordinated cell divisions, migrations, and spatial cellular arrangements. It is well established that these processes mainly rely on secretion of gonadotropins (*i.e*., LH and FSH) and androgens (*i.e*., testosterone) (Gnessi *et al.* 1997; Mackay and Smith 2007). Together with endocrine regulators, an intercellular network of transcription factors or highly regionalized paracrine secretions are involved in testis development and initiation and/or maintenance of steroidogenesis and spermatogenesis. Both endocrine and paracrine pathways mediate the testis physiology through growth factors, cytokines, and cell-cell contacts (Basciani *et al.* 2010). Numerous paracrine factors are likely to regulate cellular interactions and spermatogenesis within the testis. Among intrinsic paracrine regulators, GDNF, LIF, and FGF family have been shown to play key roles in the function and development of the testes (Tu *et al.*; Jaillard *et al.* 1987; Wang and Culty 2007; Mirzapour *et al.* 2012; Sahare *et al.* 2016, 2018) (Fig. 2.2).

The FGF family is known for their important function in tissue patterning and organogenesis (Angelin *et al.* 2012). Members of this growth factor family trigger proliferation of mesenchymal cells, migration of mesonephric cells into the testis, and formation of the interstitial compartment (Colvin *et al.* 2001; Jiang *et al.* 2013). FGF-2, also known as bFGF or FGF-β, is a canonical

member of the FGF family with multiple roles such as tissue development and repair, exerted by binding to FGF receptor 1, 2, or 3 (Ornitz and Itoh 2015). This growth factor was first isolated and characterized in bovine testes, and thereafter its expression was reported in the testes of different species (Ueno *et al.* 1987; El Ramy *et al.* 2005). FGF-2 is produced by many cell types in the testis including Sertoli cells, Leydig cells, and germ cells (Mullaney and Skinner 1992; Han *et al.* 1993). Expression of FGF-2 becomes downregulated in an age-dependent manner by Sertoli cells; however, it is deemed as a bona-fide self-renewal factor for spermatogonia (Shubhada *et al.* 1993; van Dissel-emiliani *et al.* 1996; Skinner 2005; Masaki *et al.* 2018) and has been shown to be expressed especially by A spermatogonia, pachytene spermatocytes, and spermatids (Abo-Elmaksoud and Sinowatz 2005; Jiang *et al.* 2013). Rat fetal and neonatal gonocytes co-cultured with Sertoli cells significantly increased in numbers following addition of FGF-2, while supplementation of FGF-2 neutralizing antibodies in the culture significantly decreased their numbers, indicating that FGF-2 is both a survival and mitogenic factor for gonocytes (van Dissel-emiliani *et al.* 1996). Addition of GDNF together with FGF-2 to the culture media has been shown to induce spermatogonia to increase exponentially for 2 years (Kanatsu-Shinohara 2005). Spermatogonia proliferate and survive in cultures with FGF-2 but under GDNF-free conditions and can restore fertility following GCT (Takashima *et al.* 2015; Masaki *et al.* 2018). Cultured germ cell populations exposed to FGF-2 show characteristics of more differentiated cells by expressing KIT and low SSC activity, indicative of bFGF roles in regulation of undifferentiated spermatogonia (Masaki *et al.* 2018).

The main production site of FGF-2 in the testis has remained controversial. Some reports indicated its expression by Sertoli cells (Smith *et al.* 1989; Tadokoro *et al.* 2002), whereas others showed FGF-2 release by germ cells (Han *et al.* 1993; Zhang *et al.* 2012). However, more recent work has shown that Sertoli cells may not be the only source of FGF-2 in the testis (Garcia *et al.* 2014; Masaki *et al.* 2018). Depletion of endogenous germ cells by busulfan has been associated with *fgf-2* attenuation which raised the concept that germ cells, the niche under regulation of germ cells, and/or the niche independent from the germ cells produce FGF-2 (Masaki *et al.* 2018). FGF-2 triggers germ cell divisions in the seminiferous tubules and permits RA-mediated differentiation through enhancing the expression of RA receptor (RAR) on germ cells. FGF-2 also acts on the niche to facilitate the actions of RA (Masaki *et al.* 2018). It is speculated that the niche undergoes cyclic changes of FGF-2 dominant and GDNF-dominant states. Although both GDNF and FGF-2

promote germ cell self-renewal, GDNF overexpression, which likely happens during GDNF-dominant state inhibits germ cell differentiation, while FGF-2-release allows generation of spermatogonia population with greater tendency towards differentiation (Nagano *et al.* 1999; Nagai *et al.* 2012).

The effects of FGF-2 on somatic cells of the testis have also been investigated in a number of studies (Jiang *et al.* 2013). FGF-2 significantly increased the number of Sertoli cells isolated from the fetal and newborn rats *in vitro* (van Dissel-emiliani *et al.* 1996). Fetal and mature Leydig cells have also been shown to appear positive for FGF-2 expression (Gonzalez *et al.* 1990; Han *et al.* 1993) (Fig. 2.2). This growth factor also increased the steroidogenic function of cultured Leydig cells following induction by human chorionic gonadotropin (hCG) (Sordoillet *et al.* 1992). FGF-2 has also been reported as a morphogen for formation of testis cords since it promoted cord-like structures in cultures of rat embryonic testis cells (El Ramy *et al.* 2005).

2.5.2. Glial Cell-derived Neurotrophic Factor

GDNF is a member of the transforming growth factor-beta (TGF-β) superfamily and was first extracted from rat glioma cell-line cultures (Kakiuchi *et al.* 2018). This growth factor promotes the survival of dopaminergic neurons and has been shown to influence other neuronal subpopulations (Airaksinen and Saarma 2002). Although GDNF expression is mainly reported in the central nervous system, it is also widely produced in various non-neuronal tissues such as kidney, gastrointestinal tract, and testis (Golden *et al.* 1999). GDNF plays an important role in the survival of spermatogonia since heterozygous GDNF-deficient mice show reduced germ cell proliferation, impaired spermatogenesis, and eventually Sertoli cell-only phenotype. In contrast, overexpression of GDNF has been associated with abnormal accumulation of spermatogonia, which is attributed to a block in germ cell differentiation (Meng *et al.* 2000a) as well as promotion of seminomatous tumors (Meng *et al.* 2001). Production of GDNF by Sertoli cells is regulated by FSH. This growth factor is necessary for self-renewal and inhibition of apoptosis in germ cells in a dose-dependent manner (Meng *et al.* 2000a; Bojnordi *et al.* 2014). GDNF exerts its proliferative stimulatory effects on germ cells following attachment to GFRα-1 through phosphoinositide-3 kinase (PI3K)/AKT pathway (Lee *et al.* 2007). GFRα-1 is the ligand-binding domain of GDNF and has been detected on spermatogonia (Kakiuchi *et al.* 2018) (Fig. 2.2). Crucial effects of GDNF for SSC survival and division have been shown via continuous proliferation of murine SSCs in a

serum-free culture conditions, while maintaining their potential to colonize the seminiferous tubules, and establish donor-derived spermatogenesis (Kubota *et al.* 2004b). Further work has also shown colonization potential of rabbit germ cells cultured in serum-free conditions supplemented with GDNF and as such, confirmed the critical role of GDNF in unlimited proliferation of undifferentiated spermatogonia (Kubota *et al.* 2011). Disruption of GDNF signaling by ETS variant gene 5 (*Etv5*)-knock out resulted in germ cell loss, confirming the critical role of GDNF in survival of SSCs (Simon *et al.* 2010). Similar to many species, GDNF expression in mice is cyclic since it increases during SSC proliferation and decreases during the stages where spermatogonia are quiescent and undergo differentiation (Meng *et al.* 2000a; Johnston *et al.* 2011; Sato *et al.* 2011; Grasso *et al.* 2012; Sharma and Braun 2018). GDNF also stimulates germ cell expansion *in vitro* and mouse spermatogonia survive in a long-term culture on MEF when supplemented with GDNF, EGF, LIF, and FGF-2 (Kanatsu-Shinohara *et al.* 2003). As a result, GDNF has been used as one of the major culture components for SSC culture (Kanatsu-Shinohara *et al.* 2004; Kubota *et al.* 2004a; Ogawa *et al.* 2004; Ryu *et al.* 2005).

GDNF also triggers migration of MGSCs. Formation of GDNF-receptor complex has been shown to induce the assembly of cytoskeleton in germ cells and stimulates germ cell migration *in vitro* (Dovere *et al.* 2013). Additionally, GDNF is not involved in proliferation of seminoma cell lines, but predominantly acts as an important regulator for induction of directional cell migration and promotes the invasive cell translocation *in vitro* (Ferranti *et al.* 2012; Dovere *et al.* 2013). Activation of ETV5 via GDNF also upregulates the expression of CXCR4 which in turn is required for migration of PGCs to the developing gonads as well as translocation of germ cells from the center to the basolateral compartment of the seminiferous cords in neonatal testes (Niu *et al.* 2016). GDNF also has stimulatory effects on Sertoli cell proliferation during testis development (Wu *et al.* 2005). Overall, GDNF is an essential transcription factors for normal development of spermatogonia as well as continuation of germ cell proliferation and establishment of spermatogenesis (Ara *et al.* 2003; Kanatsu-Shinohara *et al.* 2012; Kanatsu-Shinohara and Shinohara 2013).

2.5.3. Leukemia Inhibitory Factor

LIF is a multifunctional member of interleukin-6 (IL-6) family of cytokines which, once released, communicates with a receptor complex consisting of LIF receptor β and gp130 (Nicola and Babon

2015). LIF has been shown to be structurally and functionally related to IL-6, oncostatin M, and ciliary neurotrophic factor, which can all bind to specific cell surface receptors in different cell types and trigger tyrosine phosphorylation of gp130, Janus kinase 1 (JAK1), JAK2, and TYK2 kinases. This will in turn activate signal transducers and activators of transcription (STAT)-3/STAT-1 pathway, thereby induces transcriptional regulation of different genes (Nakajima and Wall 1991; Yuan *et al.* 1994). Expression of LIF and its receptor (LIFR) has been reported in both fetal and adult rodent testes with PMCs being the principal origin for LIF production (Piquet-Pellorce *et al.* 2000; Molyneaux *et al.* 2003; Dorval-Coiffec *et al.* 2005). As such, LIF is deemed as an essential paracrine factor for testis development and function. Since PMCs are located between the seminiferous and interstitial compartments, production of LIF by PMCs is speculated to affect both spermatogenesis and steroidogenesis. PMCs, Sertoli, Leydig, and germ cells all express LIFR (Piquet-Pellorce *et al.* 2000).

LIF is one of the paracrine cytokines with significant effects on propagation of germ and somatic cells (Fig. 2.2). Although LIFR is also expressed by somatic cells, germ cells are the main target for LIF paracrine signaling (Dorval-Coiffec *et al.* 2005). The widespread LIF and LIFR expression by testis somatic and germ cells implies the importance of this paracrine cytokine in testicular functions. This was also shown by *in vitro* studies where LIF supplementation to the culture medium increased survival of germ and somatic cells, and stimulated proliferation of spermatogonia in testis tissue cultures (de Miguel *et al.* 1996; Dorval-Coiffec *et al.* 2005). Also, germ cell colonies increased in the presence of LIF and transformed into more differentiated spermatogonia (Kanatsu-Shinohara *et al.* 2007; Aponte *et al.* 2008). Another study on murine PGCs showed increased proliferative activity in the presence of LIF in the media, while blocking LIFR by antibodies led to germ cell apoptosis (Pesce *et al.* 1993; Cheng *et al.* 1994). However, derivation of normal offspring from germline stem cell cultures in the absence of LIF may indicate that LIF alone is not involved in proliferation of germ cells. Further, it has been suggested that LIF may be required for initiation of germline stem cell cultures, and together with other factors is involved in transition of gonocytes into spermatogonia (Kanatsu-Shinohara *et al.* 2007). Conversely, LIF overexpression has detrimental effects on germ cells and leads to germ cell loss (Hilton and Gough 1991; Shen *et al.* 1994; Yano *et al.* 1998). The stimulatory effects of LIF on germ cell proliferation and its anti-apoptotic effects are likely mediated through Sertoli cells, since LIFR ablation in Sertoli cells of rodents leads to defective spermatogenesis (Jenab and Morris

1998; Curley *et al.* 2018). Spermatids are normally produced in LIF-deficient seminiferous tubules, pointing at sufficient support of Sertoli cells for germ cell proliferation/differentiation; however, LIFR-deficiency leads to sloughing of the epithelium, resulting in an abnormal spermatogenic cycles. As such, it is speculated that LIF is required for ensuring maturation of differentiated germ cells prior to their release into the luminal compartment and development of excurrent ductal system in the testis (Curley *et al.* 2018).

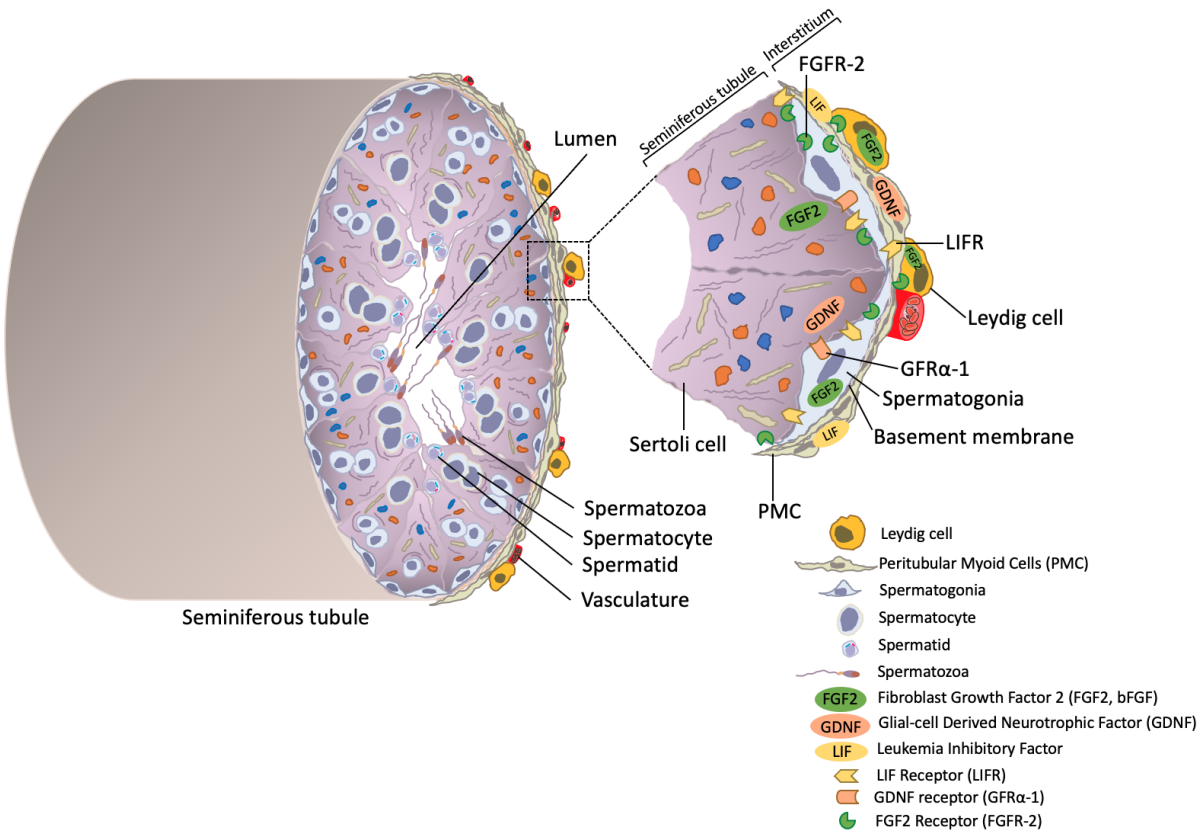

Fig. 2.2. Overview of testis structure and its potential paracrine signaling map. Gonocytes arriving at the basement membrane transform into a new germ cell identity known as spermatogonia. In an adult testis, spermatogonia undergo self-renewal divisions to sustain their population and differentiate to produce more advanced germ cells such as spermatocytes, spermatids, and ultimately, spermatozoa. Spermatogenesis and steroidogenesis are highly regulated by paracrine signalling. Among paracrine factors basic fibroblast growth factor (bFGF or FGF-2), glial-cell derived neurotrophic factor (GDNF), and leukemia inhibitory factor (LIF) play vital roles in cell-cell interactions. FGF-2 is released by PMCs, Leydig, Sertoli, and germ cells and increases self-renewal divisions of spermatogonia and somatic cells. Sertoli cells and PMCs produce GDNF, which is also an important factor for mitotic divisions of spermatogonia through interactions with GFRα-1. LIF is primarily synthesized by PMCs and interacts with its receptor on both germ and somatic cells. LIF promotes divisions of spermatogonia and somatic cells of the testis and is suggested to encourage maturation of differentiated germ cells.

2.6. Applications of Ultrasound Biomicroscopy in Reproductive Sciences

Ultrasound biomicroscopy (UBM) is a high-frequency ultrasound technique which allows real-time imaging of tissue structural details at near light microscopic resolution (He *et al.* 2012). UBM was first developed in 1989 by Pavlin's group initially to provide a means for more accurate and non-invasive examination of ocular tissues (Pavlin *et al.* 1990; Greco *et al.* 2012). Since then, applications of UBM have expanded into different clinical and research fields (Greco *et al.* 2012). Compared to conventional ultrasound machines which use low frequency ultrasound waves (*i.e.*, ~2-20 MHz), higher-frequency transducers (20-100 MHz) are utilized in UBM to record high-definition cross sectional images of the tissues (Pavlin and Foster 2012). As such, UBM transducers can provide high-definition images with up to 25 µm axial and 50 µm lateral resolution (Turnbull *et al.* 1995). UBM along with other non-invasive monitoring technologies such as computed tomography (CT), has had tremendous impact on *in situ* evaluation of organs and tissues, notably in a longitudinal approach. However, compared to other imaging techniques, UBM is superior since it is less costly and provides detailed real-time information from tissue structure and composition (Greco *et al.* 2012).

UBM has been widely used for examination of the eye and visualization of ocular structures (Pavlin *et al.* 1992; He *et al.* 2007; Pavlin and Foster 2012). Applications of UBM is not limited to imaging of ocular pathophysiology. For instance, this non-invasive monitoring method has been used to characterize the neovessel formation in mice (Hibino *et al.* 2011), visualize longitudinal follicular dynamics in mice and rats (Jaiswal *et al.* 2009), measure ovarian follicles and corpora lutea in mice (Mircea *et al.* 2009), cattle (Pfeifer *et al.* 2012), humans (Baerwald *et al.* 2009), and rabbits (Cervantes *et al.* 2013). Other applications include the study of cardiac development (Spurney *et al.* 2006), as well as cardiac structure and function following aortic constriction, or cardiomyopathy following induced heart failure in mice (Buckley and Stokes 2011; Jaffré *et al.* 2012). UBM has also been utilized to image small superficial peripheral nerves in humans (Stokvis *et al.* 2009) and embryonic brain development in mice (Turnbull *et al.* 1995). Previous applications of UBM in cancer research include analysis of melanoma xenografts and their treatment in mice (Cheung *et al.* 2005; Nuccitelli *et al.* 2006) as well as quantification of pancreatic tumor growth in mice (Snyder *et al.* 2009). Mouse pre- and post-natal development has also been investigated with UBM from day 5.5 of embryogenesis through adulthood (Foster *et al.* 2002).

UBM has been also applied for the study of testis pathophysiology. In a recent study, testis cell implants were monitored for a short-term period using UBM. In that study, dimensions and structure of the implanted testis cells were efficiently and accurately recorded and the structural changes of the implants were clearly visualized through UBM. The results were suggestive of UBM potential to be used as a possible alternative tool for examination of a wide range of superficial masses in a non-invasive manner and more accurate approach (Awang-Junaidi *et al.* 2020). Another example of UBM application in the study of male gonads is testicular UBM for evaluation of spermatogenic function in busulfan-treated mice. The latter study showed that pixel intensity returned to normal 126 days after busulfan treatment, when the spermatogenesis could be observed in the tubules, and it was concluded that UBM is an accurate tool for evaluation of spermatogenic function (Huang *et al.* 2021).

2.7. Applications of Male Germline Stem Cells in Research and Clinical Settings

As discussed above, MGSCs represent a robust population of stem cells which hold great promise for downstream applications not only in reproductive sciences but also in regenerative medicine and stem cell therapy. MGSCs can be isolated at different time points in life and cultured using different 2-D or 3-D approaches, and as such can be maintained over extended periods or differentiated to produce more advanced germ cells. Alternatively, these cells can be used for *in vivo* culture systems (*e.g*., TTX and TCAI) to study, manipulate, improve male gonadal development, or even produce mature spermatozoa. Establishment of donor-derived spermatogenesis via GCT is another important application of MGSCs, which has opened new avenues of research into transgenesis and genetic manipulation of germ cells prior to transplantation to produce genetically-modified animals. Transgenic animals, in turn, can offer enhanced productivity traits, provide organs or tissues for transplantation to humans, or serve as models for biomedical research. Additionally, combination of above-mentioned applications with current reproductive technologies such as *in vitro* fertilization (IVF) has opened more windows of opportunity for genetic conservation and fertility restoration.

One of the important applications of MGSCs is preservation of fertility in cancer patients following cytotoxic treatments such as chemo- or radiotherapy. This can be achieved by cryopreservation of small testicular samples or isolated testis cells obtained prior to gonadotoxic treatments while ensuring that the isolated samples are devoid of neoplastic cells or tissues. Cryopreserved as well

as fresh testis tissues can be used for *in vitro* tissue culture, TTX, or even isolation of testis cells. Alternatively, cryopreserved isolated testis cells can be applied in GCT, *in vitro* culture, or TCAI aimed at ectopic regeneration of testicular architecture. Cryopreservation does not hinder the spermatogenic efficiency and differentiation potential of spermatogonia as has been shown in *in vitro* studies (Suzuki and Sato 2003). Interestingly, cryopreserved testis cells possess a slightly higher fertilization rate compared to that of intact *in situ* testis cells (Sato *et al.* 2011; Yokonishi *et al.* 2014). Even live progeny has been produced following round spermatid-injection (ROSI) or ICSI using round spermatid or spermatozoa produced in the cultures of previously-cryopreserved testis tissues (Sato *et al.* 2015). The cryopreserved testis tissues and cells have been shown to retain cellular viability and differentiation potential after being grafted or implanted into immunodeficient recipient mice in TTX or TCAI studies and display similar recovery rate as fresh control tissue or cell samples (Honaramooz *et al.* 2002; Shinohara 2002; Zeng *et al.* 2009; Abrishami *et al.* 2010; Arregui and Dobrinski 2014). Particularly, combined applications of foregoing technologies such as cryopreservation, culture, and IVF provide a unique chance to prepubertal cancer patients to sire their own progeny since they are not yet able to produce spermatozoa to be preserved (Blash *et al.* 2000; Struijk *et al.* 2013; Arregui and Dobrinski 2014; Honaramooz 2014). Cryopreservation also offers the opportunity to save the testis cells or tissues from immature rare/endangered species for future applications such as *in vitro* culture, GCT, TTX, or TCAI to recover spermatozoa (Honaramooz *et al.* 2002; Zeng *et al.* 2006; Honaramooz *et al.* 2007; Watanabe *et al.* 2009; Arregui and Dobrinski 2014; Arregui *et al.* 2014; Honaramooz 2014). Using a range of domestic animals (*e.g*., sheep, goat, cattle, horse, pig, alpaca, cat, and dog) representative of endangered counterparts (*e.g.,* ungulate, equine, swine, camelid, feline, and canine species) tissue grafts have been demonstrated to retain their regeneration potential by TTX even after cryopreservation (Snedaker *et al.* 2004; Oatley *et al.* 2005; Zeng *et al.* 2006; Abrishami *et al.* 2010; Abrishami *et al.* 2010; Elzawam 2013).

Additionally, cryopreserved or fresh MGSCs can undergo genetic manipulations to develop a germ cell population carrying a specific gene transcript (Honaramooz *et al.* 2003; Honaramooz *et al.* 2003; Brinster *et al.* 2003; Honaramooz and Yang 2011; Zeng *et al.* 2012). Given the unique ability of MGSCs to undergo both proliferation and differentiation, they can be initially expanded *in vitro* to increase the number of transgenic germ cells, and colonize the recipient seminiferous tubules following GCT, thereby transmit the transgene to the next generation (Brinster 2002; Kim *et al.*

2008; Zeng *et al.* 2013; Kalds *et al.* 2019). This is especially important in large domestic species such as goats and pigs where available methods for transgene transmission are not efficient or cost-effective. Transplantation of germ cells carrying a transgene can potentially establish production of an infinite number of transgenic spermatozoa throughout the life of the recipient (Dobrinski 2008; Kim *et al.* 2008; Honaramooz and Yang 2011). Also, application of MGSCs in transgenesis will provide an approach to produce animals as donors of tissues and organs for xenotransplantation to humans. Transgenic animals can also serve as models for biomedical research or bioreactors for production of biopharmaceutical products for instance in milk-producing animals (Niemann and Kues 2003; Honaramooz and Yang 2011). Plus, GCT using transgenic MGSCs is potentially an alternative to artificial insemination for dissemination of superior farm animal genetic materials especially where limited manipulation for semen collection is allowed (Hill and Dobrinski 2005).

As discussed earlier, MGSCs have the potential to transform into more primitive developmental stages *in vitro*. These cells, known as germline-derived pluripotent stem cells, can serve as an alternative stem cell type parallel to ES cells and iPS cells to investigate the mechanisms by which cells acquire pluripotency and maintain it (Golestaneh *et al.* 2009; Ko *et al.* 2009; Chen *et al.* 2020). Also, these cells can be potentially used as a stem cell source in patients suffering from pathological conditions (*e.g.*, cardiomyopathy, neurodegenerative diseases, diabetes). Once pluripotent MGSCs are produced, they can be expanded *in vitro* and directed to differentiate into desired cell types (*e.g.*, contractile cardiomyocytes, endothelial cells, neural cells, pancreatic cells) prior to transplantation to patients (Kanatsu-Shinohara *et al.* 2004; Guan *et al.* 2006; Seandel *et al.* 2007; Izadyar *et al.* 2008; Kossack *et al.* 2009). Germline-derived pluripotent stem cells are advantageous in that they are not associated with ethical concerns raised form derivation of human ES cells, where destruction of embryos is needed, and lack the risk of immunological rejection, associated with iPS cells. Prospective applications and investigated potential of MGSCs described here have been partly investigated in animals and to a lesser extent in humans. Expectedly, feasibility of these potential approaches in clinical settings is not yet tested mainly due to ethical and safety concerns as well as low efficiency of foregoing techniques.

2.8. Conclusions

Testis is a unique organ owing to its dual function of spermatogenesis and steroidogenesis, which necessitates complexities in its structure and cellular interactions. These cell interactions are established during prenatal and postnatal development among seminiferous tubular and interstitial cells comprised of somatic cells (*e.g.*, Sertoli cells, Leydig cells, myofibroblasts, and macrophages) and MGSCs. Both testis development and function are regulated by highly coordinated and complex cellular interactions and signaling cascades. Not to mention, scarcity of testicular samples from humans or endangered/rare species makes the study of testis development and function even more challenging in these species.

Extensive studies conducted thus far on MGSCs from different species all point at their great potential to be used not only in reproductive sciences but also in stem cell therapy and regenerative medicine. Testicular cells can be cultured indefinitely, transplanted into recipient seminiferous tubules where they establish donor-derives spermatogenesis, and through TCAI/TTX regenerate fully-formed testicular tissue, induced to revert into more primitive developmental stages or differentiate into a different somatic cell lineage, or even be subjected to genetic manipulation to carry a transgene to the next generation following GCT. To this end, understanding complex processes of testis development/function, harnessing the full potential of MGSCs, and their applicability in clinical settings are not feasible without availability of accurate models which can highly mimic *in situ* conditions.

2.9. Objectives and Hypotheses

The overreaching goal of this thesis was to develop tools and protocols to enable *in vivo* and *in vitro* study of the testicular cell and tissue development in a porcine animal model. General objectives of this thesis were to establish new strategies for *in vivo* developmental study of testis cells and tissues and *in vitro* harnessing the developmental potential of isolated testis cells. Our specific objectives and hypotheses were as follows:

STUDY 1:

Objectives: To test the effects of supplementation of six different culture media (DMEM, DMEM/F12, GMEM, α-MEM, RPMI and StemPro SFM) with three different concentrations of FBS or its replacement (5%, 10% and 15%) on (1) *in vitro* proliferation and colony-formation of porcine gonocytes; and on (2) their ultrastructure and expression of gonocyte and pluripotency markers.

Hypotheses: (1) No media, sera, or serum replacement would affect the gonocyte number or their colony number/size; and (2) culturing in the selected condition would not affect the expression of germ cell or pluripotency markers (*e.g.*, NANOG, E-cadherin, SSEA-1, and POU5F1) of gonocytes and their colonies.

STUDY 2:

Objectives: To investigate the effects of different growth factors alone or in combination, on (1) *in vitro* proliferation and colony-formation of porcine gonocytes; and on (2) expression of gonocyte and pluripotency markers.

Hypotheses: Culturing with selected growth factors would not affect (1) the gonocyte number or their colony number/size; or (2) the expression of pluripotency markers (*e.g.*, NANOG, E-cadherin, SSEA-1, and POU5F1) of gonocytes and their colonies.

STUDY 3:

Objective: To investigate trans-differentiation potential of porcine gonocytes and their colonies, developed in the optimized culture condition from study 2 into cells with origins from the three germinal layers (ectoderm, mesoderm, and endoderm).

Hypothesis: Once cultured under appropriate conditions, porcine gonocytes would differentiate into derivatives of all three primary germinal layers and express the lineage-specific markers detectable by RT-PCR or immunocytochemistry.

STUDY 4:

Objectives: (1) To validate the use of UBM as a feasible and reliable technique for non-invasive monitoring of the testis tissue grafts and cell implants; and (2) to correlate the UBM data with physical attributes of the retrieved samples (*e.g.,* graft or implant dimension and volume).

Hypotheses: (1) The use of UBM would be feasible and reliable for monitoring the grafted testis tissues/implanted cells; and (2) the UBM data would be positively correlated with the physical attributes of retrieved testis tissue grafts/cell implants.

STUDY 5:

Objectives: (1) To perform longitudinal evaluation of the grafts and implants using UBM and histology; and (2) to compare pre- and post-retrieval UBM and microscopic measurements of the grafts and implants over a 6-month period (*e.g.,* composition and pixel intensity, detectability of blood vessels and descriptive comparison).

Hypotheses: (1) UBM would be able to demonstrate long-term 3-D growth and compositional changes of the samples; and (2) UBM findings would be positively correlated with the histological attributes of the retrieved samples.

CHAPTER 3

EFFECTS OF DIFFERENT CULTURE CONDITIONS ON PROLIFERATION, COLONY-FORMATION, AND PLURIPOTENCY STATE OF PORCINE MALE GERM CELLS [1, 2]

3.1. Abstract

Gonocytes are progenitor germ cells in the neonatal testis with important potential applications in fertility restoration and transgenesis. Using stepwise experiments, we examined the effects of different media combined with fetal bovine serum (FBS) and/or knockout serum replacement (KSR) on the *in vitro* proliferation, colony-formation, ultrastructure, and expression of pluripotency markers of porcine gonocytes. Testis cells from 1-wk-old piglets were cultured for 28 days in 6 different culture media (DMEM, DMEM/F12, GMEM, MEM, StemPro, and RPMI), each supplemented with 5%, 10%, or 15% FBS and/or KSR. The media and FBS/KSR combination leading to the maximum number of gonocytes, and their colonies was selected for further analyses. KSR supplementation resulted in a reduced somatic cell propagation and increased gonocyte colony formation ($P < 0.001$). Culturing in DMEM+15%FBS led to the greatest number of gonocytes ($P < 0.001$), while the largest diameter and greatest number of colonies were formed in DMEM+5%FBS+10%KSR cultures ($P < 0.001$). Gonocytes and their colonies in DMEM+15%FBS expressed all the examined gonocyte and pluripotency markers. KSR alone did not support gonocyte propagation, likely due to a reduced somatic cell proliferation; however, the combination of FBS and KSR increased gonocyte colony formation and their size.

3.2. Introduction

Male germline stem cells (MGSCs) include primordial germ cells (PGCs), gonocytes, and spermatogonial stem cells (SSCs). During fetal development, PGCs differentiate into a transitory population of germ cells known as gonocytes or prospermatogonia (De Felici 2016). Shortly after

[1] This manuscript has been submitted for publication in *Theriogenology* under joint co-authorship with Ali Honaramooz.

[2] As first author, MAF contributed to the experimental design, conducted the study, and wrote the first draft of the manuscript. AH contributed to the experimental design, revised the manuscript, and supervised the project.

birth, gonocytes move from the center toward the basement membrane of the seminiferous cords and transform into SSCs (Brinster 2002). Being the foundational source of all subsequent germ cell types, SSCs can both proliferate to maintain their stem cell pool and differentiate into more specialized germ cells to transfer genetic information to the next generation (Jiang 2001; Chikhovskaya *et al.* 2014). SSCs are surrounded by the stem cell niche components including the extracellular matrix, Sertoli cells, peritubular myoid cells, Leydig cells, and blood vessels, all contributing to the structural and functional support of SSCs (Kuijk *et al.* 2009; Phillips *et al.* 2010; Ibtisham and Honaramooz 2020; Ibtisham *et al.* 2020). Within this niche, Sertoli cells play a pivotal role in regulating the proliferation and differentiation of SSCs by providing essential nutrients as well as mediating the endocrine and paracrine signals (Phillips *et al.* 2010).

Among different types of MGSCs, gonocytes are relatively accessible and easily identifiable due to being the only type of germ cells in the neonatal testis, their unique morphological features, and the availability of gonocyte-specific biomarkers. Hence, gonocytes provide a feasible model for the study and manipulation of MGSCs (de Rooij and Russell 2000; Meng *et al.* 2000a; Culty 2009; Awang-Junaidi and Honaramooz 2018). PGCs, on the other hand, are only accessible through collection of embryos and at limited numbers, (Jiang and Short 1998a; Ohta *et al.* 2004; Awang-Junaidi and Honaramooz 2018) and SSCs are a rare population of germ cells in the testis, and in the absence of unequivocal cell-specific markers, true SSCs can only be verified using the germ cell transplantation assay (Ibtisham and Honaramooz 2020; Ibtisham *et al.* 2020).

MGSCs have great potential in being used as a cell source for restoration of fertility, regenerative medicine, and transgenesis. Upon germ cell transplantation into a recipient animal's seminiferous tubules, MGSCs obtain/display stemness due to their potential to colonize the recipient testis and establish donor-derived spermatogenesis (Jiang and Short 1998b; Jiang 2001; Yang and Honaramooz 2011; Sahare *et al.* 2018). MGSCs from immature and pubertal donors have also been shown to possess the ability to spontaneously transform into embryonic-like stem cells *in vitro* (Jiang and Short 1998a; Jiang 2001; Bai *et al.* 2018). Therefore, MGSCs can be potentially used as an alternative source for regenerative therapy, which is otherwise largely limited to embryonic stem (ES) cells or induced pluripotent stem (iPS) cells (Seandel *et al.* 2007; Zheng *et al.* 2013). The use of MGSCs would circumvent some of the ethical concerns surrounding the use of ES cells or safety concerns over the use of iPS cells, which require incubation with potentially

carcinogenic transcription factors. Transplantation of MGSCs from a fertile donor can overcome certain types of infertility (Zheng *et al.* 2013), and auto-transplantation of MGSCs from cryopreserved biopsies may also be considered for the restoration of fertility following gonadotoxic cancer treatments (Hwang and Lamb 2010). Additionally, the transplantation of genetically modified MGSCs can be used as an alternative approach to the currently inefficient methods of generating transgenic farm animals (Ibtisham and Honaramooz 2020).

Downstream applications of MGSCs in reproductive biology and technology require their scale up *in vitro* (Guan *et al.* 2006; Phillips *et al.* 2010). *In vitro* culture can be used to expand MGSCs from scarce resources such as small biopsies and to obtain high numbers of these cells by promoting their proliferation. *In vitro* culture is also a valuable tool to elucidate mechanisms by which proliferation and differentiation of MGSCs are regulated (Phillips *et al.* 2010; Bai *et al.* 2018). For instance, successful and efficient colonization of germ cells in the recipient seminiferous tubules largely depends on the number of transferred MGSCs, necessitating enrichment of SSCs or gonocytes prior to transplantation (Dobrinski *et al.* 1999; Awang-Junaidi and Honaramooz 2018). In neonatal murine testes and porcine seminiferous cords, gonocytes only comprise ~2% (Huckins 1971; Tagelenbosch and De Rooij 1993; Li *et al.* 1997; Orwig *et al.* 2002) and ~7% (Honaramooz *et al.* 2005) of the cell population, respectively. Also, conventional methods of cell isolation lead to testis cell populations comprised of only up to ~10% gonocytes (van Dissel-Emiliani *et al.* 1989; Li *et al.* 1997; van Den Ham *et al.* 1997; Honaramooz *et al.* 2005; Goel *et al.* 2007). Nevertheless, cell-specific markers such as germ cell markers (*e.g.* DAZL, VASA) (Castrillon *et al.* 2000; Reijo *et al.* 2000) and gonocyte markers (*e.g.* DBA, UCH-L1, THY-1) (Goel *et al.* 2007; Yang *et al.* 2010; Zheng *et al.* 2014) can be used for subsequent enrichment through magnetic activated cell sorting (MACS) or fluorescent activated cell sorting (FACS) (Kim *et al.* 2010). However, cell sorting methods have low efficiency in enrichment of large quantities of MGSCs in large domestic animals including pigs for subsequent applications (Kim *et al.* 2010). Efficient enrichment of gonocytes have also been shown using Nycodenz gradient centrifugation and differential plating (Yang and Honaramooz 2011), but are of limited use for SSCs.

Expectedly, in culture conditions, medium and serum play crucial roles in cell survival and proliferation (Zheng *et al.* 2013; Sahare *et al.* 2016, 2018; Suyatno *et al.* 2018). However, thus far,

few studies have examined optimal conditions for *in vitro* culture of MGSCs from large animals (Awang-Junaidi and Honaramooz 2018; Bai *et al.* 2018; Sahare *et al.* 2018), and none have systematically examined the effects of media type or sera on long-term culture of porcine gonocytes. Porcine gonocytes were selected in the present study since they provide a more relevant model for the study of germ cells in prepubertal boys and a suitable model for the study of stem cell pluripotency (Dirami *et al.* 1999; Goel *et al.* 2007; Petersen *et al.* 2009; Awang-Junaidi and Honaramooz 2018; Sahare *et al.* 2018; Awang-Junaidi *et al.* 2020). In two-dimensional (2-D) culture systems, Dulbecco's modified Eagle's medium (DMEM), Dulbecco's modified Eagles medium and Ham's F12 (DMEM/F12; 50%/50% vol/vol), and minimum essential medium (MEM), supplemented with either serum or serum replacement, are the most prevalent medium/serum sources for *in vitro* culture of MGSCs (Kanatsu-Shinohara *et al.* 2011, 2014; Sadri-Ardekani *et al.* 2011; Sahare *et al.* 2018). Given the indispensable effects of media and sera on survival of gonocytes, we designed the present study to optimize our previously established culture conditions (Awang-Junaidi and Honaramooz 2018) by investigating the effects of six different media supplemented with one of three concentrations of fetal bovine serum (FBS) and/or knock-out serum replacement (KSR) on long-term porcine gonocyte proliferation, colony-formation, and expression of pluripotency-determining factors.

3.3. Materials and Methods

3.3.1. Study Design

The present study consists of two stepwise experiments, as schematically shown in Figure 3.1. We first tested the effects of six different media combined with various individual concentrations of FBS or KSR on the number of gonocytes or their colonies and their expression of pluripotency-determining factors, using our previously reported general culture conditions (Awang-Junaidi and Honaramooz 2018; Awang-Junaidi *et al.* 2020). The culture medium which improved the proliferation of gonocytes and enhanced their colony-formation was selected to be combined with increasing concentrations of FBS along with decreasing concentrations of KSR. In Experiment 3.2, the combination culture condition which enhanced gonocyte proliferation and colony-formation the most was selected to examine the expression of pluripotency-determining factors of cultured gonocytes and their resultant colonies. Also, the culture condition leading to the greatest number of large embryoid body-like colonies (EBLCs) was then selected as the optimal condition

for subsequent cultures to examine the ultrastructure of EBLCs by transmission electron microscopy (TEM).

3.3.2. Castration of Animals, Cell Isolation, and Culture

Castration of 1-wk-old donor Yorkshire-cross piglets (n = 230; Camborough-22 line 65; PIC Canada, Winnipeg, MB, Canada) and isolation of testis cells were carried out as described in our previous studies (Yang *et al.* 2010; Awang-Junaidi and Honaramooz 2018; Awang-Junaidi *et al.* 2020). In total, 51 combinations of media and sera (*i.e.*, treatment groups) were tested. For each treatment group, three replicates of isolated cell suspensions were prepared (each round of testis cell isolation was considered as a replicate), and for each replicate we used ~3 testes. Cell quantification and viability assessments were performed as described previously (Awang-Junaidi and Honaramooz 2018; Awang-Junaidi *et al.* 2020). Relative number of gonocytes was calculated using a gonocyte-specific marker.

In Experiment 3.1, testis cells were cultured using 6 different media listed in Table 3.1 in an optimized condition reported previously by our laboratory (Awang-Junaidi and Honaramooz 2018). Each medium was supplemented with one of three concentrations (5%, 10%, or 15%) of either FBS (catalogue no. A15-701; PAA Laboratories, Etobicoke, ON, Canada) or KSR (catalogue no. 10828028, Gibco, Thermo Fisher Scientific, Waltham, MA, USA). StemPro-SFM medium is supplied as a basal medium along with a proprietary nutrient supplement to be mixed by users. Hence, in addition to using the basal StemPro-SFM medium when adding different concentration of FBS or KSR, we also tested it using its own nutrient supplement-only. Each of the three cell isolate replicates for each treatment was seeded in two separate wells of a single 6-well plate, and the cells were maintained by changing the media every 7 days for 28 days. The cultured cells were briefly monitored daily under an inverted phase-contrast microscope (Nikon, Eclipse TS100).

As a follow up to Experiment 3.1, using the medium which led to the overall highest numbers of gonocytes on Day 28, we also tested the effects of supplementation with even higher concentrations (20%) of FBS or KSR under otherwise similar culture conditions as above. To test the effects of combined FBS and KSR concentrations in Experiment 3.2, the same medium (leading to the highest numbers of gonocytes) was also selected and supplemented with a

combination of increasing concentrations of FBS (0%, 5%, 10%, or 15%) and decreasing concentrations of KSR (15%, 10%, 5%, or 0%).

3.3.4. Evaluation of Cultured Gonocytes and Gonocyte Colonies

In each experiment, on Days 7, 14, 21, and 28, randomly selected wells from all three replicates of each treatment were used for morphometrical evaluations and visual quantification of gonocytes. Quantification of EBLCs was performed on Day 28 of culture. Selected wells were observed using an inverted phase-contrast microscope equipped with a camera for photomicrography (Sony α5000, Sony Corporation, Tokyo, Japan). Images were captured from randomly selected fields of view at 40× and 200× (n = 10 images per magnification). Using ImageJ software (ImageJ, U.S. National Institutes of Health, Bethesda, MD, USA), the number of individual gonocytes, and if present, EBLCs was quantified at 40× magnification. The average diameter of EBLCs along the X and Y axes was measured and calculated in all captured images at 200× magnification. Given that gonocytes in culture appear as individual cells or colonies (Awang-Junaidi and Honaramooz 2018), two or more gonocytes with identifiable interface were still considered as separate entities.

3.3.5. Sampling and Immunocytochemistry

Sampling and immunocytochemistry were performed on both cultured and smears of freshly-isolated testis cells as described previously (Awang-Junaidi and Honaramooz 2018). Antibodies used in the present study are summarized in Table 3.2 and fluorescein isothiocyanate (FITC)-labelled *Dolichos biflorus* agglutinin (DBA-FITC; catalogue no. FL1031; Vector Labs, Burlington, ON, Canada) was used as a gonocyte-specific marker (Goel *et al.* 2007). Photomicrographs of the stained samples were captured at 400× magnification by using specific filter sets to visualize 4′, 6-diamidino-2-phenylindole (DAPI), FITC, and Alexa Fluor 594 as described our previous work (Awang-Junaidi *et al.* 2020).

3.3.6. RNA Extraction and RT-PCR Analysis

To confirm the expression of pluripotency markers, reverse-transcriptase polymerase chain reaction (RT-PCR) analysis was used. Total RNA was extracted from both freshly isolated testis cells and samples of cultured cells on Days 7, 14, 21, and 28. To obtain a single cell suspension from cultured cells, randomly selected wells at each time-point were trypsinized as described

above and the harvested cells were centrifuged. The supernatant was removed, and pelleted cells were resuspended in PBS, and centrifuged again. The supernatant was removed, and the resultant cells as well as testis cells obtained from fresh samples underwent RNA extraction using Invitrogen RNAqueous Micro Total Isolation Kit (catalogue no. AM1931; Thermo Fisher Scientific), according to the manufacturer's instructions. Next, contaminating gDNA was eliminated and complimentary DNA (cDNA) was synthetized using the Primer Mix and iScript gDNA Clear cDNA Synthesis Kit (catalogue no. 172-5034; Bio-Rad, Mississauga, ON, Canada). Developed cDNA was amplified using Ssofast EvaGreen Supermix (catalogue no. 1725200; Bio-Rad), according to the manufacturer's instructions. The primers used for RT-PCR analyses are shown in Table 3.3. A 2% agarose gel was prepared and the PCR products, stained with ethidium bromide, were run and visualized under ultraviolet light.

3.3.7. Transmission Electron Microscopy

Preparation of culture wells for TEM was performed as described previously (Awang-Junaidi *et al.* 2020). Briefly, cells and EBLCs in the optimal treatment condition (selected for increasing the number and size of EBLCs) were fixed on Day 28 with 2% glutaraldehyde in 0.1 M sodium cacodylate buffer (pH = 7.2) at 4° C. Fixed cells and EBLCs were then immersed in 0.1 M sodium cacodylate buffer, stored at 4° C overnight, immersed in 1% osmium tetroxide for 1 h, and washed with distilled water. Cells and EBLCs were dehydrated in ethanol, covered by two changes of absolute ethanol and LR White resin mix (1:1 and 1:2) for 1 h, and immersed in 100% resin for 2 h. The samples were sealed, and polymerization was performed at 65° C overnight. Following polymerization, the samples were split, separated, and blocked. Sectioning was performed at 100 nm using Leica Ultracut UCT and the prepared samples were examined under a transmission electron microscope (HT7700, Hitachi), using an accelerating voltage of 80 kV.

3.3.8. Statistical Analyses

Data are presented as mean ± standard error of mean (SEM) and $P < 0.05$ was considered as significant. All the data were analyzed using *t-test*, one- or two-way analysis of variance (ANOVA) and Tukey's HSD was used as the post hoc test, unless stated otherwise. For all data analyses Statistical Package for Social Sciences was used (IBM SPSS Statistics for Macintosh, Version 26.00; IBM Corporation, Armonk, NY, USA).

3.4. Results

3.4.1. Morphometrical and Developmental Assessment

3.4.1.1. Experiment 3.1: Effects of Individual Concentrations of FBS and KSR

Rather unexpectedly, in groups treated with StemPro medium with or without FBS/KSR, the cell confluency was less than ~10% after 7 days in culture (Fig. 3.2A). As such, StemPro medium group was removed from statistical analyses. Similarly, in all KSR-supplemented media, the cell confluency did not advance beyond ~20%, while colonization of gonocytes was improved (Fig. 3.2B). Hence, the groups supplemented with KSR were included in the analyses of EBLC numbers. In all remaining groups, the pattern of morphometrical cellular changes was similar.

Heterogenous populations of round floating cells were observed immediately after culturing of isolated testis cells. In the following 24 h, floating cells started to settle and adhere to the bottom of the culture well, forming a monolayer. By Day 3, gonocytes appeared as large round cells and started to attach to the adherent monolayer. By Day 5, further attachment of somatic cells formed a wave-shaped monolayer, with round gonocytes sitting on the top (Fig. 3.2C). By Day 7, extension of somatic cells formed ~90% confluency in the groups treated with DMEM, DMEM/F12, α-MEM, GMEM, and RPMI, supplemented with different concentrations of FBS.

On Day 7, gonocytes appeared individually or within clusters of 2 or more cells. Somatic cells appeared as fibroblast-like cells and by Day 7 they formed organized round patterns (Fig. 3.2D). These patterns, previously termed ‘circular arrangements’ (Awang-Junaidi *et al.* 2020), consisted of aggregated somatic cells in specific locations, while embracing a few clustered gonocytes via their cytoplasmic extensions. By Day 14, clustered gonocytes within the circular arrangements formed 3-D colonies with indistinct cytoplasmic membrane between individual cells within the colony (Fig. 3.2E and 3.2F). These structures, previously termed EBLCs (Awang-Junaidi *et al.* 2020) were seen exclusively within circular arrangements. When FBS was used as a source of serum, EBLCs formed in all treatment groups except GMEM-, RPMI-, and StemPro-treated groups. By Day 28, the number of gonocytes and EBLCs increased in all above-mentioned treatment groups, while the DMEM cultures had the greatest number of gonocytes and EBLCs. Since FBS supported *in vitro* propagation of testis cells, a new treatment group comprised of all six media supplemented with 20% FBS was also included in follow up analyses.

In FBS-supplemented cultures, an interaction was found between the medium type and FBS concentration on the number of gonocytes on Day 28 ($P < 0.001$; Fig. 3.3), where DMEM+15% FBS led to the greatest number of gonocytes. Among different medium types, the maximum number of gonocytes was found in cultures treated with DMEM ($P < 0.001$), and the maximum number of EBLCs was found in cultures with DMEM supplemented with 10-20% FBS. Also, in cultures provided with DMEM+15% FBS, the number of gonocytes and EBLCs increased by ~2 and ~3 folds, from Day 7 to Day 28, respectively ($P < 0.001$ for both).

In cultures where KSR was used, the morphology of post-seeding floating cells was not different from that of FBS-supplemented media. However, the cytoplasmic extensions of somatic cells did not develop compared with FBS-supplemented groups, the monolayer did not form the wave-shaped appearance, and cell confluency did not increase beyond ~20%. However, compared with FBS-supplemented groups, gonocytes showed a greater tendency to aggregate and form small clusters with the same appearance as small EBLCs (Fig. 3.4). The number of small EBLCs was affected by the interaction between KSR concentration and medium type, where numerically, the greatest number of small EBLCs was found in groups provided with DMEM+5% KSR ($P = 0.005$). Compared with the cultures supplemented with FBS, KSR-supplemented cultures with DMEM developed greater numbers of EBLCs at each concentration ($P = 0.001$; Fig. 3.5A), but smaller EBLC diameters by 53% ($P < 0.001$; Fig. 3.5B). Increasing the FBS concentration increased EBLC formation, while increasing the KSR concertation, decreased EBLC formation in DMEM (serum type*serum percentage $P = 0.001$).

Gonocytes comprised ~39% of the isolated cells based on the ratio of DBA-positive cells. The average cell viability in cultures of DMEM+15% FBS on Day 28 and fresh cell isolates was ~95%. In cultures of DMEM+15% FBS, the number of gonocytes and their resultant EBLCs increased by ~2 and ~3 times from Day 7 to Day 28, respectively.

3.4.1.2. Experiment 3.2: Effects of Combined Concentrations of FBS and KSR

Since DMEM optimally supported gonocyte proliferation and EBLC formation in Experiment 3.1, we tested this medium supplemented with increasing concentrations of FBS and decreasing concentrations of KSR in Experiment 3.2. Here, the morphology of gonocytes, somatic cell monolayer, and EBLCs conformed with those found in DMEM+15% FBS in all the treatment

groups except for cultures supplemented with only KSR, where the cell confluency was less than ~20% with large numbers of small gonocyte aggregates.

On Day 28, the greatest gonocyte and EBLC numbers were developed in cultures of DMEM+15% FBS and DMEM+5% FBS+10% or 15% KSR, respectively ($P < 0.001$; Fig. 3.6A and 3.6B). Overall, largest EBLCs were found in combined concentrations of FBS and KSR ($P < 0.001$; Fig. 3.6C). Thus, DMEM+15% FBS was selected as the optimal condition for increasing the gonocyte number and DMEM+5% FBS+10% KSR was selected as the optimal condition to improve EBLC development for subsequent study of their ultrastructure on Day 28.

3.4.2. Immunocytochemistry

Gonocytes appeared positive for DBA as a gonocyte-specific marker both on smears of freshly-isolated cells and after 28 days in culture. EBLCs were also positive for DBA in optimal conditions developed for EBLC formation (Fig. 3.7). The DBA signal was identified on the surface of gonocytes and EBLCs but not in their nuclei (Fig. 3.7). Furthermore, gonocytes in fresh cell isolates appeared positive for SSEA-1, as a porcine germ-cell and pluripotency-determining marker. The expression of POU5F1, NANOG, and E-cadherin as pluripotency-determining markers was not observed in freshly-isolated testis cells, while cultured gonocytes and their developed EBLCs appeared positive for these markers both in the nuclei and cytoplasm (Fig. 3.7).

3.4.3. Gene Expression Analyses

Gene transcripts of pluripotency-determining factors, comprised of *POU5F1, FUT4* (gene for SSEA-1)*, NANOG*, and *E-cadherin* were confirmed in samples obtained from cultured gonocytes, while freshly-isolated testis cells were only positive for *FUT4*. Quantification of fold change in expression level of these transcript markers revealed that the expression levels of *POU5F1*, *NANOG*, and *E-cadherin* were maintained from Day 7 to Day 28 of culture. Similarly, *FUT4* expression levels did not change from cell isolation to Day 28 of culture (Fig. 3.8).

3.4.4. Ultrastructural Assessment of Cultured Gonocytes and EBLCs in Selected Media

TEM was used to elucidate the underlying cellular structures and organelles as well as physical contacts between the cells. The number of gonocytes was relatively lower in cultures with DMEM+5% FBS+10% KSR than in cultures with DMEM+15% FBS. However, the overall appearance of gonocytes, somatic cell monolayer, and EBLCs was similar to that found in the

basic conditions composed of DMEM+15% FBS. Somatic cells adhered to the culture well, forming a flat and thin cellular layer (Fig. 3.9A). Gonocytes appeared as round single cells or in contact with each other while located on top of the monolayer. They possessed a large nucleolus with electron-dense heterochromatin associated with the nuclear envelope and randomly distributed euchromatin, giving the nucleolus a spongy-shape appearance (Fig. 3.9B). Gonocytes and EBLCs in the selected culture condition showed large numbers of electron-lucent vesicles in the cytoplasm (Fig. 3.9C and 3.9D). Gonocytes also possessed small cytoplasmic projections devoid of microtubules. EBLCs appeared as syncytia with multiple nuclei without a distinctive membrane separating them and contained the same cytoplasmic organelles as individual gonocytes. The gonocytes were in close contact with somatic cells while maintaining a physical gap in between (Fig. 3.9C). The main organelles observed within the cytoplasm of somatic cells included rough endoplasmic reticulum with stacks of paired membranes, sparse mitochondria, and lysosomes. Also, smooth endoplasmic reticulum mainly appeared as interconnecting tubules within these cells.

Table 3.1. Name and specification of media used in treatment groups

Name of the media	Abbreviation	Company	Catalogue number
Dulbecco's modified Eagle's medium	DMEM	Corning	12-604F
Dulbecco's modified Eagle's medium and Ham's F12	DMEM/F12	Corning	10092CV
α-Minimum essential medium	α-MEM	Gibco	12561056
Glasgow's minimum essential medium	GMEM	Gibco	11710035
Roswell Park Memorial Institute medium	RPMI	Gibco	11875093
StemPro-34 serum free medium	StemPro-SFM	Gibco	10639011

Table 3.2. Summary of primary and secondary antibodies used for immunofluorescence assay

Antibody	Company	Catalogue number	Dilution
Rabbit anti-POU5F1	Abcam	AB18976	1:200
Mouse anti-SSEA-1	Santa Cruz Biotechnology	sc-21702	1:200
Mouse anti-NANOG	Sigma-Aldrich	N3038	1:200
Rabbit anti-E-cadherin	Abcam	15148	1:200
Alexa Fluor 594 goat anti-rabbit	Abcam	AB150088	1:200
Alexa Fluor 594 goat anti-mouse	Abcam	150116	1:200

FITC, fluorescein isothiocyanate; POU5F1 or OCT4, octamer-binding transcription factor 4; SSEA-1, stage-specific embryonic antigen; NANOG, homeobox NANOG; E-cadherin, epithelial-cadherin

Table 3.3. Primers used for RT-PCR analysis

Target	Direction	Primer sequence (5′-3′)	Annealing Temperature (° C)	Product size (BP)
POU5F1	Forward	AGAGAAAGCGGACAAGTA	51.7	299
	Reverse	ATCCTCTCGTTGCGAATA		
FUT4	Forward	GGGTTACCAGACCAGCTTTAC	62	206
	Reverse	TCATCACAGCCAGCTTCTTC		
NANOG	Forward	CCTCAACGACAGATTTCAGAGG	62	227
	Reverse	GGCATCCTTGGTGATAGGAATAG		
E-cadherin	Forward	GAGATTCCGGGACTCACAATAG	62	228
	Reverse	CACAGGACAAGGTAGGAAACA		
GAPDH	Forward	TCGGAGTGAACGGATTTG	62	219
	Reverse	CCTGGAAGATGGTGATGG		

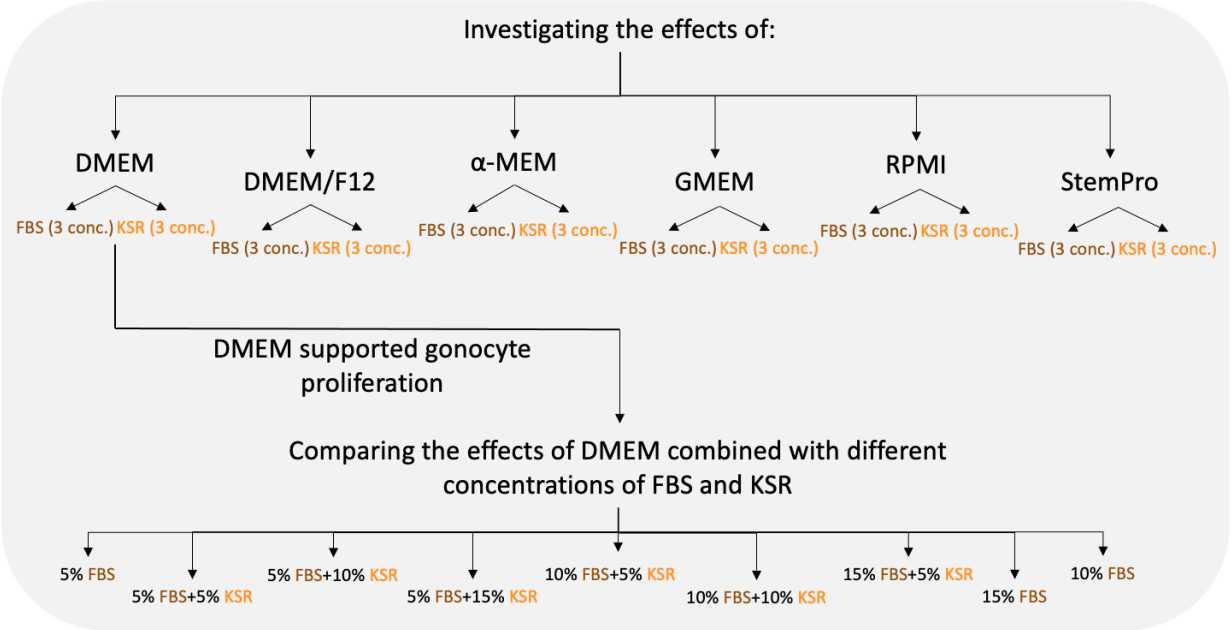

Fig. 3.1. Schematic overview of the experimental design. In Experiment 3.1, we tested the effects of six different media supplemented with three different concentrations of fetal bovine serum (FBS) or knock-out serum replacement (KSR) on gonocyte proliferation, colony-formation, and pluripotency. After culturing the cells for 28 days, DMEM+15% FBS was found as an optimal combination to increase the number of cultured gonocytes among different combinations. Hence, the cultured cells and colonies in this combination were also tested for the expression of pluripotency-determining transcription factors. In Experiment 3.2, we compared the effects adding to DMEM a combination of FBS and KSR at different concentrations. DMEM+5% FBS+10% KSR resulted in the largest and greatest number of embryoid body-like colonies (EBLCs) and as such, this treatment group was used to increase EBLCs for the study of their ultrastructure using transmission electron microscopy (TEM).

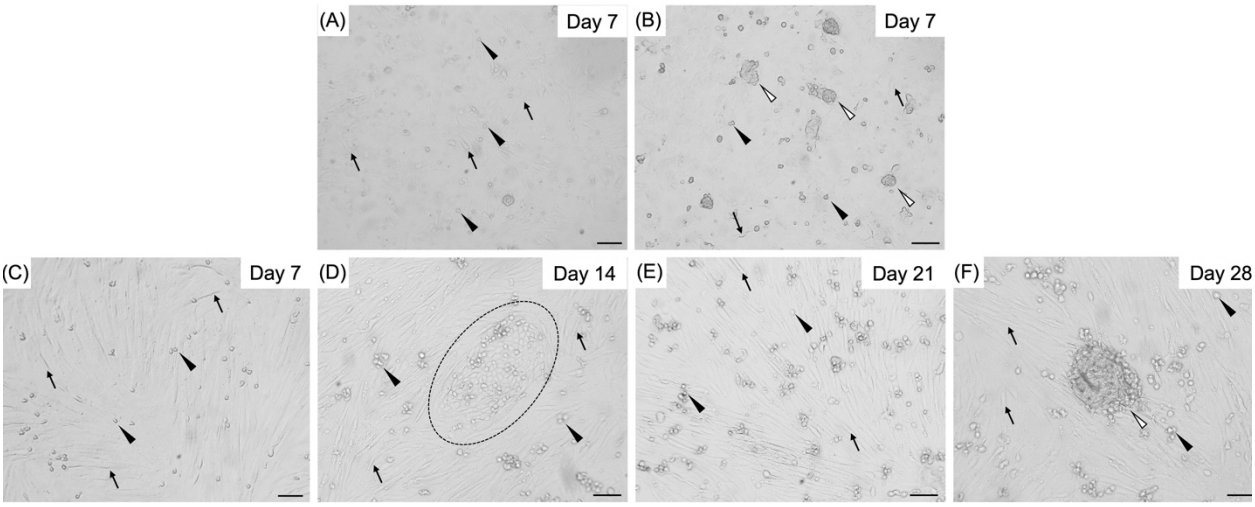

Fig. 3.2. Representative images demonstrating varying developmental status of cultured testis cells in different media and serum/serum replacement combinations. (A) After 1 wk of culture, the somatic cells (arrows) in StemPro medium (containing its proprietary supplement) did not reach the optimal confluency. The same morphology of the cells was observed when StemPro medium was supplemented with serum or serum replacement. Consequently, gonocytes (black arrowheads) did not increase in numbers, likely because their survival largely depends on support of the somatic cells. (B) Confluency of somatic cells (arrows) did not improve beyond 20% in any media supplemented with KSR-only. Gonocytes (black arrowheads) showed a greater tendency to form clusters and small embryoid body-like colonies (EBLCs; white arrowheads) in the presence of KSR. (C-F) Maximum number of gonocytes (black arrowheads) was found in cultures with DMEM+15% FBS, where somatic cells (black arrows) formed a complete wave-shaped monolayer on the culture well surface by Day 7 (C). These cells formed circular arrangements (dotted circle) within the monolayer by Day 14 (D). Over time, gonocytes increased in numbers by Day 21 (E) and merged to form large embryoid body-like colonies (EBLCs; white arrowhead) by Day 28 (F). (Scale bar = 100 μm)

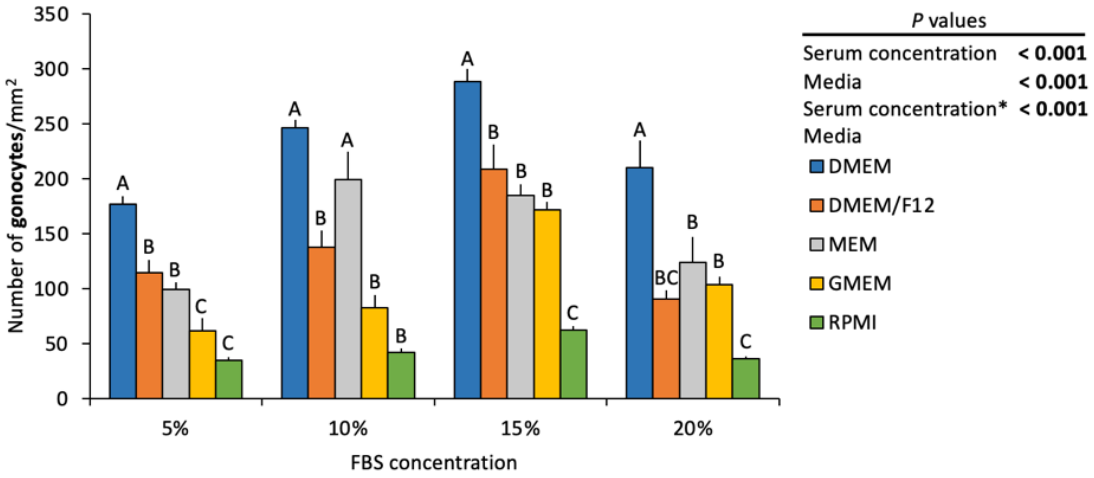

Fig. 3.3. Effects of different media supplemented with various serum concentrations on gonocyte numbers after 28 days of *in vitro* culture. The gonocyte numbers (mean ± SEM) was affected by an interaction between the media type and serum concentrations, where DMEM+15% FBS was selected as the optimal combination as it resulted in the numerically greatest gonocyte numbers ($P < 0.001$). Since StemPro media did not support gonocyte propagation, it was removed from the analysis. The minimum number of gonocytes was found in GMEM and RPMI supplemented with any serum concentration. Media types with different letters in each serum concentration group differ significantly, and $P < 0.05$ was considered significant.

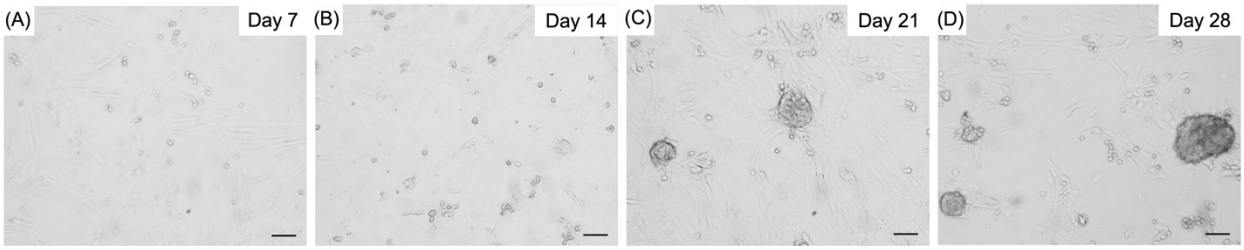

Fig. 3.4. Representative images of testis cells cultured in DMEM+10% KSR. When supplemented with KSR-only, somatic cell confluency did not increase beyond 20% and as a result, the number of gonocytes was also smaller than that found in FBS-supplemented media. By Day 7, somatic cells formed spindle-shaped extensions on the culture dish (A), and their confluency gradually increased by Day 14 (B). In the presence of KSR, gonocytes showed a greater tendency to form small clusters, which gradually transformed into EBLCs by Day 21 (C). These EBLCs increased in size by fusion of adjacent individual gonocytes by Day 28 (D). The same morphology was observed in all KSR concentrations. (Scale bar = 100 μm)

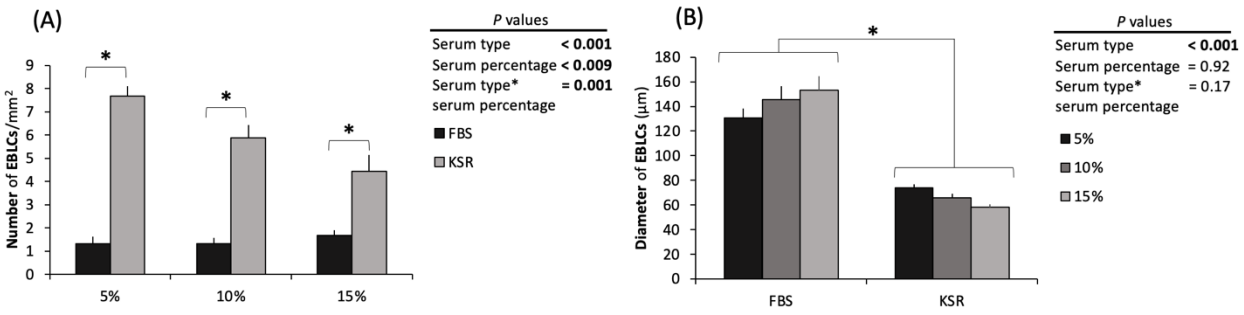

Fig. 3.5. Effects of DMEM combined with serum or serum replacement on EBLC numbers (mean ± SEM) (A) and diameters (mean ± SEM) (B). Greater numbers of EBLCs developed by Day 28 in groups supplemented with KSR (A). However, the diameters of EBLCs in KSR-supplemented groups were smaller than those formed in FBS-supplemented groups on Day 28 ($P < 0.001$) (B). Increased serum concentration led to an increase in EBLC formation, whereas less EBLCs were formed following increasing KSR concentrations (interaction $P = 0.001$). Asterisks denote significant differences and $P < 0.05$ was considered as the significance level.

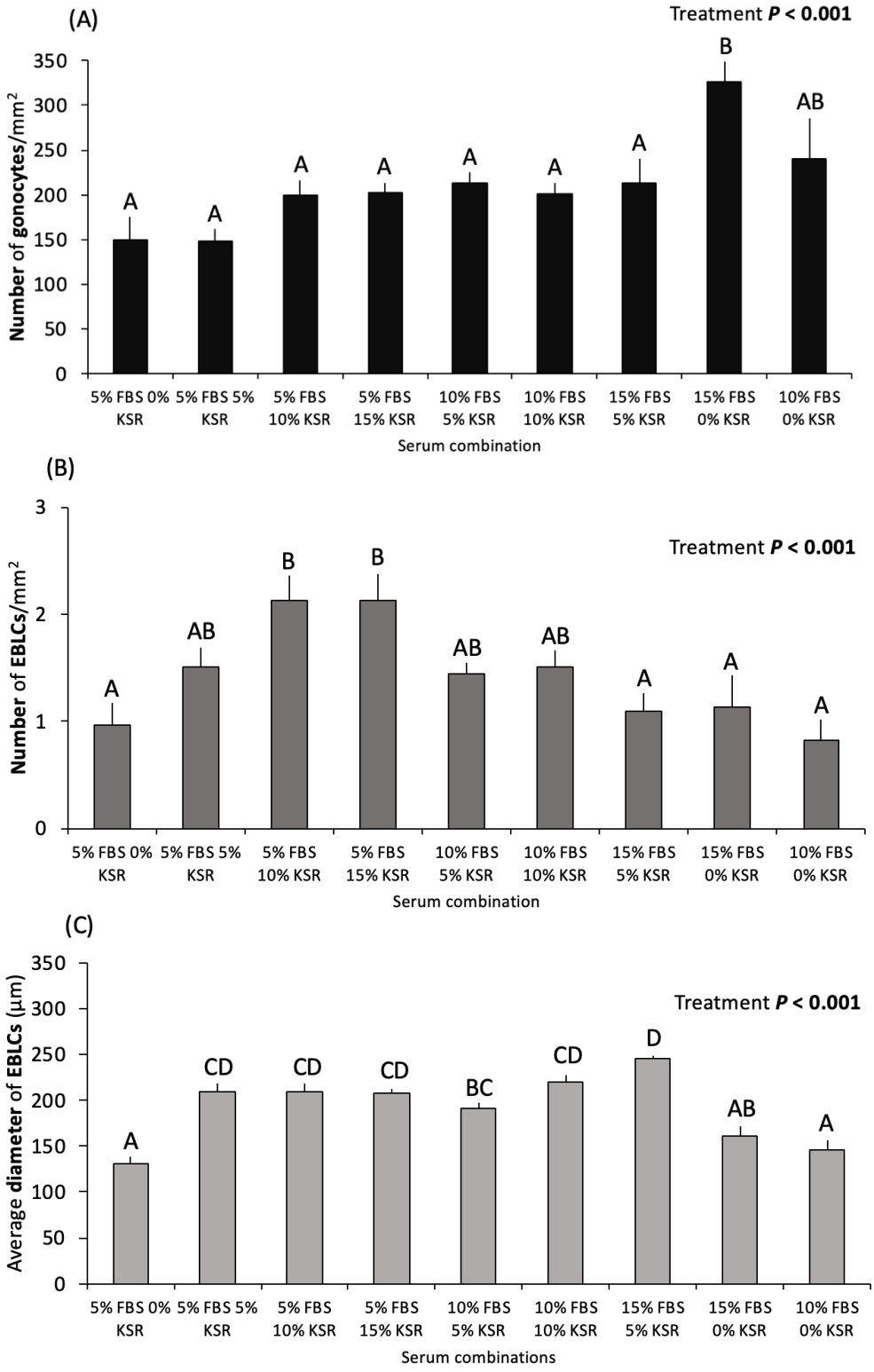
(A)
Treatment P < 0.001
Number of gonocytes/mm²
350
300
250
200
150
100
50
0
A
A
A
A
A
A
A
B
AB
5% FBS 0% KSR
5% FBS 5% KSR
5% FBS 10% KSR
5% FBS 15% KSR
10% FBS 5% KSR
10% FBS 10% KSR
15% FBS 5% KSR
15% FBS 0% KSR
10% FBS 0% KSR
Serum combination
(B)
Treatment P < 0.001
Number of EBLCs/mm²
3
2
1
0
A
AB
B
B
AB
AB
A
A
A
5% FBS 0% KSR
5% FBS 5% KSR
5% FBS 10% KSR
5% FBS 15% KSR
10% FBS 5% KSR
10% FBS 10% KSR
15% FBS 5% KSR
15% FBS 0% KSR
10% FBS 0% KSR
Serum combination
(C)
Treatment P < 0.001
Average diameter of EBLCs (µm)
350
300
250
200
150
100
50
0
A
CD
CD
CD
BC
CD
D
AB
A
5% FBS 0% KSR
5% FBS 5% KSR
5% FBS 10% KSR
5% FBS 15% KSR
10% FBS 5% KSR
10% FBS 10% KSR
15% FBS 5% KSR
15% FBS 0% KSR
10% FBS 0% KSR
Serum combinations

Fig. 3.6. Average number of gonocytes (mean ± SEM) (A) and EBLCs (mean ± SEM) (B) as well as the diameter of EBLCs (mean ± SEM) (C) in DMEM supplemented with combined concentrations of FBS and KSR on Day 28 of culture. Since DMEM supported the proliferation of testis cells and formation of the somatic cell monolayer, it was supplemented with combined concentrations of FBS and KSR to find the optimal conditions for gonocyte proliferation and EBLC formation. Among different treatments, the maximum number of gonocytes was observed in DMEM+15% FBS ($P < 0.001$) (A), while the maximum number of EBLCs developed in cultures with DMEM+5% FBS+10% or 15% KSR ($P < 0.001$) (B). Combined concentrations of FBS and KSR also led to formation of larger EBLCs compared with cultures where FBS- or KSR-only were used ($P < 0.001$) (C). Different letters denote significant differences and $P < 0.05$ was considered significant.

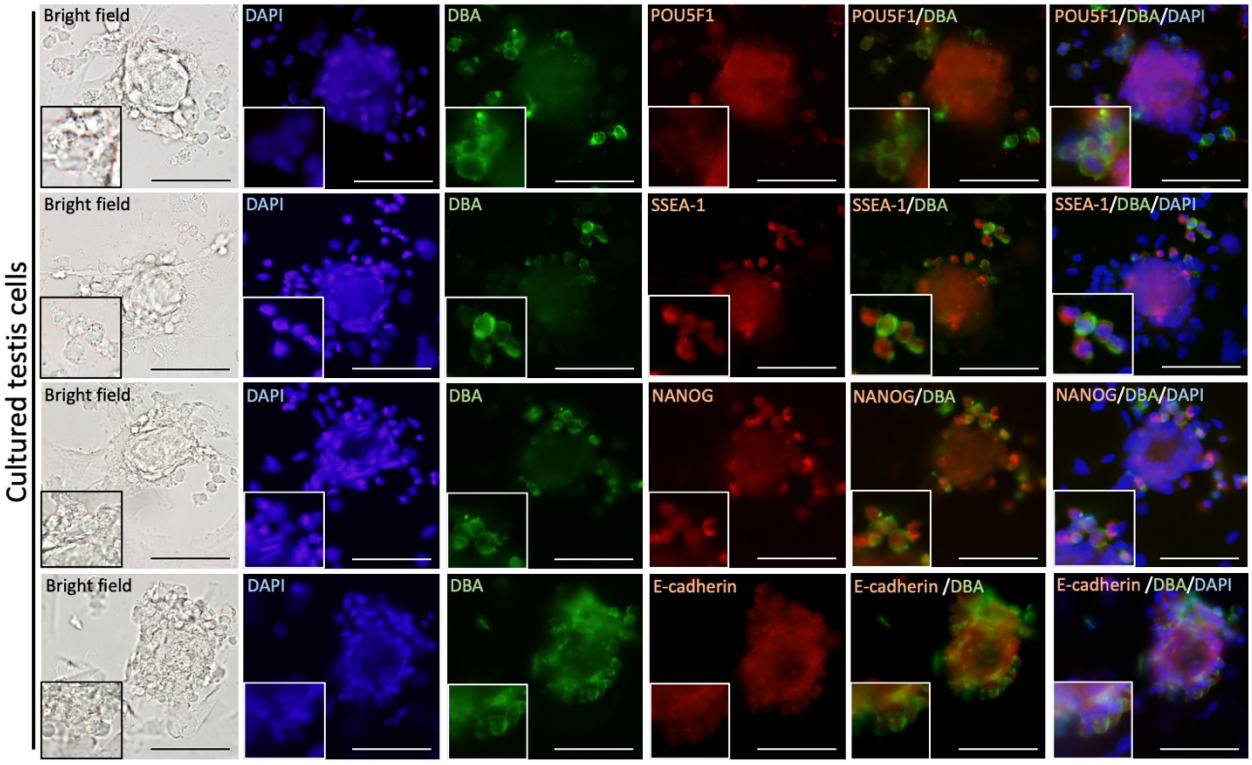
Cultured testis cells
Bright field
DAPI
DBA
POU5F1
POU5F1/DBA
POU5F1/DBA/DAPI
Bright field
DAPI
DBA
SSEA-1
SSEA-1/DBA
SSEA-1/DBA/DAPI
Bright field
DAPI
DBA
NANOG
NANOG/DBA
NANOG/DBA/DAPI
Bright field
DAPI
DBA
E-cadherin
E-cadherin /DBA
E-cadherin /DBA/DAPI

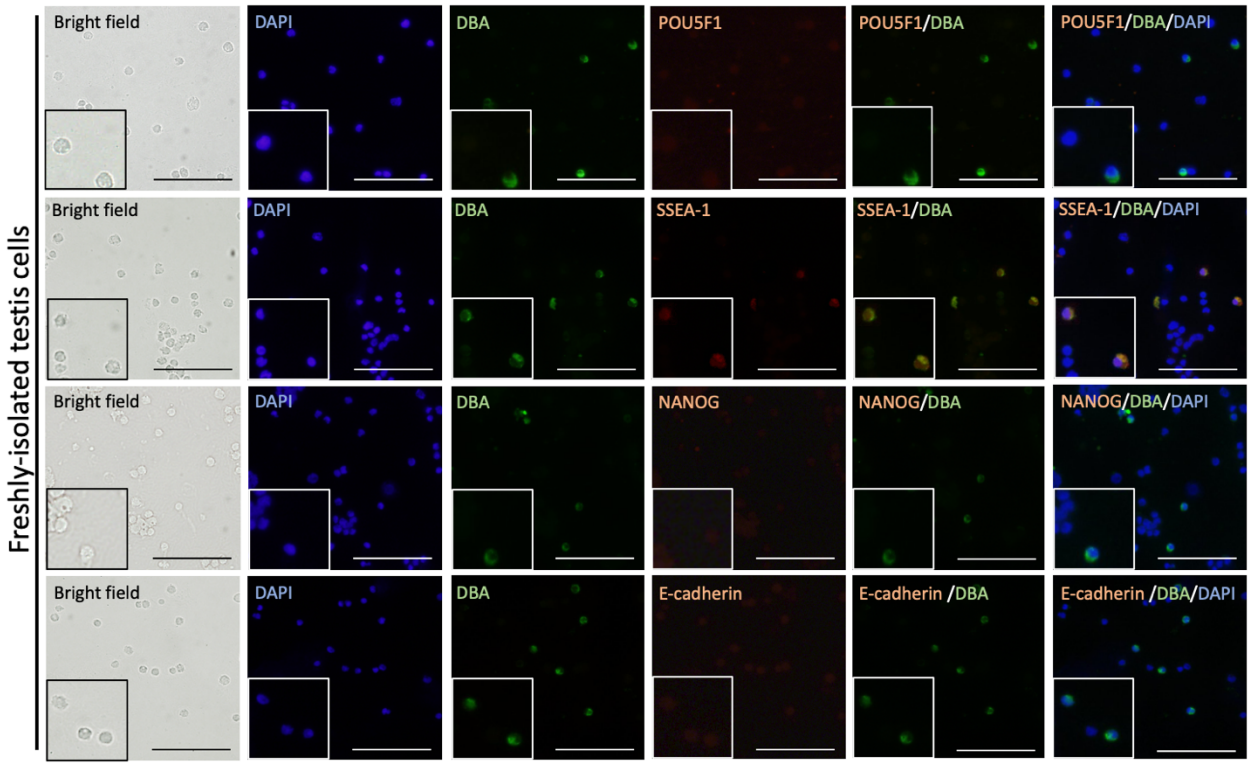
Freshly-isolated testis cells
Bright field
DAPI
DBA
POU5F1
POU5F1/DBA
POU5F1/DBA/DAPI
Bright field
DAPI
DBA
SSEA-1
SSEA-1/DBA
SSEA-1/DBA/DAPI
Bright field
DAPI
DBA
NANOG
NANOG/DBA
NANOG/DBA/DAPI
Bright field
DAPI
DBA
E-cadherin
E-cadherin /DBA
E-cadherin /DBA/DAPI

Fig. 3.7. Double immunocytochemistry of freshly-isolated and 28-day cultured porcine testis cells for gonocyte-specific and pluripotency-determining markers. Fluorescein isothiocyanate (FITC)-labeled *Dolichos biflorus* agglutinin (DBA-FITC) was used as a gonocyte-specific marker and pluripotency-determining markers including POU5F1, stage-specific embryonic antigen-1 (SSEA-1), homeobox NANOG, and anti-epithelial-cadherin (E-cadherin) in both gonocytes and EBLCs. Co-localization of the signals was indicative of germ- and stem-cell potential of 28-day cultured gonocytes. Cultured gonocytes and their developed EBLCs appeared positive for all pluripotency and gonocyte markers while testis cells in freshly-isolated cell smears appeared negative for POU5F1, NANOG, E-cadherin as pluripotency markers but were positive for SSEA-1. This may point to the *in vitro* changes in gonocytes to a pluripotent state in our optimized culture conditions while maintaining their germ cell potential. DAPI was used to stain the nuclei. Insets show a higher magnification. (Scale bar = 100 μm)

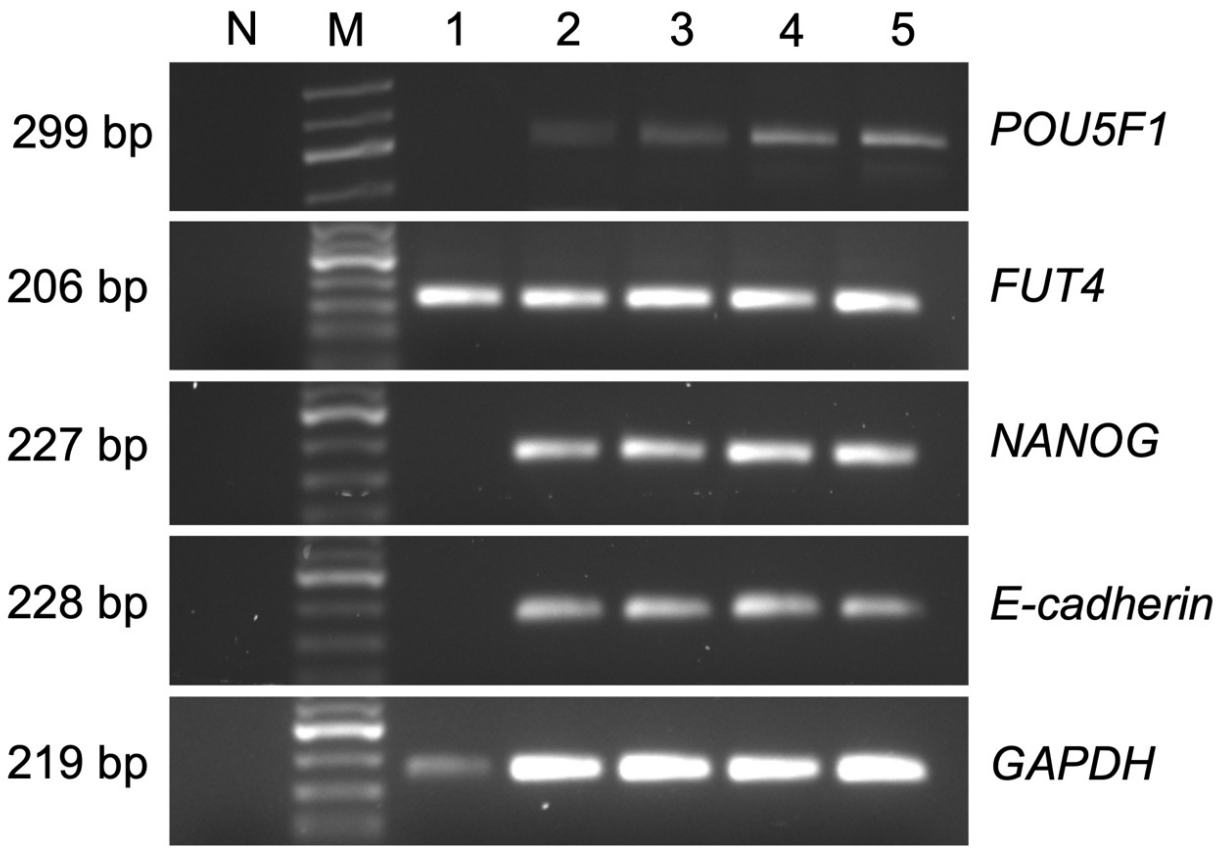

Fig. 3.8. Expression of pluripotency-determining gene transcripts in samples of freshly-isolated testis cells from neonatal piglets and those cultured for 7, 14, 21, or 28 days. In all the sampling time points, cultured testis cells showed positive expression of *POU5F1, FUT4, NANOG*, and *E-cadherin*. Freshly-isolated testis cells only appeared positive for *FUT4* as a common germ- and stem cell marker, and were negative for pluripotency-determining factors including *POU5F1*, *NANOG*, and *E-cadherin*. N, no template control; M, 50-bp DNA ladder; Lines 1-5, cDNA obtained from freshly-isolated testis cells, or those cultured for 7, 14, 21, or 28 days, respectively.

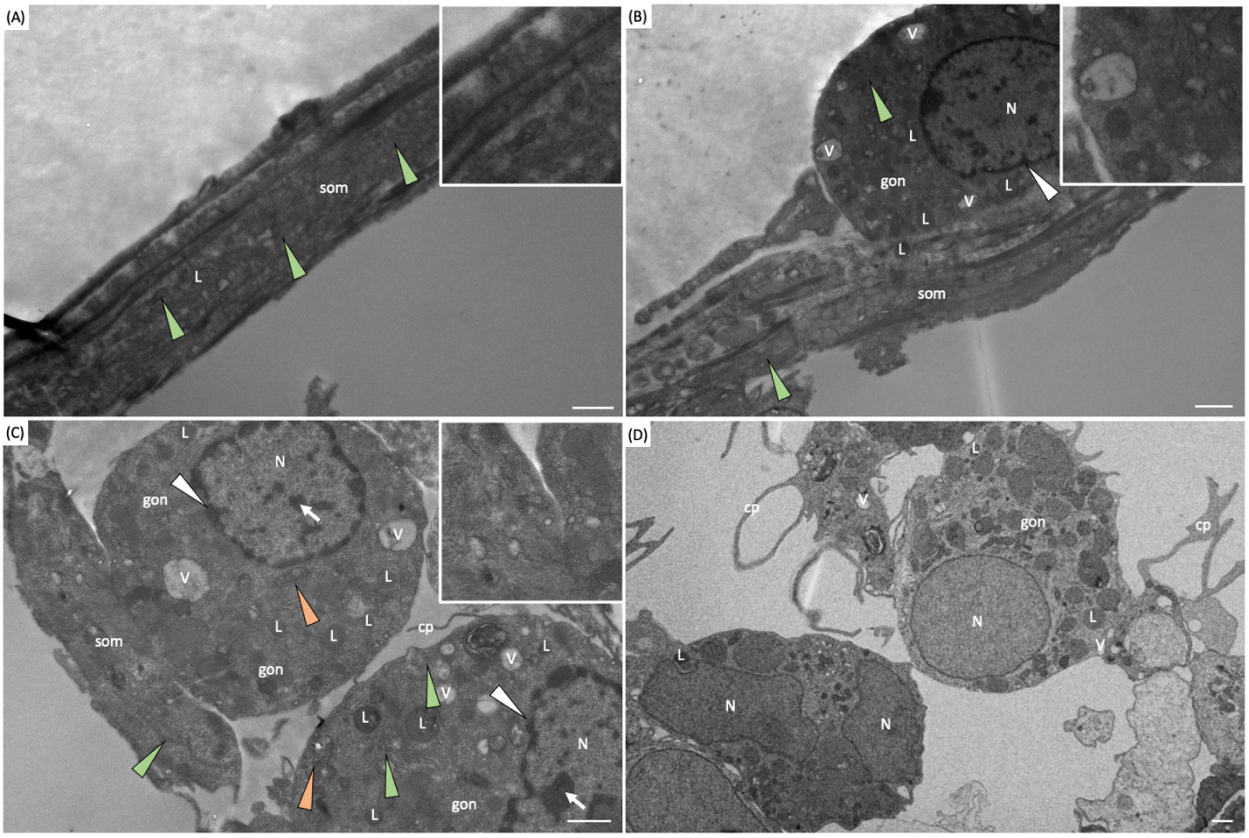

Fig. 3.9. Transmission electron microscopy of cultured porcine testis cells in the selected media and serum combination (DMEM+5% FBS+10% KSR). A somatic cell monolayer (som) covered the culture wells by Day 7 (A). The somatic cells contained different organelles including extended membrane stacks of rough endoplasmic reticulum (green arrowheads) and lysosomes (L). Gonocytes (gon) and somatic cells maintained a gap (B and C), which along with cytoplasmic projections (cp), enabled gonocytes to migrate freely on top of the monolayer. Gonocytes also contained multiple organelles including a large nucleus (N) which contained nucleoli (white arrows) and heterochromatin clusters (white arrowheads), rough endoplasmic reticulum (green arrowheads), lysosomes (L), mitochondria (orange arrowheads), and electron-lucent vesicles (V). Gonocytes appeared as singles (B), or in close contact with each other (C). Gonocytes initially formed clusters and merged to form 3-D colonies (D). Morphologically, gonocytes and EBLCs developed in DMEM supplemented with both FBS and KSR contained a large number of electron-lucent vesicles. (Scale bar = 2 µm)

3.5. Discussion

To our knowledge, the present study is the first to systematically investigate the effects of different culture media and various levels of serum or serum replacement on *in vitro* propagation of neonatal porcine gonocytes, their colony-formation potential, and expression of pluripotency-determining factors. Here, we defined an optimal combination of medium and serum/serum replacement which maximized the proliferation of gonocytes, encouraged their colony-formation, and induced their spontaneous transformation into a pluripotent state without addition of growth promoting factors or other supplements. We also examined the ultrastructure of EBLCs developed in the optimized medium and serum combination and found that each EBLC is comprised of a large syncytium with multiple nuclei and similar cytoplasmic organelles as in their surrounding gonocytes.

Development of a simple culture condition to maintain and propagate MGSCs remains a key challenge since the safety concerns in their downstream applications depend largely on their *in vitro* culture components. Medium and serum are the two main culture components, which expectedly affect the proliferation and colony-formation of MGSCs. We showed here that DMEM sufficiently supported *in vitro* propagation of gonocytes and somatic cells. DMEM is a standard media widely used for the culture of testis cells of different species (Wang *et al.* 2015; Niu *et al.* 2016; Awang-Junaidi and Honaramooz 2018; Sahare *et al.* 2018; Awang-Junaidi *et al.* 2020) and has twice the amino acid concentration and four times the amount of vitamins compared with DMEM/F12 and α-MEM. This composition might be an underlying mechanism for its great support for cell propagation and colony-formation in the present study (Schultheiss *et al.* 2013; Inoue *et al.* 2020). Although porcine gonocytes were previously cultured in DMEM/F12 (Goel *et al.* 2007), we showed moderate gonocyte proliferation in this medium, which might be the result of incomplete compatibility of porcine testis cells with components or concentrations of nutrients in this medium.

Similarly, we found limited growth of testis cells in α-MEM. α-MEM has been widely used to maintain a range of cells *in vitro* including neurons (Kanoh *et al.* 1991; Roudebush *et al.* 1994), osteoblasts (Coelho *et al.* 2000; Mizuno *et al.* 2000), and mesenchymal stem cells (Meuleman *et al.* 2006; Kang *et al.* 2012). This medium has a simple composition containing almost a quarter as much vitamins, amino acids, and glucose as DMEM, which can explain limited gonocyte proliferation in our study (Kanatsu-Shinohara *et al.* 2012; Aoshima *et al.* 2013; Kim *et al.* 2014;

Sahare *et al.* 2016; Suyatno *et al.* 2018). Here, we also showed reduced proliferative activity of testis cells in GMEM and RPMI media. GMEM is a modification of Eagle's medium with two times the levels of amino acids, vitamins, and tryptose phosphate broth. Although GMEM has been widely used to culture embryonic stem cells (Hamilton *et al.* 2019), its components may have contributed to the limited testis cell proliferation in the present study. We also found lowest testis cell proliferation in cultures containing RPMI medium. This medium is characterized by low levels of magnesium and calcium and high levels of phosphate (Yao and Asayama 2017), which may indicate that these two minerals play a key role in metabolism and proliferation of cultured testis cells and their absence can potentially limit germ cell proliferation. Overall, similar to our results, a previous study on mouse MGSCs showed that α-MEM, GMEM, and RPMI cannot support murine testis cell propagation *in vitro* (Kanatsu-Shinohara *et al.* 2014).

In the present study, StemPro with or without serum/serum replacement also failed to support gonocyte and somatic cell survival, indicating that it either lacks supportive components for somatic cell proliferation or has components which hamper their expansion. Somatic cells are crucial for survival and proliferation of gonocytes, and as such underdeveloped monolayer leads to loss of non-adherent gonocytes in culture (van Dissel-Emiliani *et al.* 1993; Awang-Junaidi and Honaramooz 2018). StemPro has also been used for *in vitro* culture of mouse SSCs but with limited cell proliferation, which further supports our findings (Kanatsu-Shinohara *et al.* 2014).

KSR is a serum-free formulation and a more defined substitute for FBS. Using KSR also provides more consistency since it eliminates batch to batch production variations in components (Hua *et al.* 2009). Compared with KSR, greater support of FBS for proliferation of testis cells can be attributed to the presence of various known and unknown compounds in the serum. In KSR-supplemented media, limited cell confluency and reduced somatic cell growth might have in turn encouraged gonocyte aggregation and formation of smaller EBLCs. Similar to our findings, previously, KSR supplementation increased colonisation of cultured bovine SSCs (Youssefi *et al.* 2016). Although in theory KSR is a more reliable and consistent alternative source for FBS, available literature on its application in culture of germ cells of different species shows an inconsistency in using a homogenous feeder layer to support the germ cell growth (Sato *et al.* 2011; Aoshima *et al.* 2013; Zhang *et al.* 2017). Taken together, enhanced proliferative potential of MGSCs in the presence of KSR might be due to the effect of serum replacement combined with

the support of an exogenous feeder layer (Wang and Hna 2008). However, in contrast to previous reports, we used testicular somatic cells as the feeder layer to eliminate this potential confounding influence when examining the direct effects of media and serum/serum replacement.

In studies on culture of MGSCs, the basal media is typically supplemented with either serum or serum replacement (Zhang *et al.* 2017; Awang-Junaidi and Honaramooz 2018; Sahare *et al.* 2018; Awang-Junaidi *et al.* 2020). As such, in Experiment 3.2 we investigated the effects of combined concentrations of FBS and KSR with DMEM on *in vitro* culture of neonatal porcine gonocytes. We showed that 15% FBS alone best suits gonocyte proliferation, where gonocytes could increase by up to ~35% compared with 10% FBS in DMEM in long-term culture. However, lowered numbers of gonocytes in cultures with 20% FBS are possibly the result of somatic cell overpopulation, which in turn limited the gonocyte proliferation. As described in previous reports, somatic cells tend to overgrow in the culture of testis cells, which is likely triggered by a combination of unknown factors in FBS (Shikina and Yoshizaki 2010; Zheng *et al.* 2014). Additionally, increases in concentration of FBS led to increased numbers of EBLCs. Given the pivotal role of somatic cells in providing the necessary foundation for EBLC formation, increased FBS concentration may have led to increased somatic cell population, which in turn provided the basis for formation of gonocyte clusters and subsequently EBLC formation. Here, we also showed that gonocytes and somatic cells require a proportionally combined concentration of FBS and KSR for enhanced EBLC formation. Perhaps combined FBS and KSR concentrations imposed a dual effect on cultured testis cells, where FBS enhanced somatic cell proliferation, which in turn led to formation of circular arrangements. Exposure to KSR on the other hand, encouraged gonocyte cluster- and EBLC formations. Similar results were shown previously in bovine SSC cultures (Youssefi *et al.* 2016). In addition, here, EBLCs in the combined FBS and KSR-supplemented media had larger diameters compared with FBS- or KSR-only cultures. *In vitro* aggregation of porcine gonocytes and subsequent formation of colonies have also been reported in different culture conditions (Goel *et al.* 2007, 2009; Kuijk *et al.* 2009; Lee *et al.* 2013; Awang-Junaidi and Honaramooz 2018). Here, the three-dimensional appearance of EBLCs resembled that of pluripotent ES cell colonies in culture (Lee *et al.* 2013; Sahare *et al.* 2016).

Introducing an alternative source for ES cells and iPSCs is of great interest since currently the application of these cells in stem cell therapy and regenerative medicine is associated with ethical

and safety concerns. Here, we demonstrated that cultured gonocytes and EBLCs express a number of pluripotency-determining factors that are typically present in ES cells and their colonies (Goel *et al.* 2009; Chen *et al.* 2010; Shi and Jin 2010; Wolf *et al.* 2011; Yang *et al.* 2015; Devi *et al.* 2017; Choi *et al.* 2019; Awang-Junaidi *et al.* 2020). We showed that the expression of all examined markers started from the first wk in culture without fold changes in their expression level over time. This is indicative of spontaneous changes happening in gonocytes when grown in our selected cultures. Among these markers, POU5F1 plays a central role in self-renewal of pluripotent ES cells (Nichols *et al.* 1998). Here, we also observed SSEA-1 expression in freshly-isolated and cultured gonocytes. In line with our findings, this marker is present in ES cells, neonatal murine germ cells, porcine PGCs, and spermatogonia in prepubertal pig testis (Goel *et al.* 2007; Kim *et al.* 2013; González and Dobrinski 2015). Additionally, here, expression of NANOG and E-cadherin was detected as early as 7 days in our selected cultures. Hence, this phenomenon also points at dedifferentiation of gonocytes to a more primitive stage in our selected cultures. Spontaneous dedifferentiation of human, porcine, and bovine germ cells in culture conditions has been also shown previously (Hoei-Hansen *et al.* 2005; Mirzapour *et al.* 2012; Kim *et al.* 2014). Collectively, this is an outstanding achievement since these cells can serve as an alternative source for ES cells and iPSCs. This in turn can eliminate the ethical concerns associated with the use of ES cells or limitations in development and use of iPSCs due to exogenous confounding factors.

TEM findings further confirmed our light microscopy observations where gonocytes represented different populations of cells, ranging from single, paired, or clustered groups to EBLCs. EBLCs contained multiple nuclei and a large cytoplasm, which perhaps formed during the fusion of cytoplasmic membranes of adjacent gonocytes. Because these cells were obtained from a mixed population of testis cells of healthy 1-wk old piglets and cultured for 4 weeks, senescence or pathological conditions as the leading cause of EBLC formation is not likely (Miething 1993, 1995; Gallagher *et al.* 2013; Hutson *et al.* 2013). Extensive migration ability of MGSCs has been shown following transplantation of germ cells from a donor male to the recipients, where the transplanted cells translocate from the luminal compartment of the seminiferous tubules to the basal compartment in order to colonize the recipient testis (Brinster and Zimmermann 1994; Brinster 2002; Honaramooz and Yang 2011). We speculate that a similar underlying trigger which initiates the migration of MGSC that find themselves ‘misplaced’ upon germ cell transplantation can possibly stimulate gonocytes to move *en masse* towards a more suitable environment which

in our 2-D cultures seemed to be the monolayer circular arrangements. The nature of such a trigger is not clear but it likely includes transcription factors produced by misplaced gonocytes and/or somatic cells that activate signalling cascades within gonocytes that initiate further development of the F-actin filaments, cytoskeleton, and extension of gonocyte cytoplasmic projections. Additionally, a narrow gap between gonocytes and the monolayer indicates the non-adherent nature of gonocytes, consistent with their extensive mobility. Also, compared with our findings in a previous report, (Awang-Junaidi *et al.* 2020) gonocytes and EBLCs in our selected media and serum combination (DMEM+5% FBS+10% KSR), possessed large numbers of electron-lucent vesicles in the cytoplasm; their presence can possibly point at greater secretory activity of gonocytes and EBLCs exposed to our selected culture conditions.

In conclusion, among the commonly used media, DMEM shows a greater support for the culture of gonocytes. This medium supplemented with 15% FBS or with a combination of 5% FBS+10% KSR provides the optimal condition to maximize the number of gonocytes and their resultant EBLCs, respectively. Importantly, gonocytes cultured in DMEM+15% FBS, without addition of growth factors or other supplements, spontaneously dedifferentiate into primitive stages and express markers that are normally present in ES cells. Overall, our findings provide a means to easily obtain large numbers of MGSCs. Furthermore, our results are indicative of the great potential of neonatal germ cells to be used as a source of stem- and germ cells for downstream applications in regenerative medicine, fertility preservation, or transgenesis.

Transition

In Chapter 3, we tested the effects of different media and serum/serum replacement combinations on proliferation, colony-formation, and pluripotency of porcine gonocytes and reported the optimal conditions to increase these cells and their colonies in an *in vitro* environment. In order to further enhance gonocyte proliferation and colony-formation, in Chapter 4 we used our selected condition in Chapter 3 to test the effects of individual or combined concentrations of three main growth factors on proliferation of gonocytes and formation of their colonies. In Chapter 4, we also evaluated the expression of pluripotency markers in the selected conditions.

CHAPTER 4

CULTURE SUPPLEMENTATION OF BFGF, GDNF, AND LIF ALTERS *IN VITRO* PROLIFERATION, COLONY-FORMATION, AND PLURIPOTENCY OF NEONATAL PORCINE GERM CELLS [3, 4]

4.1. Abstract

Gonocytes in the neonatal testis have male germline stem cell properties and as such have important potential applications in fertility preservation and regenerative medicine. Such applications require further studies aimed at increasing gonocyte numbers and evaluating their pluripotency *in vitro*. The objective of the present study was to test the effects of basic fibroblast growth factor (bFGF), glial cell-derived neurotrophic factor (GDNF), and leukemia inhibitory factor (LIF) on *in vitro* propagation, colony-formation, and expression of pluripotency markers of neonatal porcine gonocytes. Testis cells from 1-wk-old piglets were cultured in basic media (DMEM+15% FBS), supplemented with various concentrations of bFGF, GDNF, and LIF, either individually or in combinations, in a stepwise experimental design. Gonocytes and/or their colonies were evaluated every 7 days and the gonocyte- (DBA) and pluripotency-specific markers (POU5F1, SSEA-1, E-cadherin, and NANOG) assessed on Day 28. Supplementation of a basic medium consisting of DMEM+15% FBS with only 10 ng/mL bFGF can effectively maximize *in vitro* proliferation of porcine gonocytes. Furthermore, supplementation of LIF alone to the basic media can enhance porcine gonocyte colony-formation while the addition of 10 ng/mL bFGF+100 ng/mL GDNF+1500 U/mL LIF significantly increases EBLC diameters. The resultant gonocytes and colonies expressed both germ cell- and pluripotency-specific markers. These results shed light on growth hormone requirements of porcine gonocytes for *in vitro* proliferation and colony-formation.

[3] This manuscript has been submitted for publication in *Cell & Tissue Research* under joint co-authorship with Fahar Ibtisham, Tat-Chuan Cham, and Ali Honaramooz.

[4] MAF contributed to the experimental design, performed the study, and wrote the first draft of the manuscript. FI and TCC contributed to the collection of the samples and revised the manuscript. AH contributed to the experimental design, revised the manuscript, and supervised the project.

4.2. Introduction

During embryonic development, primordial germ cells (PGCs) colonize the developing gonad and form a transient population of primitive germ cells known as gonocytes (*i.e.*, prospermatogonia) that reside in the center of testicular cords (Culty 2009). After birth, these gonocytes gradually migrate towards the cordal basement membrane and transform into spermatogonial stem cells (SSCs). In the mature testis, SSCs maintain a reserve stem cell population within the seminiferous tubules by way of self-renewal while simultaneously producing generations of spermatogonia committed to successive divisions and differentiation. As such, SSCs establish and sustain a continuous process of spermatogenesis to produce a life-long supply of spermatozoa (Brinster 2002; Culty 2009; Ibtisham *et al*. 2020; Kuijk *et al*. 2009).

When SSCs, gonocytes, and even PGCs were transplanted into the testis of recipients, they were able to colonize the recipient seminiferous tubules and initiate donor-derived spermatogenesis (Brinster and Zimmermann 1994; Orwig *et al*. 2002; Chuma *et al*. 2005). Given this ability, SSCs, gonocytes, and PGCs are referred to as male germline stem cells (MGSCs) (Ibtisham and Honaramooz 2020). Importantly, the transfer of MGSCs from a fertile donor into the testes of an infertile mouse can restore the fertility potential of the recipient (Kanatsu-Shinohara *et al*. 2003; Kubota *et al*. 2004). SSCs in particular can be cultured long-term or cryopreserved for years, and still maintain their potential to initiate spermatogenesis when transferred into recipient testes (Kanatsu-Shinohara 2005; Wu *et al*. 2012). Furthermore, SSCs and gonocytes from diverse species, including pigs, can be genetically manipulated prior to the transplantation into wild-type recipient testes to generate transgenic-sperm producing recipients (Honaramooz *et al*. 2008; Zeng *et al*. 2013, 2012). Transplantation of germ cells (containing SSCs) is hence viewed as an alternative strategy to produce transgenic founders, especially in farm animals, where true embryonic stem cell lines are not yet available (reviewed in Honaramooz and Yang 2011; Ibtisham *et al.* 2020; Savvulidi *et al*. 2019). Interestingly, upon being cultured, mouse germ cells can form embryonic stem (ES)-like cells and colonies that express several pluripotency-determining markers and have the potential to contribute to development of chimeras (Guan *et al.* 2006; Kanatsu-Shinohara *et al.* 2004). Therefore, MGSCs hold great promise for various basic and clinical applications including potential use in genetic conservation, infertility treatment, and regenerative medicine (Chen *et al*. 2020; Wang *et al*. 2015).

The potential use of MGSCs for downstream applications depends greatly on our expanding ability to isolate, identify, enrich, culture, and manipulate these cells *in vitro*. Among MGSCs, gonocytes tend to be most readily available, given that they are the only type of germ cell present in the neonatal testis. Relatively large numbers of gonocytes can be collected from the neonatal testes of livestock (*e.g.*, after routine castration of piglets) and identified using their unique morphology or specific cell-surface markers (*e.g.*, VASA, DAZL, DBA, and UCH-L1) (Awang-Junaidi and Honaramooz 2018; Culty 2009; Goel *et al*. 2007). Upon enzymatic digestion of neonatal rodent or porcine testis tissue using conventional protocols, ~2% or ~7% of the resultant testis cells are expected to be gonocytes (Lee *et al*. 2013; Honaramooz *et al*. 2005). There is a direct relationship between the number of donor germ cells transplanted and the degree of recipient testis colonization (Honaramooz and Yang, 2011). Therefore, different approaches have been taken to increase gonocyte numbers, including *in vitro* proliferation in culture, differential plating, magnetic activated cell sorting (MACS), fluorescence activated cell sorting (FACS), and the utilization of cell-specific markers (Kim *et al*. 2010). To obtain an enriched population of neonatal porcine gonocytes, we have developed an optimized three-step enzymatic digestion method which yields cell aggregates comprised of ~40% gonocytes (Yang and Honaramooz 2011; Yang *et al*. 2010). Further, a combination of the foregoing cell isolation method with Nycodenz centrifugation and differential plating can result in a highly enriched and homogenous cell population, comprised of ~90% gonocytes (Yang and Honaramooz 2011).

Each of these approaches for obtaining a sufficient proportion of MGSCs may be suitable for different applications. While isolation and enrichment of MGSCs from a fresh tissue may seem ideal, it is not always possible nor desirable to use fresh tissue as the primary source. For example, one of the envisioned clinical applications for MGSCs is their use in preserving the fertility potential of preadolescent boys undergoing cancer therapy; many prepubertal oncology patients face infertility in adulthood due to the gonadotoxic effects of chemotherapy and total body irradiation. In such cases, cryopreserved tissue acts as the primary source of MGSCs. Prior to the start of these treatments, small biopsies of the immature testis tissue can be obtained and cryopreserved long-term for potential future use if the individual indeed becomes infertile (reviewed in Honaramooz 2012; Ibtisham and Honaramooz 2020). While there seem to be no limit in the number of years cryopreserved MGSCs can maintain their developmental potential (Wu *et al*. 2012), the small size of a typical single testis biopsy (~31 mg) is unlikely to provide enough

MGSCs to repopulate the recipient testis without their further *in vitro* expansion (Wu *et al*. 2009). Further, the investigation into optimal culture conditions is also required for fundamental understanding and manipulation of male germ cells. Optimizing culture conditions for MGSCs is especially important for their *in vitro* development, proliferation, differentiation, and eventual production of haploid germ cells. Additionally, optimized culture systems would enable experimentations that are otherwise difficult to be performed *in vivo*, such as the pharmaceutical or toxicological study of new drugs or potential toxicants on development of neonatal human germ cells. Other applications include the study of mechanisms of testicular tumors, genetic causes of male infertility, or even correction of genetic disorders causing infertility (reviewed in Ibtisham and Honaramooz 2020). Cultured germ cells can also develop ES-like cells and colonies to be used as a source of pluripotent stem cells or undergo *in vitro* differentiation into any of the three germinal layer lineages for downstream applications in cell-based therapy (Kubota and Brinster 2006; Mirzapour *et al*. 2012; Phillips *et al*. 2010).

Within the *in vivo* environment of the seminiferous tubules, germ cell survival, proliferation, and differentiation depend on a variety of growth factors and cytokines released by the stem cell niche. Expectedly, these growth factors are equally important for the proliferation of germ cells *in vitro*. Among these growth factors are different types of fibroblast growth factors (FGF) which are necessary for fetal and neonatal testis development (Shubhada *et al.* 1993; Skinner 2005; van Dissel-Emiliani *et al*. 1996). For instance, basic fibroblast growth factor (bFGF), a member of the FGF family, is involved in the proliferation of testis somatic cells (*e.g.*, Sertoli and Leydig cells) and has stimulating effects on gonocyte self-renewal. The expression of *Etv5*, a transcription factor essential for self-renewal of SSCs, is also upregulated by bFGF; indicative of direct and indirect effects of this growth factor on proliferation of spermatogonia (Phillips *et al*. 2010; Schlesser *et al*. 2008). Another major regulator of the seminiferous niche is the glial cell-derived neurotrophic factor (GDNF) secreted by Sertoli cells (Tadokoro *et al*. 2002; Takahashi 2001). Self-renewal of gonocytes also depends on the paracrine release of GDNF; *in vivo* overexpression of this factor is shown to block SSC differentiation. Furthermore, mouse germ cells developed in culture media supplemented with GDNF successfully colonized the recipient seminiferous tubules following transplantation (Nagano *et al*. 2003). Leukemia inhibitory factor (LIF) was also shown to be an essential component for the long-term culture of PGCs and embryonic germ cells, which acts by triggering a signalling cascade involved in the propagation of stem cells (Kubota *et al*. 2004;

Piquet-Pellorce *et al*. 2000). However, the presence of growth factors can potentially lead to overgrowth of somatic cells, including fibroblasts, Sertoli cells, and endothelial cells, which in turn may hinder survival of germ cells (Guan *et al.* 2006). Importantly, there is limited information available on the effects of these growth factors on the stem cell function of porcine germ cells (Kuijk *et al.* 2009).

In preliminary studies, we tested various culture conditions, comprised of different media and serum sources, and found a combination that resulted in ~35% increase in gonocyte proliferation. Combining the latter findings with supplementation of select growth factors can potentially have additive effects on *in vitro* proliferation and colony-formation of gonocytes. As such, the objective of the present study was to test the effects of bFGF, GDNF, and LIF, supplemented individually or in combination, using a stepwise manner, on proliferation, colony-formation, and expression of the pluripotency-determining markers of neonatal porcine gonocytes.

4.3. Materials and Methods

4.3.1. Study Design

As outlined in Figure 4.1, to test the effects of individual and combined growth factors on neonatal porcine testis cells, the present study consisted of two main experiments conducted in a stepwise manner. For Experiment 4.1, using a total of 20 groups, we tested the effects of three different concentrations of three different growth factors (bFGF, GDNF, and LIF) alone by adding each to Dulbecco's modified Eagle's medium (DMEM), supplemented with either 15% fetal bovine serum (FBS) or 15% knockout serum replacement (KSR). After analyzing the effects on cultured cells, a single group with the optimal effects was selected for further investigations. In Experiment 4.2, we examined an additional 6 groups by starting with the selected group from Experiment 4.1 (a given concentration of a given growth factor), to test the effects of combining this mixture with three different concentrations of the next growth factor. This was followed by analysis and selection of an optimal group to test the effects of combining this new mixture with three different concentrations of the remaining growth factor using an additional 7 groups. A final culture condition (group with optimal concentrations of all three growth factors) was then selected to examine the expression of pluripotency-determining factors of its gonocytes and colonies.

4.3.2. Collection of Testes and Isolation of Testis Cells

The procedures used for the collection of piglet testes and isolation of testis cells have been described in greater detail (Awang-Junaidi and Honaramooz 2018). In summary, testes were obtained aseptically from ~1 wk-old Yorkshire-cross piglets (n = 180) during routine weekly castrations at a university affiliated swine facility (Prairie Swine Center, Saskatoon, SK, Canada). All experiments involving animals were reviewed and approved by the University of Saskatchewan's Institutional Animal Care and Use Committee (Protocol # 20080042). The testes were cooled immediately, transferred to the laboratory within ~1 h, and the testis parenchyma was harvested. The tissue underwent our afore-established three-step enzymatic digestion method (Yang *et al*. 2010) which yields a mixed population of testis cells containing ~40% gonocytes. We have previously shown that the characteristics of testis cells from this source are consistent over time (Yang *et al.* 2010).

For each treatment group, multiple replicates were prepared; each round of cell isolation was regarded as an individual replicate. To prepare each replicate of testis cells for culture, ~5 testes were used. Briefly, the parenchyma was completely minced for 5 min using fine scissors, the resultant suspension vortexed for 60 sec, and then digested at 37° C for 10 min using an enzymatic cocktail containing 0.2% w/v collagenase IV (catalogue no. C153; Sigma-Aldrich, St Louis, MO, USA), 0.1% w/v hyaluronidase (catalogue no. H3884; Sigma-Aldrich), and 0.01% w/v deoxyribonuclease (DNase; catalogue no. FN25; Sigma-Aldrich) in Dulbecco's modified Eagles medium (DMEM; catalogue no. 12-604F; Corning, New York, NY, USA) with 1% w/v antibiotic. The digestion was stopped by addition of fetal bovine serum (FBS; catalogue no. A15-701; PAA Laboratories, Etobicoke, ON, Canada), followed by vortexing for 30 sec, filtration using 40-µm cell strainers, centrifugation at 500× *g* at 16° C for 5 min, elimination of the erythrocytes, and two rounds of rinsing and centrifugation (Awang-Junaidi and Honaramooz 2018).

All the growth factors were reconstituted at 100 µg/mL in Dulbecco's phosphate-buffered saline (DPBS; catalogue no. 20-031-CV; Mediatech, Manassas, VA, USA), containing 0.1% bovine serum albumin (BSA; catalogue no. 2452C055; Amresco, Solon, OH, USA), aliquoted, and stored at –80° C upon arrival. To prepare different dilutions from each growth factor, prepared aliquots were thawed at 37° C and mixed with DMEM based on the final required concentration. For Experiment 4.1, after the last centrifugation, the cell pellets were resuspended in DMEM+15%

FBS or DMEM+15% KSR with 1% w/v antibiotics, supplemented with one of three individual concentrations of bFGF (0.1, 1, or 10 ng/mL; catalogue no. 233-FB-025; R&D Systems, Minneapolis, MN, USA), GDNF (10, 50, or 100 ng/mL; catalogue no. 212-GD-010; R&D Systems), or LIF (1000, 1200, or 1500 U/mL equivalent to 10000, 12000, and 15000 pg/mL, respectively; catalogue no. 7734-LF-025; R&D Systems).

For Experiment 4.2, the resultant cell pellets were mixed with DMEM+15% FBS+1% w/v antibiotics, supplemented with the optimal individual bFGF concentration and each concentration of GDNF (10, 50, and 100 ng/mL). However, due to the low cell confluency in KSR-treated wells after 21 days of culture, these were not included in further analyses. For the next step of Experiment 4.2, after the last round of centrifugation, cell pellets were mixed with DMEM+15% FBS+1% w/v antibiotics supplemented with the optimal concentrations of bFGF+GDNF in combination with each LIF concentration (1000, 1200, or 1500 U/mL). By gentle pipetting, the cell pellets were mixed with media and growth factor combinations, to prepare a single cell suspension for each treatment. For control groups in Experiment 4.1, cell pellets were resuspended in DMEM+15% FBS or DMEM+5% FBS+10% KSR without growth factor supplementation. For control groups in Experiment 4.2, pellets were mixed with DMEM+15% FBS or DMEM+5% FBS+10% KSR either without growth factor supplementation, with bFGF, or bFGF+GDNF supplementation (Fig. 4.1).

4.3.3 Evaluation of Viability and Number of Isolated Cells

Cell count and assessment of cell viability were performed immediately after isolation of testis cells and again after 28 days of culture for randomly selected culture wells (n = 3 per treatment) using the trypan blue exclusion technique. Briefly, to detach the cultured cells on Day 28, the media was removed and 1 mL of DPBS was added to each well to wash the remnant media. DPBS was then removed and 1 mL of 0.25% (w/v) trypsin in Hank's balanced salt solution (HBSS) and 2.21 mM EDTA (catalogue no. 25-053-CI; Mediatech) was dispensed in each well. The culture plates were placed at 37° C for ~3 min, 1 mL of undiluted FBS was added to each well to terminate the digestion, and the suspended cells were centrifuged at 500× g at 16° C for 5 min. The supernatant was removed, and the resultant cell pellet was resuspended in DMEM. Freshly isolated and cultured cells were each mixed with 1:1 ratio of trypan blue (100 µL of 0.4% in saline; catalogue no. T8154; Sigma-Aldrich) and 20 µL of the resultant suspension was dispensed on a

hemocytometer chamber. The number of live and dead cells were counted under a light microscope (Nikon, Eclipse E100). Percentage of cell viability and cell yield were calculated based on an average of two counts for each replicate or culture well. Also, gonocytes were visualized using a gonocyte-specific marker and their percentage was calculated on freshly isolated and cultured cell smears (Awang-Junaidi and Honaramooz 2018).

4.3.4. Cell Culture

Prepared cell suspensions for each treatment were seeded at a density of 3.0×10^5 cell/well in 6-well plates (catalogue no. 353046; Corning). The seeded cells were then provided with DMEM+15% FBS or DMEM+15% KSR, containing 1% w/v antibiotics along with individual and/or combined concentrations of bFGF, GDNF, and/or LIF (treatments). The optimal bFGF concentration which led to the maximum number of gonocytes in Experiment 4.1 was used in Experiment 4.2 in combination with different concentrations of GDNF and LIF. For control groups, cells were cultured in DMEM+15% FBS or DMEM+5% FBS+10% KSR without growth factor supplementation. More specifically, when comparing the number of EBLCs, DMEM+5% FBS+10% KSR was used as a control since we previously showed that this treatment leads to the greatest EBLC numbers in cultures without additional growth factor supplementation. The treatment groups (n = 3 replicates per treatment) were as follows:

– *Experiment 4.1 (an individual concentration of each growth factor):*

- DMEM+15% FBS supplemented with 0.1, 1, or 10 ng/mL bFGF (*i.e.*, 3 groups)
- DMEM+15% KSR supplemented with 0.1, 1, or 10 ng/mL bFGF (*i.e.*, 3 groups)
- DMEM+15% FBS supplemented with 10, 50, or 100 ng/mL GDNF (*i.e.*, 3 groups)
- DMEM+15% KSR supplemented with 10, 50, or 100 ng/mL GDNF (*i.e.*, 3 groups)
- DMEM+15% FBS supplemented with 1000, 1200, or 1500 U/mL LIF (*i.e.*, 3 groups)
- DMEM+15% KSR supplemented with 1000, 1200, or 1500 U/mL LIF (*i.e.*, 3 groups)
- DMEM+15% FBS without growth factor supplementation
- DMEM+5% FBS+10% KSR without growth factor supplementation

– *Experiment 4.2 (combined concentrations of growth factors):*

- **(First step)** DMEM+15% FBS supplemented with the selected bFGF concentration and 10, 50, or 100 ng/mL GDNF as well as three different control groups (*i.e.*, 6 groups)

- **(Second step)** DMEM+15% FBS supplemented with the selected bFGF+GDNF concentration and 1000, 1200, or 1500 U/mL LIF as well as four different control groups (*i.e.*, 7 groups)

Each replicate for each treatment group was cultured in two separate wells of a 6-well plate using our overall optimized culture conditions (Awang-Junaidi and Honaramooz 2018). The cells were incubated at 37° C with 5% CO_2 and 95% humidity and monitored twice daily using an inverted phase contrast microscope (Nikon, Eclipse TS100). The media was replenished every 7 days using the same components described above, and the cells were maintained for 28 days.

4.3.5. Imaging and Assessment of Cultured Cells

For each experiment, using an inverted phase contrast microscope equipped with a camera (Sony α5000, Sony Corporation, Tokyo, Japan), photomicrographs were captured from both wells of each replicate of all treatment groups. On Days 7, 14, 21, and 28 of culture, images were captured from randomly selected fields of view from each well at 40× and 200× magnifications (n = 10 images per magnification). On Day 28, the visual quantification and morphometrical evaluation of gonocytes and/or EBLCs (if present) were conducted using 40× magnification images using ImageJ software (ImageJ, U.S. National Institutes of Health, Bethesda, MD, USA). On Day 28, the average diameter of EBLCs in X and Y axes was also calculated using 200× magnification images. When cultured, gonocytes typically form clusters and colonies and as such, multiple gonocytes in close contact with an identifiable interface were counted as separate cells (Awang-Junaidi and Honaramooz 2018).

4.3.6. Immunocytochemistry

Cell samples from both the freshly isolated and cultured cells of different treatment groups, with the maximum number of gonocytes, were examined further for the expression of gonocyte-specific and pluripotency-determining markers. To obtain samples, the cells were cultured on 22 × 22 mm coverslips (catalogue no. 12-540B; Thermo Fisher Scientific), coated with 0.01% w/v poly-L-lysine solution. Preparation of coverslips was performed as described previously with minor modifications (Awang-Junaidi and Honaramooz 2018). Briefly, coverslips were placed in sterile metal racks (catalogue no. 114; Thermo Fisher Scientific) and immersed in 1% HCL in 70% alcohol for 10 min. Next, the racks were transferred from the acid-alcohol solution to a biosafety

cabinet under sterile conditions to air-dry for 20 min. A diluted solution of poly-L-lysine 0.01% w/v was prepared from 0.1% w/v stock solution (catalogue no. P8920; Sigma-Aldrich), in which the metal rack containing the coverslips was immersed for 20 min. The coverslips were air-dried overnight in the biosafety cabinet and were placed in each well using sterile conditions.

Gonocytes and EBLCs were identified using (FITC)-labeled *Dolichos biflorus* agglutinin (DBA-FITC; catalogue no. FL1031; Vector Labs, Burlington, ON, Canada) (Awang-Junaidi and Honaramooz 2018; Goel *et al*. 2007). POU5F1 (OCT4) (Choi *et al.* 2019; Shi and Jin 2010), homeobox NANOG (Choi *et al.* 2019; Yang *et al*. 2015), and epithelial-cadherin (E-cadherin) (Chen *et al*. 2010; Wolf et al. 2011) were used as pluripotency-determining factors, and stage-specific embryonic antigen-1 (SSEA-1) (Choi *et al*. 2019) was used as a dual germ-cell- and pluripotency-determining marker. Cell smears of the freshly isolated testis cells and coverslips with cultured cells obtained on Day 28 were washed 3 times with PBS containing 0.1% Tween-20 (PBST; catalogue no. J60304; Alfa Aesar, Tewksbury, MA, USA), followed by fixation with a 4% paraformaldehyde solution for 6 min. The samples were washed again with PBST 3 times, 3 min each, and incubated at room temperature with a blocking solution of 5% BSA for 30 min in a humidified chamber. After removal of BSA, each sample was covered with 1:100 concentration of both DBA-FITC and one of the primary antibodies at 4° C overnight. Primary antibodies for pluripotency-determining factors were anti-POU5F1 antibody (rabbit polyclonal to POU5F1; catalogue no. AB18976; Abcam, Toronto, ON, Canada), anti-SSEA-1 antibody (mouse monoclonal to SSEA-1; catalogue no. sc-21702; Santa Cruz Biotechnology; Santa Cruz, CA, USA), anti- NANOG antibody (mouse monoclonal to NANOG; catalogue no. N3038; Sigma-Aldrich), and anti-E-cadherin antibody (rabbit polyclonal to E-cadherin; catalogue no. 15148; Abcam). Next, the samples were washed 3 times, 3 min each, with PBST and covered with diluted (1:200 concentration) Alexa Fluor 594-conjugated goat anti-rabbit IgG (catalogue no. AB150088; Abcam) or Alexa Fluor 594-conjugated goat anti-mouse IgG (catalogue no. 150116; Abcam) at room temperature for 1 h. The samples were washed with phosphate buffered saline (PBS; catalogue no. 21-040-CV; Corning) 3 times, 3 min each, and placed on glass slides (catalogue no. 22-0370246; Thermo Fisher Scientific) using a mounting medium with 4′, 6-diamidino-2-phenylindole (DAPI; catalogue no. H-1200; Vector Labs).

Photomicrography from the samples was performed at 40× using a DAPI filter set (catalogue no. 49000; Chroma, Bellows Falls, VT, USA; excitation 350 nm/50 nm and emission 460 nm/50 nm), a FITC filter set (catalogue no. 49008; Chroma; excitation 470 nm/40 nm and emission 525 nm/50 nm), and a Texas Red filter set (catalogue no. 49008; Chroma; excitation 560 nm/40 nm and emission 630 nm/75 nm) to observe DAPI, FITC, and Alexa Fluor 594, respectively.

4.3.7. Extraction of RNA and RT-PCR

To determine the expression of pluripotency markers by developed gonocytes and/or EBLCs on Days 7, 14, 21, and 28, selected treatments were used for reverse-transcriptase polymerase chain reaction (RT-PCR) analysis. Cultured cells in randomly selected wells were suspended at each sampling time-point using trypsin-EDTA as described above, and the resultant suspension was centrifuged at 500× *g* at 16° C for 5 min. The cell pellet was washed with DPBS and centrifuged using the same settings. RNA extraction from the freshly isolated and cultured cells was then performed using Invitrogen RNAqueous Micro Total Isolation Kit (catalogue no. AM1931; Thermo Fisher Scientific), according to the manufacturer's instructions and as described in Chapter 3. Details of the primers used for RT-PCR analysis were as described in Chapter 3.

4.3.8. Statistical Analyses

The presented data are mean ± standard error of mean (SEM) and $P < 0.05$ was considered as significant. For all comparisons, one-way analysis of variance (ANOVA) and repeated measures ANOVA were used with Tukey's HSD as the post hoc test. All analyses were performed using the Statistical Package for Social Sciences (IBM SPSS Statistics for Macintosh, Version 26.00; IBM Corporation, Armonk, NY, USA).

4.4. Results

4.4.1. Testis Cell Count and Viability Assessment

Using the trypan blue exclusion technique, the viability of both freshly isolated and dissociated cultured testis cells from Day 28 was greater than 95% in all treatment groups. Also, using immunocytochemistry against DBA, the population of gonocytes in smears prepared from the freshly isolated testis cells was ~40%. The number of gonocytes in groups treated only with 10 ng/mL bFGF increased ~2-fold from Day 7 to Day 28. This number also increased ~3-fold in

groups treated with combined concentrations of 10 ng/mL bFGF+100 ng/mL GDNF and 10 ng/mL bFGF+100 ng/mL GDNF+1500 U/mL LIF.

4.4.2. Cell Development and Morphology

4.4.2.1. Experiment 4.1: Effects of Individual Growth Factors

The cell suspension at the time of seeding contained ~40% gonocytes. During the first 24 hr of culture, when observed using a conventional phase-contrast microscope, the cells in all treatment groups remained floating in the media and appeared heterogenous in shape. After 24 h, increasing numbers of somatic cells settled and adhered to the culture, forming sparse and irregular-shaped flattened cytoplasmic extensions, while most of the original cell mixture continued floating in the media. This pattern continued and after 7 days these somatic cells completely covered the culture well, forming a wave-shape monolayer with >90% confluency in all treatment groups (Fig. 4.2A). Round gonocytes appeared as single cells, pairs, or clusters of multiple cells sitting on top of the somatic cell monolayer (Fig. 4.2A and 4.2B). Gradually, the somatic cells extended their cytoplasmic projections further and in sparse locations formed 'circular growth arrangements', in which a disproportionate number of gonocytes aggregated and formed clusters. By Day 14, the gonocyte clusters converged to form large 3-D colonies with multiple nuclei. These colonies, known as EBLCs, appeared in miscellaneous shapes, and gradually enlarged via coalescence of surrounding individual gonocytes in all treatment groups. From Day 14 to 28, the gonocyte clusters and EBLCs became more prevalent and appeared in larger dimensions (Fig. 4.2C and 4.2D).

In all KSR-supplemented groups, regardless of the growth factor used, cell confluency did not improve beyond ~20% and somatic cells appeared sparse on the culture well (Fig. 4.2E). In all cultures with KSR, gonocytes aggregated and formed small clusters which, by Day 14, converged, formed small 3-D colonies (Fig. 4.2F) and gradually enlarged further (Fig. 4.2G and 4.2H). As a result of the underdeveloped somatic cell monolayer, low confluency, and small numbers of gonocytes, the KSR-treated groups were excluded from further analyses.

On Days 7, 14, 21, and 28, the greatest number of gonocytes was found in cultures supplemented with 10 ng/mL bFGF ($P < 0.001$; Fig. 4.3A). On Day 28, the number of gonocytes was ~44% greater in the group supplemented with 10 ng/mL bFGF compared with the control ($P < 0.001$; Fig. 4.3A) in which no growth factor was added (DMEM+15% FBS). Also on Day 28, this number

in cultures containing 10 ng/mL bFGF was ~13% or ~75% greater than those containing the highest concentrations of GDNF or LIF, respectively ($P < 0.001$; Fig. 4.3A). From Day 7 to 28, the gonocyte numbers increased by ~2-fold in the 10 ng/mL bFGF treatment group (Fig. 4.3B). However, since KSR supplementation alone did not result in satisfactory cell growth, at this time, we also tested the effects of combining FBS and KSR in the same media (DMEM+5% FBS+10% KSR) in additional cultures and compared the resultant EBLC numbers with other groups. Although the DMEM+15% FBS+10 ng/mL bFGF group had the greatest gonocyte numbers, cultures with 5% FBS+10% KSR developed the greatest number of EBLCs on Day 28 of culture ($P < 0.001$; Fig. 4.3C). Overall, the EBLC number in 5% FBS+10% KSR cultures was not different from that of groups treated with individual concentrations of LIF (Fig. 4.3C).

Largest EBLC diameters were found in groups treated with 10 ng/mL bFGF, 1500 U/mL LIF, or a combination of 5% FBS+10% KSR and without growth factor supplementation ($P < 0.001$, Table 4.1). Numerically, the largest average diameter of EBLCs was still found in the 5% FBS+10% KSR group. Other than the latter differences, the groups did not differ in any of the morphometric measurements including formation of the somatic cell monolayer, settlement of gonocytes on top of the monolayer, formation of gonocyte clusters and colonies, or development of EBLCs.

4.4.2.2. Experiment 4.2: Effects of Combined Concentrations of Growth Factors

Morphometric changes of cultured cells in groups treated with combined concentrations of growth factors followed the same pattern and timing as those described above. Since in Experiment 4.1 the greatest number of gonocytes was found in cultures with DMEM+15% FBS supplemented with 10 ng/mL bFGF, in the first step of Experiment 4.2 we tested the effects of combining 10 ng/mL bFGF and each of the three concentrations of GDNF on the number of gonocytes using the same basic media (DMEM+15% FBS). On Day 7 of culture, the group treated with an individual concentration of 10 ng/mL bFGF (DMEM+15% FBS+10 ng/mL bFGF) contained the greatest number of gonocytes compared to all other groups ($P < 0.001$). On Day 14, 21, and 28, cultures supplemented with an individual concentration of 10 ng/mL bFGF (DMEM+15% FBS+10 ng/mL bFGF) or a combination of 10 ng/mL bFGF+100 ng/mL GDNF contained the greatest numbers of gonocytes ($P < 0.001$; Fig. 4.4A). On Day 28, the number of gonocytes in cultures supplemented with 10 ng/mL bFGF-only and 10 ng/mL bFGF+100 ng/mL GDNF was ~44% and ~50% greater than that of the control group (*i.e.,* basic media without growth factors) (Fig. 4.4A). Additionally,

the number of gonocytes in cultures with 10 ng/mL bFGF+100 ng/mL GDNF increased by 3.3-fold from Day 7 to Day 28. Although the greatest gonocyte numbers were found in the growth factor-supplemented media, the number of EBLCs was still the greatest in cultures with 5% FBS+10% KSR without growth factors ($P < 0.001$).

Given the promoting effects of 10 ng/mL bFGF+100 ng/mL GDNF on gonocyte proliferation, in the second step of Experiment 4.2, this combination was mixed with each of the three concentrations of LIF (1000, 1200, or 1500 U/mL). On Day 7, cultures treated with basic media supplemented with 10 ng/mL bFGF contained the greatest number of gonocytes ($P < 0.001$), while on Day 14, 21, and 28, cultures supplemented with 10 ng/mL bFGF, 10 ng/mL bFGF+100 ng/mL GDNF, or 10 ng/mL bFGF+100 ng/mL GDNF+1500 U/mL LIF developed the greatest numbers of gonocytes ($P = 0.005$; Fig. 4.4B). Also, a ~2.8-fold increase in the gonocyte number was observed from Day 7 to 28 in cultures treated with the highest concentration of bFGF, GDNF, and LIF (10 ng/mL bFGF+100 ng/mL GDNF+1500 U/mL LIF, $P < 0.001$; Fig. 4.4C).

Additionally, the number of EBLCs was quantified and their diameters measured via photomicrographs on Day 28 in cultures supplemented with all three growth factors. The greatest number of EBLCs was found in cultures containing 5% FBS+10% KSR without growth factor supplementation ($P = 0.009$; Fig. 4.4D). However, among the groups with combined concentrations of growth factors, the largest EBLCs were developed in cultures supplemented with a cocktail of 10 ng/mL bFGF, 100 ng/mL GDNF, and 1500 U/mL LIF ($P < 0.001$, Table 4.2).

4.4.3. Double Immunocytochemistry against Pluripotency-determining and Gonocyte-specific Markers

Freshly isolated gonocytes were positive for DBA and SSEA-1 but were negative for POU5F1, NANOG, and E-cadherin. After 28 days of culture, both EBLCs and individual gonocytes were positive for DBA and POU5F1, SSEA-1, NANOG, and E-cadherin. DBA signals were found on the surface of gonocytes and EBLCs, while the expression of the other four markers was identified within the cytoplasm and nucleus of gonocytes (Fig. 4.5).

4.4.4. Gene Expression of Pluripotency-determining Factors

Samples from cultured neonatal porcine testis cells on Days 7, 14, 21, and 28 were positive for expression of *POU5F1, FUT4* (gene for SSEA-1)*, NANOG*, and E-cadherin. *FUT4* transcript

marker was also positive in freshly isolated testis cells, which conformed with the immunocytochemistry results (Fig. 4.6).

Table 4.1. X- and Y-axis average diameter (mean ± SEM) of EBLCs on Day 28 in culture wells treated with basic media (DMEM+15% FBS) supplemented with individual concentrations of bFGF, GDNF, or LIF and without growth factor supplementation (DMEM+15% FBS or DMEM+5% FBS+10% KSR)

Growth factor	Concentration	Average diameter ± SEM (µm)	Range of diameter (µm)
bFGF	0.1 ng/mL	144.24 ^{A} ± 16.47	102.96 – 209.98
	1 ng/mL	146.04 ^{A} ± 10.72	121.14 – 184.92
	10 ng/mL	194.71 ^{B} ± 11.25	167.4 – 243.15
GDNF	10 ng/mL	145.40 ^{A} ± 14.15	109.73 – 199.82
	50 ng/mL	147.77 ^{A} ± 15.48	107.54 – 209.20
	100 ng/mL	148.13 ^{A} ± 14.61	103.95 – 197.11
LIF	1000 U/mL	150.36 ^{AC} ± 13.03	122.14 – 202.57
	1200 U/mL	151.86 ^{AC} ± 8.93	123.20 – 175.43
	1500 U/mL	188.01 ^{BC} ± 8.73	148.3 – 203.20
5% FBS+10% KSR	-	209.05 ^{B} ± 9.69	118.60 – 348.72
15% FBS	-	161.13 ^{AC} ± 12.14	49.81 – 264.67

^{A,B,C} Diameters with different superscripts are significantly different ($P < 0.05$).

Table 4.2. X- and Y- axis average diameter (mean ± SEM) of EBLCs on Day 28 in culture wells treated with basic media (DMEM+15% FBS) supplemented with 10 ng/mL bFGF, combined concentrations of bFGF, GDNF and LIF or without growth factor supplementation (DMEM+15% FBS or DMEM+5% FBS+10% KSR)

Growth factor combination	LIF Concentration	Average diameter ± SEM (µm)	Range of diameter (µm)
10 ng/mL bFGF	-	194.71 ± 11.25 ^{AC}	167.4 – 243.15
10 ng/mL bFGF+100 ng/mL GDNF	-	206.45 ± 12.50 ^{A}	163.51 – 262.99
10 ng /mL bFGF+100 ng/mL GDNF+LIF	1000 U/mL	220.70 ± 7.35 ^{A}	196.33 – 245.02
	1200 U/mL	223.06 ± 8.88 ^{A}	204.23 – 259.17
	1500 U/mL	265.29 ± 9.71 ^{B}	226.82 – 307.33
5% FBS+10% KSR	-	209.05 ± 9.69 ^{A}	118.60 – 348.72
15% FBS	-	161.13 ± 12.14 ^{C}	49.81 – 264.67

^{A,B,C} Diameters with different superscripts are significantly different ($P < 0.05$).

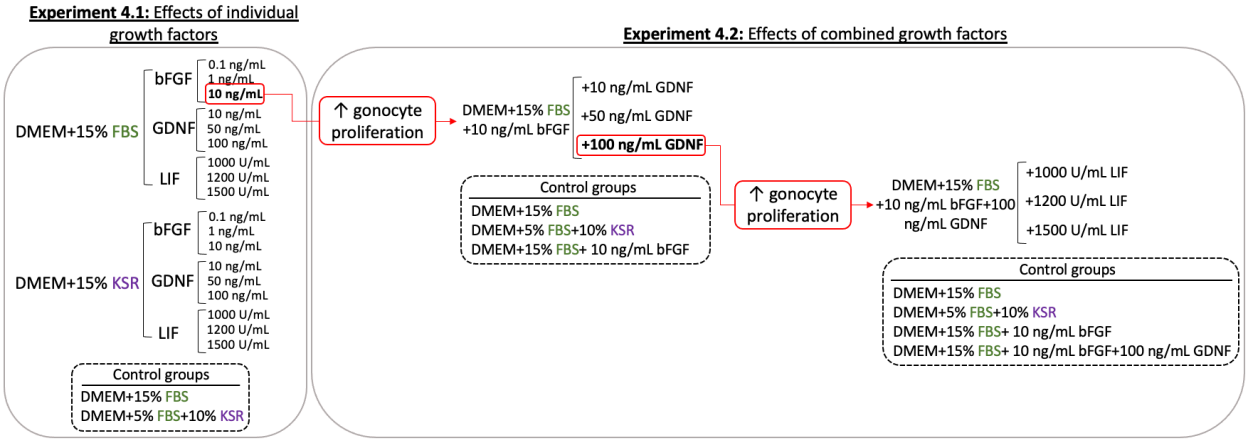

Fig. 4.1. Schematic overview of the experimental design. In Experiment 4.1, isolated testis cells were cultured in a basic medium with FBS (DMEM+15% FBS) or with KSR (DMEM+15% KSR), supplemented with individual concentrations of bFGF (0.1, 1, or 10 ng/mL), GDNF (10, 50, or 100 ng/mL), or LIF (1000, 1200, or 1500 U/mL). The culture condition most supportive of gonocytes proliferation was selected to be used in Experiment 4.2. In Experiment 4.2, the optimal growth factor concentration (10 ng/mL bFGF) was combined with each of the three concentrations of GDNF (10, 50, or 100 ng/mL) to be tested on their effects on proliferation of gonocytes. The optimal combined bFGF and GDNF concentration was then mixed with each of the three concentrations of LIF (1000, 1200, or 1500 U/mL) in the next step to be tested for their effects on gonocyte proliferation and colony-formation. Among all treatments, the selected culture condition resulting in the highest number of gonocytes was selected to determine the expression of germ cell- and pluripotency-markers by gonocytes and EBLCs.

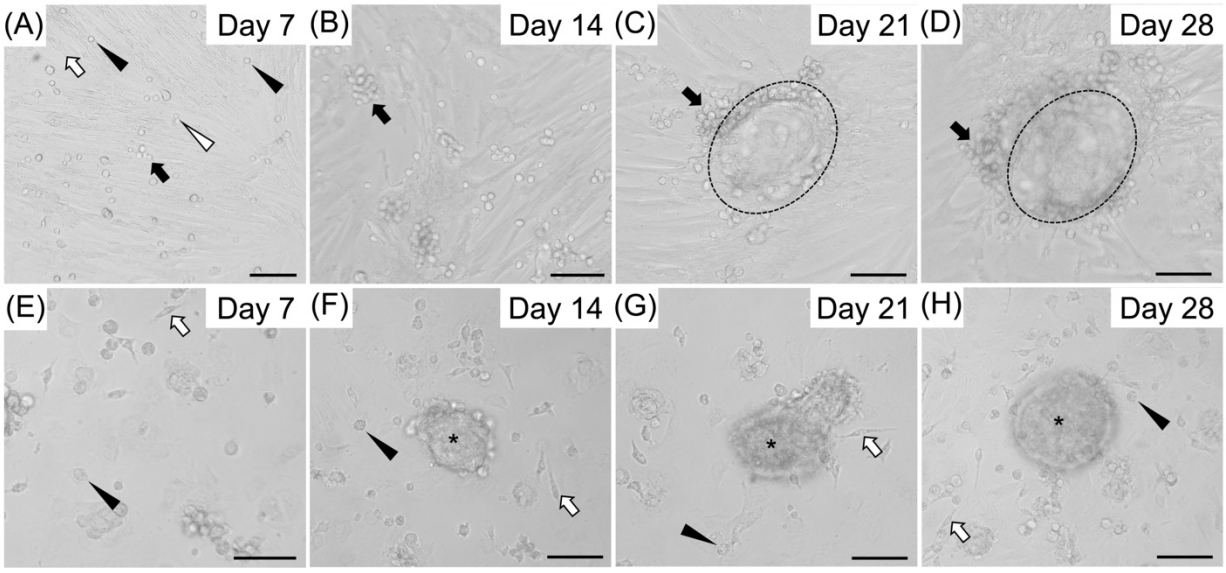

Fig. 4.2. Representative photomicrographs of cultured cells in groups treated with 10 ng/mL bFGF. Gradual morphometrical changes of the cultured testis cells were similar among treatment groups, where FBS or KSR was added to the media. (A-D) Addition of FBS to the cultures led to greater somatic cell confluency. (A) Somatic cells adhered to the bottom of the culture well by Day 7 and appeared as spindle-shape formations (white arrows). Single (black arrowheads), paired (white arrowhead), and clustered (black arrows) gonocytes appeared on top of the somatic cell monolayer with loose attachments. (B) By Day 14, gonocytes formed larger clusters (black arrow) and showed greater tendency to aggregate in circular arrangements. (C) By Day 21, clustered gonocytes converged to form large 3-D colonies, namely embryoid body-like colonies (EBLCs) (dotted circle). (D) Coalesce of individual gonocytes surrounding multi-nucleated EBLCs resulted in their gradual enlargement by Day 28 (black arrows). (E and F) When KSR was used as an alternative to FBS, somatic cell confluency did not increase beyond 20% (white arrow) after 7 days of culture and gonocytes formed small 3-D colonies by Day 14 (asterisk). (G and H) These colonies seemed to slightly increase in size by Day 28 of culture (asterisks). Although growth factors were supplemented, the underdevelopment of somatic cell monolayer (white arrows) may have resulted in decreased gonocyte proliferation (black arrowhead) and as such cultures with KSR supplementation were not included in further analyses. (Scale bar = 100 μm)

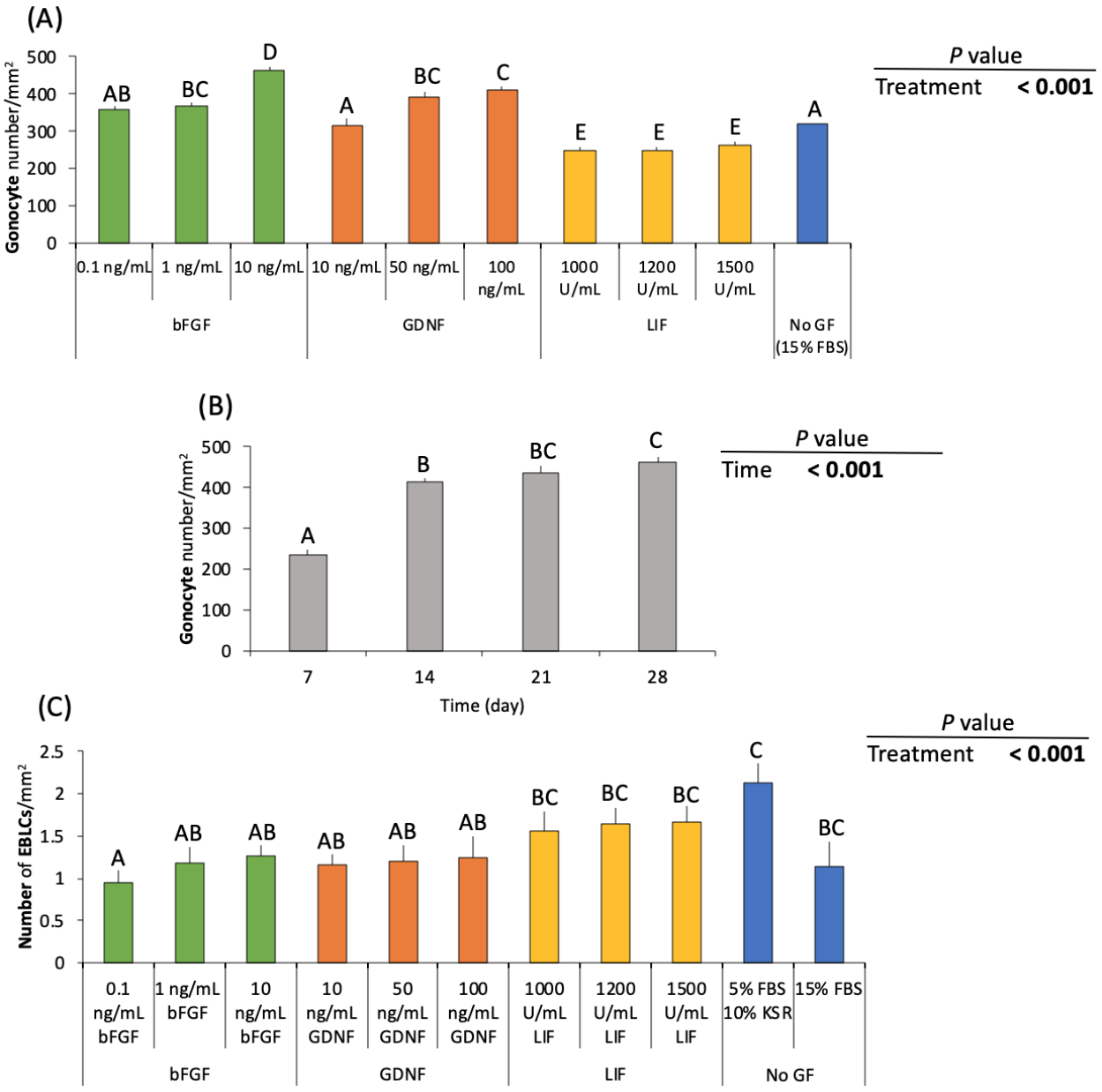

Fig. 4.3. Number of gonocytes (mean ± SEM) in different treatment groups on (A) Day 28 and (B) over time changes in the number of gonocytes in cultures supplemented with 10 ng/mL bFGF. Visual quantification of gonocytes was performed every 7 days. (A) When three tested growth factors were added individually to the culture media, the highest number of gonocytes was found in groups supplemented with 10 ng/mL bFGF in all the time points including Day 28 of culture ($P < 0.001$). (B) Also, gonocyte numbers increased by ~2-fold from Day 7 to Day 28 in cultures

supplemented with 10 ng/mL bFGF ($P < 0.001$). Exogenous bFGF supplementation along with production of endogenous bFGF by the somatic cells in culture is speculated to provide greater support for Sertoli cell survival, which in turn may have resulted in improved gonocyte proliferation. When comparing the number of developed EBLCs, LIF and combined concentrations of 10% KSR+5% FBS seemed to have promoting effects on aggregation and colonization of gonocytes ($P < 0.001$). Different letters denote significant differences and $P < 0.05$ was considered as significant.

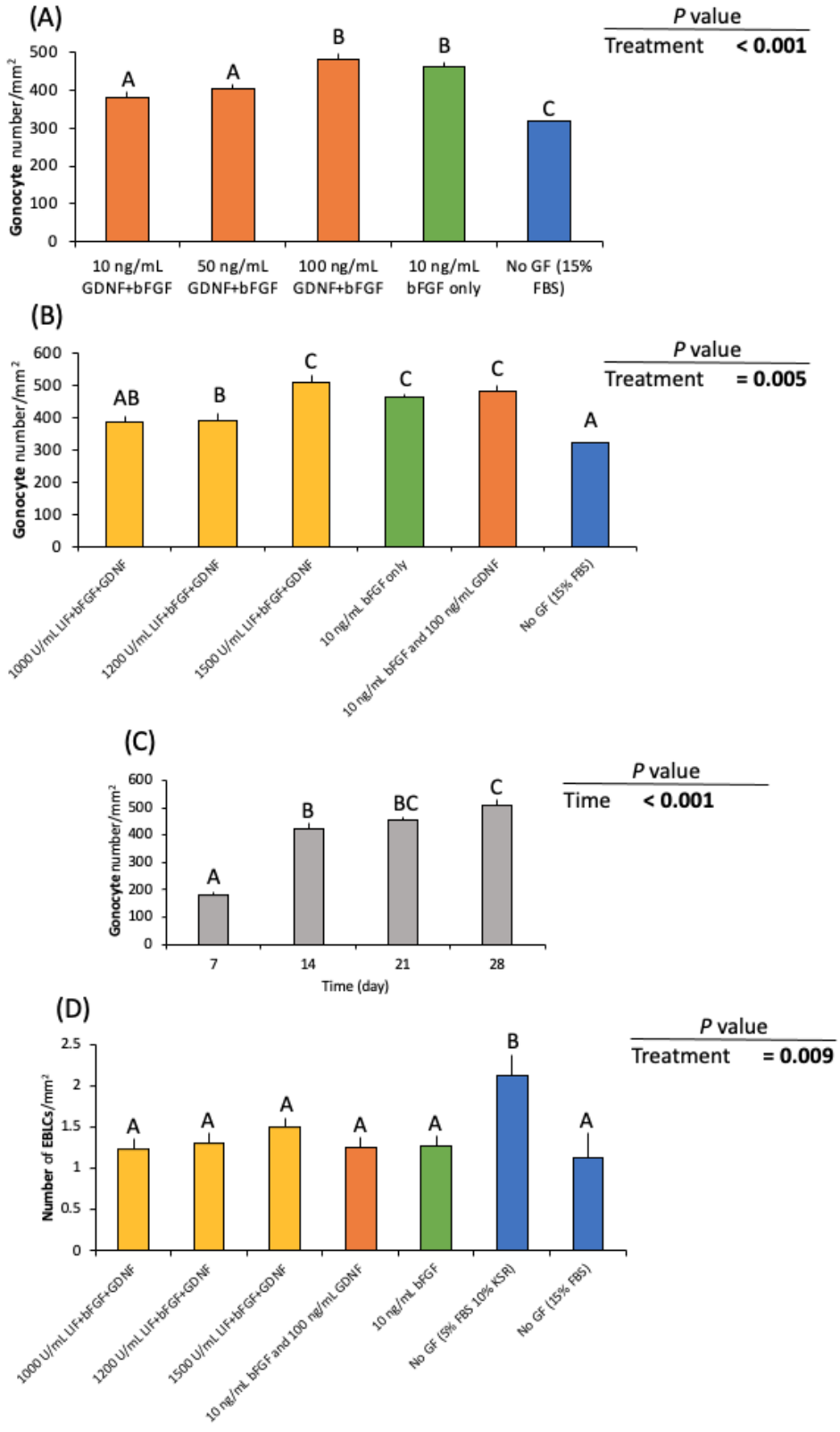
(A)
Gonocyte number/mm²
500
400
300
200
100
0
A
A
B
B
C
10 ng/mL GDNF+bFGF
50 ng/mL GDNF+bFGF
100 ng/mL GDNF+bFGF
10 ng/mL bFGF only
No GF (15% FBS)
P value
Treatment < 0.001
(B)
Gonocyte number/mm²
600
500
400
300
200
100
0
AB
B
C
C
C
A
1000 U/mL LIF+bFGF+GDNF
1200 U/mL LIF+bFGF+GDNF
1500 U/mL LIF+bFGF+GDNF
10 ng/mL bFGF only
10 ng/mL bFGF and 100 ng/mL GDNF
No GF (15% FBS)
P value
Treatment = 0.005
(C)
Gonocyte number/mm²
600
500
400
300
200
100
0
A
B
BC
C
7
14
21
28
Time (day)
P value
Time < 0.001
(D)
Number of EBLCs/mm²
2.5
2
1.5
1
0.5
0
A
A
A
A
A
B
A
1000 U/mL LIF+bFGF+GDNF
1200 U/mL LIF+bFGF+GDNF
1500 U/mL LIF+bFGF+GDNF
10 ng/mL bFGF and 100 ng/mL GDNF
10 ng/mL bFGF
No GF (5% FBS 10% KSR)
No GF (15% FBS)
P value
Treatment = 0.009

Fig. 4.4. Number of gonocytes (mean ± SEM) in cultures supplemented with combined concentrations of growth factors. (A) Since 10 ng/mL bFGF led to increased gonocyte numbers in Experiment 4.1, combined bFGF and GDNF concentrations were added to the basic media. In long-term culture, highest number of gonocytes was found in groups supplemented with 10 ng/mL bFGF or 10 ng/mL bFGF+100 ng/mL GDNF ($P < 0.001$). (B) In the second step, a cocktail of growth factors, consisting of 10 ng/mL bFGF+100 ng/mL GDNF with each of the three concentrations of LIF was supplemented. Greatest number of gonocytes was obtained in groups treated with maximum concentrations of all three growth factors, 10 ng/mL bFGF-only, and 10 ng/mL bFGF+100 ng/mL GDNF ($P = 0.005$). (C) The number of gonocytes increased by ~2.8-fold from Day 7 to Day 28 in cultures supplemented with maximum concentrations of all three growth factors. Nevertheless, the same enhancing effect was found on the gonocyte numbers when 10 ng/mL bFGF alone was added to the media, which may indicate that bFGF can sufficiently support somatic cell proliferation and survival. Survival of somatic cells may have provided an increased support for gonocyte proliferation in culture conditions. Mixture of media with 5% FBS+10% KSR without added growth factors seemed to have an enhancing effect on gonocyte colonization and subsequent EBLC development, as the greatest number of EBLCs was found when FBS and KSR were both present in the culture media ($P = 0.009$). Different letters denote significant differences and $P < 0.05$ was considered significant.

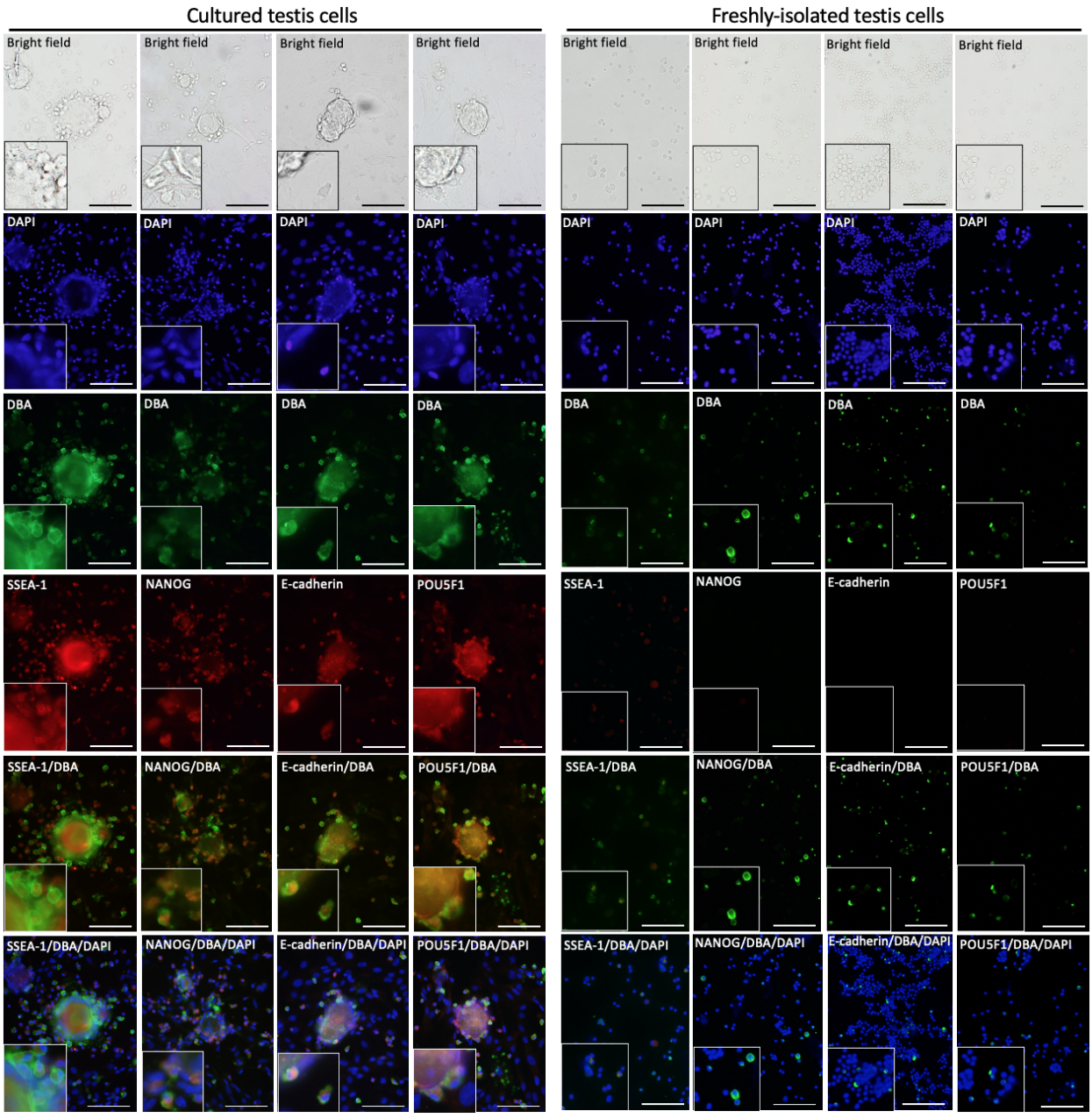

Fig. 4.5. Double-immunostaining of the freshly isolated and cultured testis cells against gonocyte- and pluripotency-specific markers. Freshly isolated testis cells appeared positive for fluorescein isothiocyanate (FITC)-labeled *Dolichos biflorus* agglutinin (DBA-FITC) as a gonocyte-specific marker and SSEA-1 as a spermatogonia and pluripotent stem cells marker. However, gonocytes in the fresh samples were negative for POU5F1, NANOG, and E-cadherin. When cultured, gonocytes which were DBA-positive also expressed pluripotency-determining factors. DBA appeared on the surface of gonocytes and SSEA-1, POU5F1, NANOG, and E-cadherin were detected in the

cytoplasm and nuclei. Co-localization of DBA and pluripotency-determining factors in cultured gonocytes is suggestive of induced reprogramming of germ cells to obtain stem cell characteristics while maintaining their germ cell potential. DAPI was used to stain the nuclei. (Scale bar = 100 μm)

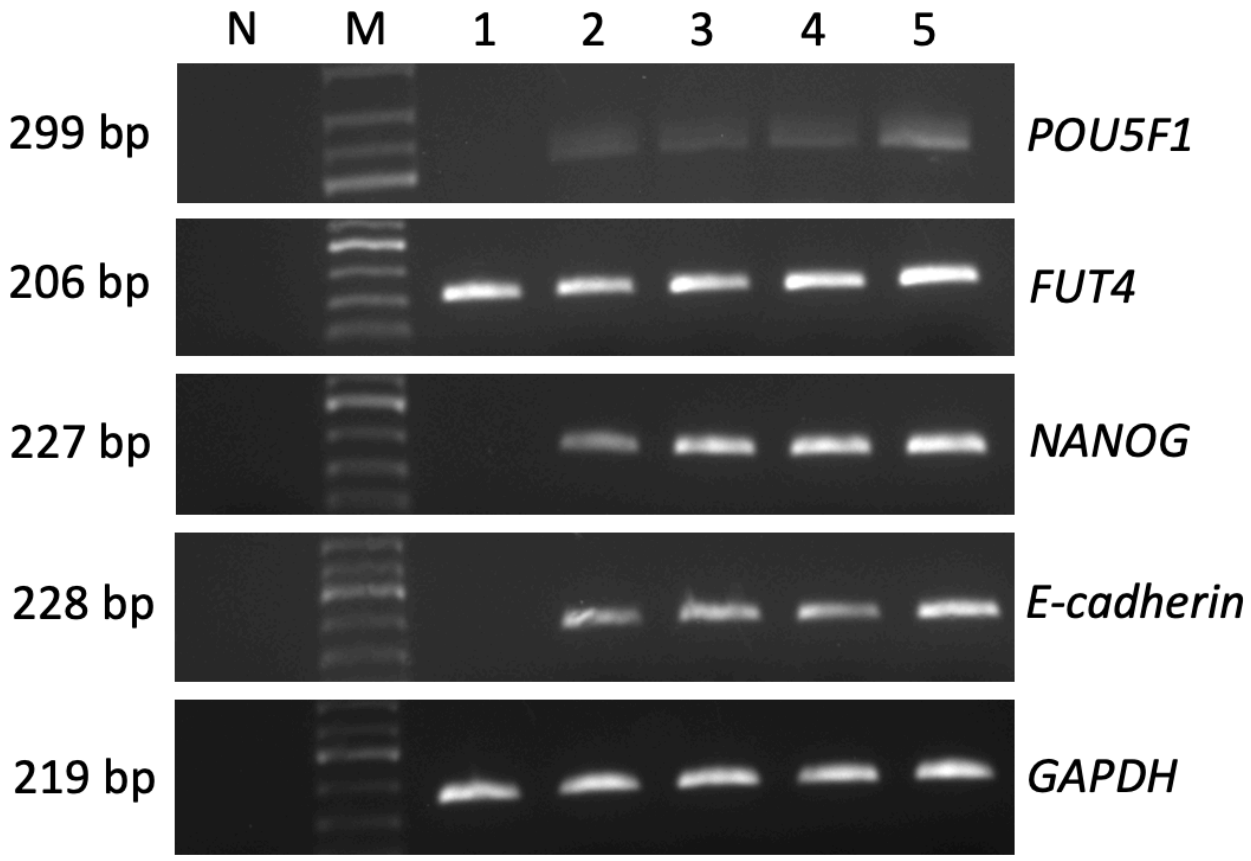

Fig. 4.6. RT-PCR analysis for detection of pluripotency-determining gene transcripts in fresh testis cell isolate and 28-day cultured testis cells. Positive expression of *FUT4* known as a marker for both pluripotent embryonic stem cells and spermatogonia was found in freshly isolated testis cells. On Day 28, cultured testis cells expressed *POU5F1, FUT4, NANOG*, and *E-cadherin*, known as pluripotent embryonic stem cell markers. N, no template control; M, 50 bp DNA ladder; Lines 1-5, amplified cDNA synthesized from samples of freshly isolated testis cells, and cultured testis cells for 1, 2, 3, and 4 weeks, respectively.

4.5. Discussion

To harness the potential of MGSCs for various downstream applications, the optimal culture conditions conducive to their *in vitro* proliferation and colony-formation must be decided. Towards this goal, the present study was designed to systematically study the effects of select key growth factors on the *in vitro* proliferation and behaviour of porcine gonocytes. In a previous study, we optimized other fundamental culture variables including cell density, gonocyte proportions, incubation temperatures, sampling, and media changing regimens (Awang-Junaidi and Honaramooz 2018). Recently, we also examined the effects of media choices (DMEM, DMEM/F12, GMEM, MEM, StemPro, and RPMI), each supplemented with 5, 10, or 15% FBS and/or KSR. In the later study, we observed that DMEM+15% FBS provided an optimal condition to support gonocyte proliferation, while DMEM+5% FBS+10% KSR promoted gonocyte colonization. Furthermore, increasing FBS concentration from 10% to 15% in long-term cultures led to an increase in gonocyte numbers by ~35%. Given a lack of background information regarding the optimal growth factors, in the present study we chose to investigate the effects of bFGF, GDNF, and LIF, three growth factors known to play important roles in germ cell proliferation and/or differentiation (Kubota *et al*. 2004; Kubota *et al*. 2004; Mirzapour *et al*. 2012; Phillips *et al*. 2010; Piquet-Pellorce *et al*. 2000).

Here, we developed a simplified culture system composed of a basic media (DMEM+15% FBS), supplemented with 10 ng/mL bFGF without passaging or adding multiple exogenous factors. This led to an increase in gonocyte proliferation by ~44%. We found that combined concentrations of 10 ng/mL bFGF+100 ng/mL GDNF, or 10 ng/mL bFGF+100 ng/mL GDNF+1500 U/mL LIF similarly promote the proliferation of porcine gonocytes. Additionally, we showed that supplementation with LIF or a combination of FBS and KSR is equally capable of maximizing EBLC formation. Importantly, the gonocytes developed in our optimized culture system co-expressed gonocyte- and pluripotency-determining factors, indicative of their spontaneous dedifferentiation to obtain the characteristics of pluripotent stem cells. Our findings especially benefit applications where large numbers of gonocytes are required as a source of potential pluripotent stem cells or for the ultrastructural study of EBLCs.

Given the non-adherent nature of gonocytes in culture, they typically require co-culturing with a supporting feeder layer (Awang-Junaidi and Honaramooz 2018; van Dissel-Emiliani *et al*. 1993).

In the present study, the somatic cells among the initial population of primary testis cells acted as the feeder layer and sufficiently supported the *in vitro* propagation of gonocytes. As such, our three-step isolation protocol (Yang and Honaramooz, 2011) resulted in a relatively high ratio of gonocytes (~40%) and sufficient numbers of somatic cells, eliminating the need for additional steps to enrich gonocyte or to use exogenous feeder cells. This may in turn have provided a balanced proportion of germ-to-somatic cells and influenced cell proliferation or differentiation. While low numbers of initial gonocytes lead to inferior culture results, additional steps taken prior to culturing to highly enrich gonocytes (to 80% or more) does not necessarily result in improved cell survival and propagation. We previously observed that enriching gonocytes to 86% in fact can lead to their apoptosis once cultured (Awang-Junaidi and Honaramooz 2018). Survival and propagation of isolated cells in the present study further support the notion that gonocytes require a proportional ratio of somatic cells to proliferate and form colonies in culture.

We recently observed that FBS sufficiently supports the growth of testicular somatic cells in culture; thereby, FBS must directly or indirectly promote the survival of germ cells which rely on the somatic cell monolayer. However, using different suppliers of the serum, batch-to-batch variations, or supplementation of serum with undefined components can affect the outcome of testis cell cultures reported by various studies. To reduce such a potential effect, we used aliquots of the same serum source/batch over the course of the present study. In Experiment 4.1, we also included groups with KSR instead of FBS for comparison, as well as to eliminate the potential confounding effects of undefined endogenous components of FBS on gonocyte proliferation and colony-formation. However, regardless of the growth factor used, the survival and propagation of somatic and germ cells were reduced in all KSR-containing cultures. Somatic cells are deemed essential for *in vitro* survival of germ cells as they support gonocytes functionality and provide them with the necessary survival components, such as cytokines and nutritional factors (van Dissel-Emiliani *et al.* 1993). As such, only FBS-supplemented media were considered in Experiment 4.2 to further improve the culture conditions.

Overall, the majority of previous studies have suggested positive effects of growth factors on proliferation and/or survival of germ cells co-cultured with various feeder layers (De Felici *et al*. 2004). Given the complexity of testing multiple growth factors with different concentrations, we added new growth factors in progressive steps. In the present study, bFGF, alone or in combination

with other growth factors, increased gonocyte proliferation in our primary culture conditions. For its effects, bFGF may have directly increased the mitotic activity of germ cells or increased somatic cell growth, which indirectly provided a greater support for germ cells. Previously, it was shown that neutralizing antibodies against bFGF can significantly reduce rat gonocyte numbers in culture. This can be indicative of a direct or indirect involvement of bFGF on the mitogenic and proliferative activity of germ cells (van Dissel-Emiliani *et al*. 1996). Similar to our findings, supplements of bFGF increased mouse and human germ cells, as well as neonatal rat gonocyte numbers following 6 days of culture (Jiang *et al.* 2013; Kanatsu-Shinohara *et al.* 2003; Mirzapour *et al.* 2012; Takashima *et al.* 2015; van Dissel-Emiliani *et al.* 1996). Also, the addition of bFGF to media has been reported to increase the formation and diameter of human SSC clusters (Mirzapour *et al*. 2012). In contrast, a negative effect of bFGF (at 10 ng/mL) on proliferation of mouse SSCs has been observed after culturing in minimum essential medium (MEM) using STO feeders (Kubota *et al.* 2004). Yet, a separate study suggested that a much lower concentration of bFGF (1 ng/mL) has the optimal supportive effects on expansion of cultured mouse germ cells, compared with higher bFGF concentrations (Matsui *et al*. 1992). Nevertheless, the use of different culture conditions, media, and feeder cells may partly explain the seemingly contradictory outcomes of foregoing studies. Here, our use of the same basic media and endogenous somatic cells as the feeder layer eliminated such potential confounding effects when testing different concentrations of different growth factors.

Growth factor bFGF belongs to a larger fibroblast growth factor family and is involved in the proliferation and differentiation of various cell types with mesodermal and neuroectodermal origin (Li 2016). It plays a key role in paracrine regulation of germ cell growth (Jiang *et al*. 2013; Li 2016; van Dissel-Emiliani *et al.* 1996) and is a potent mitogenic factor for rat Sertoli cells (van Dissel-Emiliani *et al.* 1996). Additionally, bFGF is also involved in angiogenesis surrounding the seminiferous tubules, Sertoli cell proliferation, and controlling Sertoli-germinal cell interactions (Mullaney and Skinner 1992). Interestingly, using an *in vivo* testis cell aggregate implantation model, our lab previously demonstrated that brief pre-implantation exposure of the donor cells to bFGF can result in enhanced implant weight as well as increased cross-sectional implant and seminiferous cord areas (Awang-Junaidi 2019). Other studies have also shown a supportive role of bFGF for porcine Sertoli cell growth and proliferation (Jaillard *et al*. 1987; van Dissel-Emiliani *et al.* 1996). Taken together, bFGF likely provides a greater support for Sertoli cell proliferation,

which in turn may have led to an improved re-formation of seminiferous cords *in vivo* or indirectly enhanced gonocyte proliferation *in vitro.*

We also studied the effects of GDNF, a neurotrophic factor secreted by glial cells in the central nervous system. Within the testes, GDNF is also expressed by Sertoli cells (Hofmann 2008). Given the importance of GDNF in determining germ cell fate, we tested its effects on the number of cultured gonocytes, both individually and combined with other growth factors. We showed that in all examination time points, increasing concentrations of GDNF can increase gonocyte proliferation, possibly due to the activation of various signaling cascades that trigger mitosis divisions in gonocytes (Hofmann 2008). Increased germ cell numbers in response to higher GDNF concentrations have also been observed in previous reports. For instance, mouse germ cells increased ~1.5-fold following the addition of GDNF to the culture media (Kubota *et al*. 2004). The enhancing effect of GDNF on germ cell proliferation was also shown using long- and short-term cultures of different MGSCs (Hofmann *et al*. 2005; Kanatsu-Shinohara *et al.* 2003; Kanatsu-Shinohara *et al*. 2003; Nagano *et al*. 2003). Additionally, GDNF-expressing STO feeder cells were reported to support the long-term proliferation of cultured mouse spermatogonia without a need for refreshment of the growth factor (Wei *et al.* 2016). This can be indicative of the crucial role of GDNF on *in vitro* germ cell survival. Nevertheless, a study using porcine gonocytes reported non-significant mitogenic effects of the recombinant GDNF and weak expression of GFRA1 when cultured in a serum-free medium (Kakiuchi *et al.* 2018). They concluded that although in rodents a peak expression of GDNF and GFRA1 is observed in the first week after birth, such an increase may not be present in cultured porcine testis cells (Kakiuchi *et al*. 2018). It can be postulated that different culture conditions including varying media or feeder layers in foregoing studies partly account for the discrepancies (Hofmann *et al.* 2005; Kanatsu-Shinohara *et al*. 2003; Kanatsu-Shinohara *et al.* 2003; Kuijk *et al.* 2009; Mirzapour *et al*. 2012; Nagano *et al.* 2003). GDNF has been shown to up-regulate the expression of bFGF receptors on gonocytes. Thus, GDNF can potentially render a population of MGSCs more responsive to bFGF, wherein the synergistic effects of both growth factors combined affect germ cell proliferation (Hofmann *et al.* 2005). The release of GDNF by Sertoli cells has also been shown to be regulated by follicle stimulating hormone (FSH) (Kanatsu-Shinohara 2005; Kuijk *et al*. 2009). Subsequently, a signaling cascade is induced by GDNF, leading to the expression of Ets variant gene 5 *(Etv5*) which is an important factor for the regulation of germ cell proliferation (Simon *et al*. 2007). Evaluation of seminiferous

tubules in GDNF-knockout mice showed an absence of spermatogonia, whereas its overexpression resulted in accumulation of undifferentiated spermatogonia (Kanatsu-Shinohara *et al*. 2003; Kanatsu-Shinohara *et al.* 2014). GDNF is known to be involved in the regulation of Sertoli- and germ cell communications, formation of actin cytoskeleton, and movement of germ cells towards the stem cell niche (Dovere *et al.* 2013). Due to its supportive effects on *in vitro* survival and colony-formation of mouse germ cells, GDNF has been commonly used for the establishment of long-term SSC cultures and is considered an important component for such cultures (Kanatsu-Shinohara *et al.* 2003; Kanatsu-Shinohara *et al*. 2004a; Kubota *et al.* 2004). Furthermore, it has been shown that disruption of GDNF signaling pathways can supress self-renewal of germ cells and as such, lead to formation of seminiferous tubules devoid of germ cells (Kanatsu-Shinohara *et al.* 2012; Kanatsu-Shinohara and Shinohara 2013). Overall, our findings are indicative of the stimulatory effects of GDNF on porcine gonocyte proliferation, which agrees with previous studies.

Additionally, LIF is an important pleiotropic growth factor from the interleukin-6 family and is involved in stem cell regulation (Curley *et al.* 2018). By attaching to its heterodimeric receptor, LIF initiates phosphorylation of several tyrosine residues and activates a signaling cascade involved in the maintenance or self-renewal of stem cells in many tissues (Kanatsu-Shinohara *et al.* 2007). In the present study, LIF supplementation did not significantly increase gonocyte numbers compared with the control group. It is possible that increasing LIF concentrations much beyond our highest dose (1500 U/mL) might have led to an observable effect on porcine germ cell proliferation. In the absence of previous studies using LIF on neonatal porcine testis cells, we chose the range of growth factor concentrations based on our best estimates from various other culture systems (Kanatsu-Shinohara *et al.* 2007; Kubota *et al.* 2004a; Matsui *et al*. 1992; Pesce *et al*. 1993). Here, we also observed that individual concentrations of LIF can result in the same number of EBLCs as groups exposed to mixed concentrations of FBS and KSR, a mixture we recently found to be the optimal condition for EBLC development. Moreover, when the highest concentrations of bFGF, GDNF, and LIF were supplemented in combination, the average diameter of EBLCs was ~1.3-fold greater than those developed in FBS+KSR without growth factor supplementation. In contrast to our results, porcine gonocytes cultured in GMEM and StemPro media developed relatively smaller colonies when supplemented with bFGF, GDNF and EGF (Kuijk *et al.* 2009). These conflicting results point to the importance and specificity of employed

culture conditions, such as the growth factor combination and media, on the behavior and colony-formation of porcine gonocytes. Our results indicate that LIF promotes germ cell aggregation and colonization, and, when combined with bFGF and GDNF, larger EBLC diameters may be expected. In a previous report, LIF was deemed essential for increasing the colony numbers of human SSCs co-cultured with Sertoli cells (Mirzapour *et al.* 2012); when LIF and bFGF were combined, both the number and diameter of said colonies increased. This agrees with our findings. LIF has also been found to increase colony-formation of neonatal mouse germ cells in culture (Kanatsu-Shinohara *et al.* 2007). Once released, LIF attaches to its receptor complex consisting of LIF receptor and gp130 receptor. Upregulation of gp130 expression has been detected on the surface of clustered rat germ cells and may hence be associated with enhanced colony-formation of germ cells. This may partly explain the underlying reason for the increased *in vitro* colonization of germ cells following LIF supplementation (Mirzapour *et al*. 2012; Ryu *et al.* 2004).

In the present study, after 28 days of culture, the number of gonocytes was not different between groups treated with 10 ng/mL bFGF alone and those with combined concentrations of 10 ng/mL bFGF+100 ng/mL GDNF, or with 10 ng/mL bFGF+100 ng/mL GDNF+1500 U/mL LIF. Similar to our findings, combined concentrations of seven growth factors (stem cell factor, LIF, bFGF, insulin-like growth factor, platelet-derived growth factor, murine oncostatin M, and interlukin-11) has been shown to support murine SSC culture over a 3-month period (Jeong *et al.* 2003). Our results hence indicate that the support conferred by bFGF is sufficient for long-term culture of porcine gonocytes. Therefore, in germ cell cultures, both species differences and specific culture conditions have an important influence on the survival, behavior, and differentiation fate of the cultured cells.

In addition, we observed that, starting from Day 7, gonocytes and EBLCs originating from both freshly isolated and cultured testis cells displayed co-expression of germ- and pluripotency-markers. This observation may point to the dedifferentiation potential of germ cells in our media, consisting of basic components and supplemented with bFGF. We also found that neonatal germ cells were negative for POU5F1 at the time of isolation and become positive only when cultured. POU5F1 is known as a marker for ES cells and plays a central role in pluripotency and self-renewal of stem cells during embryonic development (Nichols *et al*. 1998). Therefore, the expression of this marker by cultured gonocytes can be indicative of their transformation into a pluripotent state.

Previous studies have also shown porcine gonocytes becoming positive for POU5F1 and SSEA-1 in culture conditions (Awang-Junaidi *et al*. 2020; Goel *et al*. 2008). Another study showed successful colonization of cultured porcine gonocytes positive for POU5F1, NANOG, and PLZF following cross-species germ cell transplantation which further supports their germline stem cell potential while expressing pluripotency markers (Lee *et al.* 2013). POU5F1 expression has been shown previously to become downregulated in germ cells during embryonic development which demonstrates their differentiation to more specialized germ cells (Rajpert-De Meyts *et al.* 2004).

Here, we observed the expression of SSEA-1 by freshly isolated and cultured gonocytes. SSEA-1 is known as both a pluripotency and germ cell marker, with diminishing expression in more differentiated germ cells (Goel *et al.* 2007; González and Dobrinski 2015; Kim *et al.* 2013). Its expression has also been demonstrated by mouse blastomeres, cells of the inner cell mass, and human germline stem cells (Sivasubramaniyan *et al*. 2015; Solter and Knowles 1978). We were also able to find that gonocytes become positive for NANOG when cultured under our selected conditions, which further supports their dedifferentiation potential into more primitive stages. NANOG is an important pluripotency-determining factor and an essential regulator of ES cell population (Culty 2009; Hoei-Hansen *et al.* 2005). NANOG expression is necessary for maintaining the pluripotent state of mouse and human ES cells and as such has been used as a marker of pluripotency. The role of this factor is believed to be conserved among species (Kuijk *et al.* 2010). Similar to our findings, in bovine germ cells, NANOG and POU5F1 expression levels were enhanced after being in culture (Fujihara *et al*. 2011).

In the present study, we also observed E-cadherin expression in cultured porcine gonocytes, while freshly isolated cells appeared negative for this marker. E-cadherin is also expressed in ES cells and as such, its positive expression by cultured germ cells can similarly point to their *in vitro* reprogramming into an undifferentiated stage. E-cadherin is a protein component of adherens-type junctions and has a crucial role in the formation of cell-to-cell contacts with important functions (Redmer *et al*. 2011), such as maintaining the integrity of blastocysts during embryonic development (Larue *et al*. 1994). E-cadherin is also known as an important regulator of early differentiation, with its high rate of expression deemed essential for the maintenance of undifferentiated state in ES cells (Redmer *et al.* 2011).

Co-localization of DBA, a gonocyte-specific marker, with the above-mentioned pluripotency-determining markers in cultured gonocytes and EBLCs by Day 28 was indicative of their potential to maintain their germ cell characteristics while undergoing *in vitro* reprogramming to obtain characteristics of pluripotent stem cells. In neonatal testes, gonocytes represent a multipotent population of cells, which can undergo mitosis and differentiate into more advanced germ cells. However, the behavior of gonocytes seems to be different *in vivo*, where they do not demonstrate the tendency to undergo multi-lineage differentiation within the testis due to their special interaction with the surrounding Sertoli cells. This phenomenon is observed in both *in situ* gonocytes and those present in testis tissue grafts or cell implants in recipient mice (Awang-Junaidi *et al*. 2020; Fayaz *et al.* 2020a,b; Honaramooz *et al.* 2007, 2002; Mirzapour *et al.* 2012). However, gonocytes in a two-dimensional culture system may be expected to behave differently, given separation from the regulatory controls of Sertoli cells. As such, in 2-D systems, gonocytes display a tendency to convert into a more primitive and undifferentiated stage. Positive expression of pluripotency-determining markers by *in vitro*-developed germ cells and EBLCs is especially important due to their potential use as an alternative source for pluripotent stem cells in downstream applications. Given that general safety and/or ethical concerns limit the use of induced pluripotent stem (iPS) cells or ES cells for cell-based therapy, the development of alternative sources of pluripotent stem cells for regenerative medicine is a subject of great interest. More importantly, our optimized cell isolation method and culture conditions can lead to spontaneous increases in germ cell numbers and formation of EBLCs without a need for supplementation of the media with multiple factors. The addition of multiple factors, especially those with potential carcinogenic properties, can affect the germ cell fate and/or increase the risk of unwanted genetic and/or epigenetic aberrations in the resultant pluripotent cells, thus limiting their safety and potential use in medicine.

In conclusion, supplementation of a basic medium consisting of DMEM+15% FBS with only 10 ng/mL bFGF can effectively maximize *in vitro* proliferation of porcine gonocytes. Furthermore, supplementation of LIF alone to the basic media can enhance porcine gonocyte colony-formation while the addition of 10 ng/mL bFGF+100 ng/mL GDNF+1500 U/mL LIF significantly increases EBLC diameters. When cultured in these conditions, somatic cells form a monolayer and circular arrangements while gonocytes aggregate to produce multinucleated EBLCs. More importantly, both cultured gonocytes and their EBLCs co-express specific germ cell- and pluripotency-markers

in our selected conditions. Overall, our optimized basic culture conditions can be used to increase germ cell numbers and their colonies. This can be viewed as a successful step forward in using *in vitro* cultured gonocytes as an alternative source of pluripotent stem cells for downstream applications in cell-based therapy, transgenesis, and/or fertility preservation.

Transition

Given the ability of germline stem cells to express ES markers in culture conditions in Chapters 3 and 4, these cells may be used as an alternative to current sources of pluripotent stem cells for downstream applications in regenerative medicine. However, full potential of germline-derived stem cells such as their conversion into somatic cell lineages needs further investigation. Therefore, the study in Chapter 5 was designed and conducted to both assess the pluripotency of MGSCs using an *in vivo* implantation assay and evaluation of their tumorigenic potential as well as to evaluate their trans-differentiation potential into somatic cell derivatives of three germinal layers.

CHAPTER 5

NEONATAL PORCINE GERM CELLS DEDIFFERENTIATE AND DISPLAY OSTEOGENIC AND PLURIPOTENCY PROPERTIES *IN VITRO* [5, 6]

5.1. Abstract

Gonocytes are progenitors of spermatogonial stem cells in the neonatal testis. We have previously shown that upon culturing, neonatal porcine gonocytes and their colonies express germ cell and pluripotency markers. The objectives of present study were to investigate *in vitro* trans-differentiation potential of porcine gonocytes and their colonies into cells from three germinal layers, and to assess pluripotency of cultured gonocytes/colonies *in vivo*. For osteogenic and tri-lineage differentiation, cells were incubated in regular culture media for 14 and 28 days, respectively. Cells were cultured for an additional 14 days for osteogenic differentiation or 7 days for differentiation into derivates of the three germinal layers. Osteogenic differentiation of cells and colonies was verified by Alizarin Red S staining and tri-lineage differentiation was confirmed using immunofluorescence and gene expression analyses. Furthermore, upon implantation into recipient mice, the cultured cells/colonies developed teratomas expressing markers of all three germinal layers. Successful osteogenic differentiation from porcine germ cells has important implications for bone regeneration and matrix formation studies. Hence, gonocytes emerge as a promising source of adult pluripotent stem cells due to the ability to differentiate into all germinal layers without typical biosafety risks associated with viral vectors or ethical implications.

5.2. Introduction

Gonocytes are a transitory population of male germline stem cells (MGSCs) in the neonatal testis; they develop from fetal primordial germ cells (PGCs) and postnatally undergo transition into spermatogonial stem cells (SSCs). In mice, gonocytes proliferate within the testicular niche by embryonic day (ED) ~12.5, gradually become mitotically inactive by ED ~15.5, and then maintain their quiescent state for the remainder of the prenatal period (de Rooij 1998; Phillips *et al.* 2010).

---

[5] This study has been published. Fayaz MA, Rosa GS, and Honaramooz H (2021) *Cells* 10:2816.

[6] MAF contributed to the design of the experiments, performed the study, and wrote the first draft of the manuscript. GSR assisted in the initial experiments and revised the manuscript. AH contributed to the experimental design, revised the manuscript, and supervised the project.

The transition of gonocytes into SSCs occurs at ~6 days after birth in rodents or ~2 months in humans (Wu *et al.* 2009). SSCs, considered adult stem cells, are fundamental for spermatogenesis due to their dual potential for self-renewal and differentiation ability for subsequent mitosis and meiosis (Roosen-Runge and Giesel Jr 1950; Ibtisham *et al.* 2020). Compared to both PGCs and SSCs, gonocytes in the neonatal testis are a preferred source of MGSCs, since they offer a relatively large population, ease of accessibility, identifiable morphology, and more specific molecular markers for their identification and isolation (Lehmann 2012).

When still situated in the testis niche, MGSCs are programmed to unipotently differentiate into more specialized germ cells (Golestaneh *et al.* 2009; Azizi *et al.* 2019). However, compiling evidence demonstrates the dedifferentiation potential of MGSCs, as well as their ability to derive multipotent or even pluripotent stem cells in an *ex situ* environment (Kanatsu-Shinohara *et al.* 2004; Guan *et al.* 2006; Seandel *et al.* 2007; Kossack *et al.* 2009; Awang-Junaidi *et al.* 2020; Chen *et al.* 2020). These cells can spontaneously transform into a population of cells that express embryonic stem (ES) cell markers, otherwise if genetic manipulations were needed, they would have imposed safety concerns regarding their use and expansion (Holstein *et al.* 1996; Kanatsu-Shinohara, Inoue *et al.* 2004; Ko *et al.* 2009). The ability to dedifferentiate into a pluripotent state allows these ES-like cells to convert into other cell types from derivatives of three germinal layers (Kanatsu-Shinohara *et al.* 2004; Guan *et al.* 2006; Seandel *et al.* 2007; Chen *et al.* 2020).

Although several studies have demonstrated the potential of MGSCs as a source of pluripotent stem cells, the extent of their full potential is yet to be known and the complicated derivation process remains a major limitation in their application. Further, the conversion of MGSCs into a dedifferentiated state in the presence of exogenous factors, such as multiple growth factors and embryonic fibroblasts used as the supportive feeder layer, may pose unwanted genetic and epigenetic changes to the dedifferentiated cells; this, too, may limit their applications. Additionally, passaging of MGSCs for their expansion or induction of reprogramming can disrupt their normal cell cycle, growth, and overall physiological response to their microenvironment (Kanatsu-Shinohara *et al.* 2004). Therefore, the use of minimal exogenous factors and manipulations for induction of pluripotency in prospective studies is desirable for reducing concerns of immunogenicity, tumorigenicity, and/or viral contamination, and provides a more practical approach for *in vitro* development (Golestaneh *et al.* 2009; Chen *et al.* 2020).

Pluripotent stem cells have also been produced by introducing specific sets of pluripotency-associated genes or 'reprogramming factors' to the somatic cells. The resultant cells, known as induced pluripotent stem (iPS) cells, were developed via retroviral delivery of various transcription factors (*e.g.*, Oct3/4, Sox2, c-Myc, and Klf4) to adult dermal fibroblasts (Takahashi and Yamanaka 2006; Takahashi *et al.* 2007; Wernig *et al.* 2007), hepatocytes, gastric epithelial cells, and even neural stem cells (Aoi *et al.* 2008; Kim *et al.* 2008). However, the practicality of utilizing different stem cells in clinical settings remains limited due to the ethical and safety concerns over their source (Yang *et al.* 2019). In addition, current protocols for inducing differentiation into specific cell lineages are inefficient, time-consuming, technically complex, and are not cost effective given the requirement for multiple induction materials (Ben-Porath *et al.* 2008; Volarevic *et al.* 2018). Increased tumorigenicity of iPS cells due to introduced transcription factors, genetic instability, and biosafety risks associated with the use of viral vectors in their development further limits their applications as therapeutic agents (Chen *et al.* 2020). As a result, it is imperative to seek alternative stem cell sources that lack the biosafety risks associated with viral transduction or tumor formation, and the ethical concerns associated with the manipulation of embryos to harvest stem cells.

Our laboratory has recently shown that porcine gonocytes, co-cultured with testis somatic cells as a feeder layer, rapidly expand in our developed culture conditions composed of basic media and fetal bovine serum (FBS), with or without basic fibroblast growth factor (bFGF). More importantly, in Chapter 3 and 4 we demonstrated that porcine gonocytes are capable of spontaneous dedifferentiation into more primitive stages that express ES cell markers such as SSEA-1, POU5F1, NANOG, and E-cadherin. This is especially important since *in vitro* dedifferentiation and trans-differentiation of germ cells in previous reports required coculturing with somatic cells from other species and/or supplementation of the media with multiple exogenous factors (Azizi *et al.* 2019; Yang *et al.* 2019; Chen *et al.* 2020). In the present study, we used our recently developed culture conditions to obtain a population of ES-like cells that express pluripotency markers from porcine gonocytes, and then further evaluated their teratoma formation potential using an *in vivo* implantation assay. We also investigated the induction of their differentiation into derivatives of all three germinal layers by using a simple protocol without the addition of multiple exogenous factors. In doing so, the present study provides a much faster and safer approach for the acquisition of differentiated germinal cells than that reported in previous studies, without complicated manipulation procedures and a reduced overall differentiation cost.

5.3. Materials and Methods

5.3.1. General Experimental Design

Figure 5.1 shows the schematic representation of the experimental design. The present study was comprised of four sets of experiments used to investigate the differentiation potential and *in vivo* teratoma formation of cultured neonatal porcine gonocytes. In Experiment 5.1, cultured gonocytes were directed to differentiate into an osteogenic pathway, where differentiation was confirmed using Alizarin Red S staining. In Experiments 5.2 and 5.3, the cultured cells were directed to differentiate into derivatives of the three germinal layers (*e.g.*, ectoderm, mesoderm, and endoderm) followed by confirmation using immunocytochemistry and expression analysis for lineage-specific markers. In Experiment 5.4, the *in vivo* teratoma formation of cultured cells was tested using an implantation assay as a follow up to our previous report of their expression of several pluripotency markers.

5.3.2. Castration of Donors, Testis Cell Isolation, and Culture in Regular Media

Procedures for the castration of neonatal piglets (~1-wk old; $n = 15$ for Experiment 5.1, $n = 60$ for Experiments 5.2 and 5.3, and $n = 15$ for Experiment 5.4), testis cell isolation, and cell culture were conducted as previously described (Yang *et al.* 2010; Awang-Junaidi and Honaramooz 2018; Awang-Junaidi *et al.* 2020). Cells were cultured in Dulbecco's modified Eagle's media (DMEM; catalogue no. 12-604F; Corning, New York, NY, USA) supplemented with 10% fetal bovine serum (FBS; catalogue no. A15-701; PAA Laboratories, Etobicoke, ON, Canada) for 14 days in Experiment 5.1, 28 days for Experiment 5.4, and in DMEM+15% FBS+10 ng/mL basic fibroblast growth factor (bFGF; catalogue no. 233-FB-025; R&D Systems, Minneapolis, MN, USA) for 28 days in Experiment 5.2. However, in Experiment 5.2, following immunocytochemistry, the cells and colonies did not stain positive for the selected differentiation markers. Also, cells showed a reduced confluency following visual examination on day 4 of differentiation in Experiment 5.2. As such, we designed Experiment 5.3 where cultures were exposed to the various differentiation media for a longer period and without frequently changing the media to prevent potential interference with cell organization and interactions. In Experiment 5.3, similar seeding density, regular media composition, and incubation conditions were used as in Experiment 5.2.

5.3.3. In Vitro Osteogenic Trans-Differentiation of Porcine Germ Cells

The osteogenic differentiation media was prepared according to the manufacturer's instructions (catalogue no. A1007201; StemPro Osteogenesis Differentiation Kit, Gibco, Grand Island, NY, USA). Briefly, the differentiation supplement was mixed with base media at a 1:9 ratio. On day 14 of culture, regular media was removed, and each well was rinsed with Dulbecco's phosphate-buffered saline (DPBS; catalogue no. 20-031-CV; Mediatech, Manassas, VA, USA) and cells were exposed to the prepared osteogenesis differentiation media for 14 days. This differentiation media was replenished every 3 days and cultures were visually examined using phase-contrast microscopy.

5.3.4. In Vitro Tri-lineage Differentiation of Porcine Germ Cells

For trans-differentiation of gonocytes and colonies into derivatives of the three germinal layers, tri-lineage differentiation kits were used according to the manufacturer's instructions with modifications. On day 28 of Experiment 5.2, regular media in different wells was switched with each tri-lineage differentiation media that was developed for differentiation of human pluripotent stem cells (catalogue no. SC031B ectoderm kit; catalogue no. SC030B mesoderm kit; and catalogue no. SC019B endoderm kit; all from R&D Systems). To prepare the endoderm differentiation media-I, bFGF, Activin A, and Wnt-a were diluted 1000-fold in pre-warmed differentiation base media. To prepare the endoderm differentiation media-II, only bFGF and Activin A were diluted 1000-folds in pre-warmed differentiation base media. Each tri-lineage differentiation media was tested in a 6-well plate containing three replicates. For ectoderm and mesoderm differentiation, regular media was switched with 2.5 mL of the differentiation media and cells were incubated for 24 hr at 37° C and 5% CO_2. The media was replenished with fresh differentiation media every 24 hr on days 2 and 3. For endoderm differentiation, regular media was switched with differentiation media-I and plates were maintained in similar conditions as described above. Media-I was then replaced with media-II after 16 hr of incubation. Media-II was replenished every 12 hr on days 2 and 3. Alternatively, in Experiment 5.3, cultures were incubated with 2.5 mL of the ectoderm or mesoderm differentiation media for 7 days, but without regularly replenishing the media. For endoderm differentiation, regular media was replaced with differentiation media-I, media-I was switched with media-II after 16 hr of incubation, and the

cultures were maintained for an additional 7 days without replenishing the media. In each differentiation group, cultures were examined daily under a phase-contrast microscope.

5.3.5. Imaging and Morphometrical Assessment

Viability of freshly isolated and cultured cells was evaluated using the trypan blue exclusion technique (Yang *et al.* 2010; Awang-Junaidi and Honaramooz 2018; Awang-Junaidi *et al.* 2020). For quantification and measurements in Experiment 5.1, photomicrographs were captured from culture plates in treatment and control groups before and after staining with Alizarin Red S. In Experiments 5.2 and 5.3, photomicrographs were obtained before adding the differentiation media (day 0), as well as on days 3, 5, and 7 after incubation with differentiation media. Imaging, morphometrical assessment, and quantification protocols were carried out as described in Chapters 3 and 4.

5.3.6. Staining and Immunocytochemistry for Evaluation of Dedifferentiation and Trans-Differentiation

5.3.6.1. Alizarin Red S Staining

Calcium deposition is a known indicator of successful differentiation of stem cells into osteoblasts, and of *in vitro* bone matrix formation (Virtanen and Isotupa 1980). Therefore, on day 14 of differentiation in Experiment 5.1, Alizarin Red S staining solution was used to identify calcium deposition as described previously (Silva *et al.* 2005). Briefly, the media was aspirated, wells were rinsed with DPBS, and cells/colonies were fixed using 10% formaldehyde solution (catalogue no. HT501128; Sigma-Aldrich) for 30 min. Wells were rinsed and incubated with the staining solution at room temperature for 20 min. Wells were rinsed again with distilled water and visualized under an inverted light microscope.

5.3.6.2. Immunofluorescence Assay

In Experiments 5.2 and 5.3, cells and colonies were grown on poly-L-lysine-coated coverslips. The preparation of coverslips followed our previously described protocols (Awang-Junaidi and Honaramooz 2018). As shown in Chapter 3 and 4, culture of neonatal porcine MGSCs in regular media leads to their dedifferentiation and expression of main ES cell markers. As such, here we also evaluated the expression of POU5F1 as a representative ES marker to confirm MGSC dedifferentiation prior to their trans-differentiation (Nichols *et al.* 1998; Pan *et al.* 2002;

Zeineddine *et al.* 2014). The expression of this marker was examined immediately after cell isolation and on day 28 of culture in regular media. On day 4 of Experiment 5.2 and day 7 of differentiation in Experiment 5.3 the coverslips were removed from culture wells and stained against gonocyte- and germinal layer markers, as summarized in Table 5.1. The procedure used for immunofluorescence assay has been previously described by our laboratory (Awang-Junaidi and Honaramooz 2018; Awang-Junaidi *et al.* 2020). To double-label the cells and colonies with a gonocyte-specific marker, FITC-labeled *Dolichos biflorus* agglutinin (DBA-FITC; catalogue no. FL1031; Vector Labs, Burlington, ON, Canada) was used (Goel *et al.* 2007).

5.3.7. Gene Expression Analyses for Confirmation of Dedifferentiation and Trans-Differentiation

In Experiment 5.3, the expression of the pluripotency marker (*POU5F1*) and 6 germinal layer markers was examined using reverse-transcriptase polymerase chain reaction (RT-PCR). To confirm dedifferentiation of cultured MGSCs, expression of *POU5F1* was examined using samples of freshly-isolated testis cells and cultured cells in regular media on days 7, 14, 21, and 28. Following 7 days of culture in differentiation media, RT-PCR analysis for differentiation markers was carried out on cells and colonies from each differentiation group. The procedures for RT-PCR analyses were performed as described in Chapters 3 and 4. Selected target genes for confirmation of differentiation were as follows: *POU5F1, OTX2, GFAP, TBXT* (T-box transcription factor T; gene for Brachyury), *ACTA2* (Actin alpha 2; gene for ASM), *SOX17*, and *AFP*. The annealing temperatures, names, and primer sequences for each gene are listed in Table 5.2.

5.3.8. Subcutaneous Implantation of Cultured Cells and Colonies

Cultured cells were examined for pluripotency based on their teratogenic potential following subcutaneous injection into male hairless immunodeficient mice (n = 2; SHO, Crl: SHO-*Prkdc*^{scid}*Hr*^{hr}, strain code 474; Charles River, Montreal, Canada). On the day of implantation all media (DMEM+10% FBS) was removed, the wells were rinsed with sterile DPBS, and cells/colonies were detached using trypsin-EDTA solution as previously described (Awang-Junaidi and Honaramooz 2018). To stop the trypsin reaction, FBS was added to each well, then contents were pooled and centrifuged at 500× g at 16° C for 5 min. The supernatant was discarded, and the pellet washed with DPBS and centrifuged again using the same settings. Preparation and

anesthesia of recipient mice were as described previously (Awang-Junaidi *et al.* 2020; Fayaz *et al.* 2020a,b). For implantation procedure, 0.1 mL of the cell aggregates (equals to the content of ~3 wells) were injected subcutaneously into each of 8 sites per mouse (4 sites on the left and 4 sites on the right side of the dorsal midline) as described previously (Awang-Junaidi *et al.* 2020; Fayaz *et al.* 2020a,b). Each mouse was kept in an individual plexiglass micro-isolator cage under sterile conditions and maintained in standard temperature (22 ± 2° C) and controlled lighting photoperiod (12 hr light/dark cycles). The mice were kept for 4 wk, evaluated daily for abnormal signs, and provided with sterile water and chow *ad libitum*.

5.3.9. Retrieval of the Subcutaneous Implants and (Immuno)histochemistry

Recipient mice were sacrificed after 4 wk. The implants were retrieved, rinsed with DPBS, fixed in Bouin's solution, processed, embedded in paraffin, and sectioned at 5 µm. Among the largest sections, randomly selected samples were used for routine histology (hematoxylin and eosin; H&E staining) and immunohistochemistry against lineage-specific antibodies (*i.e.*, GFAP, ASM, and AFP). The procedure for immunohistochemistry was performed as described previously (Fayaz *et al.* 2020a).

5.3.10. Statistical Analyses

All the data are presented as the mean ± standard error of mean (SEM) from at least three independent replicates and $P < 0.05$ was considered as statistically significant. The statistical methods used for the analyses include *t-test* and one-way analysis of variance (ANOVA), and Tukey's HSD was used as the post hoc test, unless stated otherwise. All data analyses were performed using the Statistical Package for Social Sciences (IBM SPSS Statistics for Macintosh, Version 26.00; IBM Corporation, Armonk, NY, USA).

5.4. Results

5.4.1. Viability and Morphometric Assessments

The viability of the freshly isolated testis cells and cultured cells sampled on day 28 in the osteogenic differentiation group, (Experiment 5.1) and day 35 in the tri-lineage differentiation groups (Experiment 5.3), was ~90%. In Experiments 5.1, 5.2, and 5.3 and during the culture period in regular media, morphological features of the cells and colonies were similar to those reported in Chapters 3 and 4, including formation of a wave-shape monolayer after 7 days, development of

circular arrangements, and 3-D embryoid body-like colonies (EBLCs) after ~14 days (Fig. 5.2A-D).

In Experiment 5.1, EBLCs in the control group appeared light in color, while those developed in the differentiation induction media had a more compact appearance with a darker center. The margins of EBLCs developed in differentiation induction media was relatively translucent compared to their opaquer central areas (Fig. 5.2E-J). The number of EBLCs did not differ between these groups ($P = 0.56$), although the average EBLC diameter was ~26% greater in the differentiation induction media compared to control groups ($P < 0.001$; Fig. 5.2K). The average EBLC diameter in the differentiation and regular cultures were 197.16 ± 16.66 μm and 156.10 ± 10 μm, respectively.

In Experiment 5.2, cell confluency was reduced following incubation with tri-lineage differentiation media in all treatment groups. Hence, Experiment 5.2 was removed from further analyses. Following this, Experiment 5.3 was designed and conducted, wherein a modified media changing regimen was used to reduce cell loss and interference with cell organization and arrangement.

In Experiment 5.3, after 7 days of culture, the overall morphology of cells and colonies cultured in differentiation media did not differ from those developed in the regular media. However, after 7 days of incubation in differentiation media, EBLCs appeared more translucent and lighter colored compared to day 0 of differentiation (Fig. 5.3). Further, EBLCs developed in differentiation media appeared to have two different, albeit indistinct, areas: a narrow marginal region close to their edges and a more central area. Notably, while the number of gonocytes or EBLCs in differentiation media were not different from that of control groups ($0.59 < P < 0.93$), the average diameter of EBLCs was smaller than that of the control group and was reduced from day 0 to day 7 of differentiation in all tri-lineage differentiation media ($0.001 < P \leq 0.002$; Fig. 5.3).

5.4.2. Alizarin Red S Staining and Immunofluorescence Assay

5.4.2.1. Osteogenic Differentiation

All colonies developed in the differentiation group produced hydroxyapatite deposits, while none of the colonies in control group were positive for Alizarin Red S staining. No differences in the

extent of differentiation were observed between colonies in the differentiation group. In the control group, gonocytes appeared translucent without color staining and colonies showed a homogenous distribution of dark color. Conversely, all colonies in the differentiation group showed light red staining in the narrow marginal areas and dark red staining in more central areas, indicative of hydroxyapatite deposition (Fig. 5.2E-J). Gonocytes and somatic cells in the differentiation group appeared in light red color following the staining process. The overall distribution pattern of gonocytes, EBLCs, and somatic cells was similar to those observed in the control group.

5.4.2.2. Pluripotency of Germ Cells and their Differentiation into Derivatives of Three Germinal Layers

Freshly-isolated testis cells were negative for POU5F1; however, both gonocytes and EBLCs in regular media appeared positive for POU5F1 on day 28 of culture. Co-localization of DBA and POU5F1 was observed in all germ cells. DBA^{+}/$POU5F1^{+}$ cells comprised ~42 ± 4% of total number of cells in the regular media. Also, gonocytes and EBLCs in regular media were positive for Brachyury but negative for all other markers. In both regular and differentiation media, germ cells appeared positive for DBA. In differentiation groups, some cells and colonies showed strong expression of DBA but weak expression of designated lineage-specific markers. Conversely, a fraction of cells appeared strongly positive for the designated differentiation marker but showed weak expression of DBA. A similar expression pattern for each lineage-specific marker was observed in the corresponding differentiation media (Fig. 5.4A and 5.5).

5.4.3. Gene Expression Analyses

Freshly-isolated testis cells appeared negative for expression of *POU5F1*. However, in Experiment 5.3, cultured cells in regular media displayed POU5F1 expression on day 7 to day 28. In Experiment 5.3, RT-PCR for cultured cells in ectoderm, mesoderm, and endoderm differentiation media were positive for *OTX2/GFAP, TBXT/ACTA2*, and *SOX17/AFP*, respectively. Samples of freshly isolated testis cells were also positive for *SOX17, TBXT, ACTA2, OTX2*, and *GFAP*. Cells cultured in regular media (DMEM+15% FBS+10 ng/mL bFGF) were positive for *TBXT* and *ACTA2*. Also, *ACTA2* expression was evident in samples of endoderm and ectoderm differentiation cultures (Fig. 5.4B and 5.6).

5.4.4. Characterization of Dedifferentiated Cell Implants

5.4.4.1. H&E Staining

Histological examination of the injected cells/colonies (n = 16 injected aggregates) revealed gradual formation of cellular structures, which morphologically did not belong to the normal adjacent peripheral tissues. These structures were located at the expected implantation sites, including immediately ventral to the dermis and dorsal to the hypodermis. The morphologies, dimensions and extension of these tumor-like growth formations varied between injection sites and animals. These formations appeared as multicellular dense structures, were present in all implantation sites, and were encapsulated within a dense connective tissue. In sparse areas within the formations, the distribution of cells formed circular and oval patterns. In certain other areas, the formations contained distinguishable groups of cells that resembled melanocyte nests. Furthermore, increased numbers of melanocytes with melanin deposition were detected in cross-sections of all implants, representing the formation of melanomas. In addition, the formations contained bundles resembling those of peripheral nerves (Fig. 5.7A-D).

5.4.4.2. Immunohistochemistry

To confirm the differentiation of implanted cells and colonies we used antibodies associated with each germinal layer. Expression of each maker was observed in all samples but were localized to specific areas of the formations. Cells in adjacent foci to the adipose tissue appeared positive for anti-pig-AFP, which was expressed in both the nucleus and cytoplasm. Cells within and surrounding the aforementioned circular/oval patterns expressed ASM. Also, GFAP was expressed in small foci, and within the bundles resembling peripheral nerves. GFAP expression also appeared to be both nuclear and cytoplasmic (Fig. 5.7E-H).

Table 5.1. Antibodies used for immunofluorescence and immunocytochemistry

Antibody	Supplier	Catalogue no.	Dilution
Rabbit anti-POU5F1	Abcam	AB18976	1:200
Goat anti-OTX2	R&D Systems	SC031B	1:200
Mouse anti-GFAP	Novus Biological	NBP1-05197SS	1:200
Goat anti-Brachyury	R&D Systems	SC030B	1:200
Mouse anti-ASM	Novus Biological	NBP1-33006	1:200
Goat anti-SOX17	R&D Systems	SC019B	1:200
Rabbit anti-AFP	Novus Biological	NBP1-76275	1:200
Alexa Fluor 594 goat anti-rabbit	Abcam	AB150088	1:200
Alexa Fluor 594 goat anti-mouse	Abcam	150116	1:200
Alexa Fluor 594 rabbit anti-goat	Abcam	150148	1:200

Table 5.2. RT-PCR primer sequences for gene expression analyses

Target name	Direction	Primer sequence (5′-3′)	Annealing Temperature (° C)	Product size (BP)
POU5F1	Forward	AGAGAAAGCGGACAAGTA	51.7	299
	Reverse	ATCCTCTCGTTGCGAATA		
OTX2	Forward	TTTATCTGGTCTCTCTCCCTCTC	61	129
	Reverse	GTTAGTGGTGGAAAGTGGTAGG		
GFAP	Forward	CAGAGCAGGACCGAGTTTATG	61	117
	Reverse	CATAAAGAGAAGAGGGAAGGACAG		
TBXT	Forward	GGGATTTGCTTCTGGGTCTAA	63.7	124
	Reverse	GTTGAGAAGTCACTGGACAGAG		
ACTA2	Forward	CTGGGTCTGAGTCTTAGCTTTC	63.7	114
	Reverse	GATAGGATGGCTGTGTGGATT		
SOX17	Forward	CATCTCAAGTGACCCTAGTCTTTAC	61	136
	Reverse	GTTGAATCTTGAGGTCTGCCT		
AFP	Forward	GCTCCATCTCCTTGCTTTCT	66.1	100
	Reverse	AAGAGATGCCCATAAACCCTG		
GAPDH	Forward	TCGGAGTGAACGGATTTG	62	219
	Reverse	CCTGGAAGATGGTGATGG		

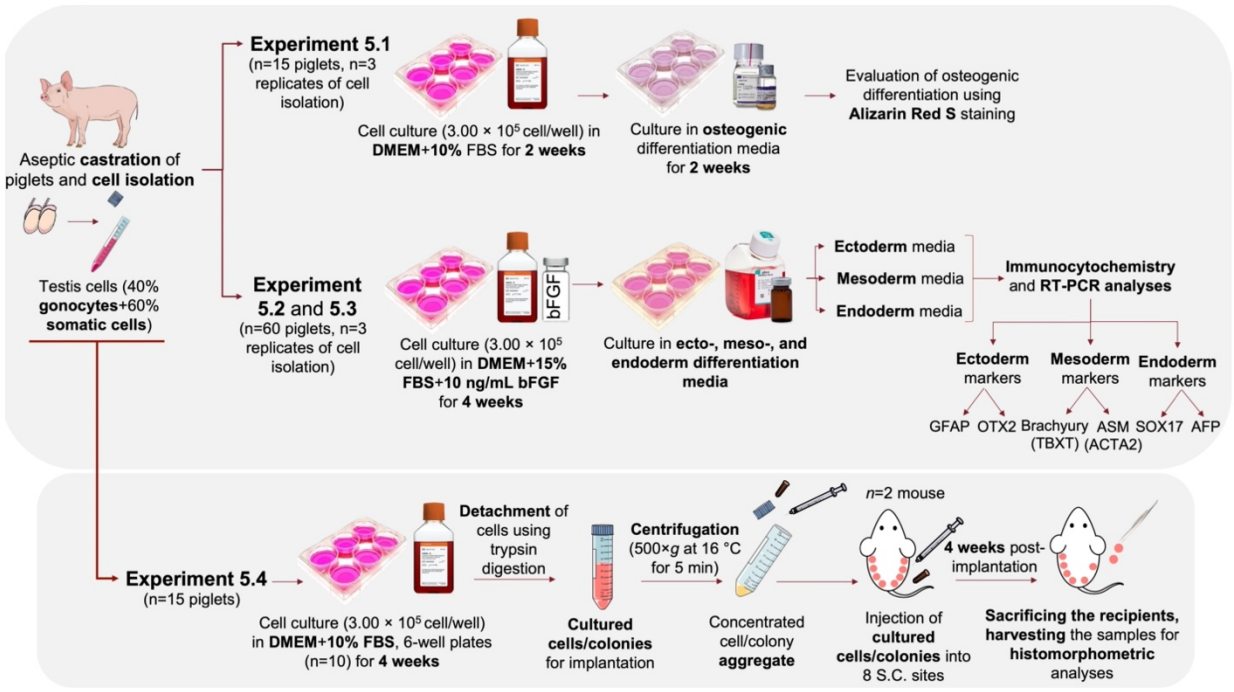

Fig. 5.1. Schematic representation of the experimental design. In Experiment 5.1, differentiation of neonatal porcine gonocytes to osteogenic pathway was investigated. Gonocytes were isolated from neonatal piglets and cultured in regular media for 2 wk to induce dedifferentiation. Media was then changed to osteogenic differentiation media to direct their differentiation into osteogenic cells. Cells and colonies were stained with Alizarin Red S for confirmation of osteogenic differentiation. In Experiments 5.2 and 5.3, to induce tri-lineage differentiation, porcine gonocytes were cultured in regular media for 4 wk to induce dedifferentiation. Cells and colonies were then cultured in ectoderm, mesoderm, or endoderm differentiation media to direct their differentiation into the respective cell derivates. Tri-lineage differentiation was confirmed by immunocytochemistry and RT-PCR analyses against markers associated with formation of ectoderm, mesoderm, and endoderm. The pluripotency and tumorigenicity of cultured gonocytes and their colonies were also investigated using an implantation assay (Experiment 5.4). Isolated testis cells were cultured for 4 wk in DMEM+10% FBS, dislodged from culture wells, and injected into the subcutaneous tissue of immunodeficient recipient mice. After 4 wk, recipient mice were sacrificed, and implants were retrieved for histomorphometric analyses.

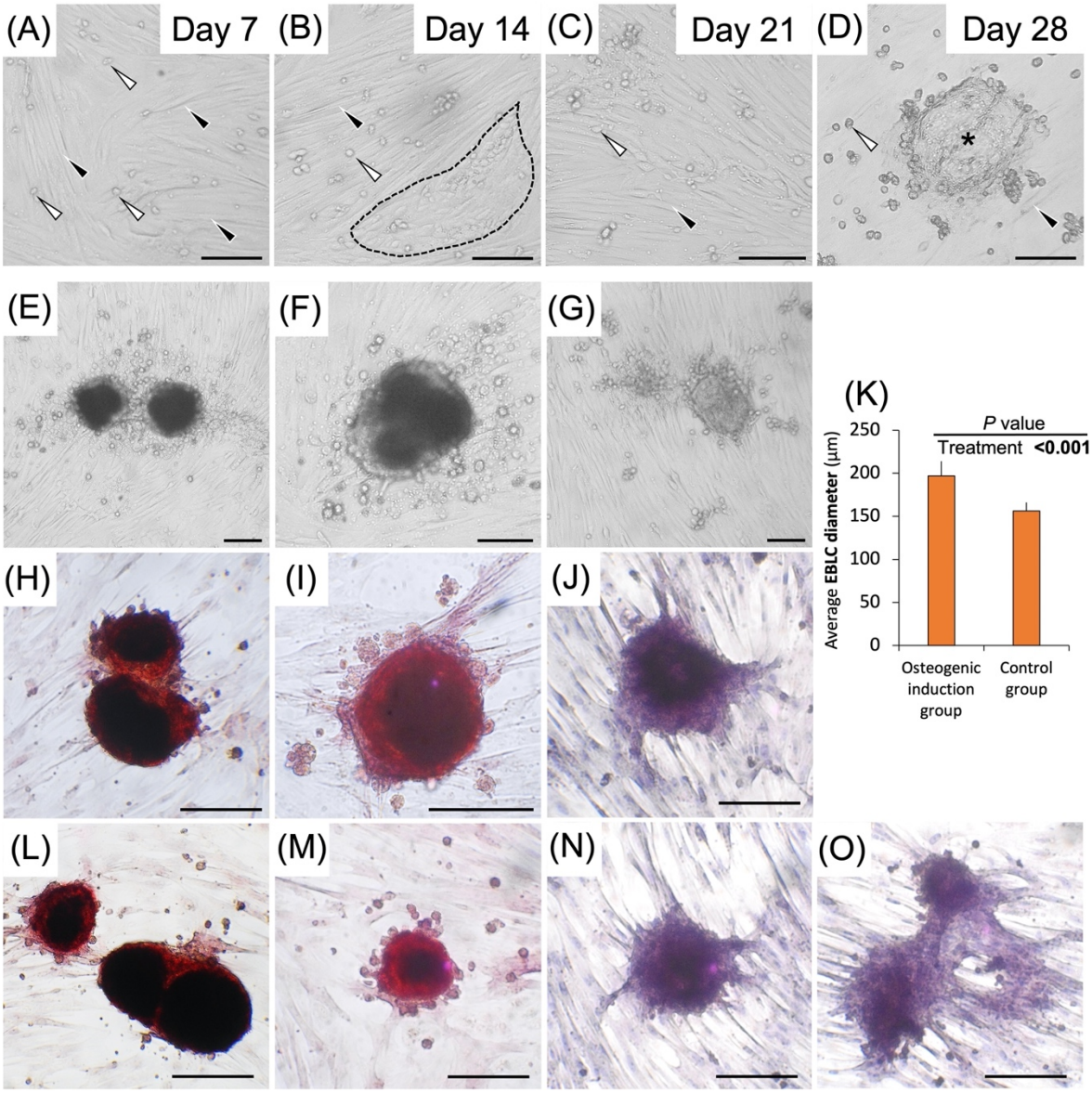

Fig. 5.2. Representative photomicrographs of culture wells in regular media and osteogenic differentiation media, as well as the average diameter of EBLCs in different groups. When cultured in regular media, by day 7, somatic cells of the testis formed a complete monolayer attached to the culture well (black arrowhead). Gonocytes were located on top of the spindle-shaped somatic cells (white arrowhead) (A). By day 14, somatic cells formed circular arrangements (black broken line) (B). In circular arrangements, gonocytes were surrounded by cytoplasmic projections of somatic cells. Gonocytes gradually increased in number by undergoing proliferation. Also, by day 14, convergence of surrounding gonocytes in circular arrangements led to formation of large multinucleated embryoid body-like colonies (EBLCs). By day 28, gonocytes increased in number

and EBLCs became larger (black asterisk) (C and D). EBLCs in osteogenic differentiation group (E, F, H, I, L, and M) possessed a more compact appearance compared to those developed in control groups (G, J, N and O). Also, EBLCs in osteogenic differentiation groups developed darker central areas and narrower translucent marginal areas. This may be related to their dome-shaped structure leading to a thicker central area compared to thinner marginal areas. EBLCs appeared positive for Alizarin Red S staining, indicative of their transformation into calcium deposition sites (H, I, L, and M), while control groups appeared negative for this staining (J, N, and O). Although the number of EBLCs did not differ between osteogenic differentiation and control groups, their average diameter was greater in differentiation group ($P < 0.001$) (K). (Scale bar = 100 μm)

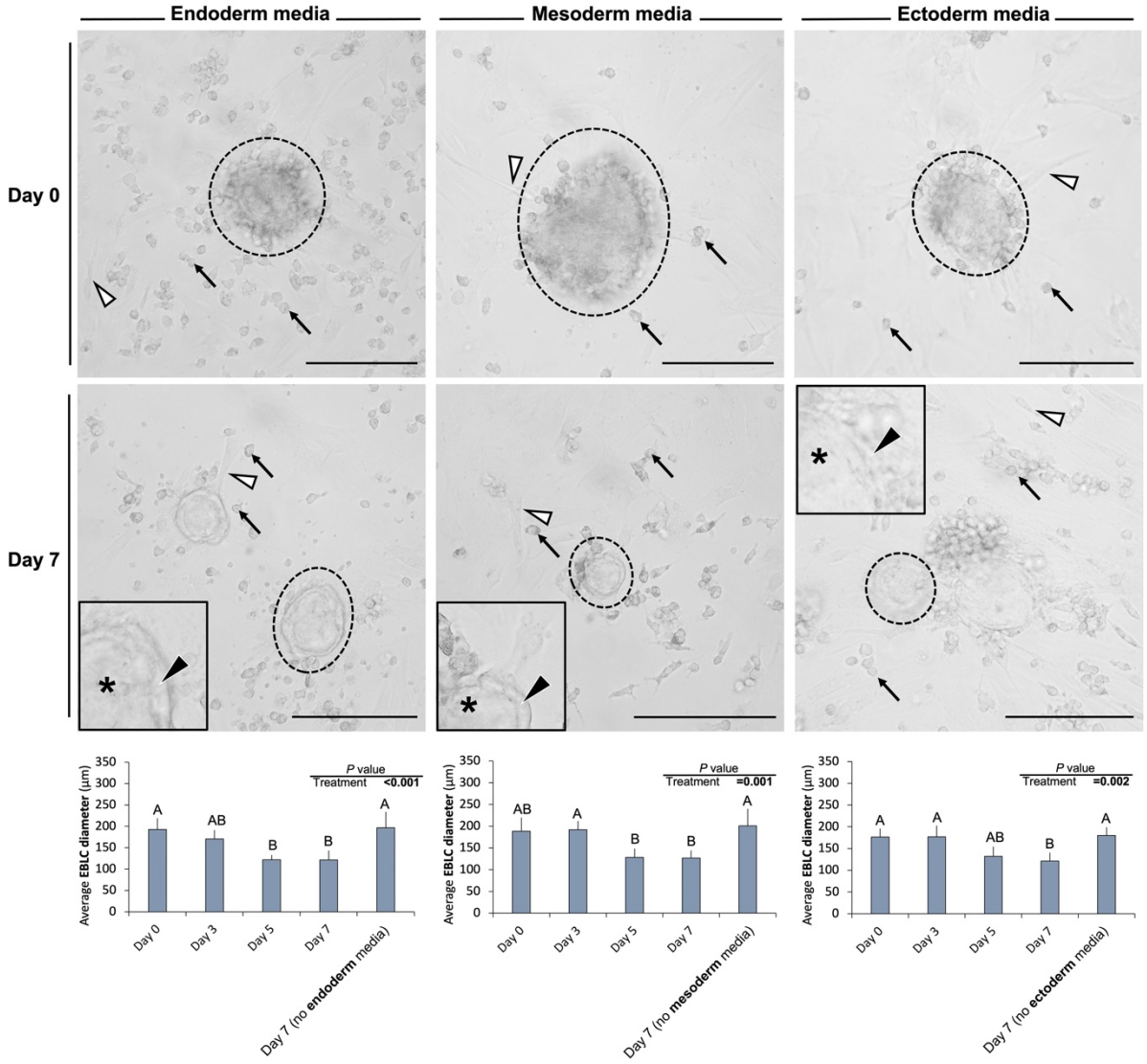

Fig. 5.3. Representative photomicrographs obtained from culture wells before (day 0) and 7 days after incubation with the tri-lineage differentiation media. The overall morphological features of gonocytes (black arrows), embryoid body-like colonies (EBLCs) (dotted circles), and somatic cell monolayer (white arrowheads) did not differ between control groups provided with regular media (DMEM+15% FBS+10 ng/mL bFGF) and treatment groups incubated with ectoderm, mesoderm, or endoderm differentiation media. However, the diameter of EBLCs decreased in the three differentiation media compared with those in the control group ($0.001 < P \leq 0.002$). Also, the EBLCs in differentiation media possessed a narrow marginal area close to the periphery (black arrowheads) and more central areas (asterisks). Insets show higher magnification. A and B denote significant differences and $P < 0.05$ was considered as significant. (Scale bar = 150 µm)

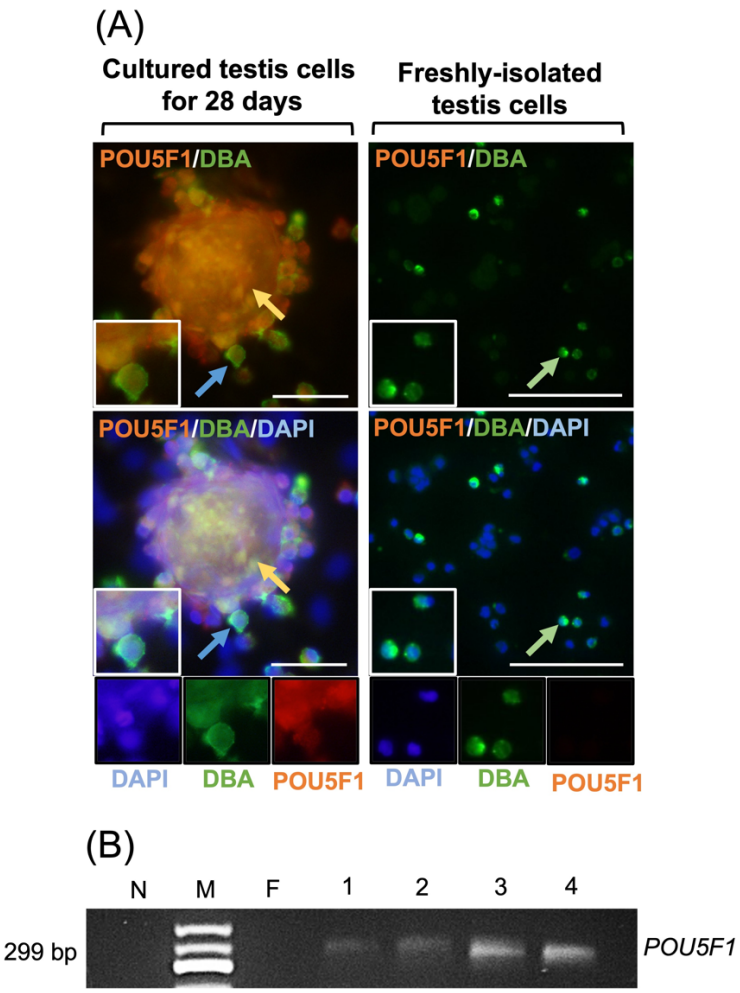

Fig. 5.4. Evaluation of POU5F1 expression as a pluripotency marker and DBA as gonocyte-specific marker by freshly-isolated and cultured porcine testis cells in regular media. Following isolation of testis cells, gonocytes were positive for DBA (green arrows) but negative for POU5F1. When cultured in regular media, gonocytes (blue arrows) and EBLCs (yellow arrows) were positive for both POU5F1 and DBA (A). Also, testis cells appeared negative for *POU5F1* immediately after isolation in RT-PCR analyses, while in samples of day 7, 14, 21, and 28, cultured testis cells appeared positive for this marker (B). These findings are indicative of spontaneous MGSC reversion into more primitive developmental stages. N, no template control; M, 50 bp DNA ladder; F, freshly isolated testis cell sample; Lines 1-4, cultured cells and colonies in regular media for 7, 14, 21, or 28 days, respectively. Insets display higher magnification. (Scale bar = 50 µm)

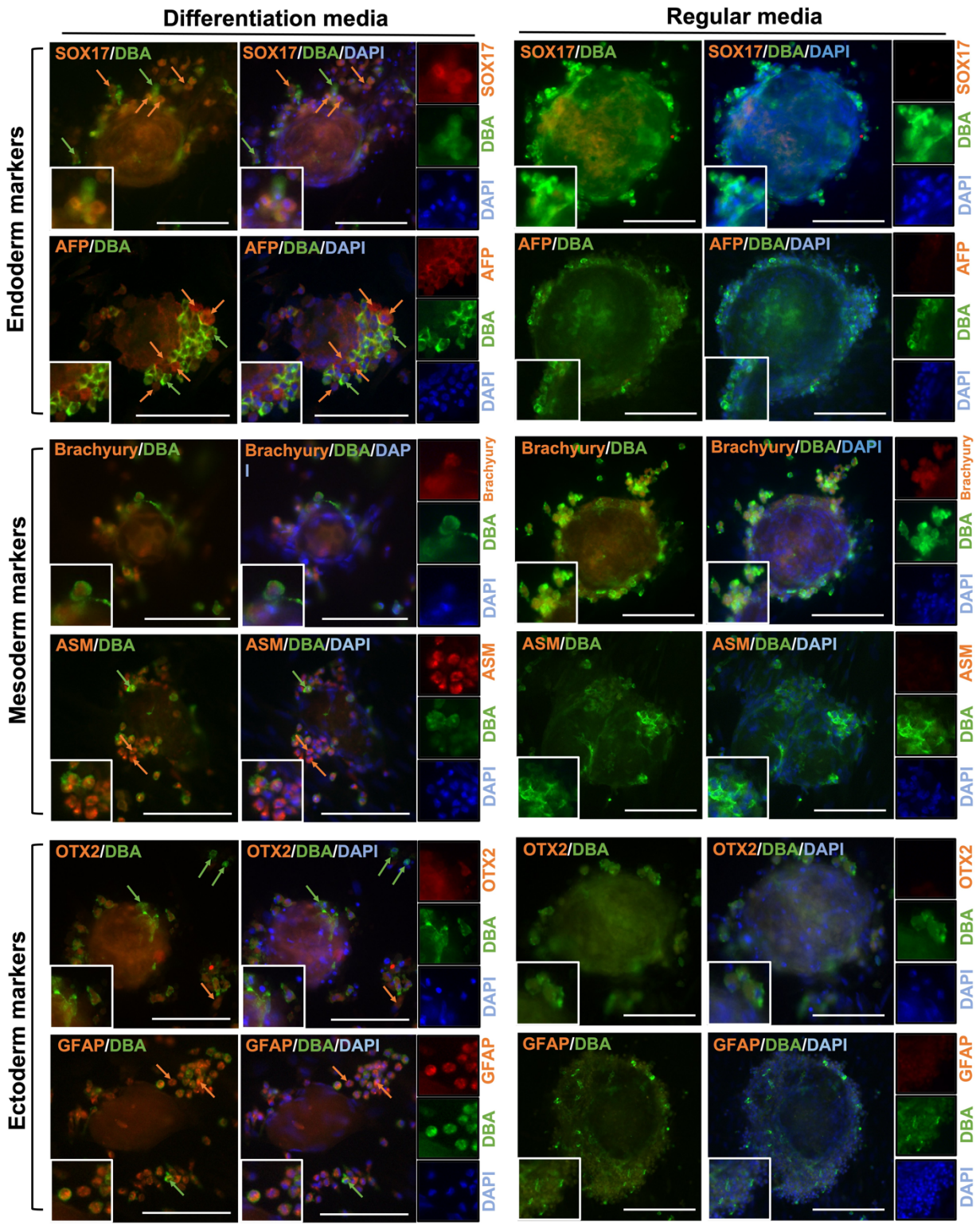

Fig. 5.5. Expression of a gonocyte-specific marker (DBA) and markers of endoderm (SOX17 and AFP), mesoderm (Brachyury and ASM), and ectoderm (OTX2 and GFAP) by cultured gonocytes

and their colonies in regular and differentiation media. Overall, gonocytes and embryoid body-like colonies (EBLCs) were positive for DBA. Many gonocytes showed strong expression of DBA (green arrows) but weak expression of lineage-specific markers. Other gonocytes showed strong expression of the lineage-specific markers (orange arrows) when cultured in corresponding media. EBLCs appeared positive for all three lineage differentiation markers. When cultured in regular media, gonocytes and EBLCs were positive for DBA and Brachyury, but were negative for OTX2, SOX17, AFP, ASM, and GFAP. This may indicate that gonocytes in differentiation media are gradually converting into a new population of cells with similar biomolecular properties as cells of three germinal layer derivatives. (Scale bar = 100 μm)

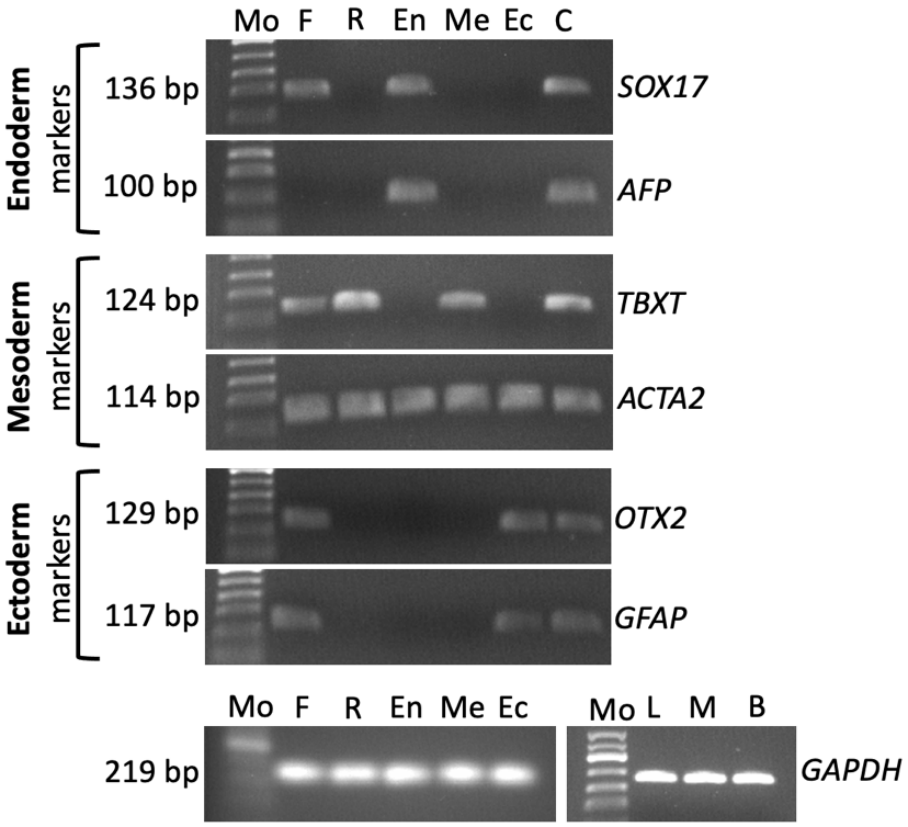

Fig. 5.6. Gene expression analyses of germinal layer-specific markers using RT-PCR. Expression of germinal layer markers was positive in respective differentiation media. Also, freshly isolated testis cell samples were positive for the expression of *SOX17, TBXT, ACTA2, OTX2*, and *GFAP*. Cultured testis cells in regular media (DMEM+15% FBS) were positive for mesoderm markers (*TBXT* and *ACTA2*). *ACTA2* expression was also positive in cultures of endoderm and ectoderm differentiation media in addition to cultures treated with mesoderm differentiation media. Mo, 50 bp DNA ladder; F, freshly isolated testis cell sample; R, cultured cells and colonies in regular media; En, cultured cells and colonies in endoderm differentiation media; Me, cultured cells and colonies in mesoderm differentiation media; Ec, cultured cells and colonies in ectoderm differentiation media; C, positive control (liver sample for *SOX17* and *AFP*; muscle sample for *TBXT* and *ACTA2*; brain sample for *OTX2* and *GFAP*); L, liver sample; M, muscle sample; B, brain sample.

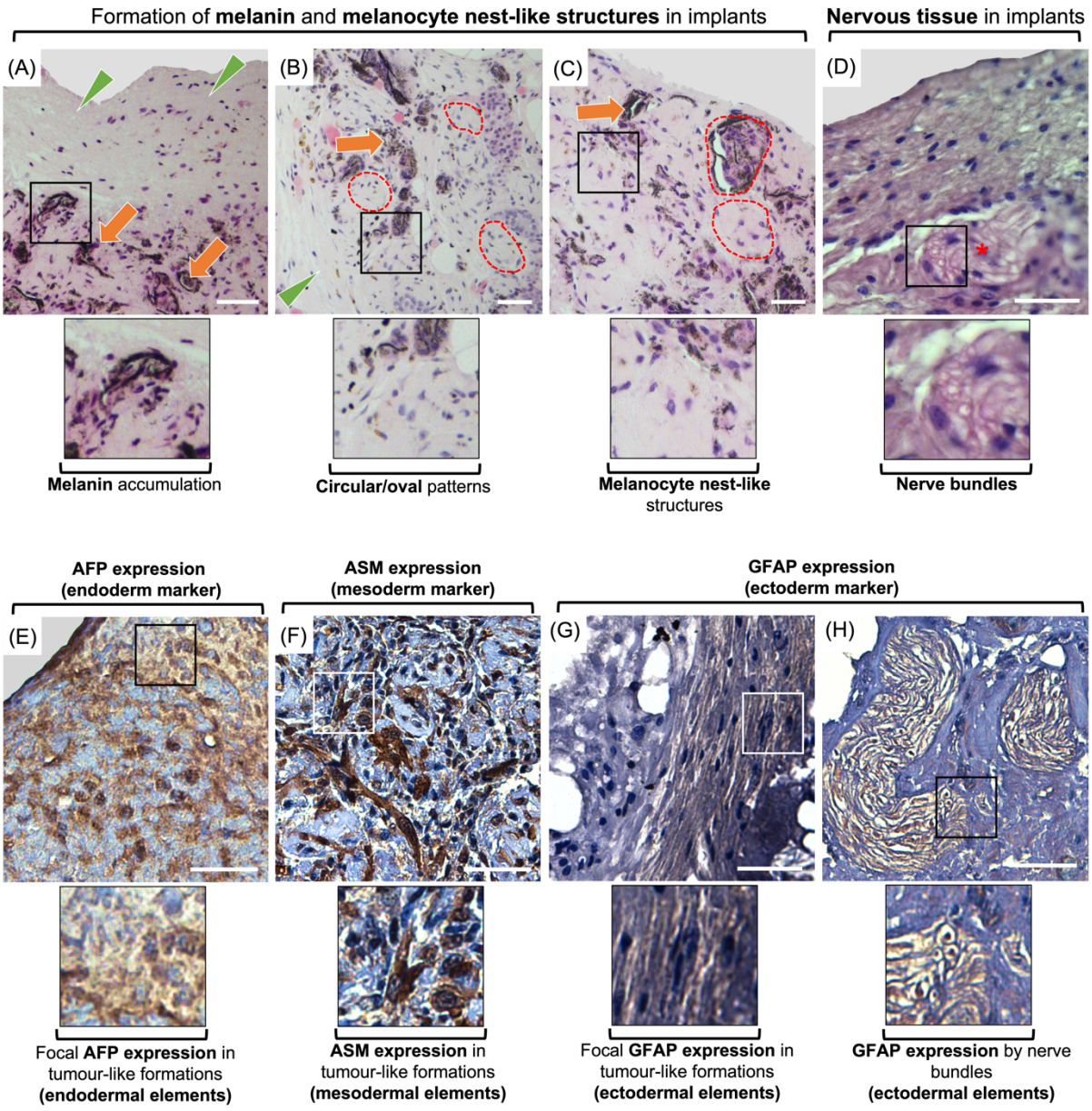

Fig. 5.7. Representative photomicrographs captured from (immuno)histological sections of dedifferentiated cell implants. Implants were stained using H&E (A-D) or labelled with lineage-specific antibodies including AFP (E), ASM (F), or GFAP (G and H). The implants were surrounded by a dense fibrous capsule (green arrowhead) (A and B). Implants developed into tumour-like growth formations containing circular and/or oval patterns as well as large numbers of melanocytes with remarkable accumulation of melanin pigments (orange arrows) (A, B, and C). The distribution pattern of the cells resembled nests of melanocytes (red broken lines) (B and C). Within these formations were also located the bundles resembling those of peripheral nerves

(asterisk) (D). AFP as endoderm marker was expressed in foci of implanted cells/EBLCs (E). Focal AFP expression can be attributed to endodermal elements in tumour-like formations. Also, limited expression of ASM was observed by the cells inside and surrounding the circular patterns (F), which can be deemed as the presence of differentiated myofibroblasts. Small foci within the formations and nerve bundle-like structures both appeared positive for GFAP as neuroectodermal marker (G and H), which can point at development of ectodermal components within the formations. Squares display higher magnification. (Scale bar = 50 μm)

5.5. Discussion

In previous works as well as the present Chapter, our laboratory has shown that gonocytes from neonatal porcine testis can spontaneously dedifferentiate and express pluripotency-associated markers when cultured under basic conditions (Awang-Junaidi *et al.* 2020). Given the potential of these cells in conversion into a pluripotent state, here we first developed a population of dedifferentiated gonocytes using our previously established culture conditions, evaluated their potential to generate derivatives of three germinal layers *in vitro*, and assessed their pluripotency and plasticity using an *in vivo* implantation assay. As such, the present study is the first to show that, upon providing the appropriate media and supplements, dedifferentiated porcine gonocytes and their colonies can undergo osteogenic differentiation *in vitro* and can convert into cells of the three germinal layers (*i.e.,* ectoderm, mesoderm, or endoderm). Additionally, we showed that implantation of cultured gonocytes and their colonies into the subcutaneous tissue of recipient mice can lead to development of tumor-like growth formations. These formations contain areas which morphologically resembled ectoderm, mesoderm, or endoderm-derived tissues and express markers that are present in all three germinal layers. This observation further confirms the unique potential of gonocytes to spontaneously transform into a pluripotent state under simple *in vitro* conditions. The dedifferentiation and trans-differentiation potential of germ cells is a remarkable finding that sheds light on their unique conversion potential and can open new avenues of research into their applications in stem cell therapy and regenerative medicine.

In Experiment 5.1 of the present study, we successfully induced osteogenic differentiation in gonocyte colonies. Osteoblasts have mesodermal origin and are specialized mesenchymal cells that synthesize bone matrix (Mackie 2003; Franz-Odendaal *et al.* 2006). Here, we used simple culture conditions to develop pluripotent germline stem cells in a short-term culture (~2 wk) and transformed them into osteogenic cell derivatives with bone matrix deposition potential. Following differentiation, morphological features of EBLCs stained with Alizarin Red S resembled those of *in vitro* developed osteoblast colonies which typically possess darker color in the central areas and lighter color in the marginal areas (Yin *et al.* 2007; Orriss *et al.* 2012). This morphological pattern of EBLCs features a dome shape appearance and greater calcium deposition in the central areas compared to the narrow marginal areas. Previously, embryonic chicken SSCs were shown to undergo directional differentiation into osteoblasts by cultivation for multiple passages on a feeder

layer and in media composed of multiple growth factors and/or other supplements (Li *et al.* 2010). Although successful, trans-differentiation rate of chicken SSCs was 75-80%. In contrast, we showed that all EBLCs developed from porcine testis cells transformed into calcium phosphate deposition sites and appeared positive for Alizarin Red S staining; all in a relatively short period of time and without supplementation of multiple exogenous factors. In another study, bovine germ cells were co-cultured with Sertoli cells for 21 days in a differentiation induction media to become trans-differentiated into osteoblasts followed by confirmation of differentiation using Alizarin Red S staining (Qasemi-Panahi *et al.* 2011). Although multiple studies have already shown mesenchymal and ES cell potential to convert into osteogenic cell lineages (Parikka *et al.* 2005; Hanna *et al.* 2018), successful generation of osteogenic progenitors from porcine germ cells acts as an even stronger indication of similar potential in human germ cells, given the anatomical and physiological similarities between pigs and humans. As such, our findings introduce a new avenue for application of these cells in bone regeneration and matrix formation. Of notable importance, using MGSCs for the purpose of bone regeneration in an autologous manner does not carry the same ethical concerns associated with the use of ES cells, nor the biosafety risks associated with the use of iPS cells.

In addition to the osteogenic differentiation, we also examined the conversion potential of cultured gonocytes into cell derivatives of all three germinal layers. As mentioned above, Experiment 5.2 was not continued due to limited cell growth and negative expression of lineage-specific markers following brief exposure to the differentiation media. Limited cell growth in Experiment 5.2 can be attributed to an underdeveloped somatic cell monolayer, which is essential for survival of non-adherent gonocytes (Awang-Junaidi and Honaramooz 2018; Awang-Junaidi *et al.* 2020). We suggest that perhaps the frequent replenishment of the differentiation media in Experiment 5.2 led to physical detachment of the monolayer and/or removed essential components that were naturally produced by cultured cells. However, in the immunofluorescence results of Experiment 5.3 we showed decreased intensity of DBA expression and increased intensity of lineage-specific markers, including AFP/SOX17 in endoderm differentiation group, ASM in mesoderm differentiation group, and GFAP/OTX2 in ectoderm differentiation group, all indicative of gradual conversion of gonocytes into other cell lineages.

The expression of transcription factors examined in the present study are critical for normal formation and development of germinal layers during embryonic development (Eng 1985; Babai *et al.* 1990; Ang *et al.* 1994; Abe *et al.* 1996; de Jong *et al.* 2008; Bernardo *et al.* 2011; Mortensen *et al.* 2015). Here, positive expression of SOX17 in freshly isolated testis cells is in agreement with previous studies on isolated human PGCs and gonocytes (Irie *et al.* 2015; Fang *et al.* 2020). Conversely, negative expression of SOX17 in cultures of regular media may be indicative of germ cell transformation into more primitive developmental stages. SOX17 is a key transcription factor in the development of endoderm as its mutation leads to defective intercellular transport in endoderm (Viotti *et al.* 2012; Fang *et al.* 2020). Additionally, we used AFP as a secondary endoderm marker. Expression of AFP is typically upregulated in nonseminomatous germ cell tumors (Bostwick 2006) and expectedly was not expressed in our fresh testis cell samples. Here, mesoderm and ectoderm cultures were also negative for AFP, perhaps due to the lack of chemical components required for directing cell differentiation towards definitive endodermal lineages. Components of endoderm differentiation media such as bFGF, Wnt-a, and Activin A play important roles in enhancement of definitive endoderm-associated gene expression and cell viability in a dose dependent manner (Yao *et al.* 2006; Xu *et al.* 2011; Qu *et al.* 2017; Diekmann *et al.* 2019). The same interplay can be speculated between these components in our culture system, leading to expression of endodermal gene transcripts.

Here, we also showed mesoderm differentiation cultures became Brachyury^{+} while endoderm and ectoderm differentiation cultures appeared Brachyury^{-}. Brachyury is a factor required for posterior mesoderm formation (Barresi *et al.* 2014). In agreement with our observations, a previous study on mouse germ cells showed fresh testis lysates and germ cell enriched cultures were positive for Brachyury, which the authors concluded was essential for mouse germ cell self-renewal (Wu *et al.* 2011). Interestingly, multipotent germline stem cells developed from murine testis cells were also positive for Brachyury (Baba *et al.* 2007). This further supports our finding regarding Brachyury^{+} cultures in regular media, which were previously demonstrated to express pluripotency-associated markers (Awang-Junaidi *et al.* 2020). Additionally, ASM as a secondary marker for mesoderm differentiation was positive in all samples. This could have occurred due to contaminating peritubular myoid cells and/or blood endothelial cells; however, in immunocytochemistry, ASM expression was localized to the cells surrounding the EBLCs, which also weakly expressed DBA. This may point at gradual transformation of DBA^{+} cells to cells with mesodermal origin.

Identification and positive expression of ASM has been also reported in previous studies on primate testis cell culture (Langenstroth *et al.* 2014; Sharma *et al.* 2019). ASM is one of the actin isoforms responsible for mechanical tension of the cells (Wang *et al.* 2006).

Here, like SOX17, the expression of OTX2 and GFAP was downregulated in germ cells during culture in regular media. OTX2 is required for neuroectoderm differentiation (Boyl *et al.* 2001; Li and Joyner 2001; Beby and Lamonerie 2013; Yang *et al.* 2019) and is inherently expressed in porcine brain and reproductive tissues (Wang *et al.* 2016; Dawson *et al.* 2018). Additionally, Leydig cells possess neuroendocrine features and are immunopositive for neuroectodermal and astrocyte markers such as GFAP (Apte *et al.* 1998; Davidoff *et al.* 2002). Thus, positive GFAP expression by freshly isolated cells can be explained by the presence of Leydig cells, which once isolated and cultured in regular media, perhaps downregulated its expression.

In Experiments 5.1 and 5.3, migrating gonocytes formed clusters and colonies which transformed into EBLCs. Although smaller in size, the morphology of the EBLCs in Experiment 5.3 was comparable to those of Experiment 5.1. The presence of two indistinct peripheral and central areas in EBLCs can be explained by their dome-shape appearance, which normally have thinner marginal areas and thicker central areas. This can lead to a more translucent edge and opaque centre in EBLCs.

We have previously shown that MGSCs in regular media dedifferentiate and express a number of ES cell markers (Awang-Junaidi *et al.* 2020). Similarly, to confirm dedifferentiation of cultured MGSCs in regular media into primitive developmental stages, here we examined their expression of POU5F1 as one of the accepted and important ES markers (Nichols *et al.* 1998; Pan *et al.* 2002; Zeineddine *et al.* 2014). As demonstrated previously, unlike freshly-isolated testis cells which are negative for this marker, cultured cells showed positive POU5F1 expression (Awang-Junaidi *et al.* 2020). Here we showed that all MGSCs in culture conditions appeared both DBA- and POU5F1-positive. This further confirms that MGSCs are able to spontaneously revert to a dedifferentiated state and express markers that are mutually present in ES cells. As such, in the present study we used an implantation assay to evaluate their tumorigenic potential and examined the expression of selected germinal layer biomarkers (*i.e.,* AFP, ASM, and GFAP) in retrieved samples. In all injection sites, multicellular tumor-like formations contained foci with positive cells for AFP, ASM, or GFAP. AFP is a known marker for nonseminomatous germ cell tumors (Milose *et al.*

2012), and its expression may point at development of endodermal component within our observed formations (Jacobsen 1983; Lempiäinen *et al.* 2014; Mosbech *et al.* 2014). ASM expression was similarly observed in sparse locations of our retrieved samples. ASM expression is associated with mesodermal differentiation in tumors derived from pluripotent stem cells (Wakao *et al.* 2012; Wagner *et al.* 2020). Here, we also observed GFAP expression in focal areas within the formations. The morphology and pattern of diffuse GFAP-positive areas partly resembled those observed in previously reported glial cell neoplastic tissues containing polygonal and spindle shape cells with indistinct cellular borders (Akiyama *et al.* 2014). Additionally, nerve bundle-like structures within these formations appeared positive for GFAP, which may suggest the presence of a neuroectodermal component. Increased GFAP expression has been attributed to neuroectodermal component in teratomas (Sundström *et al.* 1999; Gu *et al.* 2011). Importantly, excessive accumulation of melanin and development of melanocyte nests further confirms the presence of ectodermal tissue in the developed tumor-like formations. Thus, the overall morphological and immunohistochemical attributes of the implanted cells and EBLCs point at their potential contribution to formation of tumor-like structures which contain endodermal, mesodermal, and ectodermal components. The tumorigenic potential is one of the staple characteristics of ES- or iPS cells derived from somatic cells (Wakao *et al.* 2012). Additionally, by definition, pluripotent stem cells can give rise to the cells of all three germinal layers, whereas multipotent stem cells can differentiate to particular tissue types/cell lineages but not all, which suggests that similar to ES- or iPS cells, developed germ cell-derived stem cells in our culture conditions can be classified as pluripotent (Singh *et al.* 2016). As such, gonocytes in our primary culture conditions spontaneously underwent reprogramming into a pluripotent state in a relatively shorter time (~4 wk post-implantation) as confirmed by the implantation assay. Additionally, we successfully converted these cells into cell derivatives from all three germinal layers, which has not been achieved previously. Harvesting germ cells from primary culture is important since multiple passages and removal of the cells from their microenvironment causes unwanted changes to their physiological and biochemical properties (Goel *et al.* 2009). Such changes can generate confounding factors for their downstream applications and pose negative effects on their proliferation and differentiation potential at genetic or epigenetic levels (Goel *et al.* 2009).

In conclusion, neonatal porcine gonocytes represent a promising source of adult stem cells. In our culture conditions, these stem cells undergo dedifferentiation into more primitive developmental

stages. When implanted into recipient mice, the cultured gonocytes and their colonies develop formations with morphological and biomolecular characteristics of all three germinal layers, which further confirms their plasticity. Furthermore, cultured gonocytes and their colonies effectively convert into derivatives of ectodermal, mesodermal, and endodermal germinal layers in trans-differentiation media. *In vitro* dedifferentiation and subsequent conversion of neonatal gonocytes into osteogenic cells and derivatives of three germinal layers are important observations since this *in vitro* system can provide an easily accessible and abundant source of adult stem cells for numerous downstream applications in regenerative medicine. More importantly, unique conversion potential of neonatal gonocytes into other cell types makes them a potentially attractive autologous pluripotent cell source since their use eliminates ethical implications and the biosafety risks associated with viral vectors to induce pluripotency, and they can be easily produced *in vitro* without addition of multiple extrinsic factors. The capacity of neonatal germ cells to differentiate into cells of all embryonic germinal layers highlights their importance and warrants further research including on their putative differentiation triggers. Such studies may put these cells in a privileged position to treat tissues of high interest in regenerative medicine, especially those that present low regeneration rates such as neural tissue, tendon, or cartilage when compared to other better studied multipotent stem cells. More specifically, the testicular biopsies obtained from preadolescent boys can potentially serve as a dual source of germ cells for fertility restoration and germ cell-derived pluripotent stem cells for development of somatic cells and tissues. As such, MGSCs offer an autologous alternative stem cell source to the available adult stem cells such as cord blood stem cells with similar potentials. It goes without saying that any *in vivo* application of these cells should be preceded with extensive assessments of any potential risk for tumor development.

Transition

Beside *in vitro* models for the study of testis cells and tissues, *in vivo* models have been developed and optimized over time to provide invaluable information about testis development and cell-cell interactions. These models include testis tissue xenografting and testis cell aggregate implantation which are known as versatile tools to study testis morphogenesis and function especially where *in situ* studies are not possible. These models also allow testing the effects of various factors on testis formation and function. To introduce a non-invasive approach for *in vivo* study of testicular morphogenesis and testis tissue development in Chapter 6 we used ultrasound biomicroscopy in a validation study. We successfully established a non-invasive and accurate approach for monitoring the ectopic testis tissue grafts and cell implants located in the recipient host by using ultrasound biomicroscopy. The study presented in Chapter 6 would eliminate the need for multiple surgical sampling following grafting/implantation thereby reducing the risk of infection in recipients and increasing the accuracy of morphometric sample evaluation.

CHAPTER 6

VALIDATION OF ULTRASOUND BIOMICROSCOPY FOR THE ASSESSMENT OF XENOGENEIC TESTIS TISSUE GRAFTS AND CELL IMPLANTS IN RECIPIENT MICE [7, 8]

6.1. Abstract

Subcutaneous grafting/implantation of neonatal testis tissue/cells from diverse donor species into recipient mice can be used as an *in vivo* model to study testis development, spermatogenesis, and steroidogenesis. Ultrasound biomicroscopy (UBM) allows obtaining high definition cross-sectional images of tissues at microscopic resolutions. The present study was designed to 1) validate the use of UBM for non-invasive monitoring of grafts/implants over time, and to 2) correlate UBM findings with the morphological attributes of recovered grafts/implants. Testis tissue fragments (~14 mm^3, each) and cell aggregates (100×10^6 cells, each) obtained from 1-wk-old donor piglets (n = 30) were grafted/implanted under the back skin of immunodeficient mice (n = 6) in eight analogous sites per mouse. Three-dimensional transcutaneous Doppler UBM was performed and a randomly-selected graft and its corresponding implant were recovered at 2, 4, 6, and 8 wk. Graft/implant weight (P = 0.04) and physical height (P = 0.03) increased over time. The dynamics of physical length and volume increases over time differed between tissue grafts and cell implants (P = 0.02 and 0.01 for sample type*time interactions, respectively). UBM-estimated volume was correlated with the post-recovery weight and volume of the grafts/implants (r = 0.98 and r = 0.99, respectively; $P < 0.001$). Pre- and post-recovery length and height of the grafts/implants were positively and strongly correlated (r = 0.50, P = 0.01; r = 0.70, P = 0.001) and so were the areas covered by cordal, non-cordal or fluid-filled cavities between UBM and histology (r = 0.87, $P < 0.001$). UBM findings correlated with physical attributes of the grafts/implants, validating its use as a non-invasive high-fidelity tool to quantify the developmental

[7] This study has been published. Fayaz MA, Awang-Junaidi AH, Singh J, and Honaramooz H (2020) *Andrology* 8:1332–1346.

[8] MAF contributed to the experimental design, performed the study, analyzed the data, and wrote the first draft of the manuscript. AHAJ contributed to performing the study and analyses. JS contributed to the experimental design and revised the manuscript. AH supervised the study, contributed to the experimental design, and revised the manuscript.

changes in ectopic testis tissue grafts and cell implants, potentially leading to a reduction in the number of recipient mice needed for similar experiments.

6.2. Introduction

(Xeno)grafting of testis tissue fragments and implantation of testis cell aggregates from various donor species into phylogenetically-distant recipients are powerful new tools in reproductive biology and technology (Honaramooz *et al.* 2002; Honaramooz *et al.* 2007). These models can provide an easy access within a mouse recipient to study spermatogenesis, steroidogenesis, and testis development/function from diverse donor species, where *in situ* studies are inherently difficult (*e.g.*, large animals) or impossible (*e.g.*, humans) (Honaramooz 2014). For instance, testing the effects of different drugs or potential environmental toxicants, all without experimenting on the target donor species *per se* can be achieved using these models. Salvaging the genetic potential of recently deceased newborn endangered/valuable males or preserving the fertility potential of prepubertal boys undergoing gonadotoxic cancer treatments are among some other important applications of these models.

In the first successful report of testis tissue xenografting (TTX), testis fragments from neonatal donor mice, pigs, and goats developed under the back skin of recipient mice, formed complete spermatogenesis, and eventually produced fertilization-competent sperm (Honaramooz *et al.* 2002). This model was then applied using a diverse range of donor species including laboratory, domestic, and non-domestic animals, as well as primates (Honaramooz 2014). TTX has been successfully used to preserve the genetic potential of immature mammalian species; however, development of testis tissue from mature donors has been less successful, possibly due to the inability of mature somatic cells to proliferate and support the grafted tissue in the new environment (Honaramooz *et al.* 2002; Schlatt *et al.* 2006; Arregui *et al.* 2008).

Interestingly, ectopic subcutaneous implantation of pig testis cell suspensions, obtained after complete enzymatic dissociation of tissue to obtain single cells, into immunodeficient recipient mice resulted in post-implantation cellular rearrangements and regeneration of a functional testis tissue (Honaramooz *et al.* 2007). This *de novo* tissue formation was rather surprising as the newly-formed tissue was morphologically and functionally identical to the age-matched testis tissue (Honaramooz *et al.* 2007). Re-organization of the implanted cells was evident as early as 4 days post-implantation and led to the re-formation of seminiferous cords within 2 wk (Honaramooz *et*

al. 2007). Using other species such as rodents (Kita *et al.* 2007) and sheep (Arregui *et al.* 2008) as donors of testis cells, for this *in vivo* system, has also led to similar results. Although the TTX model is easier to perform, implantation of testis cell aggregates provides easier access for manipulation of individual cells when the behavior and developmental potential of testis stem cells are examined under different conditions (Dobrinski 2007).

So far, all studies using these two models have employed surgical recovery of the grafts/implants as the endpoint for evaluating the development of testis tissue/cells (Honaramooz *et al.* 2002; Honaramooz *et al.* 2007; Honaramooz 2014). Therefore, examining the developmental events within grafts/implants are limited by the number of timepoints that samples can be surgically recovered. Moreover, samples recovered from the subcutaneous tissue undergo multiple steps of fixation and tissue processing, which in turn, leads to tissue shrinkage and underestimation of their actual dimensions. Surgical procedures in general, and especially repeated sample recoveries in immunodeficient recipient mice carry complications such as potential for infection. Hence, it is desirable to employ novel imaging modalities that allow non-invasive, accurate, and repeated evaluation of the growth and structural changes in the grafted/implanted tissues/cells.

Ultrasound biomicroscopy (UBM) is a fairly new technology used in both diagnostic and research fields. First introduced in 1989, this high-resolution non-invasive imaging tool was originally designed for examination of the anterior chamber of the eye (Sherar *et al.* 1989). UBM utilizes a high-frequency transducer (20-100 MHz) to capture high-definition cross-sections of living objects at microscopic resolutions (Pavlin and Foster 2012). Compared with conventional clinical ultrasound systems, the frequencies used in UBM result in higher resolution (up to 25 μm axial and 50 μm lateral resolution), but with lower tissue penetration depth (Ishikawa and Schuman 2004; Kumar *et al.* 2016). Because of its low cost, high speed, accuracy, and non-invasiveness, UBM has been widely used in imaging of laboratory animals, especially to investigate pathogenesis of diseases and embryonic development of mice (Turnbull *et al.* 1995; Foster *et al.* 2002; Goertz *et al.* 2002; Zhou *et al.* 2003; Cheung *et al.* 2005). This technology has been successfully used in reproductive sciences to visualize the ovarian follicular development and cumulus-oocyte-complexes in laboratory animals (Jaiswal *et al.* 2009; Mircea *et al.* 2009) as well as in farm animals (Pfeifer *et al.* 2012, 2014) and humans (Baerwald *et al.* 2009; Pfeifer *et al.* 2014). UBM has also been utilized in three-dimensional (3-D) measurements of melanomas in

mice where the UBM-measured dimensions were shown to be in excellent agreement with those measured using the caliper volume of tumors (Turnbull *et al.* 1995; Cheung *et al.* 2005). Although UBM has been used in a number of applications including in oncology, embryology, and developmental biology (Liu *et al.* 1998) no study has validated its use for monitoring the developmental changes in tissue grafts/cell implants *in vivo*.

In this study, we used UBM to examine ectopically grafted/implanted tissues/cells to study their volume, dimensions, and composition prior to sample recovery. We captured consecutive 2-D UBM images, followed by reconstruction of 3-D views for volumetry. The recovered samples underwent morphometric and histologic analyses to compare with the UBM data. Our objectives were 1) to validate the use of UBM as a non-invasive and practical tool to monitor the development of testis tissue grafts/cell implants, and 2) to correlate the UBM data with the physical and histological attributes of recovered samples.

6.3. Materials and Methods

6.3.1. Study Design

Figure 6.1 summarizes the experimental design used in this study. Testis tissue fragments and testis cell aggregates were prepared from testes of 1-wk-old piglets. The tissue grafts and cell implants were placed within the dorsal subcutaneous tissue of recipient mice (n = 6) on 4 parallel sites on each side of the body. The grafting/implantation sites were examined every 2 wk using transcutaneous ultrasound (UBM) for 8 wk followed by randomized recovery of corresponding grafts and implants. Physical attributes of the recovered samples including their weight, volume, and dimensions were measured followed by histological analysis of the samples. All experiments involving animals were reviewed and approved by the University of Saskatchewan's Institutional Animal Care and Use Committee (Protocol # 20080042).

6.3.2. Preparation of Testis Tissue Fragments and Testis Cell Aggregates

Testis tissue fragments and testis cell aggregates were prepared using aseptic castration of 1-wk-old donor Yorkshire-cross piglets (n = 30; Camborough-22 line 65; PIC Canada, Winnipeg, MB, Canada) at a university-affiliated swine facility. Castration of animals and cell dissociation were performed as described in Chapter 4. The resultant cell-pellet was mixed with 30 mL of DMEM

with 10% FBS and 1% antibiotics to prepare a single-cell suspension and was refrigerated before transfer.

6.3.3. Recipient Mice and Grafting/Implantation Procedures

Recipient mice were male double-homozygous severe combined hairless immunodeficient outbred (SHO, Crl: SHO-*Prkdc*^{scid}*Hr*^{hr}, strain code 474; Charles River, Montreal, Canada, $n = 6$) at 7 wk of age at the time of grafting/implantation. The mice were kept individually in plexiglass micro-insulator cages under sterile conditions, standard temperature (22 ± 2° C), and controlled lighting photoperiod (12 hr light/dark cycles). Sterile water and mouse chow were provided *ad libitum*. The mice were acclimatized for 1 wk prior to the study and were handled aseptically. For the induction and maintenance of anesthesia, isoflurane at 5% and 2% in oxygen were used, respectively, and the mice were placed on a heat pad on sternal recumbency. After the surgical preparation of the skin, each mouse received 4 longitudinal linear incisions through the dorsal skin, each ~0.5 cm, on the right side of the midline. Using blunt dissection, small subcutaneous pouches were formed through each incision, in which testis tissue grafts were embedded. The incision sites were closed using metal wound clips (Michel Clips 7.5 mm, Miltex, York, PA, USA).

Testis cells were prepared as described above and kept at 4° C overnight. On the day of implantation (same day as grafting), the cells were prepared for injection by centrifugation at 500× *g* for 5 min at 16° C leading to aggregation of highly concentrated cellular sediments containing 100×10^7 cells per mL. Using a 1-mL syringe attached to a 22-gauge needle, 0.1 mL of the cell aggregates were injected subcutaneously in each of the 4 contralateral sites on the left side of the midline. The tissue grafts and cell implants were assigned a letter (L or R = left or right) and a number (1 to 4, in order of cranial to caudal position) to track samples (Fig. 6.1).

6.3.4. UBM Examination

3-D transcutaneous Doppler UBM (VisualSonics Vevo3100, 32-55 MHz MX550D transducer, VisualSonics, Toronto, ON, Canada) was performed on all surgical/injection sites prior to graft/implant recovery. The mice underwent UBM examination every 2 wk for 8 wk. For each UBM examination, the animals were anesthetized using isoflurane as described above, placed on the heated UBM stage on sternal recumbency, and the skin over the grafted/implanted sites was covered by an ultrasound gel (EcoGel 200; catalogue no. 40JB; Eco-Med Pharmaceutical Inc,

Mississauga, ON, Canada). The B-mode setting was used to perform 3-D measurements of the grafts/implants using a 3-D-motor-driven 32-55MHz transducer. Machine settings were as follows: MX550D transducer with the central frequency of 32-55, 100% power, radio frequency of 2 kHz, master gain of 35 decibel and, 0.1 mm delay, field of view of 15×14.08 mm, 19 frames per second, and a dynamic range of 70 decibel.

The transducer was placed on the ultrasound gel and its position was maintained steady as soon as the target tissue was completely within the borders of the image. The focal points and 3-D range were then adjusted based on the lateromedial dimension of the graft. The transducer notch was located cranially and by slight movements of the 3-D motor, consecutive images (X and Y dimensions = 15 mm, axial and lateral pixel sizes = 12.0 × 55.2 μm) were captured every 0.038 mm (Z dimension) starting from the point where the graft/implant was observed from lateral to medial for the tissue grafts and medial to lateral for the cell implants. Once the imaging of a graft/implant was completed, the transducer, mounted on a stand, was moved using levers to be adjusted for the next imaging site until all remaining grafts/implants were examined.

The ultrasound findings were used in a correlation analysis with the physical and histological attributes of the samples recovered immediately following the imaging process. The specifications evaluated in the 2-D UBM images included volume, length (craniocaudal axis), width (lateromedial axis), and height (dorsoventral axis) of all samples. Given the noticeable heterogenic echogenicity of cell implants, we also quantified the relative hyperechoic, hypoechoic, and anechoic areas by manually outlining their boundaries on UBM images, and by quantifying the pixel intensity and pixel heterogeneity of each area. The relative surface areas occupied by the differing echogenicities were then used in correlation analyses with the putative corresponding areas on histological cross-sections of the same cell implants. The length, height, and relative areas, as well as the pixel intensity and heterogeneity of samples were measured in the largest 2-D UBM planes. Length and height were measured using the designated software (Vevo Lab, Version 3, Fujifilm VisualSonics Inc, Toronto, ON, Canada) and the pixel intensity and heterogeneity as well as the relative areas were measured using ImageJ (ImageJ, U.S. National Institutes of Health, Bethesda, MD, USA). Width measurements were made by multiplying the step size (0.038 mm) by the recorded number of images from one side to the other. UBM volume measurements were performed using the Cavaleri principle of stereological approach for volume

calculations (segmentation volume measurement) (Elliot *et al.* 1996; Cheung *et al.* 2005). For this purpose, using the same software, 3-D images were segmented into 1-mm slices, each consisting of 26 two-dimensional images (1 mm slice ÷ 0.038 mm step size), followed by calculation of the area of each graft/implant by manually outlining their boundaries in a randomly-selected 2-D image within the first 1-mm slice, skipping 26 images, and repeating the same measurement for each of the following slices. Each delineated area (in mm^2) was then multiplied by the inter-slice interval (0.038 mm step size × 26 = 1 mm) to obtain the volume of a section (in mm^3), followed by adding all the section volumes to calculate the total volume of an individual mass (Fig. 6.2).

6.3.5. Graft and Implant Sample Recovery, and Physical Evaluation

Three of the 6 recipient mice were randomly selected to undergo UBM scanning and sample recovery at 2 and 6 wk post-procedure, and the remaining three mice at 4 and 8 wk. After scanning all grafts/implants in each mouse, one tissue graft and its corresponding cell implant were surgically recovered. For the recovery from each mouse, a site was randomly chosen to avoid the potential confounding effects of graft/implant site. The physical volume, weight, and dimensions of the recovered grafts/implants were also measured for comparison with the UBM data. For gross measurement of sample dimensions, immediately after recovery, each sample was placed on a stage with backlight for added clarity, and close-up photomacrographs were captured dorsally with a camera (Sony α5000, Sony Corporation, Tokyo, Japan) mounted on a stabilized macro stand to document the length and width, followed by repositioning the sample laterally for documenting its height. The macrographs were used to calculate the gross dimensions of the grafts/implants using ImageJ. Volume of the recovered samples was calculated using a water displacement method. Briefly, the water level within a graduated 1-mL pipette (polystyrene serological pipette, Fisherbrand Scientific Company, Toronto, ON, Canada) was recorded before and after submerging the recovered samples. The difference was recorded as the physical volume of the graft/implant and was used to compare with the UBM measurements of volume.

6.3.6. Histological Analyses

Using Bouin's solution, the recovered grafts/implants were fixed overnight, followed by rinsing 3 times with and maintaining in 70% ethanol until the processing time with an automated tissue processor (Leica ASP300 S tissue processor, Leica Biosystems Corporation, ON, Canada). Samples were embedded in paraffin and sectioned at 5 μm, starting from where the tissue was first

observed within the blocks. Every 5 sections were placed on a single slide, followed by skipping 15 sections before another slide was prepared. Starting from the first slide, every 5th slide (~375 µm interval) was stained with hematoxylin and eosin (H&E).

Histological analyses were performed using a calibrated binocular microscope equipped with digital photomicrography (Northern Eclipse Image Analysis software version 7.0, Empix Imaging, Mississauga, ON, Canada). Descriptive side-by-side comparisons of histological cross-sections with their corresponding 2-D UBM images were performed using the largest diameter of the samples. In the same sections, the areas of seminiferous cords (cordal), connective tissue (non-cordal), and fluid-filled cavities were also measured using ImageJ.

6.3.7. Statistical Analyses

The data presented are mean ± standard error of mean (SEM) and $P < 0.05$ was considered as significant. All the data were analyzed using *t-test*, one- or two-way analysis of variance (ANOVA), or Pearson correlation coefficient analysis, unless stated otherwise. Bland-Altman plotting (Giavarina 2015) was utilized to examine the differences between the two methods of volume measurements. Simple linear regressions were used to show relationships between UBM and physical as well as between UBM and histological measurements. Statistical Package for Social Sciences was used for all data analysis (IBM SPSS Statistics for Macintosh, Version 23.00; IBM Corporation, Armonk, NY, USA).

6.4. Results

6.4.1. UBM Assessment

Detection of the tissue grafts and cell implants was performed using UBM at 2, 4, 6, and 8 wk post-procedure. As shown in Figure 6.3, testis grafts ($n = 12$) and implants ($n = 12$) were detectable under the skin as non-uniform masses that appeared ellipsoid, sphere, hemisphere, or irregular in shape. The 2-D ultrasound images contained sufficient contrast to allow differentiation of different areas or layers within the grafts and implants, suggestive of being made of different structural compositions. As early as 2 wk post-procedure, encapsulation of the grafts and implants within the subcutaneous tissue was evident using UBM (Fig. 6.3A). The mouse skin appeared as a thick hyperechoic structure covering the dorsal border of the grafts and implants (Fig. 6.3A). The skin and apposing capsule of samples were of similar echogenicity and thus could not be differentiated.

The capsule on the ventral aspect was only partially observed and appeared as a hyperechoic line (Fig. 6.3A).

While the tissue grafts appeared as homogenous structures (Fig. 6.3D), cell implants consisted of multiple layers with differing echogenicity (Fig. 6.3B). In two of the three cell implants collected at earlier stages (2 and 4 wk), a centrally-located anechoic region was detected, indicating a fluid-filled cavity (Fig. 6.3C). These cavities decreased in size by 4 wk (3.41 ± 2.3 mm at 2 wk and 0.17 ± 1 mm at 4 wk) and were absent in 6- and 8 wk implants.

The diameters (length, width, and height) measured at the largest cross-sectional UBM images of samples at each time point are displayed in Figure 6.4, where only the length of samples increased over time (P = 0.02; Fig. 6.4A). For the UBM-measured volume (using 3-D segmentation), an interaction was found between the sample type and time (P = 0.01), where the UBM volume increased over time for tissue grafts but not for cell implants (Fig. 6.4G and 6.5).

6.4.2. Physical and Morphometric Assessment

As shown in Figure 6.6, the recovered samples had various shapes including lenticular, spherical, ellipsoid, and in some cases irregular. There were no discernible differences in shape or texture between the recovered tissue grafts and cell implants at any time point; both types of samples had connective tissue capsules and a few visible blood vessels.

Physical measurements showed an increase in the height (P = 0.03) of recovered samples over time (Fig. 6.4F). For the physical length, there was an interaction (P= 0.02) between the time and sample type, where the length of cell implants decreased at 4 wk and the length of tissue grafts increased at 8 wk. The length of cell implants was also greater than that of tissue grafts at 2 wk (P = 0.03; Fig. 6.4B). The overall weight of the samples increased (P = 0.04) over time from 36.9±5 mg at 4 wk to 83.3±20 mg at 8 wk for grafts, and from 23.8±5 mg to 69±22 mg for implants at the same period of time (Fig. 6.6). For the physical-measured volume of recovered samples (using water displacement), there was an interaction between the sample type and time, where the physical volume increased over time only for tissue grafts (P = 0.01; Fig. 6.4H).

6.4.3. Histological Assessment

In histological examinations, all grafts (n = 12) and implants (n = 12) were surrounded by a fibrous capsule; in tissue grafts branching of the connective tissue from the capsule divided the tissue into groups of seminiferous cords.

The histology of tissue grafts resembled that of a normal neonatal/immature testis tissue, comprising of seminiferous cords with gonocytes and Sertoli cells, surrounded by peritubular myoid cells, and the interstitial tissue housing Leydig cells and fibroblasts. Gonocytes within the cords were located centrally, next to the basement membrane of the cords, or in between.

Cellular organization and/or cord formation were observed in all histological cross-sections of cell implants. While at 2 wk these cellular arrangements were observed immediately interior to the capsule of the implants, by 4 wk, convoluted cords were completely formed and distributed further into the implants. The central areas were occupied by connective tissue and/or fluid-filled cavities to various degrees. Cross-sections of the newly formed cords contained the expected cellular components; multiple Sertoli cells and a few gonocytes, which were mostly located away from the basement membrane. Although sections of tissue grafts at 2 wk also contained large areas of interstitial and connective tissue lacking cords, the fluid-filled cavities were only observed in some cell implants; two out of the three recovered cell implants at 2 wk and one out of the three implants at 4 wk. Therefore, cross-sectional histology of implants could be divided into capsular, cordal formation layer, and central areas/cavities; the cavities were replaced by connective tissue in more developed implants.

6.4.4. Comparative Analysis

Side-by-side comparison of the UBM and histological images of implants at 2 wk revealed that the peripherally-located hypoechoic areas on UBM images coincided with the presence of newly-formed seminiferous cords in histological sections. Conversely, centrally-located hyperechoic areas of the implants corresponded to the non-cordal regions in histological sections, while as expected the anechoic regions corresponded with fluid-filled cavities (Fig. 6.3A-C, 6.7, and 6.8). This described pattern for the distribution of cords in cell implants was observed for UBM/histology images of the majority but not all implants; in some samples the distribution appeared more random in both UBM and the corresponding histological sections. Given the visible

morphological changes between 2 wk cell implants (some containing fluid-filled cavities) and later stages (Fig. 6.7), we used cell implants from 2 and 6 wk to represent early and late developmental stages for further comparisons between UBM and histological attributes. An interaction was found between the area type (cordal, non-cordal, and fluid-filled cavity) and time of sampling on the relative areas (%) in the largest histological sections ($P = 0.03$; Fig. 6.8A-C). The percentage of non-cordal areas increased by ~88% from 2 wk to 6 wk, whereas the percentage of cordal areas did not change (Fig. 6.8C). The overall percentage of cordal areas was ~95% higher than that of non-cordal areas in 2-D UBM images ($P = 0.004$; Fig. 6.8D-F). The pixel intensity of UBM images did not differ between the cordal and non-cordal areas or over time. However, the pixel heterogeneity showed a tendency to decrease from 2 to 6 wk ($P = 0.07$; Fig. 6.8G and 6.8H).

The Pearson correlation coefficient analyses showed a strong positive correlation between the percentage of measured areas between UBM images and histological cross-sections ($r = 0.87$, $n = 15$, $P < 0.001$; Fig. 6.8I). The physical and UBM measurements of length and height of the grafts and implants were also strongly and positively correlated ($r = 0.50$, $n = 24$, $P = 0.01$; and $r = 0.70$, $n = 24$, $P = 0.001$, respectively; Fig. 6.9A and 6.9B). Similarly, sample volumes measured using UBM were strongly and positively correlated with both sample volumes measured using water-displacement method ($r = 0.99$, $n = 24$, $P < 0.001$; Fig. 6.9C) and sample weights ($r = 0.98$, $n = 24$, $P < 0.001$). Bland-Altman analysis showed an equal frequency of data points above and below the mean percentage differences of volume between the two approaches of volume measurement, indicating an agreement between the two methods (Fig. 6.9D). Moreover, the difference between the two methods of volume measurement decreased over time ($P = 0.001$; Table 6.1). Using simple linear regression, the following equations were calculated to quantify the relationships between UBM, physical, and histological measurements:

Physical volume = $-3.78 + (0.95 \times \text{UBM volume})$

Physical length = $1.76 + (0.61 \times \text{UBM length})$

Physical height = $1.29 + (0.91 \times \text{UBM height})$

Percentage of histological areas = $10.4 + (0.74 \times \text{percentage of UBM areas})$

Table 6.1. Percentage difference (% of increases/decreases, mean ± SEM) in biomicroscopy (UBM) and physical measurements of the length, width, height, and volume of grafts and implants

Parameters	Sample	2 wk	4 wk	6 wk	8 wk
Length	Implant	–7 ± 7	25 ± 16	7 ± 3	17 ± 9
	Graft	21 ± 7	13 ± 2	16 ± 13	–2 ± 14
Width	Implant	51 ± 2	67 ± 7	64 ± 6	61 ± 4
	Graft	57 ± 1	61 ± 9	68 ± 5	60 ± 8
Height	Implant	–29 ± 33	–29 ± 12	–38 ± 11	–34 ± 10
	Graft	–32 ± 12	–35 ± 22	–50 ± 19	–75 ± 15
Volume	Implant	22 ± 1^{a}	17 ± 4^{ab}	11 ± 2^{b}	9 ± 4^{b}
	Graft	19 ± 1^{a}	16 ± 1^{ab}	11 ± 1^{b}	6 ± 2^{b}

Note: Percentage increases/decreases in values between the UBM and physical measurements were calculated using $\frac{(UBM\ value - physical\ value)}{UBM\ value} \times 100$

Positive numbers indicate that UBM values were greater than physical values by the given percentage.

Negative numbers indicate that UBM values were smaller than the physical values by the given percentage.

Numbers with different superscripts within each row differ significantly ($P < 0.05$).

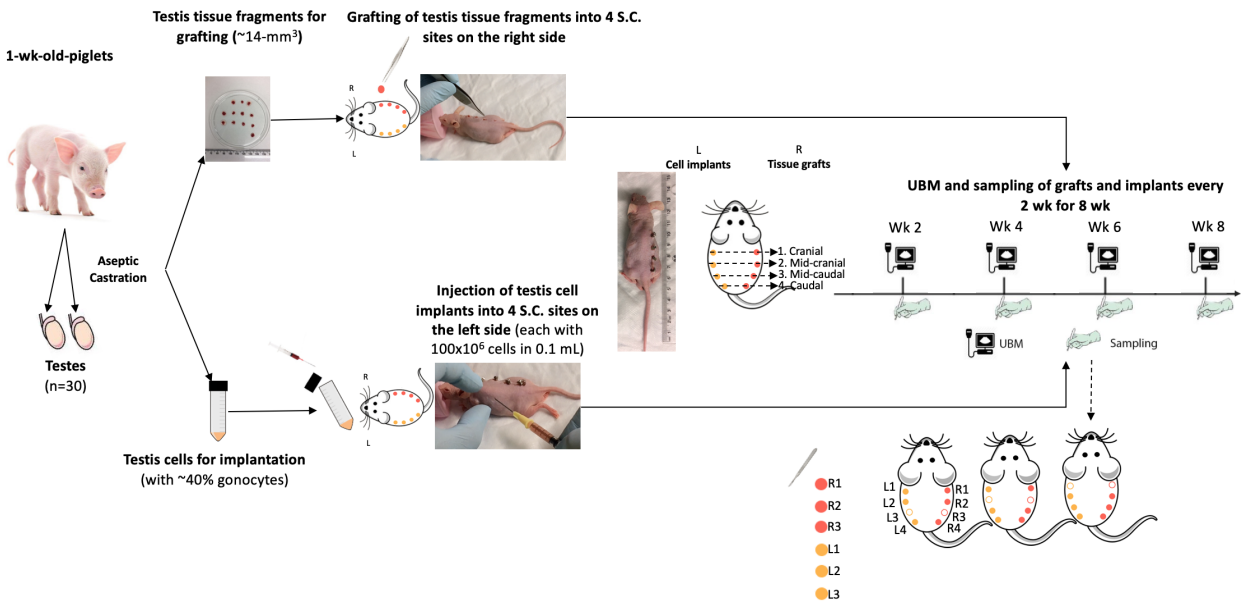

Fig. 6.1. Schematic representation of the experimental design. Neonatal testes (n = 30) were obtained after aseptic castration of 1-wk-old piglets. The testis parenchyma was either cut into small fragments for grafting or underwent tissue digestion for cell-aggregate implantation. Testis tissue grafts were placed subcutaneously in 4 sites on the right (R) side, and cell implants were injected subcutaneously into 4 contralateral sites on the left (L) side. The grafting and implantation sites were examined using ultrasound biomicroscopy (UBM) at 2, 4, 6, and 8 wk post-grafting/implantation. After each UBM examination, one randomly-selected tissue graft and its respective cell implant (R1-R3/L1-L3) were recovered for physical and histological evaluations.

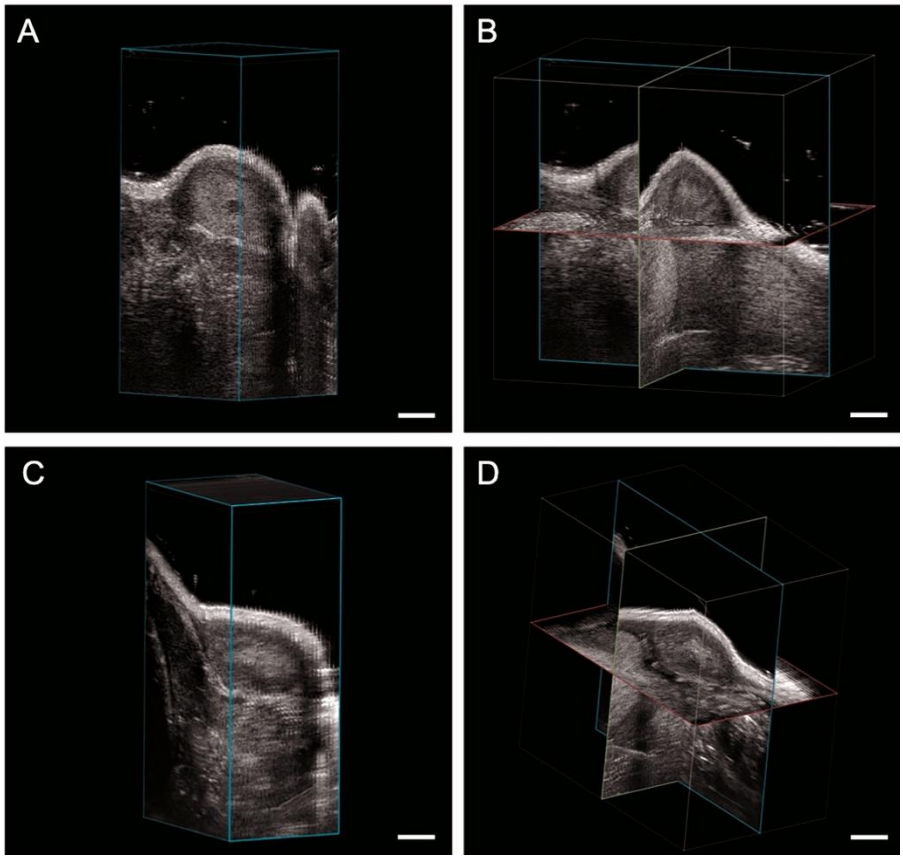

Fig. 6.2. Representative ultrasound biomicroscopy (UBM) images used for segmentation volume measurement of testis cell implants. Cube views (A and C) and cross views (B and D) of the cell implants at 2 and 8 wk, respectively. (A and C) The target implant is shown within a cube with six rectangular faces which can be moved in different axes, making it possible to observe the cross-sectional views from different aspects. In cross views, three movable planes are shown, which can also be displaced along different axes. All samples (grafts and implants) were segmented into multiple slices with 1 mm intervals. (Scale bar = 1 mm)

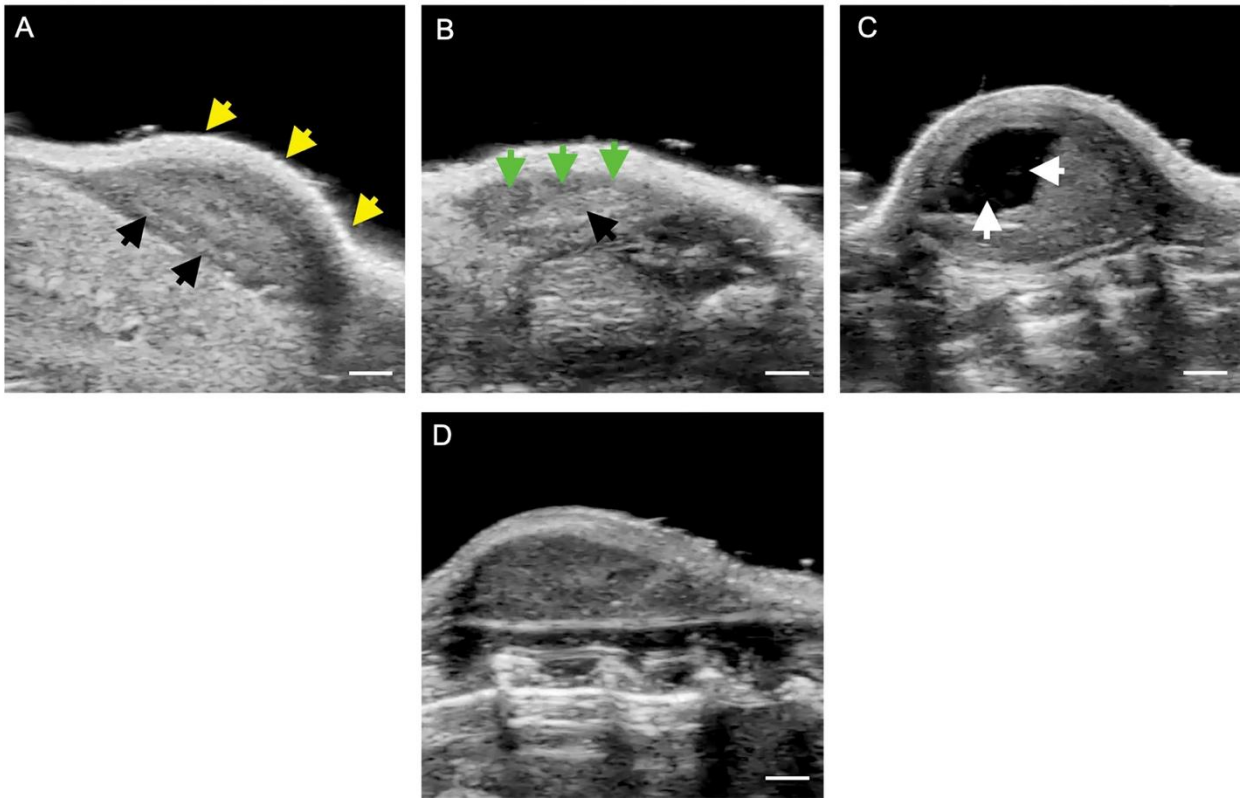

Fig. 6.3. Representative two-dimensional (2-D) ultrasound biomicroscopic (UBM) images of cell implants at 2 wk (A and C) and 4 wk (B) post-implantation, or tissue graft at 2 wk (D). (A) A 2-wk cell implant with a hyperechoic line (yellow arrows) representing the dorsal skin and a thin layer representing the ventral capsule (black arrows). (B) A 4-wk cell implant with hypoechoic areas (green arrows) with newly formed parenchymal testis tissue seen mostly in the peripheral regions, in contrast to the central hyperechoic area (black arrow), corresponding to more compact cellular areas. (C) In a few cell implants, including in this 2-wk sample, fluid-filled cavities (white arrows) were detected, which had disappeared by 6 wk. (D) Uniform appearance of a 2-wk testis tissue graft encapsulated in the subcutaneous tissue of the recipient mouse. (Scale bar = 1 mm)

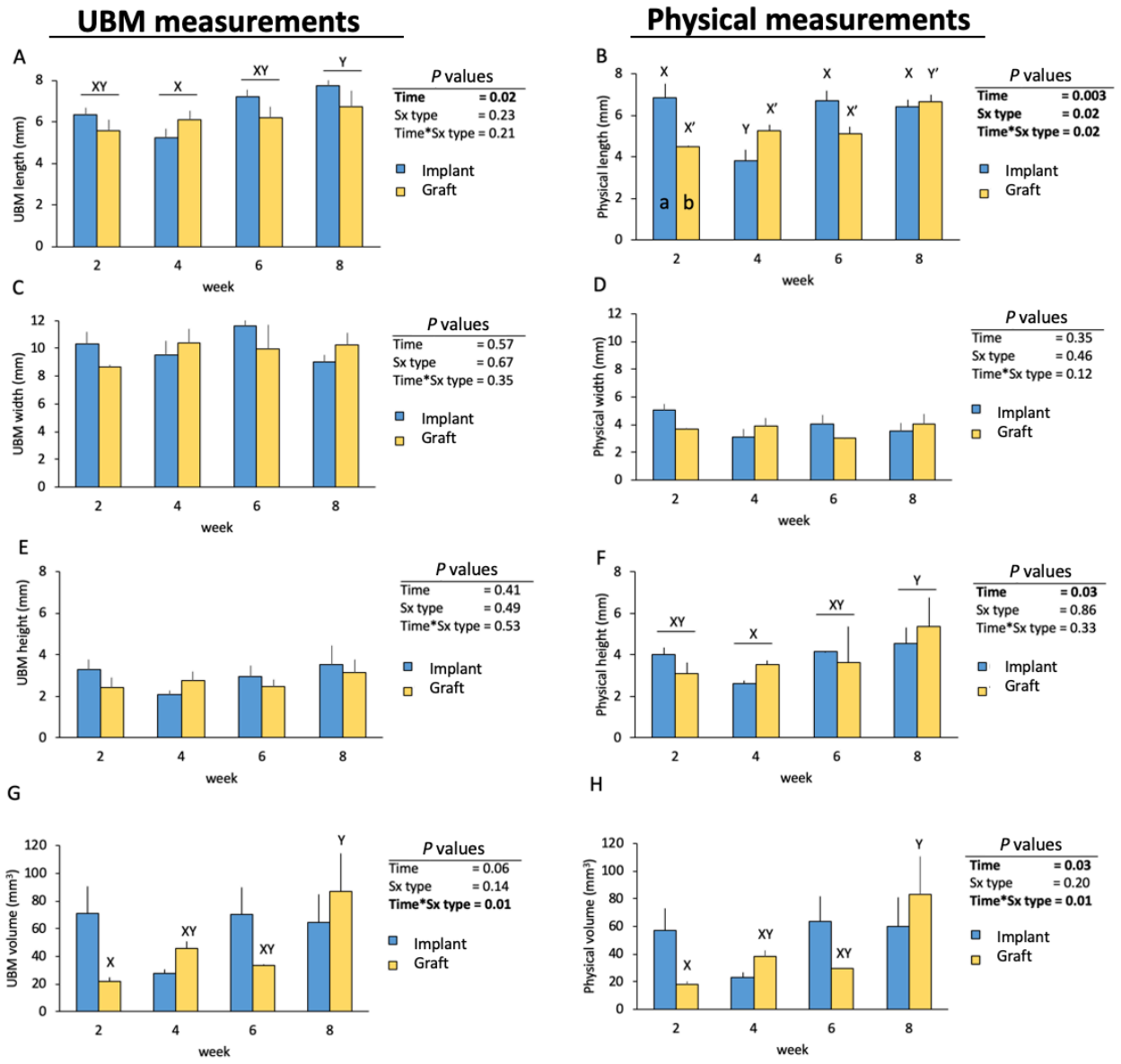

Fig. 6.4. Ultrasound biomicroscopic (UBM) and physical measurements (mean±SEM) of tissue grafts and cell implants. "Sx" denotes tissue grafts or cell implants. "X, X′, Y, and Y′ ", denote statistically significant differences over time. "a" and "b" denote statistically significant differences between tissue grafts and cell implants and $P < 0.05$ was considered as significant.

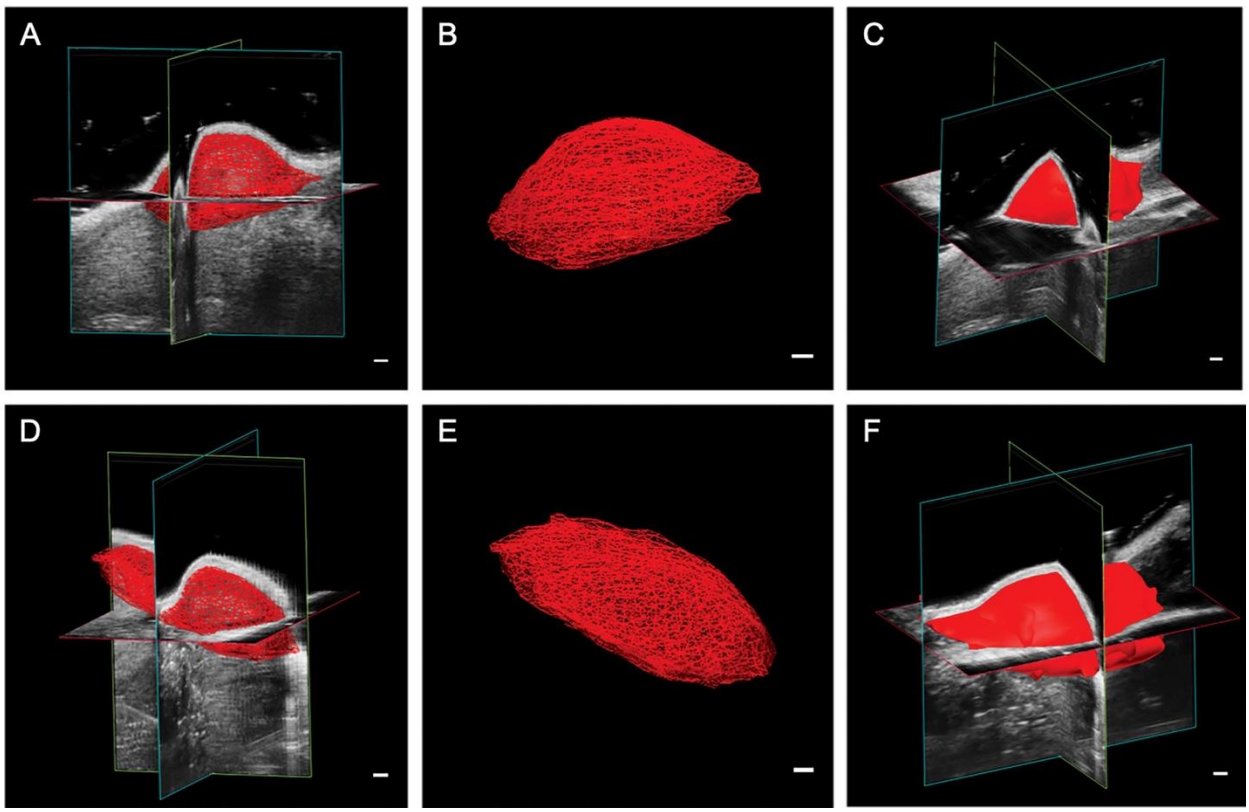

Fig. 6.5. Representative three-dimensional (3-D) reconstructed images from ultrasound biomicroscopy (UBM) of testis tissue grafts and cell implants. 3-D volumetric mesh and reconstructed 3-D image of a cell implant examined at 2 wk (A-C) or 8 wk (D-F). In order to measure the volume of each sample, 3-D images were segmented into parallel slices (Vevo LAB, Version 3, Fujifilm VisualSonics Inc, Toronto, ON, Canada). Within every two-dimensional (2-D) cross-sectional slice, the area occupied by the sample was measured followed by multiplication of the inter-slice interval by the measured area. Sample boundaries were outlined manually on each of the cross-sectional views, followed by combining the obtained 2-D images. The resulting 3-D view is presented as a mesh/wire-frame view. (Scale bar = 1 mm)

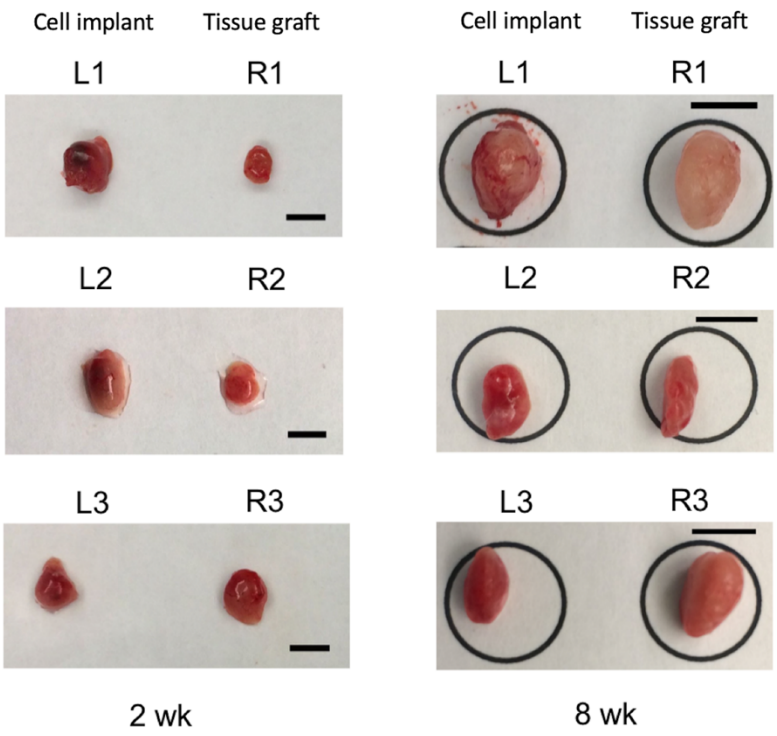

Fig. 6.6. Representative macrophotographs of testis tissue grafts and cell implants recovered after 2 or 8 wk post-grafting/implantation. Recovered samples appeared in various shapes, but all were covered by connective tissue and blood vessels. “R” and “L” letters denote tissue grafts or cell implants that were recovered from the right or left sides of the back skin of recipient mice, respectively. (Scale bar = 5 mm)

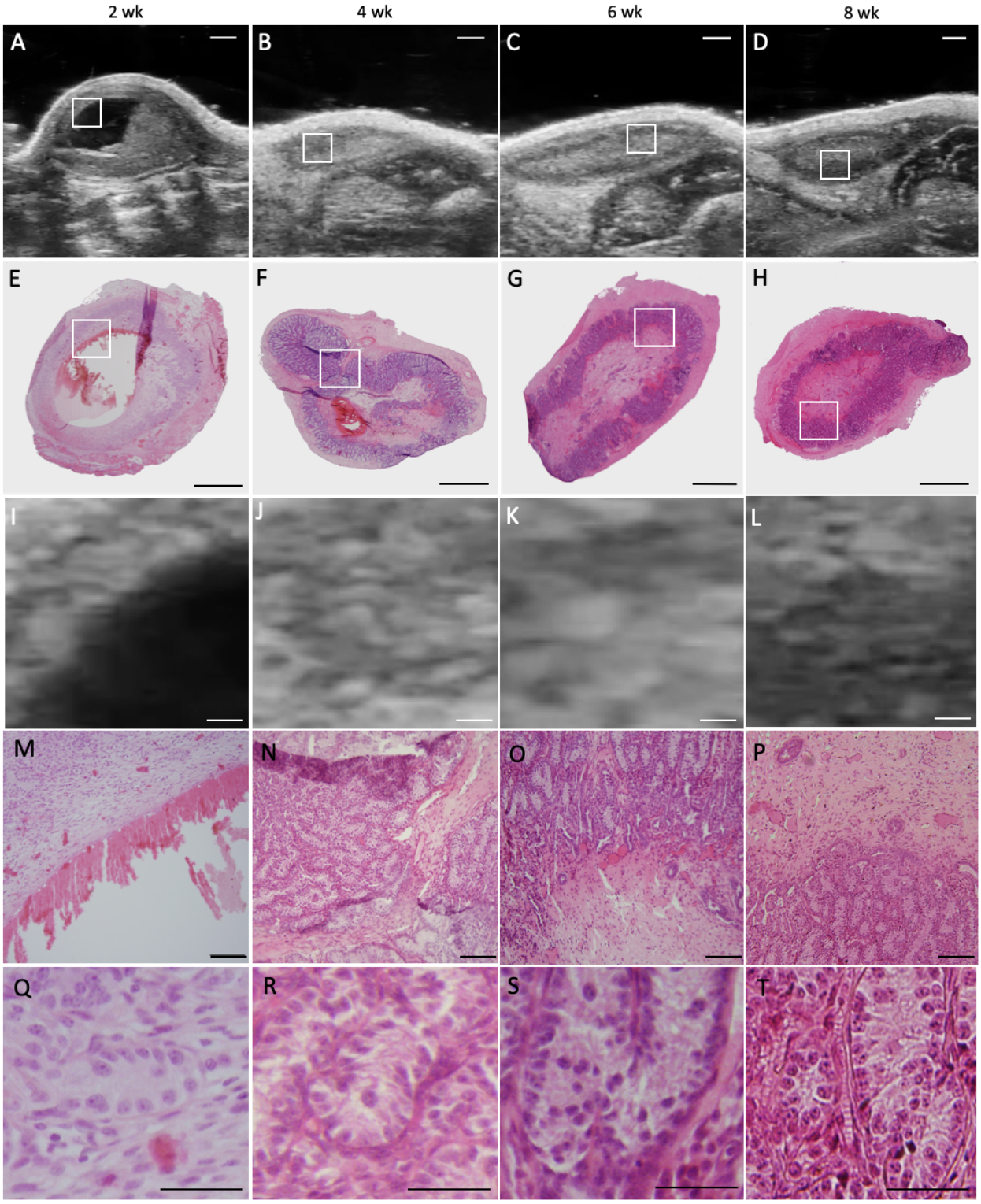

Fig. 6.7. Representative images of testis cell implants obtained using ultrasound biomicroscopy (UBM) and histology at different time points. Cell organization and seminiferous cord formation appeared within the periphery and gradually developed toward more central areas. Fluid-filled

cavities seen in a few cell implants at earlier time points were disappeared and replaced with cellular structures and connective tissue by 6 wk. The areas occupied by seminiferous cords appeared hypoechoic (darker) when compared to the areas occupied by dense cellular formations. Compared to the newly formed cords at 2 wk (M and Q), more developed cords appeared at 8 wk (P and T) post-implantation. (Scale bar for A-H = 1 mm, for I-P = 100 μm, and for Q-T = 50 μm)

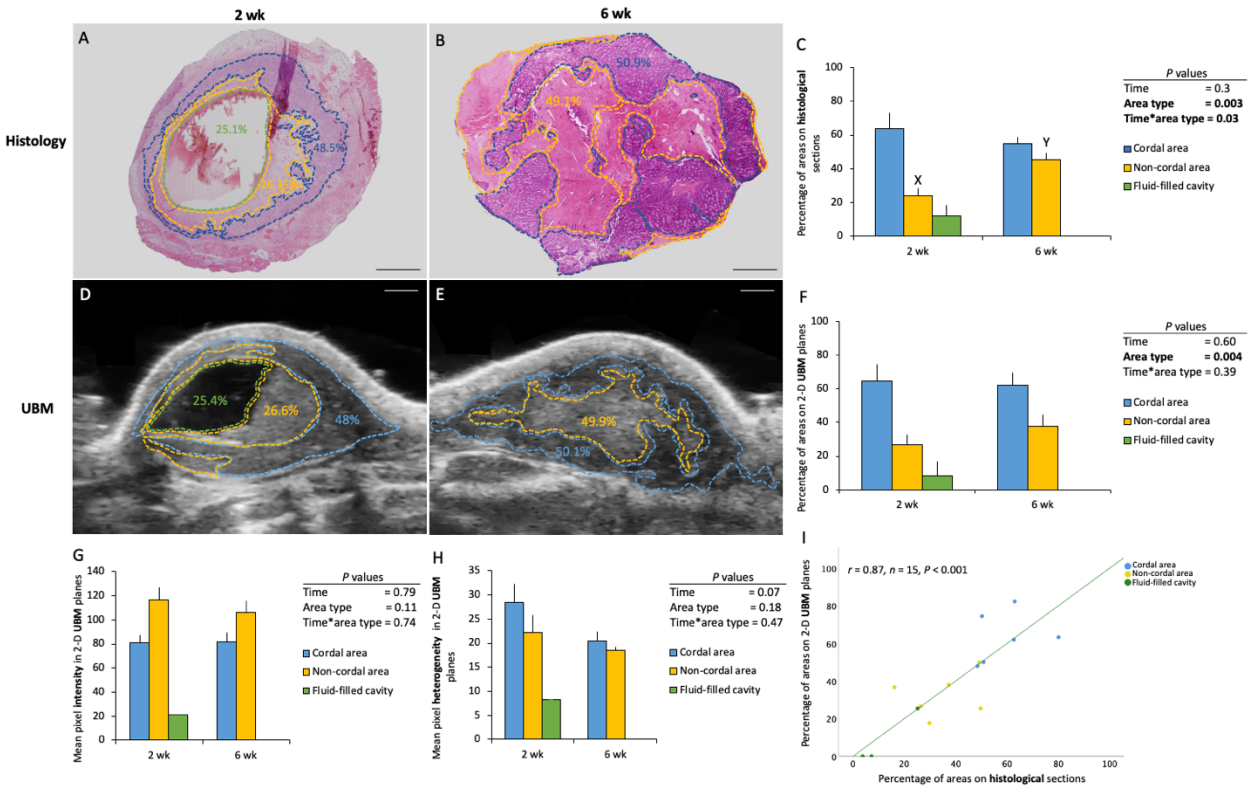

Fig. 6.8. The percentage (mean±SEM) of cordal, non-cordal and fluid-filled cavity areas delineated on histological cross-sections and 2-D UBM images of implants (A-F and I), as well as the UBM pixel intensity and pixel heterogeneity (mean±SEM) (G and H) in recovered implants at 2 and 6 wk. Replacement of the fluid-filled cavities with connective tissue, may have resulted in an increase in the percentage of non-cordal areas from 2 to 6 wk, whereas the percentage of cordal areas did not change on histological cross-sections. The overall percentage of cordal areas was significantly greater than that of non-cordal areas at both time points in UBM images (A-F). The percentage of corresponding areas were strongly and positively correlated between UBM images and histological cross-sections ($r = 0.87$, $n = 15$, $P < 0.001$), indicating the reliability of UBM in differentiating structural differences between the cordal, non-cordal and fluid-filled cavity areas (I). The differences in echotexture between the cordal and non-cordal areas allowed distinguishing the two areas on UBM images; however, the pixel intensity values did not differ between the two areas. The pixel heterogeneity tended to decrease from 2 to 6 wk, indicating that the cordal and non-cordal areas had become more homogenous over time (G and H). Area type denotes cordal/non-cordal areas and areas of fluid-filled cavities. X and Y denote statistically significant differences and $P < 0.05$ was considered as significant. (Scale bar = 1 mm)

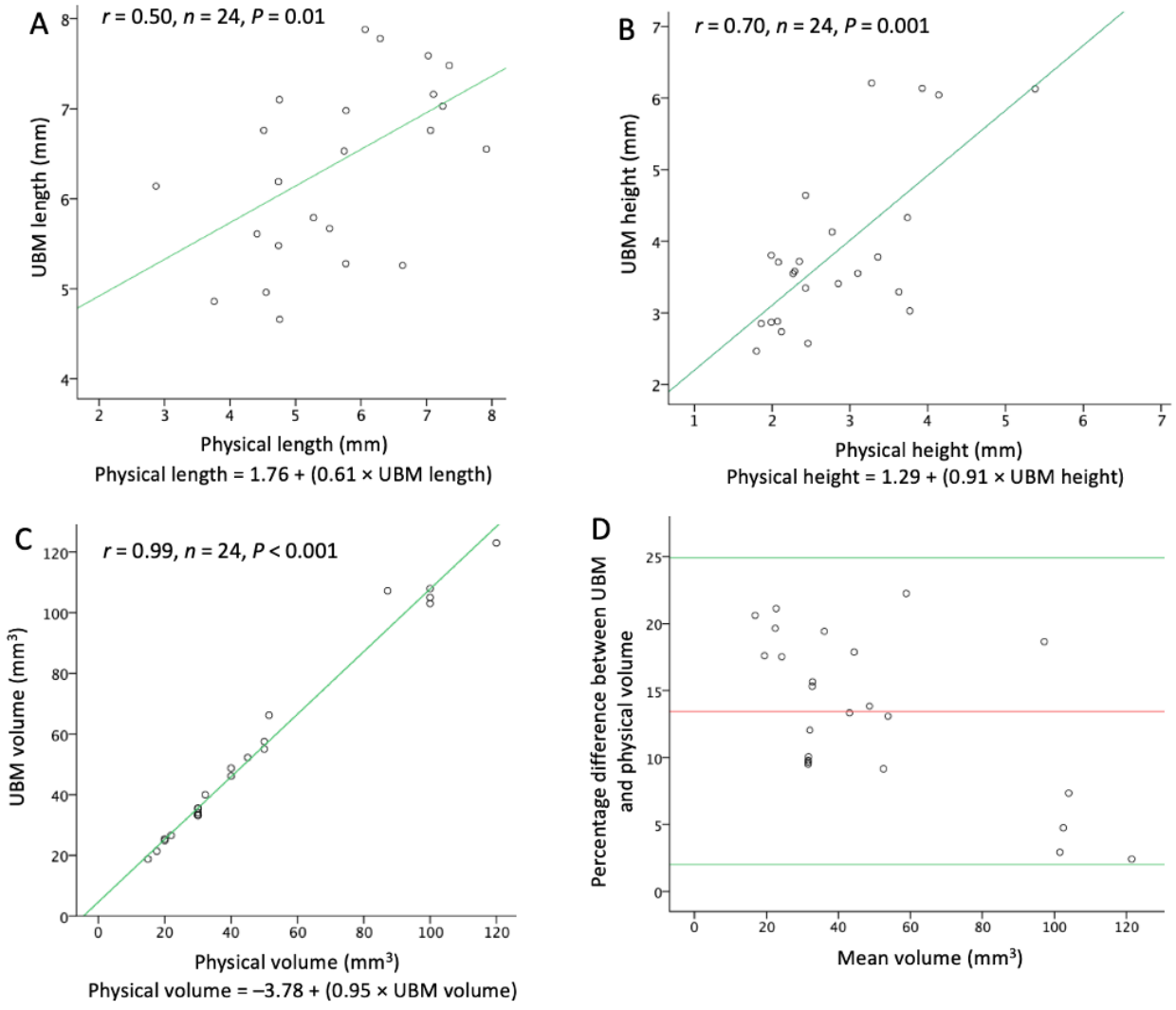

Fig. 6.9. Comparison between physical and UBM attributes of the grafts and implants. Correlations between the UBM *vs.* physical measurements of length (A), height (B), and volume (C) of the grafts and implants. (D) Bland-Altman analysis of volume measurements using percentage differences between UBM and physical volume of the grafts and implants ($\frac{(UBM\ value - physical\ value)}{UBM\ value} \times 100$). Positive correlations were found between the physical and UBM measurements of length ($r = 0.50$, $n = 24$, $P = 0.01$), height ($r = 0.70$, $n = 24$, $P = 0.001$), and volume ($r = 0.99$, $n = 24$, $P < 0.001$) of the grafts and implants (A-C). (D) The same number of data points were found above and below the mean difference of two methods of volume measurements, indicating agreement between the two volume measurement methods.

6.5. Discussion

The objective of the present study was to validate the use of UBM for non-invasive assessment of testis tissue grafts and cell implants in an immunodeficient mouse model. Here, we found positive correlations between the pre-recovery UBM and post-recovery morphometrical measurements for both testis tissue grafts and cell implants. We also found positive correlations between the UBM and histological attributes of cell implants. Using these correlations, we were able to define equations to allow future experiments to use UBM estimates to calculate the expected physical dimensions and volumes of grafts and implants, as well as the relative histological areas within implants. We also found strong agreements between UBM images and histological micrographs, which would allow distinguishing cellular layers and other histological attributes of the samples by using UBM imaging. We therefore validated the use of UBM as a non-invasive, accurate, and repeatable monitoring method for the assessment of testis tissue grafts and cell implants in prospective studies. As such, our results have important implications including a potential reduction of the required number of recipient animals in various studies using subcutaneous grafting or implantation.

An indispensable component of studies using testis tissue xenografting and testis cell implantation models is the evaluation of graft or implant development, which thus far has only been achieved after physical removal of grafts or implants for (immuno)histochemical analyses (Honaramooz *et al.* 2002; Honaramooz *et al.* 2007; Arregui and Dobrinski 2014). UBM has facilitated several fields of basic research and clinical applications, including developmental biology (Hibino *et al.* 2011) female reproductive biology,(Baerwald *et al.* 2009; Jaiswal *et al.* 2009; Mircea *et al.* 2009; Pfeifer *et al.* 2012, 2014), cardiology (Spurney *et al.* 2006; Buckley and Stokes 2011; Jaffré *et al.* 2012), neurology (Stokvis *et al.* 2009), oncology (Turnbull *et al.* 1995; Cheung *et al.* 2005; Nuccitelli *et al.* 2006; Snyder *et al.* 2009), embryology (Foster *et al.* 2002), and ophthalmology (Pavlin *et al.* 1992; He *et al.* 2007; Pavlin and Foster 2012). In a recent feasibility study, we showed that UBM has the potential to be used as a predictive tool for the development of testis tissue grafts and cell implants (Awang-Junaidi *et al.* 2019). However, the present study is the first to validate the use of UBM as a non-invasive tool for the long-term *in vivo* monitoring and assessment of grafts and implants.

A previous study using neoplastic xenografts showed high accuracy of UBM in 3-D segmentation volume estimation (Cheung *et al.* 2005). Hence, we applied the same principles for the precise volume measurements of testis tissue grafts and cell implants. We also used echogenicity and 3-D rendering of UBM images for the qualitative and quantitative evaluation of grafts and implants. These approaches have been shown to be effective in estimating the thickness of follicular walls, granulosa- and theca-cell layers, as well in describing follicular dynamics using UBM in mouse and bovine models (Baerwald *et al.* 2009; Mircea *et al.* 2009; Pfeifer *et al.* 2012).

In the present study, in histological cross-sections of cell implants there was an 88% increase in the percentage of non-cordal areas from 2 to 6 wk, whereas the percentage of cordal areas over the same period remined unchanged (Fig. 6.8C). This may be explained by the replacement of fluid-filled cavities at 2 wk with connective tissue at later time points. More importantly, the established positive correlations between the UBM and histological measurements of cordal/non-cordal areas and fluid-filled cavity were indicative of the UBM potential in detecting various textures and structural components to predict the histological attributes of cell implants. Although the differences in echotexture were sufficient to visually differentiate between the putative cordal and non-cordal areas, the pixel intensity values did not differ between these two areas to quantify the differences (Fig. 6.8G). However, there was a tendency for pixel heterogeneity to decrease over time (Fig. 6.8H), indicating that the tissues were becoming more homogeneous from 2 to 6 wk. These differences need to be tested in a larger study.

In the present study, the overall developmental patterns observed in the histological cross-sections of grafts and implants conformed to those shown in relevant previous studies in which neonatal pig testis cells and tissues were also implanted or grafted into host mice (Honaramooz *et al.* 2002; Honaramooz *et al.* 2007). These patterns for cell implants included extensive cellular re-arrangement and re-organization, leading to the formation of seminiferous cords by 2 wk and tubular lumen and complete tissue formation by 4 wk (Dobrinski 2007; Honaramooz *et al.* 2007). The developmental patterns of piglet testis tissue xenografts resembled those of the *in situ* testis tissue, where seminiferous cords gradually developed and transformed into fully functional seminiferous tubules over time (Honaramooz *et al.* 2002).

Furthermore, the observed strong and positive correlations between pre- and post-recovery volumes, and height and length measurements were indicative of UBM validity in predicting the

growth and physical development of testis tissue grafts and cell implants. Bland-Altman analysis of the two volume estimation approaches (3-D segmentation and water displacement) showed the reliability of our estimated values and agreements between pre- and post-recovery volume measurements.

Although UBM and physical measurements of length were positively correlated for all samples, when considered as a whole, mean UBM values of width and length were numerically greater than those of physical measurements. Lack of a correlation between the UBM and physical measurements of sample widths, as well as smaller physical width and length measurements may have resulted from the rounding of grafts and implants upon recovery, likely due to removal of the surrounding physical restrictions such as attachments to adjacent tissues. The physical heights of samples were greater than those of UBM, again supporting the speculation about rounding of samples after recovery. Alternatively, sample heights recorded by UBM may represent potentially underestimated values, given the undetectability of the ventral capsular border of most samples. Therefore, it is recommended that our proposed coefficients be used in future experiments to predict the post-recovery physical attributes of samples more accurately from UBM estimates.

Although positively correlated, the physical measurements of volume were lower than those estimated from UBM. This difference may be due to tissue shrinkage and/or fluid loss from the fluid-filled cavities as a result of physical manipulation of cell implants during sample recovery. Nevertheless, the UBM estimated length, height, and volume of the samples corresponded to those of physical evaluations, validating the use of UBM for axial and volumetric estimation of testis grafts and implants. The average UBM volume of tissue grafts and cell implants changed from 13.49±0.94 mm^3 and 100 mm^3 at the time of grafting or implantation to 22.23±2.29 mm^3 and 71.12±19.56 mm^3 at 2 wk, respectively. The volume decreases observed for cell implants may be as a result of resorption of the remnant media, which was mixed in with the donor cells during implantation.

Retrospective comparison of images from 2 wk implants revealed that relatively less echogenic (darker) areas near the margins of cell implants in UBM images coincided with the presence of newly-formed testis tissue containing seminiferous cords in histological cross-sections. Conversely, relatively hyperechoic areas of the implants in UBM images corresponded with the non-cordal regions in histological cross-sections, which were located more centrally (Fig. 6.4B).

The observed preferential pattern of cordal distribution around the periphery may indicate that these areas benefited from accessibility to diffusion from the host and earlier development of new blood supply (Schlatt *et al.* 2006). Using testis tissue xenografting models, it has been proposed that limited central vascularization combined with high oxygen and metabolic demands of the implanted cells during re-organization may lead to better development of testicular cords in the peripheral regions of the grafts (Schlatt *et al.* 2006; Ntemou *et al.* 2019). In our study, only cell implants showed the differential pattern of cordal development whereas all grafts displayed a uniform distribution of cords. However, in a study using young chicks, auto-transplanted testis tissue grafts maintained tubular structures in peripheral areas and their central areas undergoing necrosis (Cheng *et al.* 2017). Similarly, earlier reports of testis tissue xenografting from neonatal piglets into recipient mice also showed more advanced development in the periphery of some grafts (Honaramooz *et al.* 2002). These observations are consistent with our observation of preferential cordal distribution pattern within the cell implants.

The interaction between the sample type and time for sample volumes in both UBM and histological measurements ($P = 0.01$ for both) indicated that the volume of tissue grafts increased towards wk 8 by ~290%, measured using UBM, and by ~360%, measured using the displacement method (Fig. 6.4G and 6.4H). While for cell implants the volume change over time was not significant, their initial reduction in volume may be explained by resorption of fluids from 2 to 4 wk, followed by limited growth from 4 to 8 wk mainly in their periphery.

Taken together, the present study supports the use of UBM data for examining and predicting the *ex situ* development of testis tissue grafts and cell implants. These results may also indicate the potential use of UBM for other organ systems or neoplasia where detection of superficial structures or masses and their changes over time are being investigated. The accuracy and non-invasiveness of UBM are also important advantages in its use as an *in vivo* evaluation technique.

The present study was designed to compare the UBM data of recovered testis tissue grafts and cell implants with their physical and histological attributes in order to validate the use of UBM for monitoring the development of grafts and implants. The correlations found between the approaches showed that UBM can be used as a consistent, accurate, and non-invasive alternative to surgical recovery of multiple samples over time for monitoring the development of such grafts and implants. Thereby validating UBM as a high-fidelity, facile, and informative tool for the *in vivo*

assessment of physical growth and structural changes of grafts and implants. The potential replacement of repeated surgical sample recoveries with UBM can reduce fatality rates among the immunodeficient host mice which, in turn, can result in a reduced number of animals required for future studies for similar applications.

Transition

In Chapter 6, by using side-by-side comparison of UBM images and histological cross-sections of obtained samples in a short-term study (2 mo) we validated the use of UBM as a non-invasive and accurate approach to monitor the development of ectopic testis tissue grafts and cells implants. Therefore, we designed and conducted a long-term study in Chapter 7 to repeatedly use UBM for over time evaluations of the samples and to demonstrate the gradual changes in grafts and implants mainly by utilizing this approach.

CHAPTER 7

LONG-TERM MONITORING OF DONOR XENOGENEIC TESTIS TISSUE GRAFTS AND CELL IMPLANTS IN RECIPIENT MICE USING ULTRASOUND BIOMICROSCOPY [9, 10]

7.1. Abstract

Testis tissue xenografting (TTX) and testis cell aggregate implantation (TCAI) from various donor species into recipient mice are novel models for the study and manipulation of testis formation and function in target species. Thus far, the analysis of such studies has been limited to surgical or post-mortem retrieval of samples. Here, we used ultrasound biomicroscopy (UBM) to monitor the development of neonatal porcine testis grafts/implants in host mice for 24 wk, and to correlate UBM and (immuno)histological changes. This led to 1) long-term visualization of gradual changes in volume, dimension, and structure of grafts and implants, 2) detection of a 4-wk developmental gap between grafts and implants, and 3) revealing differences in implant development depending on the craniocaudal site of implantation on the back of host mice. Our data support the reliability and precision of UBM for longitudinal study of transplants, which eliminates the need for frequent surgical sampling.

7.2. Introduction

In situ study of testis development and function is challenging; this is especially the case for non-rodent animals, endangered species, and humans. The advent of innovative *in vivo* and *in vitro* testis culture systems has made it feasible to overcome the conventional limited access to the male gonads in various target species. Testis tissue xenografting (TTX) and testis cell aggregate implantation (TCAI) were among the first *in vivo* models to offer alternative strategies for the study of male gonadal development, spermatogenesis, and steroidogenesis of various donor species within a host mouse. These models have ever since led to more in-depth understanding of

---

[9] This study has been published. Fayaz MA, Awang-Junaidi AH, Singh J, and Honaramooz A (2020) *Ultrasound in Medicine & Biology* 46:3088–3103.

[10] MAF contributed to the experimental design, performed the study, analyzed the data, and wrote the first draft of the manuscript. AHAJ contributed to performing the study and analyses. JS contributed to the experimental design and revised the manuscript. AH supervised the study, contributed to the experimental design, and revised the manuscript.

the pathobiology of the testis in a wide range of species than comparable animal models (Honaramooz 2014; Ibtisham *et al*. 2020).

TTX leads to physical growth and maturational development of the grafted tissue, induction of complete spermatogenesis, and even production of fertilization-competent sperm (Honaramooz *et al.* 2002). Similarly, *de novo* morphogenesis of functional testis tissue makes TCAI a unique model for the developmental studies (Honaramooz *et al.* 2007). By now, a range of species have been used as donors in TTX and TCAI studies, and as such these two models have provided an invaluable opportunity to investigate testis development and function, conservation of fertility potential of endangered mammalian species, and prepubertal boys undergoing gonadotoxic cancer treatments (Gassei *et al.* 2006; Honaramooz *et al.* 2007; Kita *et al.* 2007; Arregui *et al.* 2008; Aeckerle *et al.* 2013; Honaramooz 2014; Sharma *et al.* 2018; Ibtisham and Honaramooz 2020).

When neonatal/immature testis is used as donor tissue, testicular development and xenogeneic spermatogenesis can be expected in TTX, perhaps with a notable exception of human testis tissue as donor (Schlatt *et al.* 2006; Arregui *et al.* 2008b; Honaramooz 2014; Tharmalingam *et al.* 2018; Ibtisham *et al*. 2020). Previous studies showed that especially male SCID mice (irrespective of gonadal status) provide a more suitable recipient model (Abbasi and Honaramooz 2010) and grafting 8 or 16 fragments per recipient mouse leads to better overall development in TTX studies (Abbasi and Honaramooz 2011b). Recently, we optimized TCAI by showing the feasibility of a less invasive approach involving a bolus injection of very large numbers of concentrated cells (*i.e.*, 100×10^6 per implant) containing high percentage of gonocytes (*i.e.*, ~40%) (Awang-Junaidi *et al.* 2020) rather than depositing unknown numbers of cells through surgically created wounds as a conventional method (Honaramooz *et al.* 2007).

Initially, evaluations of grafts from TTX and TCAI experiments were primarily restricted to terminal collection of all samples from groups of mice undergoing euthanasia (Honaramooz *et al.* 2002, 2007). We later showed that surgical removal of a few randomly-selected samples at each of several time points can provide sufficient indications about the developmental status of grafts or implants over time (Abbasi and Honaramooz 2011a, 2011c, 2012; Fayaz *et al.* 2020b). However, surgical retrieval of sample grafts and implants is still invasive, and the retrieved samples need to be processed for histological assessments. Thus, although informative, this longitudinal sampling approach carries the usual surgical risks, especially because of repeated

surgeries, and can also lead to inaccurate volume measurements of grafts/implants due to fixation and histological processing leading to tissue shrinkage. More importantly, histological assessment of samples can only provide retrospective information about the tissue status at the time of retrieval, and since the number of grafts/implants per mouse are limited, only a few observational time points can be included in a longitudinal TTX or TCAI study (Honaramooz 2014). Therefore, non-invasive real-time monitoring modalities that can be repeated over time will provide invaluable information and are advantageous from several perspectives.

Ultrasound biomicroscopy (UBM) is well-suited to provide the repeatability and precision required for non-invasive acquisition of data in various clinical and research settings, including female reproductive tissue and organs (Baerwald *et al.* 2009; Jaiswal *et al.* 2009; Mircea *et al.* 2009; Pfeifer *et al.* 2012; Pfeifer *et al.* 2014). In short-term feasibility and validation studies (Awang-Junaidi *et al.* 2020; Fayaz *et al.* 2020b), conducted up to 2 or 8 wk, respectively, we showed that UBM is an accurate tool for evaluation of testis tissue xenografts and cell implants in host mice. However, foregoing short-term studies may not reflect the complete developmental changes in samples, and the post-retrieval evaluations of samples were mainly focused on macroscopic aspects. Also, a study with focus on UBM practicality in screening the over time changes in sample structure and effects of grafting/implantation location based on the echotexture is deemed essential. Therefore, the present study was designed to (1) repeatedly apply UBM for the non-invasive and long-term (24 wk) monitoring of orthogonal dimension and volume changes in samples to encompass the putative length of the pre-pubertal process of donor pigs (~6 mo) and through spermatogenesis and to (2) use histology and UBM to evaluate the long-term structural and developmental changes in testis tissue xenografts and cell implants from neonatal donor pigs in recipient mice. We hypothesised that UBM can be used accurately and independently to determine long-term orthogonal dimensions, volumes, and compositional changes in samples. We also hypothesised that longitudinal UBM and histological attributes of retrieved samples will be positively correlated.

7.3. Materials and Methods

7.3.1. Preparation of Testis Tissue Fragments and Cells

A schematic representation of the study design is provided in Figure 7.1. Small fragments of testis parenchyma (~14 mm^3 each) and isolated testis cells, composed of 40% gonocytes, were prepared

as described previously and in Chapter 6 (Yang *et al.* 2010; Yang and Honaramooz 2011; Fayaz *et al*. 2020b) using the obtained testes from 1-wk-old Yorkshire-cross piglets (n = 30). Prepared fragments were kept on ice-cold medium mixed with antibiotics (10,000 I.U. penicillin and 10,000 µg streptomycin; catalogue no. 30-002-CI; Mediatech) until TTX into immunodeficient recipient mice and the resultant cell pellets were prepared and refrigerated for TCAI procedure, as previously described (Awang-Junaidi *et al.* 2020; Fayaz *et al*. 2020b). All experiments involving animals were reviewed and approved by the University of Saskatchewan's Institutional Animal Care and Use Committee (Protocol # 20080042).

7.3.2. Procedures for TTX and TCAI

The recipient mice were ~7-wk-old male severe combined hairless immunodeficient (SHO, Crl: SHO-*Prkdc*^{scid}*Hr*^{hr}, strain code 474; Charles River, Montreal, Canada, n = 6). The acclimatization, care, handling, anesthesia, and surgical procedures of mice were as described in Chapter 6. TTX and TCAI were performed on the same day as was described in detail in our previous studies (Awang-Junaidi *et al*. 2020; Fayaz *et al*. 2020b). Grafts were designated a letter (R for right) and a number (1-4, corresponding to their cranial through caudal position), and implants were similarly designated L1-L4 (Fig. 7.1).

7.3.3. UBM of the Grafts and Implants

Using 3-D transcutaneous colour Doppler UBM (VisualSonics Vevo3100, 32-55 MHz MX550D transducer, VisualSonics, Toronto, ON, Canada), all grafts and implants were examined weekly for the first 8 wk, followed by once every 4 wk for up to 24 wk. The examination process was performed as previously described in more details (Awang-Junaidi *et al.* 2020; Fayaz *et al.* 2020b). In addition to B-mode for determination of size, volume, and pixel intensity/heterogeneity, colour Doppler mode was used to detect the flow-dependent signals.

Measurements and quantifications on UBM images were performed for all examination time points, and the UBM measurements were correlated with corresponding histological measurements. As described previously (Fayaz *et al.* 2020b), tissue grafts demonstrated a more homogenic structure, whereas cell implants consisted of areas with varying echogenicities, corresponding with areas with cord formation (cordal areas), areas with connective tissue (non-cordal areas), and fluid-filled cavities on histological cross-sections. Reconstruction of 3-D

images, volume measurement, orthogonal dimension measurement, and hyperechoic and hypoechoic area measurements were performed as described previously (Robb 1995; Fenster and Downey 2000; Cheung *et al*. 2005; Fayaz *et al*. 2020b). For 3-D reconstruction, the most caudal graft and its corresponding cell implant were used (*i.e.*, R4 and L4); these were not included in samplings and hence were present in all recordings of all recipient animals over time. The same graft and implant were used for 3-D reconstruction at each time point (Fig. 7.2). Sample volumes were also measured using the Cavaleri principle of stereological approach and on 2-D images recorded through the B-mode (Elliot *et al.* 1996; Cheung *et al.* 2005; Fayaz *et al.* 2020b). Length, height, and width were also measured as described previously (Fayaz *et al*. 2020b) and cordal volume was quantified using multiplication of the obtained UBM volume by the percentage of cordal areas, measured on 2-D UBM images for each implant. Using the colour Doppler mode, flow-dependent signals appearing within the boundaries of each sample in three consecutive images were considered as an individual blood vessel in Vevo LAB software. Two or more signals within 0.25 mm distance were considered as the same individual vessel.

7.3.4. Sample Retrieval and Histological Evaluations

Recipient mice were randomly assigned a number (# 1-6). At 2, 6, and 16 wk, mice # 1, 2, and 3 underwent sampling, while the remaining three recipients (# 4, 5, and 6) were used for sampling at 4 and 8 wk. At each sampling time point, after UBM examination of all grafts and implants out of R1-3 grafts and L1-3 implants, one of each sample was randomly selected for retrieval. Therefore, at each sampling time point a total of 3 grafts and 3 implants was obtained for further evaluations. The most caudal grafts and implants (*i.e.*, R4 and L4) were not included in random sampling and remained intact in all recipients, to be used as a time-course control within each animal and for 3-D re-construction of grafts and implants over time. The remaining grafts and implants were all retrieved at the time of euthanasia at 24 wk. The procedure for sample retrieval was as described previously (Fayaz *et al.* 2020b).

Physical dimensions of the obtained samples were documented using photomacrographs and the samples were then fixed and processed for histology as previously described (Fayaz *et al.* 2020b). 2-D UBM images and histological attributes of each sample were compared at the largest diameter. The two slides immediately following the H&E-stained slide were used for immunohistochemistry and trichrome staining, respectively. To test the validity of our previously-calculated equations

(Fayaz *et al.* 2020b) for dimension estimation of grafts and implants in this study, we randomly selected grafts and their corresponding implants at 16 and 24 wk, and used their measured physical volume, length, and height in correlation analyses to be compared with the expected dimensions calculated based on our established equations.

7.3.5. Immunohistochemistry and Trichrome Staining

To identify germ cells in sample cross-sections, expression of the ubiquitin C-terminal hydrolase-1 (UCH-L1, also known as PGP9.5) was evaluated. Briefly, among five sections on an individual slide, one was randomly selected, deparaffinized in xylene, and dehydrated through descending grades of alcohol. Antigen retrieval was performed at 98° C in citrate buffer (catalogue no. H3300; Vector Laboratories, Burlingame, CA, USA) and Tris (hydroxymethyl) aminomethane-Ethylenediaminetetraacetic acid (Tris-EDTA) (Tris; catalogue no. T87602; Sigma-Aldrich; EDTA; catalogue no. E9884; Sigma-Aldrich) for 30 min, each. The slides were washed with 0.1 M phosphate buffered saline (PBS; catalogue no. BP243820; Fisher scientific, Toronto, ON, Canada) three times, followed by incubation with 0.3% w/v hydrogen peroxide in distilled water (H_2O_2; catalogue no. 7722841; RW consumer products, Winnipeg, MB, Canada) for 30 min to block endogenous peroxidase activity. Sections were covered with 2.5% horse serum (catalogue no. S-2012; Vector Laboratories), for 30 min in a moist chamber at room temperature to block non-specific proteins. The blocking solution was then removed and the primary antibody (1:200 mouse monoclonal to UCH-L1; catalogue no. ab8189; Abcam, Toronto, ON, Canada) was used to cover the sections at 4° C overnight. Subsequently, slides were washed three times with 0.1 M PBS and incubated for 1 hr with the secondary universal antibody (horse anti-mouse/rabbit IgG; catalogue no. BP-1400; Vector Laboratories) at room temperature in a moist chamber. Sections were again washed three times with PBS and covered with 3,3'-Diaminobenzidine (DAB) chromogen (catalogue no. SK-4105; Vector Laboratories) for 3 min, immersed in distilled water for 5 min, and counter-stained with hematoxylin for 5 min (catalogue no. H-3401; Vector Laboratories). Sections were dehydrated with alcohol, cleared with xylene and mounted using a mounting medium (Fisher Chemical Permount mounting medium, catalogue no. SP15-100; Fisher scientific).

Trichrome staining was performed using a trichrome staining kit (catalogue no. ab150686; Abcam) by following manufacturer's instructions. Briefly, the sections were deparaffinized as described

above, hydrated in distilled water, and placed in Bouin's solution in a 56° C water bath for 1 hr, followed by 10 min of cooling at room temperature. The sections were then rinsed with tap and distilled water, respectively, followed by immersion in a working solution of Weigert's hematoxylin for 5 min and under running tap water for 2 min. The Biebrich scarlet/acid fuchsin solution was used for 15 min, followed by rinsing the slides in distilled water. In the next step, the sections were covered with phosphomolybdic/phosphotungstic acid for 10 min. Aniline blue solution was then applied for 5 min, and the slides were rinsed with distilled water and covered with 1% acetic acid solution for 3 min. The sections were dehydrated using 95% and 100% alcohol, respectively, cleared using xylene, and mounted with the mounting medium.

7.3.6. Histomorphometric Analyses

Photomicrographs were obtained using a calibrated binocular microscope equipped with digital photomicrography (Northern Eclipse Image Analysis software version 7.0, Empix Imaging, Mississauga, ON, Canada) and measurements on obtained images were performed using ImageJ (ImageJ, US national Institutes of Health, Bethesda, Maryland, USA). One photomicrograph was captured at 40 × magnification and 10 photomicrographs were captured from randomly selected fields of view at 200 × magnification from each of the three stained slides.

As was described previously, using low magnifications on H&E-stained slides, cordal and non-cordal areas as well as areas of the total section and fluid-filled cavities were measured by outlining their boundaries (Fayaz *et al*. 2020b). Measured areas were then used in correlation analyses with similar measurements performed on the largest 2-D UBM images. Diameter and density of cords were measured using images obtained at higher magnifications. To compare the grafts and implants at a more comparable developmental stage, the diameter and density of cords in implants were also compared with those of grafts of one and two earlier time points.

Slides stained against UCH-L1 were used to quantify the percentage of seminiferous cords or tubules with the most advanced germ cells to assess their development at each sampling time point. Cords or tubules were categorized based on the presence of 1) Sertoli cell-only, 2) gonocyte/spermatogonia, 3) spermatocytes, 4) round spermatids, and 5) elongated spermatids as the most advanced stages. Using trichrome-stained slides and ImageJ, the total area of blood vessels was measured by outlining the basement membrane of the vessels. Also, on the same

sections, the number of blood vessels was counted and used in correlation analyses with the number of flow-dependent signals, detected in colour Doppler mode.

7.3.7. Statistical Analyses

The data presented are mean ± standard error of mean (SEM) and $P < 0.05$ was considered statistically significant. All the analyses were performed using *t-test*, one- or two-way analysis of variance (ANOVA), one- or two-way repeated measures ANOVA, or Pearson correlation coefficient analysis, unless stated otherwise. Simple linear regression was used to find the relationship between UBM and histological measurements. Statistical Package for Social Sciences (IBM SPSS Statistics for Macintosh, Version 23.00; IBM Corporation, Armonk, NY, USA) was used for statistical data analyses.

7.4. Results

7.4.1. UBM Evaluations

As early as 1 wk and throughout the examination time points, all samples were detectable by UBM under the skin and appeared in various shapes, ranging from sphere, hemisphere, and ellipsoid to irregular (Fig. 7.2). The dorsal skin of mice covering grafts and implants appeared as a hyperechoic (white) band. Located immediately under the skin, grafts (n = 24) and implants (n = 24) were surrounded by a fibrous capsule which appeared as a hyperechoic line, notably at the ventral boundary of the samples (Fig. 7.3).

Overall, unlike tissue grafts which displayed a relatively homogenous echogenicity, cell implants were composed of varying echogenicities indicative of multiple zones (Fig. 7.4). These zones included hypoechoic areas adjacent to the boundaries, hyperechoic areas near the center, and anechoic areas (dark) also located in the center of the cell implants. Hypoechoic, hyperechoic, and anechoic areas on 2-D UBM images corresponded with the cordal areas, non-cordal areas, and fluid-filled cavities on histological cross-sections, respectively (Fig. 7.3 and 7.4). At wk 1, the cavities were present in ~92% of cell implants, while this number decreased to ~8% by wk 5, and to 0% by wk 6 (Fig. 7.3J, 7.3K, and 7.3L).

Changes in the average UBM volume (through 3-D segmentation), cordal volume, and orthogonal diameters (length, width, and height) at the largest 2-D UBM images of samples are shown in Figure 7.5 The pattern of these changes was not similar between grafts and implants. Overall, the

UBM volume and diameters of implants initially decreased to wk 3 but was followed thereafter by a progressive increase over time, while the volume and diameter of grafts gradually increased from the first UBM examination to wk 24. The UBM implant volume decreased by ~37% from wk 1 to 3, while the graft volume increased by ~235% within the same period (P = 0.001; Fig. 7.5A). Similarly, from wk 1 to 4, the UBM length of implants decreased by ~8%, while for the grafts this measurement was up by 12% (P = 0.004; Fig. 7.5B). Also, the UBM width of implants deceased by ~17% from wk 1 to 3, when grafts width increased by ~6% in the same period (P < 0.001; Fig. 7.5C). Likewise, from wk 1 to 4, the implants height decreased by ~35%, while grafts height increased by ~22% (P < 0.001; Fig. 7.5D). The overall UBM-estimated cordal volume increased by ~245% from wk 2 to 24 in all implants (P < 0.001), but this was also influenced by the location of implants; the cordal volume of cranial and mid-cranial implants was ~50% greater than that of mid-caudal and caudal implants (P = 0.02; Fig. 7.5E). For pixel intensity in 2-D UBM images of implants, an interaction was found between the area type (cordal *vs.* non-cordal areas) and time of UBM examination (P < 0.001), where cordal pixel intensity decreased by ~30% from wk 3 to 24, while non-cordal pixel intensity remained unchanged (Fig. 7.5F). Over time, pixel heterogeneity showed a tendency to decrease for both area types (P = 0.08). At wk 1, 20, and 24, pixel heterogeneity of cordal areas was ~8%, ~9%, and 3% greater than that of non-cordal areas, respectively (P < 0.001; Fig. 7.5G). The overall number of flow-dependent signals (vessels) in the colour Doppler mode increased over time (P < 0.001). Also, at 2- and 24-wk grafts contained ~40% and ~28% greater number of signals compared with implants, respectively (P = 0.01; Fig. 7.5H).

7.4.2. (Immuno)histological Evaluations

All samples were visible at every retrieval point to be surgically removed from the subcutaneous tissue. In the largest histological sections, a dense connective tissue surrounded both grafts (n = 24) and implants (n = 24). For grafts, the interstitial tissue seemed to be interconnected with the fibrous capsule via branches (Fig. 7.3 and 7.4). Also, the distribution pattern of cords and interstitial tissue appeared random throughout the histological cross-sections of the grafts. For implants, the initial cellular organization and cord formation were first observed at wk 2 near the fibrous capsule, further cellular alignments formed morphologically normal seminiferous cords by wk 4 and cordal area expanded more centrally, while the central areas were mainly occupied by

fluid-filled cavities and/or connective tissue (Fig. 7.3P, 7.3Q, and 7.3R). The same cordal distribution pattern was observed in all implants collected at all sampling time points. The fluid-filled cavities were observed in histological sections of two implants at 2 wk, one implant at 4 wk, whereas no cavity was present at 6 wk or later. The histological appearance of tissue grafts at 2 wk was similar to that of age-matched testis tissue, composed of clusters of seminiferous cords surrounded by interstitial tissue (Fig. 7.3G, 7.3H, and 7.3I). Within each cord, Sertoli cells with detectable nuclei surrounded germ cells and cords gradually underwent developmental changes and luminal formation by wk 4. Expectedly, in 2-wk implants, cellular alignments and initial cords were observed which further developed into tubules at later time points.

Previously, based on a short validation study, we established equations to calculate the expected physical measurements based on UBM measurements (Fayaz *et al*. 2020b). Here we utilized the equations to test their accuracy by calculating the expected attributes of samples obtained at much later time points (wk 16 and 24) and comparing them with actual measured values. The expected measurements of volume, length, and height calculated using our previously established equations (Fayaz *et al.* 2020b) were strongly and positively correlated with the actual physical measurements of representative samples at wk 16 and 24 (volume: $r = 0.99$, $n = 12$, $P < 0.001$; length: $r = 0.95$, $n = 12$, $P < 0.001$; height: $r = 0.97$, $n = 12$, $P < 0.001$).

The overall diameter and density of cords increased over time ($P < 0.001$ for both; Fig. 7.6A and 7.6B). Also, diameter of cords in grafts was greater than that of implants at all sampling time points except for wk 2 ($P < 0.001$). The density of cords was also greater in grafts at wk 2, 6, 8, 16, and 24 ($P < 0.001$). When comparing implants at a given time point with grafts of two time points earlier, to correct for the perceived delayed development of implants, the diameter of cords was ~22% greater only in 24-wk implants compared to 8-wk grafts ($P < 0.001$). Similar to the diameter, the density of cords was not different at earlier time points with 4 wk developmental interval between grafts and implants but at later time points with 10 and 16 wk intervals, density of cords was greater in grafts ($P < 0.001$).

In sections stained against UCH-L1, the percentage of Sertoli cell-only cords or tubules decreased by ~48% from wk 4 to 24 in both grafts and implants ($P < 0.001$) and overall ~15% more cords/tubules in grafts displayed this morphology than implants ($P = 0.001$; Table 7.1). From wk 2 to 8, gonocytes/spermatogonia were the most advanced germ cell type present in both sample

types (Fig. 7.7). However, from wk 2 to 8, the percentage of cords/tubules with gonocytes/spermatogonia as the most advanced germ cells increased by ~28% in both sample types, followed by ~64% decrease from wk 8 to 24 ($P < 0.001$). Overall, the number of gonocyte/spermatogonia-containing cords/tubules were ~10% greater in implants than grafts ($P = 0.005$; Table 7.1). Spermatocytes were first observed in grafts and implants at wk 16. In grafts, the percentage of cords/tubules containing round and elongated spermatids were 10.97 ± 1.35 and 7.00 ± 1.52, respectively, while no spermatids were detected in the corresponding implants.

Masson's trichrome staining allowed visualization of collagen and muscle fibers located at the basement membrane of vascular walls, and thereby allowed identification of blood vessels in histological sections (Fig. 7.8). In both grafts and implants, the number of detected vessels decreased over time ($P < 0.001$; Fig. 7.6C), whereas their total measured area increased ($P = 0.006$; Fig. 7.6D).

7.4.3. UBM vs. Histological Findings

Comparison between 2-D UBM images and their corresponding histological sections revealed that the observed ventral hyperechoic line in 2-D UBM images corresponded to a dense fibrous capsule in histological sections. This capsule was not limited to the ventral boundary in histological sections and surrounded both sample types. Only the ventral part of the capsule was discernible in 2-D UBM images. Also, in histomorphometric evaluations, the capsule showed thinner interconnecting branches with interstitial connective tissue within the tissue grafts, which was not identifiable by UBM (Fig. 7.3).

Cordal, non-cordal, and fluid-filled cavity areas on histological sections corresponded to the hypo- (dark), hyper- (white), and anechoic (black) areas on 2-D UBM images, respectively (Fig. 7.3J-3R and Fig. 7.4). These areas on the largest 2-D UBM images were strongly and positively correlated with their corresponding areas on histological cross-sections ($r = 0.81$, $n = 25$, $P < 0.001$; Fig. 7.9A). In implants, the distribution of cords appeared to be random but was near the fibrous capsule, while the cavities and non-cordal areas were located centrally at all examinations and sampling time points (Fig. 7.4). Although cords developed towards the central areas, still the density of cords was lower in the central *vs.* peripheral areas of implants at wk 24. Also, the total pixel intensity of implants on the largest 2-D UBM images was positively correlated with the percentage of non-cordal areas on the largest histological cross-sections ($r = 0.87$, $n = 24$, $P <$

0.001; Fig. 7.9B). In grafts, uniform echogenicity and distribution of cords was found in 2-D UBM images and histological sections, respectively. In 2-D UBM images anechoic areas of fluid-filled cavities were identified in 6 and 2 cell implants at wk 2 and 4, respectively, whereas in histological sections, these cavities appeared in 2 and 1 implants at wk 2 and 4, respectively. Cavities and movements of their contents were detectable as early as 1 wk by UBM and medial to lateral changes to their 2-D shape could be visualized by movements of the probe. In histological sections, the architecture of these cavities as well as their surrounding cellular and non-cellular zones were visualized with more accuracy. Additionally, the number of flow-dependent signals, recorded in colour Doppler mode, was negatively correlated with the number of vessels on histological sections including capillaries ($r = –0.43$, $n = 24$, $P = 0.002$; Fig. 7.8).

Table 7.1. Histomorphometric analysis of cell implants and tissue grafts at different retrieval time points showing the percentage (mean ± SEM) of cords/tubules with the most advanced germ cells.

		week					
Parameter	**Sx type**	**2**	**4**	**6**	**8**	**16**	**24**
Sertoli cell-only cords/tubules	**Implant**	46.21 ± 0.72^{A}	44.55 ± 0.95^{A}	33.39 ± 0.1^{B}	31.64 ± 3.83^{B}	30.60 ± 3.56^{B}	23.41 ± 1.51^{C}
	Graft	52.70 ± 2.58^{A}	48.49 ± 1.91^{A}	39.51 ± 0.67^{B}	39.16 ± 2.20^{B}	33.77 ± 2.73^{B}	25.029 ± 1.30^{C}
Gonocyte/ spermatogonia	**Implant**	53.78 ± 0.72^{A}	55.44 ± 0.96^{AB}	66.60 ± 0.06^{BC}	68.35 ± 3.83^{C}	36.08 ± 0.60^{D}	25.36 ± 5.88^{D}
	Graft	47.29 ± 2.60^{A}	51.51 ± 1.92^{AB}	60.49 ± 0.68^{BC}	60.83 ± 2.20^{C}	27.25 ± 3.38^{D}	21.47 ± 6.78^{D}
Spermatocyte	**Implant**	-	-	-	-	33.31 ± 3.90	51.22 ± 6.93
	Graft	-	-	-	-	38.96 ± 4.27	35.52 ± 3.59
Round spermatid	**Implant**	-	-	-	-	-	-
	Graft	-	-	-	-	-	10.97 ± 1.35
Elongated spermatid	**Implant**	-	-	-	-	-	-
	Graft	-	-	-	-	-	7 ± 1.52

Numbers with different superscripts within each row differ significantly ($P < 0.05$). Sx = sample.

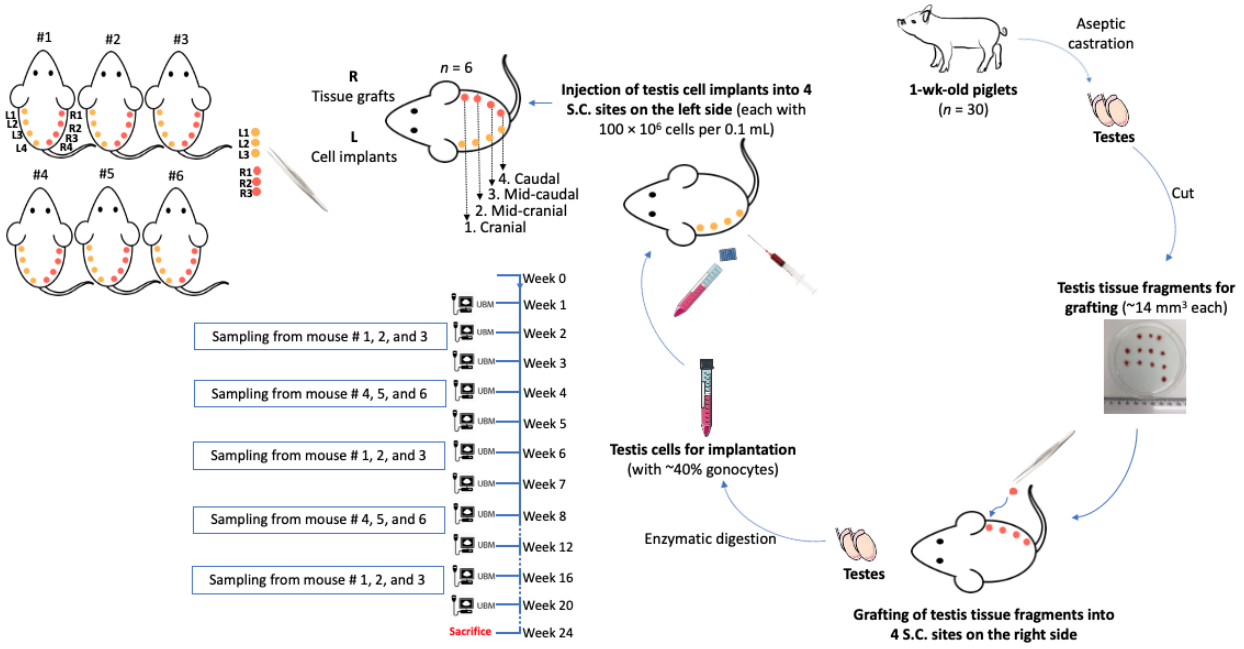

Fig. 7.1. Experimental design of the present study. Teste (n = 30) were collected by aseptic castration of 1-wk-old piglets and the parenchyma was used to prepare small fragments (~14 mm^3). Using the same source, testis cell aggregates, comprised of ~40% gonocytes, were isolated (100 × 10^7 cells/mL) by enzymatic digestion. Dorsal skin of immunodeficient recipient mice (n = 6) was prepared, testis tissue grafts embedded in small subcutaneous pouches on 4 grafting sites on the right side and cell implants injected into 4 contralateral sites on the left side (0.1 mL/injection site). Starting from wk 1 post-grafting/implantation, each site was examined using ultrasound biomicroscopy (UBM) every wk for the first 8 wk and then every 4 wk until 24 wk. Following UBM examination, randomly-selected grafts and corresponding cell implants were surgically removed for (immuno)histochemical evaluation at 2, 4, 6, 8, and 16 wk. Grafts and implants, included in the retrieval were defined as R1-R3/L1-L3. Nevertheless, the most caudal samples (*i.e.*, R4 and L4) were not retrieved and served as time-course control as well as for 3-D reconstruction.

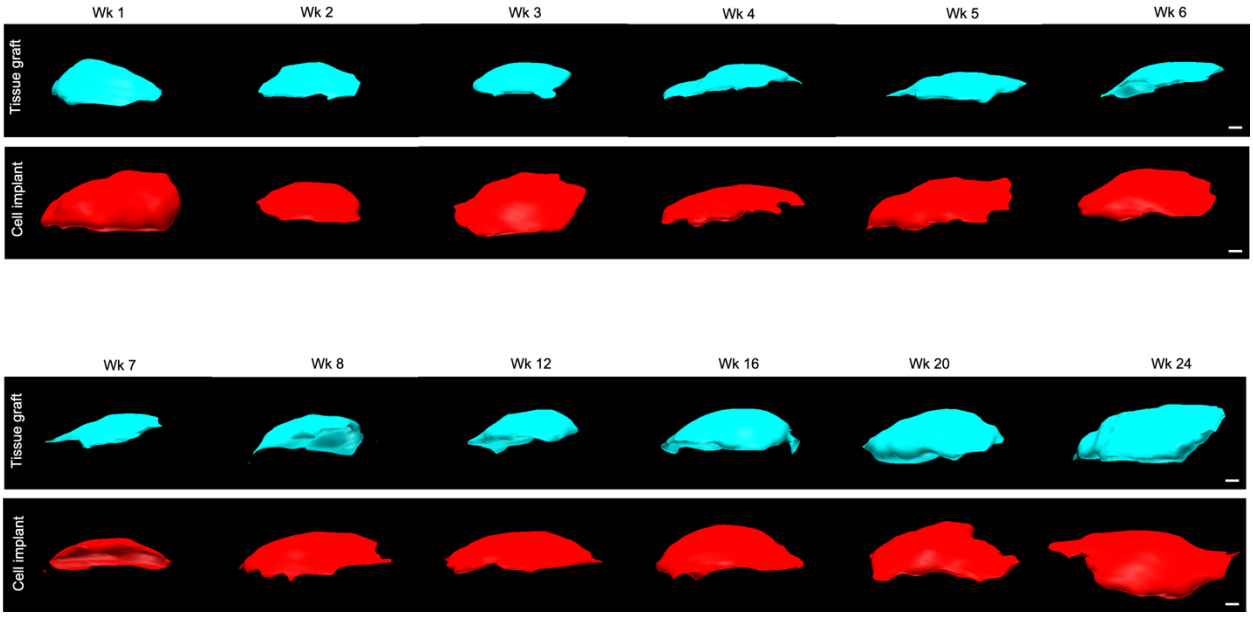

Fig. 7.2. Three-dimensional (3-D) reconstruction of a representative subcutaneous tissue graft and its contralateral cell implant from wk 1 to 24. Using a built-in feature of the Vevo Lab software (Vevo LAB, Version 3, Fujifilm VisualSonics Inc, Toronto, ON, Canada), the borders of each sample were delineated every 0.5 mm on 2-D UBM images in three axes in order to construct polyhedral 3-D representation of each sample. Reconstructed images could be moved in different orientations for a better visualization of their 3-D growth estimation analysis and shape changes. (Scale bar = 1 mm)

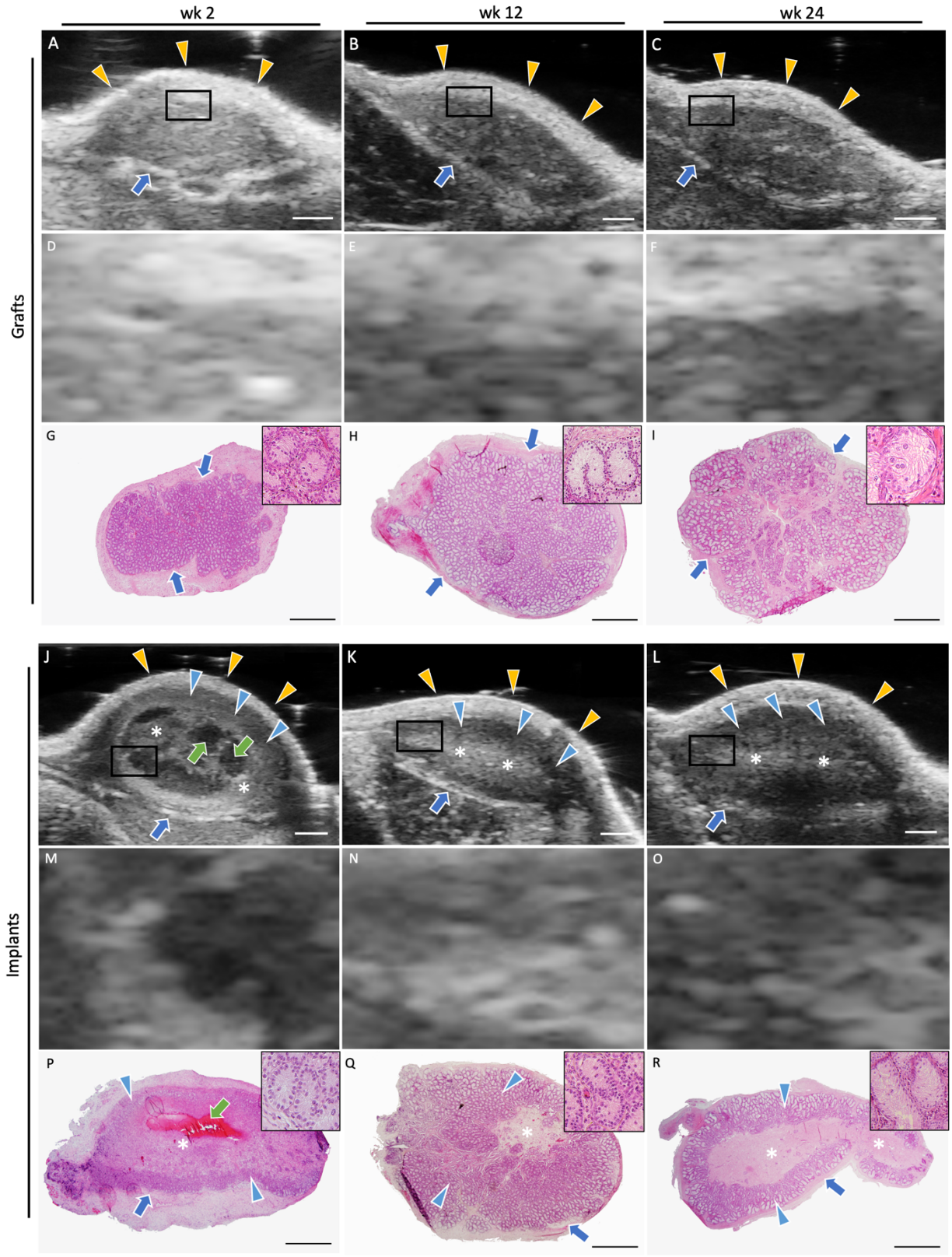
wk 2
wk 12
wk 24
Grafts
Implants
A
B
C
D
E
F
G
H
I
J
K
L
M
N
O
P
Q
R

Fig. 7.3. Representative 2-D UBM images and largest histological sections of grafts (A-I) and implants (J-R). Both sample types were covered by dorsal skin on the top (yellow triangles; A-C and J-L) and fibrous capsule, which could only be detected in the lower boundary of grafts and implants (blue arrows; A-C, G-I, J-L, and P-R). The tissue grafts were composed of seminiferous cords/tubules in histological sections, representing a homogenous structure in 2-D UBM images. However, cell implants consisted of different echogenic areas. By comparing UBM with the largest histological sections, these areas could be defined as cordal areas (blue triangles; P-R), appeared as hypoechoic (grey; J-L), non-cordal areas (white asterisks; P-R), appeared as hyperechoic (white asterisks; J-L), and fluid-filled cavity areas (green arrows; P), appeared as anechoic (dark; J). The contents of cavities were absorbed and replaced by connective tissue by wk 6. (Scale bar = 1 mm)

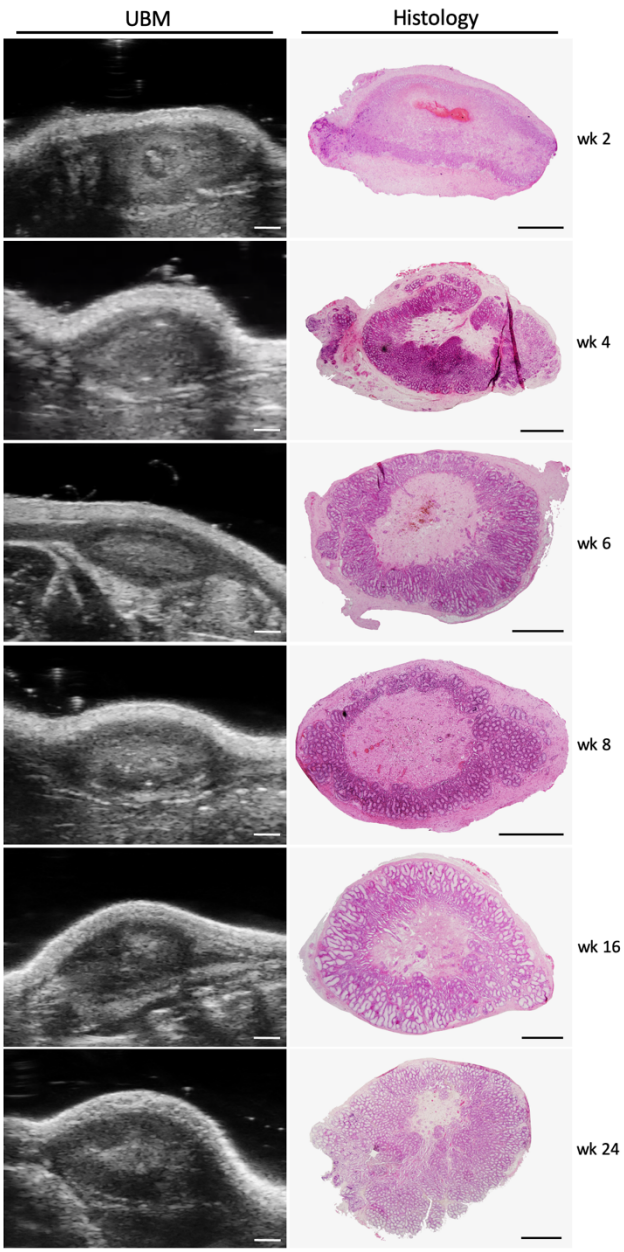

Fig. 7.4. Histological sections and their corresponding 2-D UBM images of representative cell implants at the largest section and at different time points. The fluid-filled cavities with eosinophilic content in histological sections appeared as anechoic areas in 2-D UBM images. In UBM examination, these cavities were present in 6 implants at wk 2 and were disappeared and replaced by connective tissue by wk 6. By wk 24, implants size and density of cords increased. Also, the cords transformed into tubules, containing more advanced germ cells. (Scale bar = 1 mm)

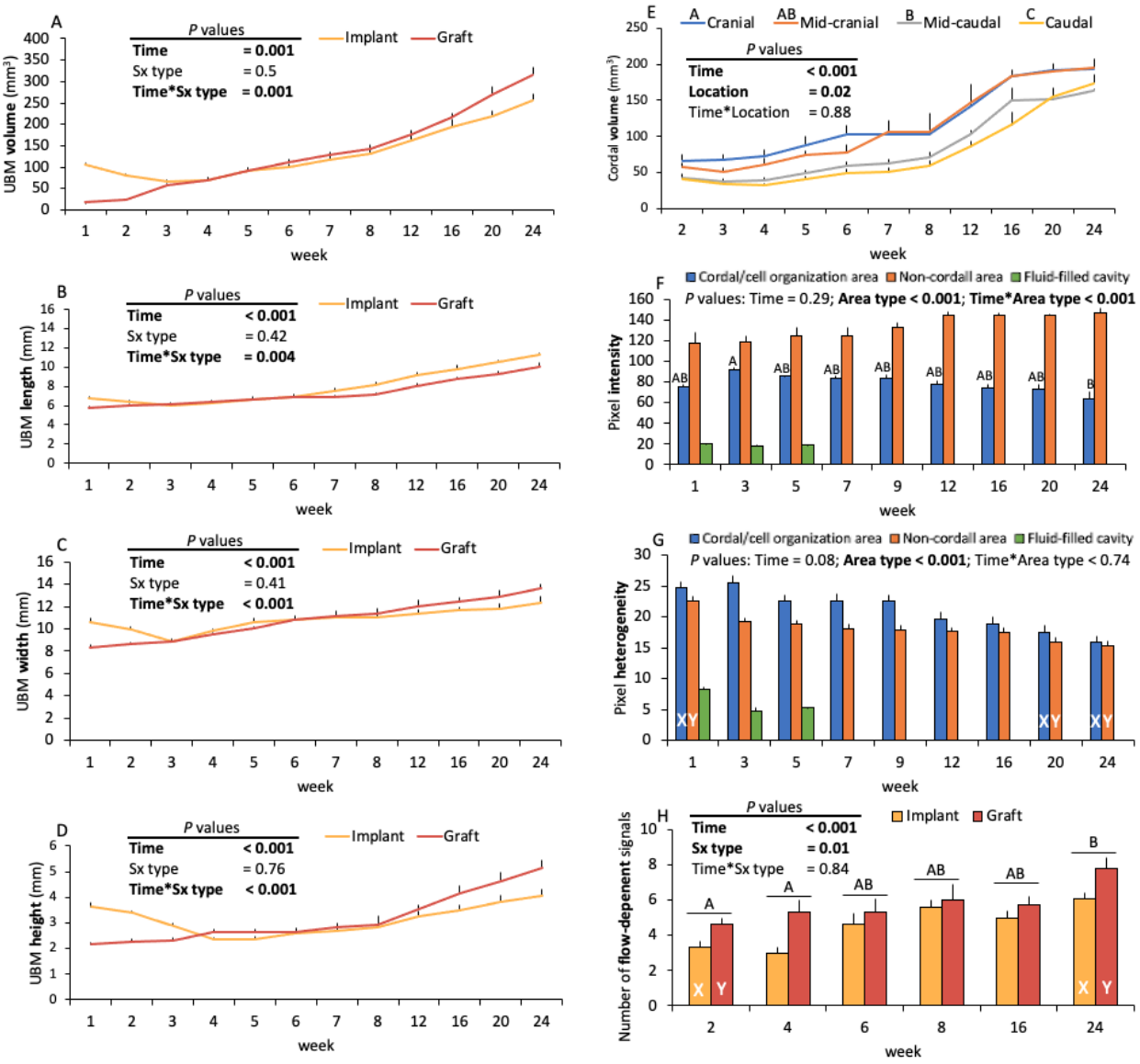

Fig. 7.5. UBM measurements (mean ± SEM) of tissue grafts and cell implants. "Sx" denotes tissue grafts or cell implants. "Location" denotes cranial, mid-cranial, mid-caudal and caudal grafting/implantation sites on the dorsal skin of recipients. "Area type" denotes cordal, non-cordal, and fluid-filled cavity area. The first and second numbers on the horizontal axis refers to examination wk of the grafts and implants, respectively (H). "A, B, and C" denote statistically significant differences between locations (E) or over time (F and H). "X and Y" denote statistically significant differences between cordal/non-cordal area (G) or tissue grafts/cell implants (H) and $P < 0.05$ was considered as significant.

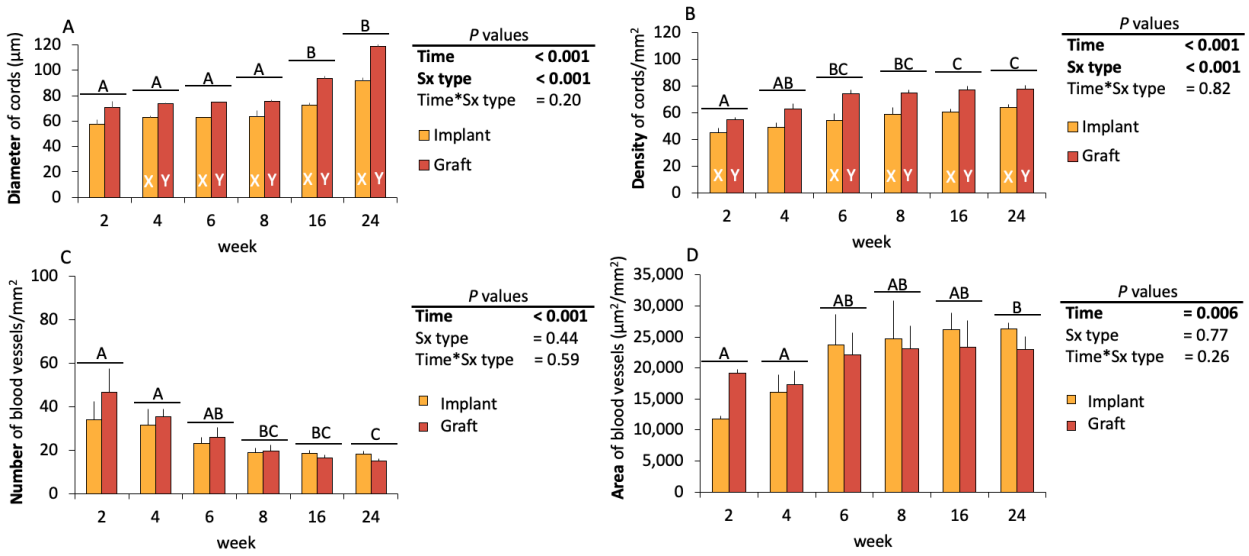

Fig. 7.6. Histological measurements (mean ± SEM) of retrieved samples. (A and B) Diameter and density of cords increased over time ($P < 0.001$ for both). Also, the diameter and density of cords in grafts were greater compared to those in implants retrieved at a later time point ($P < 0.001$). (C and D) Although in histological sections, number of blood vessels gradually decreased ($P < 0.001$), their area increased ($P = 0.006$). This may indicate over time formation of vascular anastomoses and integration of small capillaries to form larger vessels. "A and B" denote over time statistically significant differences. "X and Y" denote statistically significant differences between tissue grafts and cell implants and $P < 0.05$ was considered as significant.

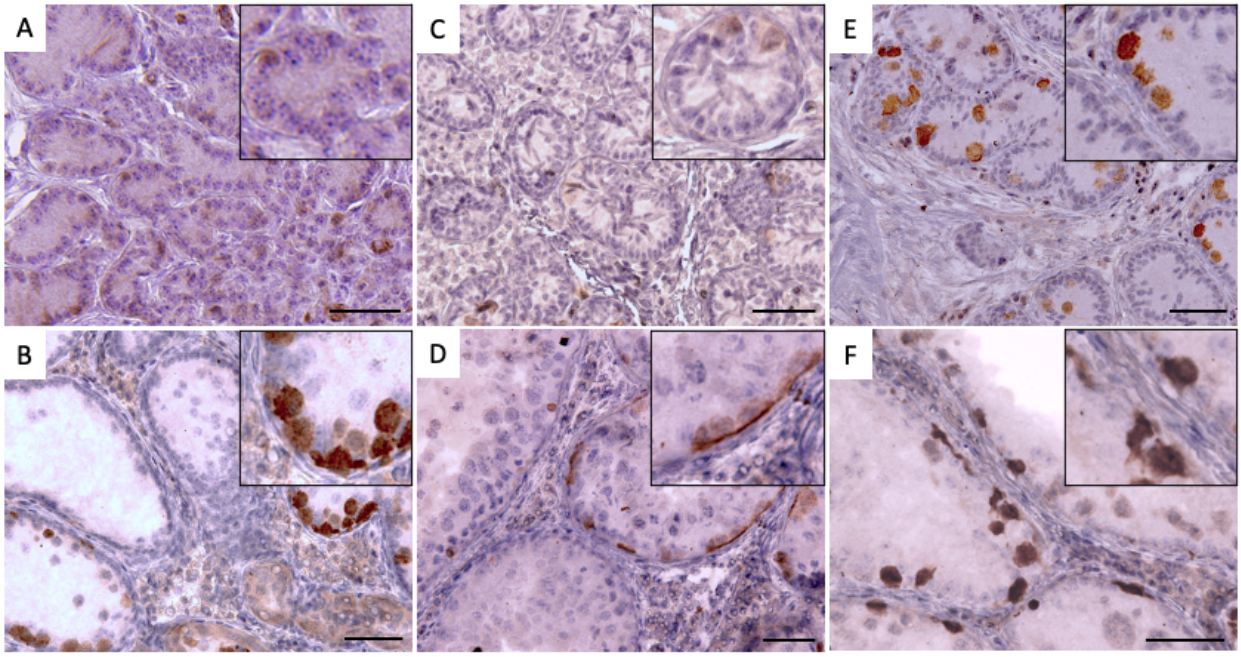

Fig. 7.7. Immunolocalization of UCH-L1 (PGP9.5) in germ cells of cell implants (A and B) and tissue grafts (C, D, E, and F). Gonocytes/spermatogonia were the most advanced germ cells in 2-wk implants (A) and grafts (C). Elongated and round spermatids were first identified in tissue grafts at wk 24 (D), while spermatocytes were the most advanced germ cells in implants at wk 24 (B). Representative tissue grafts at wk 1 (E) and wk 23 (F) were used as controls. (Scale bar = 50 µm)

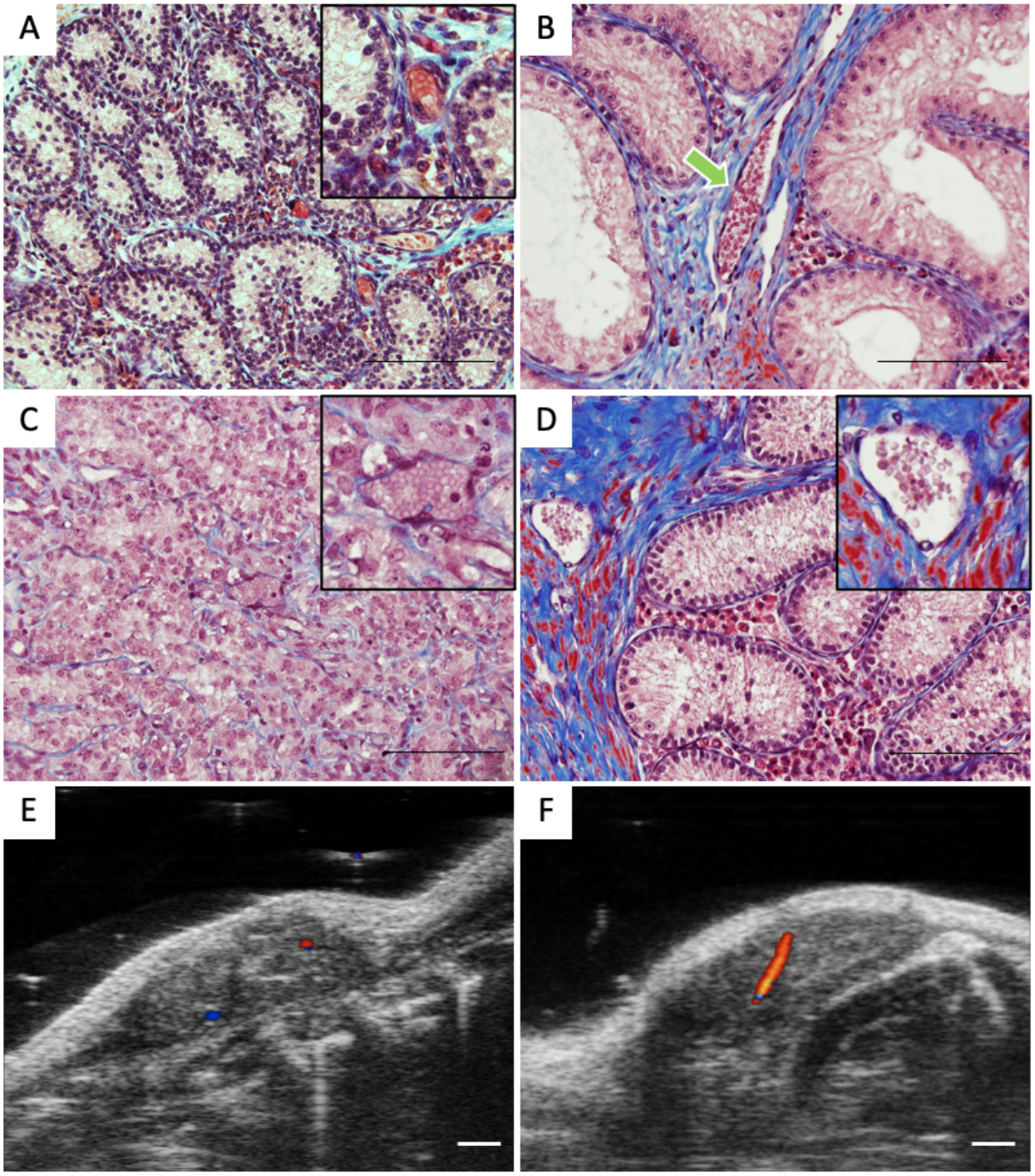

Fig. 7.8. Representative photomicrographs of grafts (A and B) and implants (C and D) at wk 2 (A and C) and 24 (B and D) as well as representative 2-D UBM images of implants at the largest section in colour Doppler mode at wk 2 (E) and 24 (F). Masson's Trichrome staining (A-D) was used to visualize the vascular wall in grafts and implants and to quantify the blood vessel number/area. Using this staining, muscle and collagen fibers appeared in red and blue colours,

respectively (A-D). The number of blood vessels in histological sections decreased over time, while their area increased, possibly due to convergence of small capillaries to form large vessels. However, flow-dependent signals increased in colour Doppler mode, indicative of greater detectability of larger vessels by UBM. Inset or green arrow shows a representative blood vessel within the graft/implant. (Scale bar = 100 μm A-D, 1 mm E-F)

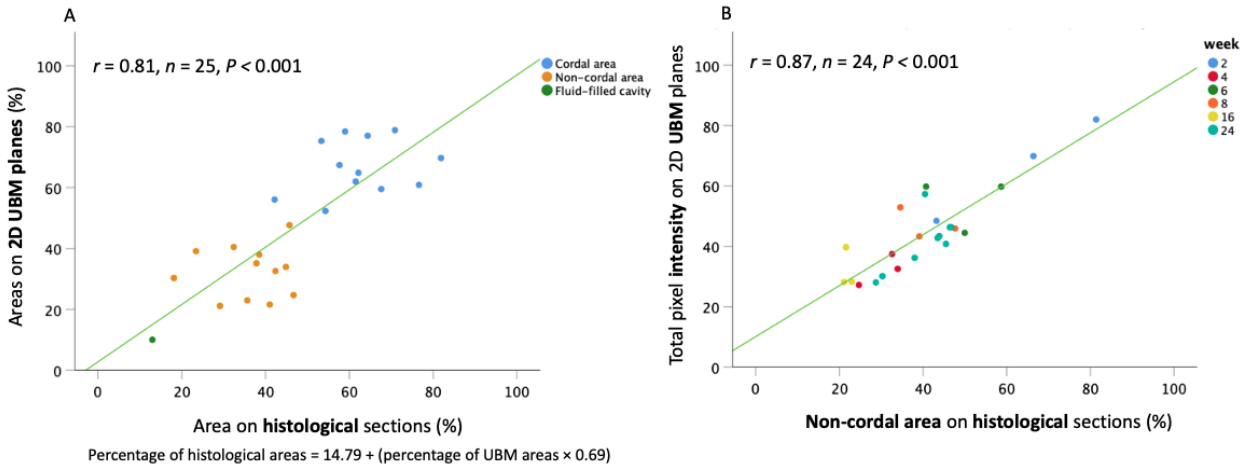

Fig. 7.9. Correlation analysis between UBM and histological attributes of retrieved samples. A positive correlation between percentage of areas in UBM and histological sections ($r = 0.81$, $n = 25$, $P < 0.001$) was indicative of UBM accuracy in predicting area of cordal, non-cordal and fluid-filled cavities (A). Similarly, positive correlation between total pixel intensity on 2-D UBM images and non-cordal area of implants ($r = 0.87$, $n = 25$, $P < 0.001$) points at UBM ability in differentiating the components within an investigated mass without the need of sample retrieval (B).

7.5. Discussion

Longitudinal changes in ectopic testis tissue grafts and cell implants were evaluated using UBM and (immuno)histology of samples retrieved over a 24-wk period. Previously, we demonstrated the feasibility of UBM and validated this approach for examination of grafts and implants in two separate studies (Awang-Junaidi *et al.* 2020; Fayaz *et al.* 2020b). Here, for the first time, we applied this repeatable monitoring approach to visualize changes in volume, dimensions, and structures of grafts and implants in a long-term study and used (immuno)histochemical analyses to support the accuracy of UBM measurements. More importantly, to demonstrate the developmental gap between the grafts and implants, we used a novel approach in our analyses, where, for the first time, we showed a developmental gap of ~4 wk between grafts and implants by comparing two sample types at various time points. Additionally, using UBM, we also revealed differences in developmental potential for *de novo* formation of seminiferous cords depending on the craniocaudal site of implantation. To our knowledge, the present study is the first to describe side-by-side and gradual histological and UBM changes in tissue grafts and cell implants over a 6-month period by obtaining samples at various time points.

As a novel imaging multimodality, UBM has been successfully used in a range of studies to visualize different structures *in vivo* and *in vitro* (Baerwald *et al.* 2009; Mircea *et al.* 2009; Greco *et al.* 2012; Pfeifer *et al.* 2012; Awang-Junaidi *et al.* 2020; Fayaz *et al.* 2020b). In female reproductive biology, due to its high accuracy, UBM has been used to study the ovarian dynamics and details in various species (Baerwald *et al*. 2009; Jaiswal *et al*. 2009; Mircea *et al.* 2009; Pfeifer *et al.* 2012, 2014). Similarly, TTX and TCAI studies require a reliable and consistent assessment methodology; however, until recently there was no standardized method for evaluation of xenogeneic testis tissue grafts and cell implants, other than their surgical retrieval and/or post-mortem histopathological analyses of samples (Honaramooz *et al.* 2002, 2007). To address this limitation, we recently performed proof-of-concept and validation studies on the use of UBM for non-invasive monitoring of grafts and implants in short-term experiments (Awang-Junaidi *et al.* 2020; Fayaz *et al.* 2020b). In the latter studies we showed the UBM reliability and accuracy for *in vivo* examination of grafts and implants.

Here, the initial decrease in dimensions and volume of implants may be explained by gradual absorption of remnant media injected along with cell aggregates, especially since dimensions and

volume of the corresponding grafts increased from wk 1 to 24. Following the initial decrease, the constant increase in implants volume/orthogonal dimensions up to wk 24 may be due to both cavity replacement with connective tissue and gradual development of cordal areas. In implants, the percentage of cordal areas on histological sections was previously shown to remain unchanged between wk 2 and 6 (Fayaz *et al.* 2020b). However, UBM cordal volume increased over time in all implantation locations. Being consistent with previous findings (Awang-Junaidi *et al.* 2020), we speculate that the greater cordal volume in more cranial implants, compared with more caudal implants, is the result of vicinity to blood supply from larger arteries such as branches of the subclavian artery and/or less cutaneous tension providing more favorable conditions for implant development. The increase in cordal volume from wk 2 to 24 is likely because of expansion of the cordal areas toward the center of implants over time (Fig. 7.5E). Additionally, positive correlations between the percentage of areas on 2-D UBM images and histological sections further supported the accuracy and reliability of UBM in predicting the cordal/non cordal areas or volumes in implants, indicating that such UBM estimations can reliably represent actual morphological changes (Fig. 7.9A). Similarly, given the hyperechoic appearance of non-cordal areas (Fayaz *et al.* 2020b), the total pixel intensity on 2-D UBM images and non-cordal areas on histological sections were positively correlated and thereby, corresponding areas can be reliably measured on 2-D UBM images (Fig. 7.9B).

The combined effects of gradual cordal development, lumen formation, and increased diameter and density of cords, may have led to the observed decreased cordal echogenicity and as such, reduced the cordal pixel intensity over time. Conversely, unchanged non-cordal pixel intensity may point to the echogenic nature of connective tissue with limited structural changes over time due to their relatively constant cellular and extra cellular matrix contents (Fig. 7.5F, 7.6A, and 7.6B). The observed changing patterns of cordal/non-cordal pixel intensities can also highlight the ability of UBM in detecting gradual cordal development and differentiating components within a mass. This finding is in agreement with previous studies where UBM was reported to be an effective tool in visualizing detailed structures such as small antral follicles, luteal tissue, and stroma of mouse and human ovaries (Baerwald *et al.* 2009; Mircea *et al*. 2009). Higher pixel heterogeneity in cordal areas compared with non-cordal areas could be possibly due to cellular organization and cordal formation leading to varying echogenic spots, all within the cordal areas. Given the echogenic nature of the connective tissue, interstitial spots within the cordal areas

contained dense connective tissue and as such, appeared as hyperechoic spots; in contrast, cordal formation spots were less echogenic, which, taken together, led to greater pixel heterogeneity in cordal areas (Fig. 7.3J-R and 7.5G).

As previously described in our preliminary study, color Doppler UBM can be effectively used to detect flow-dependent signals (Awang-Junaidi *et al.* 2020). Flow-dependent signals and blood vessels were detected as early as wk 1 in UBM images and wk 2 in histological sections, respectively, in interstitial and peripheral connective tissues. Prevalence of cellular arrangements and small capillaries near the implant boundaries, as observed during our colour Doppler examinations, may suggest that testis cells initially become attracted to areas with better access to blood vessels. Over time, the vessels further penetrated toward the center of implants. The observed pattern of vessel development from periphery to the center was also supported by histological observations.

We also found that the number of flow-dependent signals increased by 68% in grafts and 83% in implants from wk 1 to 24. Expectedly, the additional time required for cellular reorganization in implants leads to a developmental delay compared with age-matched grafts (Honaramooz *et al.* 2007; Fayaz *et al.* 2020b). To compensate for this developmental delay, we compared the implants of a given time point with grafts of an earlier time point. However, despite shifting the relative developmental stage of implants back by 2 wk, a greater number of flow-dependent signals was detected in 4-wk grafts compared with 6-wk implants. This might indicate that similar to initiation of spermatogenesis that was reported to occur at least 3 wk later in implants compared with grafts (Honaramooz *et al.* 2007), different stages of vascular development may also be delayed by 3 wk or more.

UBM did not detect the same extent of vessels as that observed in histological sections of the same samples. This is perhaps not surprising given the vast difference between the two approaches and may be partly due to the low sensitivity of colour Doppler mode in detection of weak flow-dependent signals. In histological examinations, the number of vessels decreased by 67% in grafts and 47% in implants from wk 1 to 24, which was also revealed by a negative correlation between the number of flow-dependent signals in UBM and the number of vessels in histological sections (Fig. 7.6C). However, the area occupied by these vessels (per mm^2) in the largest histological

sections increased by 20% in grafts and 123% in implants (Fig. 7.6D), indicating that small vessels converge to form large blood vessels that can be detected by UBM (Fig. 7.8).

Furthermore, the estimated physical measurements, obtained from our previously-introduced equations (Fayaz *et al.* 2020b) were all positively and strongly correlated with the actual measured values, suggesting that these equations can be used reliably in future experiments to predict the size and volume of grafts and implants.

As was described previously, cordal development commences earlier within tissue grafts, while cell implants need to undergo cellular reorganization and cord formation in the first ~2 wk following implantation (Fayaz *et al.* 2020b). Here, since diameter and density of cords in grafts were greater than those of implants at multiple time points, the developmental delay was then adjusted in analyses by comparing implants with grafts of two earlier time points. Using these comparisons, we showed that the initial developmental status of implants was not different from that of grafts obtained 4 wk earlier, indicative of ~4 wk of developmental delay for cell implants. At later time points, when the developmental gap was larger, expectedly, the diameter of cords was greater in implants; however, density of cords was still greater in grafts. This may indicate that the density of cords in grafts undergoes an exponential increase over time. Overall, grafts seemed to adapt to the new *in vivo* environment sooner and show a greater diameter and density of cords especially at later stages of the study. This phenomenon may be suggestive of an amplified developmental gap between grafts and implants at later time points and warrant further investigation.

In the present study, we observed a decrease of ~48% in the overall number of Sertoli cell-only cords and tubules, alongside an increased number of germ cell-containing cords/tubules for both grafts and implants, which point to the gradual proliferation and differentiation of germ cells. Compared with implants, grafts possessed a higher percentage of Sertoli cell-only cords/tubules. This may be indicative of greater germ cell loss in the grafts or an abundance of germ cells within the newly formed cords of implants. This was rather surprising and is likely as a result of using testis cells with a high proportion of gonocytes (~40%) for implants. The increase in gonocyte proportion was a strategy we have started to implement (Awang-Junaidi *et al.* 2020; Fayaz *et al.* 2020b) to overcome an earlier reported problem where the newly-formed cords/tubules in implants tended to contain few or no germ cells (Honaramooz *et al*. 2007; Dores and Dobrinski 2014).

However, even though a lower number of cords/tubules contained germ cells in grafts, they were more efficient at later stages in giving rise to more developed germ cells such as round and elongated spermatids. The percentage of spermatogonia-containing cords/tubules gradually decreased in both sample types, which was expected as gonocytes differentiated, leading to appearance of cords/tubules with more advanced germ cells.

We first identified spermatocytes at 16 wk in both sample types and spermatids at 24 wk in grafts but not in their corresponding implants. The absence of spermatids in cell implants by 24 wk can further highlight our proposed increase in the developmental gap between grafts and implants over time. Here, although germ cell differentiation up to the elongated spermatid stage was evident in tissue grafts by 24 wk, no sperm was found, suggesting that complete development of the grafts and implants would have required more time. This finding is in line with previous TTX studies, where fully formed sperm appeared at later time points (by ~27 wk in grafts and ~30 wk in cell implants) (Honaramooz *et al.* 2002, 2007; Abbasi and Honaramooz 2010) (Table 7.1).

Overall, UBM and histomorphometric findings in the present study suggest that UBM can be used to accurately document the long-term development of xenogeneic testis tissue grafts and cell implants. In agreement with previous reports (Dada *et al.* 2011; Schöne *et al.* 2016; Awang-Junaidi *et al.* 2020; Fayaz *et al.* 2020b), the present results are indicative of high potential of UBM in predicting the changes in sample size and structural composition. Therefore, UBM can be used independently to evaluate testis grafts and implants at various time points, which eliminates the need for frequent sample retrieval for (histo)morphometrical evaluations and, as such, reduces the number of animals required in future experiments. This is an important consideration in time-course experiments, especially where recipient animals such as immunodeficient models are being used. Also, UBM is unique in that it can provide non-invasive repeated measurements of the same samples to improve the analysis power while reducing the overall number of samples needed. Furthermore, evaluation using UBM can lead to more consistent results, which circumvents some of the potential bias caused by incomplete sample retrieval and/or distortion due to fixation process, commonly observed in histological evaluations.

In conclusion, the present study is first to reveal different developmental levels between grafting/implantation locations in recipient mice by using long-term side-by-side UBM and histomorphometric comparison of grafts and implants. In addition, for the first time, we

demonstrated accurate estimation of developmental gap between the xenogeneic tissue grafts and cell implants. The strong correlations and agreements between histology and UBM findings in the present study showed that UBM can be used independently for visualization of changes in orthogonal dimensions, volume, and structural composition of grafts/implants in both short- and long-term studies. Therefore, given the non-invasiveness and repeatability of UBM, it can be introduced as an excellent tool for longitudinal studies of testis grafts and implants with high consistency. Although this study was conducted using superficial testis grafts and implants, the same approach can potentially be applied for the study of superficial neoplastic masses in mouse models.

CHAPTER 8

GENERAL DISCUSSION AND FUTURE DIRECTIONS

8.1. General Discussion

Testis is a multifunctional organ and the prominent source for production of spermatozoa and androgens throughout the reproductive life of an individual. The dual function of spermatogenesis and steroidogenesis by the testes requires a complex structural foundation to allow signaling cascades, cell-cell interactions, and paracrine regulation within and among different testicular compartments. Despite multiple studies and tremendous progress on understanding the pathophysiology of the male reproductive system, and particularly the gonads, our knowledge of testis development and function is limited due to its structural, functional, and developmental complexities. Alternative strategies such as *in vitro* and *in vivo* culture systems have contributed significantly to exploration of unknown and complex aspects of testis formation and function. Therefore, we used these approaches to study some of the underlying factors which can possibly affect regulation of testicular cell and/or tissue development using porcine testis as donor tissue. The following paragraphs contain a brief description of general discussion of our findings in each study, as well as a general conclusion based on our overall findings.

8.1.1. In Vitro Effects of Different Media and Serum Types on Porcine Germ Cell Proliferation, Colony-Formation, Ultrastructure, and Potency

Germline stem cells are a promising source of adult stem cells with dual potential of proliferation and differentiation towards production of spermatozoa. These cells possess a range of potential applications from GCT and fertility preservation to tissue regeneration and stem cell therapy (Jiang and Short 1998a; Bai *et al.* 2018; Chen *et al.* 2020). Therefore, as demonstrated in Chapter 3, using stepwise experiments, we tested the effects of 6 different culture media (*i.e.*, DMEM, DMEM/F12, GMEM, α-MEM, RPMI and StemPro SFM) each supplemented with 3 different concentrations of FBS and/or KSR on porcine germ cell proliferation, colony-formation, ultrastructure, and expression of pluripotency markers in a long-term co-culture of germ-Somatic cells. We showed that DMEM+15% FBS could effectively increase the number of germ cells, while culture in combination of DMEM+5% FBS+10% KSR resulted in greater tendency of gonocytes to form colonies. Using TEM, we showed germ cells were floating and non-adherent in nature whose

survival largely depends on their communication to and attachments with somatic cell monolayer. We also found that most populations of germ cells in culture developed pseudopodia, enabling them to freely migrate on top of the monolayer and towards each other, thereby initially forming colonies and EBLCs at later developmental stages. Using TEM and immunofluorescence assay, we found the EBLCs to be multi-nucleated large structures surrounded by individual gonocytes. One of the exciting findings in our study was that gonocytes cultured in DMEM+15% FBS, without addition of growth factors or other supplements, spontaneously reprogrammed into primitive stages and expressed markers that are normally present in ES cells such as POU5F1, SSEA-1, NANOG, and E-cadherin. This is especially important since generation of ES cell-like cells from MGSCs typically require addition of different factors (*e.g*., growth factors or cytokines), multiple passages, or exposure of the cells to gene transcripts to induce pluripotency (Jiang and Short 1998a; Seandel *et al.* 2007; Zhang *et al.* 2013; Bai *et al.* 2018; Chen *et al.* 2020). Thus, our findings offered a facile approach to increase the number of MGSCs and were indicative of great potential of neonatal germ cells to be used as a source of adult stem cells for applications in regenerative medicine, restoration of fertility, or transgenesis.

8.1.2. Effects of Individual and Combined Growth Factor Concentrations on Porcine Germ Cell Proliferation, Colony-Formation, and Potency

As discussed earlier, numerous applications of MGSCs, including gonocytes, make them an attractive source for *in vitro* studies. Gonocytes are considered a superior source of MGSCs due to their identifiable morphology, feasibility of using cell-specific markers for their identification and isolation, and relatively greater population in the neonatal testes. Hence, in Chapter 4, using the selected base media composition in Chapter 3 we designed stepwise experiments to explore the effects of individual or combined supplementation of staple growth factors including bFGF, GDNF, and LIF on propagation, colony-formation, and expression of pluripotency markers by gonocytes. The greatest number of gonocytes were found in culture when media was supplemented with 10 ng/mL bFGF and they formed the largest colonies when media was supplemented with bFGF+100 ng/mL GDNF+1500 U/mL LIF. Also, following growth factor supplementation, resultant gonocytes and colonies expressed both germ cell- and pluripotency-specific markers (*i.e*., POU5F1, SSEA-1, NANOG, E-cadherin). It can be speculated that increased bFGF concentration in the media led to formation of a more robust somatic cell monolayer which in turn provided a

better support for germ cell survival and expansion. Similar to our findings, it has been shown that supplementation of media with combined growth factors including SCF, LIF, bFGF, IGF enhances colony formation of murine germ cells in both cell and tissue culture systems (Jeong *et al.* 2003; Kanatsu-Shinohara *et al.* 2007). Overall, the results of our study in Chapter 4 clarified unknown effects of crucial growth factors that are normally involved in *in situ* paracrine signaling on porcine gonocyte survival and proliferation. In addition, our developed culture composition could be applied for *in vitro* expansion of pluripotent germ cells and their subsequent downstream applications in cell-based therapy, transgenesis, and/or conservation of fertility potential. Given the structural and physiological similarities between human and porcine testis tissue, in particular, our results provided a strong proof-of-concept for the same potential in human germline stem cells.

8.1.3. Dedifferentiation and Trans-Differentiation Potential of Porcine Germ Cells

When located in the testis, MGSCs such as gonocytes are unipotently restricted to undergo proliferation to maintain their population or differentiation to develop more specialized germ cells. Commitment of gonocytes to establish the SSC pool and ultimately initiation of spermatogenesis is regulated by their surrounding niche and particularly their engulfing Sertoli cells. As has been shown in Chapters 3 and 4 porcine gonocytes have the remarkable feature of expressing pluripotency-determining factors when cultured *in vitro*. This unique characteristic of gonocytes is thought to be the result of their release from *in situ* restrictions, which spontaneously induce them to return to primitive stages. In Chapter 5, we investigated *in vitro* trans-differentiation of these cells into somatic cells derivatives of three germinal layers (*i.e*., endoderm, mesoderm, and ectoderm) and also assessed the pluripotency of dedifferentiated gonocytes using an *in vivo* implantation assay. Using differentiation media, specifically designed to direct the differentiation of stem cells into osteogenic pathway, we showed that EBLCs formed after ~14 days of culture transformed into hydroxyapatite deposition sites, confirmed by Alizarin Red S staining. We also showed that gonocytes and EBLCs exposed to tri-lineage differentiation media gradually lost expression of gonocyte-specific marker (DBA), while a fraction of germ cells displayed stronger expression of lineage-specific markers (*i.e*., SOX17 and AFP for endoderm, Brachyury and ASM for mesoderm, and OTX2 and GFAP for ectoderm) both at gene and protein expression levels. Expression of these markers has been previously shown to be crucial for normal development of germinal layers during embryogenesis (Eng 1985; Babai *et al.* 1990; Ang *et al.* 1994; Abe *et al.*

1996; de Jong *et al.* 2008; Bernardo *et al.* 2011; Mortensen *et al.* 2015). This was indicative of gradual gonocyte conversion into new population of cells with biomolecular properties of three germinal layers. A remarkable finding in this study was development of tumour-like formations following implantation of dedifferentiated gonocytes and colonies. These formations showed circular/oval patterns and melanin pigmentation. The observed patterns represented similar appearance as nests of melanocytes. Additionally, bundles resembling peripheral nerves were also observed within these formations. Furthermore, the formations appeared positive for expression of lineage-specific markers including AFP, ASM, and GFAP at localized foci, which might be indicative of their differentiation into cell derivatives from three germinal layers. Our observations in this study confirmed the potential of gonocytes to convert into a pluripotent state previously shown in Chapters 3 and 4. Importantly, the study in this chapter has been the first to induce tri-lineage differentiation in dedifferentiated porcine MGSCs in a shorter period of time, using primary cultures and without passaging the cells, which otherwise would have posed unwanted changes to their *in vitro* niche and biochemical properties. These changes would have possibly generated confounding factors and negative effects on their self-renewal or differentiation properties (Goel *et al.* 2009). Possible application of germ cell derived-pluripotent stem cells eliminates the ethical concerns associated with ES cells and biosafety risks of iPS cells where viral vectors are required for their derivation (Chen *et al.* 2020). Dedifferentiation and trans-differentiation potential of porcine gonocytes are outstanding findings in that they open windows of opportunity for further research on their applicability in clinical settings.

8.1.4. Validation of UBM for In Vivo Examination of Testis Tissue Grafts and Cell Implants

Beside *in vitro* culture systems*, in vivo* testis tissue and cell culture, known as TTX and TCAI, respectively, are invaluable models which provide an easy access in a mouse model to study various aspects of spermatogenesis, steroidogenesis, and testis development. Testis tissue and isolated testis cells retain their developmental potential even after being separated from the parenchyma and are able to ultimately generate spermatozoa when grafted/implanted into the subcutaneous tissue of immunodeficient recipient mice (Honaramooz *et al.* 2002; Honaramooz *et al.* 2007; Honaramooz 2014). Studies using TTX and TCAI models has so far applied surgical recovery of the grafts/implants as the endpoint for examination of the developmental status of the samples. This is a limiting factor since the number of examination time points for sample

development depends on the number of grafts/implants. Additionally, post-retrieval fixation and processing pose unwanted changes to the samples such as tissue shrinkage, and in turn will lead to underestimation of actual dimension measurements. Not to mention, multiple surgical procedures on immunodeficient mice increases the risk of infection or post-surgical complications. UBM has been applied in different research studies and clinical fields, which overall point at its accuracy and reliability in real-time displaying detailed tissue structures including reproductive tissues (Pavlin *et al.* 1992; Turnbull *et al.* 1995; Foster *et al.* 2002; Cheung *et al.* 2005; Nuccitelli *et al.* 2006; Spurney *et al.* 2006; He *et al.* 2007; Baerwald *et al.* 2009; Snyder *et al.* 2009; Stokvis *et al.* 2009; Jaiswal *et al.* 2009; Mircea *et al.* 2009; Buckley and Stokes 2011; Hibino *et al.* 2011; Pavlin and Foster 2012; Pfeifer *et al.* 2012; Jaffré *et al.* 2012; Cervantes *et al.* 2013). Therefore, in an attempt to develop an alternative non-invasive and repeatable approach for assessment of grafts/implants in Chapter 5, we compared and correlated a number of UBM attributes obtained from UBM examination of the samples prior to their retrieval with their histomorphometric measurements obtained post-retrieval. We showed strong positive correlations between UBM and histological attributes of the samples such as dimensions and volume and revealed UBM accuracy in showing detailed structural changes in the samples through different echotextures within the samples. The correlations between pre- and post-retrieval measurements showed that UBM was a consistent, accurate, and non-invasive alternative to surgical retrieval of tissue grafts and cell implants to monitor their development over time. Application of UBM could reduce the fatality among the recipient mice, which in turn would reduce the number of animals required for studies with similar applications.

8.1.5. Long-term Examination of Tissue Grafts and Cell Implants Using UBM

UBM has shown great promise as a non-invasive examination tool in different fields including male reproductive biology (Huang *et al.* 2021). Also, given the accuracy of UBM in showing detailed structural and 3-D changes in both testis tissue grafts and cell implants in Chapter 5, we designed and conducted a longitudinal study (Chapter 6) to repeatedly apply this non-invasive monitoring tool for evaluation of grafts and implants in immunodeficient recipient mice. In this study, we maintained the grafts and implants in recipients for 24 weeks, during which each sample was examined every week for the first 2 months followed by monthly examinations up to the end of the study. The remarkable findings in this study included feasibility of displaying long-term

changes in graft/implant volume, dimension, and structure, a 4-week developmental gap between two sample types, and greater support of the cranial grafting/implantation sites for tissue development. The developmental gap between grafts and implants was expectedly the result of the time required for re-organization of the testis cells in implants. Since tissue grafts normally undergo luminal formation, germ cell differentiation, and spermatogenesis immediately following grafting, they possessed a relatively more developed structure compared to their implant counterparts. Cells within implants, on the other hand, undergo extensive re-arrangements to first re-organise themselves, leading to initial formation of testicular cords, which expectedly set their developmental status behind the grafts. Based on the presence of different germ cell types, cordal development, and (immuno)histochemical properties of grafts/implants, here we reported a 4-week developmental gap between two sample types. Another remarkable finding in the present study was varying developmental potential between the graft/implants based on their craniocaudal location. Samples located cranially showed relatively greater development, which was possibly due to the superior blood supply (*i.e*., branches of subclavian artery) or less cutaneous tension in cranial compared to more caudal locations. We showed that UBM could be used independently for examination of changes in orthogonal dimensions, volume, and structure of samples in short- and long-term studies, which is also in agreement with previous reports (Dada *et al.* 2011; Schöne *et al.* 2016; Awang-Junaidi *et al.* 2020). Taken together, this study has been the first to utilize UBM for longitudinal evaluation of grafts/implants showing possible applicability to examine and monitor diverse range of superficial structures including neoplastic masses.

8.2. Future Directions

8.2.1. Manipulation of Culture Conditions to Enhance Proliferation of Gonocytes

The developed culture conditions in this thesis (Chapters 3 and 4) can be further manipulated by supplementation of different growth factors or various combinations of serum/serum replacements to further enhance the proliferation of germ cells or possibly monitor alteration in their *in vitro* behavior. These changes could include supplementation of the cultures with different concentrations of FBS and KSR at different time points (*e.g.*, week 1, 2, 3) and/or supplementation of media with additional growth factors which was not investigated in this thesis (*e.g.,* IGF, SCF, RA, FGF-9, EGF) followed by daily or weekly examination to investigate any possible change in gonocyte proliferation, colony-formation, or potency. The effects of media composition could also

be monitored using live-cell imaging and ultrastructural analysis by TEM to detect possible alterations in development of cytoplasmic extensions by gonocytes, their migratory behavior, or gonocyte/colony structure. In addition to foregoing sera sources and cytokines, culture media could be supplemented with hormones (*e.g.*, LH, FSH, testosterone, DHT, or progesterone) or additives (*e.g.*, proteins, amino acids, or vitamins) to possibly enhance gonocyte survival and proliferation. Since germ cells have been occasionally reported to become overwhelmed by excessive proliferation of somatic cells, they could be co-cultured with mitotically inactivated cells as a substitute for endogenous testis somatic cells (Nagano *et al.* 1998; Wei *et al.* 2016).

8.2.2. Assessment of Pluripotency State of Cultured Germ Cells Following Injection into Immunodeficient Recipients using UBM

As we showed in Chapter 5, once cultured, neonatal porcine gonocytes convert into a population of cells with similar biomolecular properties as ES cells and following implantation into the subcutaneous tissue of immunodeficient mice, the cells and colonies generate tumour-like formations. UBM could be applied for examination of orthogonal dimensions and structural composition of the formations in future studies. Notably, UBM (*i.e.*, Colour Doppler mode) could be advantageous in identification of neovessel formation within these neoplastic masses since their formation and development expectedly require a high blood supply. Given the accuracy of UBM in providing detailed structure of testis grafts and implants, this monitoring method could be used at different examination time points (weekly or monthly) following implantation while the recipients are maintained for a longer period of time (>2 months) to allow the implants to undergo further development.

8.2.3. Non-invasive Examination of Gonad and Accessory Sex Gland Development in Mice using UBM

Application of UBM in reproductive research has been limited to visualization of female gonads or ovarian follicular dynamics in laboratory animals (Jaiswal *et al.* 2009; Mircea *et al.* 2009; Pfeifer *et al.* 2012, 2014; Cervantes *et al.* 2013) and assessment of spermatogenic function in male mice following busulfan treatment (Huang *et al.* 2021). However, no study has utilized this monitoring approach for examination of male gonadal development and accessory sex glands from prenatal to maturity. Given the accuracy of this technique in displaying slight structural differences in different locations of the grafts and implants, shown and discussed in the present thesis, the

same approach could be used to study *in situ* testis and accessory sex gland development within a mouse model.

REFERENCES

Abbasi S., and Honaramooz A. (2010). Effects of recipient mouse strain, sex and gonadal status on the outcome of testis tissue xenografting. *Reprod. Fertil. Dev.* **22**, 1279–1286. doi:10.1071/rd10084

Abbasi S., and Honaramooz A. (2011a). Salvaging Genetic Material from Endangered Species: Xenografting of Testis Tissue from Immature Bison and Deer Donors into Recipient Mice Results in Complete Spermatogenesis. *Biol. Reprod.* **85**, 174. doi:10.1093/biolreprod/85.s1.174

Abbasi S., and Honaramooz A. (2011b). The number of grafted fragments affects the outcome of testis tissue xenografting from piglets into recipient mice. *Vet. Med. Int.* **2011**, 1–7. doi:10.4061/2011/686570

Abbasi S., and Honaramooz A. (2011c). Xenografting of testis tissue from bison calf donors into recipient mice as a strategy for salvaging genetic material. *Theriogenology* **76**, 607–614. doi:10.1016/j.theriogenology.2011.03.011

Abbasi S., and Honaramooz A. (2012). Feasibility of salvaging genetic potential of post-mortem fawns: Production of sperm in testis tissue xenografts from immature donor white-tailed deer (Odocoileus virginianus) in recipient mice. *Anim. Reprod. Sci.* **135**, 47–52. doi:10.1016/j.anireprosci.2012.09.007

Abe K., Niwa H., Iwase K., Takiguchi M., Mori M., Abé S.-I., Abe K., and Yamamura K.-I. (1996). Endoderm-specific gene expression in embryonic stem cells differentiated to embryoid bodies. *Exp. Cell Res.* **229**, 27–34.

Abel M. H., Baker P. J., Charlton H. M., Monteiro A., Verhoeven G., De Gendt K., Guillou F., and O'Shaughnessy P. J. (2008). Spermatogenesis and sertoli cell activity in mice lacking Sertoli cell receptors for follicle-stimulating hormone and androgen. *Endocrinology* **149**, 3279–3285.

Abo-Elmaksoud A., and Sinowatz F. (2005). Expression and localization of growth factors and their receptors in the mammalian testis. Part I: Fibroblast growth factors and insulin-like growth factors. *Anatomia* **34**, 319–334.

Abrishami M., Abbasi S., and Honaramooz A. (2010). The effect of donor age on progression of spermatogenesis in canine testicular tissue after xenografting into immunodeficient mice. *Theriogenology* **73**, 512–522.

Abrishami M., Anzar M., Yang Y., and Honaramooz A. (2010). Cryopreservation of immature porcine testis tissue to maintain its developmental potential after xenografting into recipient mice. *Theriogenology* **73**, 86–96.

Achermann J. C., and Hughes I. A. (2011). Chapter 23 - Disorders of Sex Development. 'Williams Textbook of Endocrinology (Twelfth Edition)'. (Eds S Melmed, KS Polonsky, PR Larsen and HM Kronenberg) pp. 868–934. (W.B. Saunders: Philadelphia) doi:https://doi.org/10.1016/B978-1-4377-0324-5.00023-7

Adams I. R., and McLaren A. (2002). Sexually dimorphic development of mouse primordial germ cells: switching from oogenesis to spermatogenesis. *Development* **129**, 1155–1164.

Adham I. M., Emmen J. M. A., and Engel W. (2000). The role of the testicular factor INSL3 in establishing the gonadal position. *Mol. Cell. Endocrinol.* **160**, 11–16. doi:10.1016/S0303-7207(99)00188-4

Aeckerle N., Dressel R., and Behr R. (2013). Grafting of neonatal marmoset monkey testicular single-cell suspensions into immunodeficient mice leads to ex situ testicular cord neomorphogenesis. *Cells Tissues Organs* **198**, 209–220. doi:10.1159/000355339

Airaksinen M. S., and Saarma M. (2002). The GDNF family: signalling, biological functions and therapeutic value. *Nat. Rev. Neurosci.* **3**, 383–394.

Akiyama Y., Komiyama M., Miyata H., Yagoto M., Ashizawa T., Iizuka A., Oshita C., Kume A., Nogami M., and Ito I. (2014). Novel cancer-testis antigen expression on glioma cell lines derived from high-grade glioma patients. *Oncol. Rep.* **31**, 1683–1690.

Albrecht K. H., and Eicher E. M. (2001). Evidence that Sry is expressed in pre-Sertoli cells and Sertoli and granulosa cells have a common precursor. *Dev. Biol.* **240**, 92–107. doi:10.1006/dbio.2001.0438

Almeida F. F. L., Leal M. C., and França L. R. (2006). Testis morphometry, duration of spermatogenesis, and spermatogenic efficiency in the wild boar (Sus scrofa scrofa). *Biol. Reprod.* **75**, 792–799.

Almunia J., Nakamura K., Murakami M., Takashima S., and Takasu M. (2018). Characterization of domestic pig spermatogenesis using spermatogonial stem cell markers in the early months of life. *Theriogenology* **107**, 154–161. doi:10.1016/j.theriogenology.2017.10.041

Alves-Lopes J. P., Söder O., and Stukenborg J.-B. (2017). Testicular organoid generation by a novel in vitro three-layer gradient system. *Biomaterials* **130**, 76–89.

Ang S.-L., Conlon R. A., Jin O., and Rossant J. (1994). Positive and negative signals from mesoderm regulate the expression of mouse Otx2 in ectoderm explants. *Development* **120**, 2979–2989.

Angelin B., Larsson T. E., and Rudling M. (2012). Circulating fibroblast growth factors as metabolic regulators—a critical appraisal. *Cell Metab.* **16**, 693–705.

Aoi T., Yae K., Nakagawa M., Ichisaka T., Okita K., Takahashi K., Chiba T., and Yamanaka S. (2008). Generation of pluripotent stem cells from adult mouse liver and stomach cells. *Science* **321**, 699–702.

Aoshima K., Baba A., Makino Y., and Okada Y. (2013). Establishment of Alternative Culture Method for Spermatogonial Stem Cells Using Knockout Serum Replacement. *PLoS One* **8**, 1–8. doi:10.1371/journal.pone.0077715

Aponte P. M. (2015). Spermatogonial stem cells: Current biotechnological advances in reproduction and regenerative medicine. *World J. Stem Cells* **7**, 669.

Aponte P. M., Soda T., Teerds K. J., Mizrak S. C., van de Kant H. J. G., and de Rooij D. G. (2008). Propagation of bovine spermatogonial stem cells in vitro. *Reproduction* **136**, 543–557.

Apte M. V, Haber P. S., Applegate T. L., Norton I. D., McCaughan G. W., Korsten M. A., Pirola R. C., and Wilson J. S. (1998). Periacinar stellate shaped cells in rat pancreas: identification, isolation, and culture. *Gut* **43**, 128–133.

Ara T., Nakamura Y., Egawa T., Sugiyama T., Abe K., Kishimoto T., Matsui Y., and Nagasawa T. (2003). Impaired colonization of the gonads by primordial germ cells in mice lacking a chemokine, stromal cell-derived factor-1 (SDF-1). *Proc. Natl. Acad. Sci.* **100**, 5319–5323.

Arregui L., and Dobrinski I. (2014). Xenografting of testicular tissue pieces: 12 years of an in vivo spermatogenesis system. *Reproduction* **148**, 72–84. doi:10.1530/REP-14-0249

Arregui L., Dobrinski I., and Roldan E. R. S. (2014). Germ cell survival and differentiation after xenotransplantation of testis tissue from three endangered species: Iberian lynx (Lynx pardinus), Cuvier's gazelle (Gazella cuvieri) and Mohor gazelle (G. dama mhorr). *Reprod. Fertil. Dev.* **26**, 817–826.

Arregui L., Rathi R., Megee S. O., Honaramooz A., Gomendio M., Roldan E. R. S., and Dobrinski I. (2008). Xenografting of sheep testis tissue and isolated cells as a model for preservation of genetic material from endangered ungulates. *Reproduction* **136**, 85–93. doi:10.1530/REP-07-

0433
Arregui L., Rathi R., Zeng W., Honaramooz A., Gomendio M., Roldan E. R. S., and Dobrinski I. (2008). Xenografting of adult mammalian testis tissue. *Anim. Reprod. Sci.* **106**, 65–76. doi:10.1016/j.anireprosci.2007.03.026
Ashman L. K., Cambareri A. C., To L. B., Levinsky R. J., and Juttner C. A. (1991). Expression of the YB5. B8 antigen (c-kit proto-oncogene product) in normal human bone marrow. **78**, 30–37.
Aubry F., Satie A., Rioux-Leclercq N., Rajpert-De Meyts E., Spagnoli G. C., Chomez P., De Backer O., Jégou B., and Samson M. (2001). MAGE-A4, a germ cell specific marker, is expressed differentially in testicular tumors. *Cancer Interdiscip. Int. J. Am. Cancer Soc.* **92**, 2778–2785.
Awang-Junaidi A. H., and Honaramooz A. (2018). Optimization of culture conditions for short-term maintenance, proliferation, and colony formation of porcine gonocytes. *J. Anim. Sci. Biotechnol.* **9**, 1–13. doi:10.1186/s40104-017-0222-0
Awang-Junaidi A. H., Singh J., and Honaramooz A. (2019). Effect of multiple factors on regeneration of testis tissue after ectopic implantation of porcine testis cell aggregates in mice: Improved outcomes consistency and in situ monitoring. *Reprod. Fertil. Dev.* **32**, 594–609.
Awang-Junaidi A. H., Singh J., and Honaramooz A. (2020). Regeneration of testis tissue after ectopic implantation of porcine testis cell aggregates in mice: improved consistency of outcomes and in situ monitoring. *Reprod. Fertil. Dev.* **32**, 594–609. doi:10.1071/rd19043
Awang-Junaidi A. H. (2019). In vitro and in vivo culture systems for development of porcine testis cells and tissue. University of Saskatchewan.
Awang-Junaidi A. H., Fayaz M. A., Kawamura E., Sobchishin L., MacPhee D., and Honaramooz A. (2020). Live-cell imaging and ultrastructural analysis reveal remarkable features of cultured porcine gonocytes. *Cell Tissue Res.* **381**, 361–377. doi:https://doi.org/10.1007/s00441-020-03218-5
Azizi H., Asgari B., and Skutella T. (2019). Pluripotency potential of embryonic stem cell-like cells derived from mouse testis. *Cell J.* **21**, 281–289.
Azizi H., Conrad S., Hinz U., Asgari B., Nanus D., Peterziel H., Hajizadeh Moghaddam A., Baharvand H., and Skutella T. (2016). Derivation of pluripotent cells from mouse SSCs seems to be age dependent. *Stem Cells Int.* **2016**, 1–13.
Azizi H., Skutella T., and Shahverdi A. (2017). Generation of mouse spermatogonial stem-cell-colonies in a non-adherent culture. *Cell J.* **19**, 238–249.
Baba S., Heike T., Umeda K., Iwasa T., Kaichi S., Hiraumi Y., Doi H., Yoshimoto M., Kanatsu-Shinohara M., and Shinohara T. (2007). Generation of cardiac and endothelial cells from neonatal mouse testis-derived multipotent germline stem cells. *Stem Cells* **25**, 1375–1383.
Babai F., Musevi-Aghdam J., Schurch W., Royal A., and Gabbiani G. (1990). Coexpression of α-sarcomeric actin, α-smooth muscle actin and desmin during myogenesis in rat and mouse embryos I. Skeletal muscle. *Differentiation* **44**, 132–142.
Baerwald A., Dauk S., Kanthan R., and Singh J. (2009). Use of ultrasound biomicroscopy to image human ovaries in vitro. *Ultrasound Obstet. Gynecol.* **34**, 201–207. doi:10.1002/uog.6438
Bagheri-Fam S., Sim H., Bernard P., Jayakody I., Taketo M. M., Scherer G., and Harley V. R. (2008). Loss of Fgfr2 leads to partial XY sex reversal. *Dev. Biol.* **314**, 71–83. doi:10.1016/j.ydbio.2007.11.010
Bai Y., Zhu C., Feng M., Wei H., Li L., Tian X., Zhao Z., Liu S., Ma N., and Zhang X. (2018). Previously claimed male germline stem cells from porcine testis are actually progenitor

Leydig cells. *Stem Cell Res. Ther.* **9**, 1–15.
Ballow D. J., Xin Y., Choi Y., Pangas S. A., and Rajkovic A. (2006). Sohlh2 is a germ cell-specific bHLH transcription factor. *Gene Expr. patterns* **6**, 1014–1018.
Barker D. J. P. (1990). The fetal and infant origins of adult disease. *Br. Med. J.* **301**, 1111. doi:10.1136/bmj.301.6761.1111
Barresi V., Ieni A., Branca G., and Tuccari G. (2014). Brachyury: a diagnostic marker for the differential diagnosis of chordoma and hemangioblastoma versus neoplastic histological mimickers. *Dis. Markers* **2014**, 1–7.
Basciani S., De Luca G., Dolci S., Brama M., Arizzi M., Mariani S., Rosano G., Spera G., and Gnessi L. (2008). Platelet-derived growth factor receptor β-subtype regulates proliferation and migration of gonocytes. *Endocrinology* **149**, 6226–6235.
Basciani S., Mariani S., Spera G., and Gnessi L. (2010). Role of platelet-derived growth factors in the testis. *Endocr. Rev.* **31**, 916–939.
Bassols A., Costa C., Eckersall P. D., Osada J., Sabrià J., and Tibau J. (2014). The pig as an animal model for human pathologies: A proteomics perspective. *Proteomics Clin Appl.* **8**, 715–731. doi:10.1002/prca.201300099
Beby F., and Lamonerie T. (2013). The homeobox gene Otx2 in development and disease. *Exp. Eye Res.* **111**, 9–16.
Bellve A. R., Cavicchia J. C., Millette C. F., O'brien D. A., Bhatnagar Y. M., and Dym M. (1977). Spermatogenic cells of the prepuberal mouse: isolation and morphological characterization. *J. Cell Biol.* **74**, 68–85.
Ben-Porath I., Thomson M. W., Carey V. J., Ge R., Bell G. W., Regev A., and Weinberg R. A. (2008). An embryonic stem cell–like gene expression signature in poorly differentiated aggressive human tumors. *Nat. Genet.* **40**, 499–507.
Bendel-Stenzel M. R., Gomperts M., Anderson R., Heasman J., and Wylie C. (2000). The role of cadherins during primordial germ cell migration and early gonad formation in the mouse. *Mech. Dev.* **91**, 143–152.
Berensztein E. B., Sciara M. I., Rivarola M. A., and Belgorosky A. (2002). Apoptosis and proliferation of human testicular somatic and germ cells during prepuberty: high rate of testicular growth in newborns mediated by decreased apoptosis. *J. Clin. Endocrinol. Metab.* **87**, 5113–5118.
Berger T., Mahone J. P., Svoboda G. S., Metz K. W., and Clegg E. D. (1980). Sexual maturation of boars and growth of swine exposed to extended photoperiod during decreasing natural photoperiod. *J. Anim. Sci.* **51**, 672–678.
Bernardo A. S., Faial T., Gardner L., Niakan K. K., Ortmann D., Senner C. E., Callery E. M., Trotter M. W., Hemberger M., and Smith J. C. (2011). BRACHYURY and CDX2 mediate BMP-induced differentiation of human and mouse pluripotent stem cells into embryonic and extraembryonic lineages. *Cell Stem Cell* **9**, 144–155.
Besmer P., Manova K., Duttlinger R., Huang E. J., Packer A., Gyssler C., and Bachvarova R. F. (1993). The kit-ligand (steel factor) and its receptor c-kit/W: pleiotropic roles in gametogenesis and melanogenesis. *Development* **119**, 125–137.
Birk O. S., Casiano D. E., Wassif C. A., Cogliati T., Zhao L., Zhao Y., Grinberg A., Huang S., Kreidberg J. A., and Parker K. L. (2000). The LIM homeobox gene Lhx9 is essential for mouse gonad formation. *Nature* **403**, 909–913.
Blash S., Melican D., and Gavin W. (2000). Cryopreservation of epididymal sperm obtained at necropsy from goats. *Theriogenology* **54**, 899–905. doi:10.1016/S0093-691X(00)00400-3

Bogatcheva N. V, Truong A., Feng S., Engel W., Adham I. M., and Agoulnik A. I. (2003). GREAT/LGR8 is the only receptor for insulin-like 3 peptide. *Mol. Endocrinol.* **17**, 2639–2646.

Boitani C., Di Persio S., Esposito V., and Vicini E. (2016). Spermatogonial cells: mouse, monkey and man comparison. In 'Seminars in cell & developmental biology', pp. 79–88. (Elsevier)

Bojnordi M. N., Movahedin M., Tiraihi T., Javan M., and Hamidabadi H. G. (2014). Oligoprogenitor cells derived from spermatogonia stem cells improve remyelination in demyelination model. *Mol. Biotechnol.* **56**, 387–393.

Borland K., Mita M., Oppenheimer C. L., Blinderman L. A., Massague J., Hall P. F., and Czech M. P. (1984). The actions of insulin-like growth factors I and II on cultured Sertoli cells. *Endocrinology* **114**, 240–246.

Bostwick D. G. (2006). 'Chapter 13 - Immunohistology of the prostate, bladder, testis and kidney.' (DJ Dabbs, Ed.). (Churchill Livingstone)

Bousfield G. R., Jia L., and Ward D. N. (2006). Knobil and Neill's Physiology of Reproduction. *Gonadotropins Chem. Biosynth.* 1581–1634.

Bowles J., Knight D., Smith C., Wilhelm D., Richman J., Mamiya S., Yashiro K., Chawengsaksophak K., Wilson M. J., Rossant J., Hamada H., and Koopman P. (2006). Retinoid signaling determines germ cell fate in mice. *Science* **312**, 596–600. doi:10.1126/science.1125691

Bowles J., and Koopman P. (2010). Sex determination in mammalian germ cells: Extrinsic versus intrinsic factors. *Reproduction* **17**, 427–432. doi:10.1530/REP-10-0075

Boyl P. P., Signore M., Acampora D., Martinez-Barbera J. P., Ilengo C., Annino A., Corte G., and Simeone A. (2001). Forebrain and midbrain development requires epiblast-restricted Otx2 translational control mediated by its 3′ UTR. *Development* **128**, 2989–3000.

Bremner W. J., Millar M. R., Sharpe R. M., and Saunders P. T. (1994). Immunohistochemical localization of androgen receptors in the rat testis: evidence for stage-dependent expression and regulation by androgens. *Endocrinology* **135**, 1227–1234.

Brinster R. L. (2002). Germline stem cell transplantation and transgenesis. *Science* **296**, 2174–2176. doi:10.1126/science.1071607

Brinster R. L., and Avarbock M. R. (1994). Germline transmission of donor haplotype following spermatogonial transplantation. *Proc. Natl. Acad. Sci. U. S. A.* **91**, 11303–11307.

Brinster C. J., Ryu B.-Y., Avarbock M. R., Karagenc L., Brinster R. L., and Orwig K. E. (2003). Restoration of fertility by germ cell transplantation requires effective recipient preparation. *Biol. Reprod.* **69**, 412–420. doi:10.1095/biolreprod.103.016519

Brinster R. L., and Zimmermann J. W. (1994). Spermatogenesis following male germ-cell transplantation. *Proc. Natl. Acad. Sci. U. S. A.* **22**, 11298–11302. doi:10.1073/pnas.91.24.11298

Brown M. S., Kovanen P. T., and Golstein J. L. (1979). Receptor-mediated uptake of lipoprotein-cholesterol and its utilization for steroid synthesis in the adrenal cortex. In 'Proceedings of the 1978 Laurentian Hormone Conference', pp. 215–257. (Elsevier)

Buageaw A., Sukhwani M., Ben-Yehudah A., Ehmcke J., Rawe V. Y., Pholpramool C., Orwig K. E., and Schlatt S. (2005). GDNF family receptor alpha1 phenotype of spermatogonial stem cells in immature mouse testes. *Biol. Reprod.* **73**, 1011–1016.

Buckley C. L., and Stokes A. J. (2011). Corin-deficient W-sh mice poorly tolerate increased cardiac afterload. *Regul. Pept.* **172**, 44–50. doi:10.1016/j.regpep.2011.08.006

Buehr M., Gu S., and McLaren A. (1993). Mesonephric contribution to testis differentiation in the

fetal mouse. *Development* **117**, 273–281.
Bullejos M., and Koopman P. (2001). Spatially dynamic expression of Sry in mouse genital ridges. *Dev. Dyn.* **221**, 201–205. doi:10.1002/dvdy.1134
Burgos M. H., and Fawcett D. W. (1955). Studies on the fine structure of the mammalian testis: I. Differentiation of the spermatids in the cat (Felis domestica). *J. Cell Biol.* **1**, 287–300.
Busada J. T., and Geyer C. B. (2016). The role of retinoic acid (RA) in spermatogonial differentiation. *Biol. Reprod.* **94**, 10–11.
Campagnolo L., Russo M. A., Puglianiello A., Favale A., and Siracusa G. (2001). Mesenchymal cell precursors of peritubular smooth muscle cells of the mouse testis can be identified by the presence of the p75 neurotrophin receptor. *Biol. Reprod.* **64**, 464–472.
Campos-Junior P. H. A., Costa G. M. J., Avelar G. F., Lacerda S. M. S. N., Da Costa N. N., Ohashi O. M., Miranda M. D. S., Barcelos L. S., Jorge É. C., Guimarães D. A., and De França L. R. (2014). Derivation of sperm from xenografted testis cells and tissues of the peccary (Tayassu tajacu). *Reproduction* **147**, 291–299. doi:10.1530/REP-13-0581
Capel B. (2017). Vertebrate sex determination: Evolutionary plasticity of a fundamental switch. *Nat. Rev. Genet.* **18**, 675–689. doi:10.1038/nrg.2017.60
Castrillon D. H., Quade B. J., Wang T. Y., Quigley C., and Crum C. P. (2000). The human VASA gene is specifically expressed in the germ cell lineage. *Proc. Natl. Acad. Sci. U. S. A.* **97**, 9585–9590. doi:10.1073/pnas.160274797
Cervantes M. P., Singh J., Palomino J. M., and Adams G. P. (2013). Surgical translocation and ultrasound bio-microscopy of the ovaries in rabbits. *Anim. Reprod. Sci.* **138**, 133–141.
Chambers I., Colby D., Robertson M., Nichols J., Lee S., Tweedie S., and Smith A. (2003). Functional expression cloning of Nanog, a pluripotency sustaining factor in embryonic stem cells. *Cell* **113**, 643–655.
Champy C. (1920). Quelques résultats de la méthode de culture des tissus. *Arch Zool Exp Gen* **60**, 461–500.
Chawengsaksophak K., Svingen T., Ng E. T., Epp T., Spiller C. M., Clark C., Cooper H., and Koopman P. (2012). Loss of Wnt5a disrupts primordial germ cell migration and male sexual development in mice. *Biol. Reprod.* **86**, 1–4.
Chen H., Ge R. S., and Zirkin B. R. (2009). Leydig cells: From stem cells to aging. *Mol Cell Endocrinol*. **306**, 9–16. doi:10.1016/j.mce.2009.01.023
Chen Z., Hong F., Wang Z., Hao D., and Yang H. (2020). Spermatogonial stem cells are a promising and pluripotent cell source for regenerative medicine. *Am. J. Transl. Res.* **12**, 7048–7059.
Chen Z., Niu M., Sun M., Yuan Q., Yao C., Hou J., Wang H., Wen L., Fu H., and Zhou F. (2017). Transdifferentiation of human male germline stem cells to hepatocytes in vivo via the transplantation under renal capsules. *Oncotarget* **8**, 14576–14592.
Chen Z., Sun M., Yuan Q., Niu M., Yao C., Hou J., Wang H., Wen L., Liu Y., and Li Z. (2016). Generation of functional hepatocytes from human spermatogonial stem cells. *Oncotarget* **7**, 8879–8895.
Chen T., Yuan D., Wei B., Jiang J., Kang J., Ling K., Gu Y., Li J., Xiao L., and Pei G. (2010). E-cadherin-mediated cell-cell contact is critical for induced pluripotent stem cell generation. *Stem Cells* **66**, 1173–1179. doi:10.1002/stem.456
Cheng L., Gearing D. P., White L. S., Compton D. L., Schooley K., and Donovan P. J. (1994). Role of leukemia inhibitory factor and its receptor in mouse primordial germ cell growth. *Development* **120**, 3145–3153.

Cheng P.-L., Hui-Ru W., LI C.-Y., Chen C.-F., and Chen H.-C. (2017). Characterization of the testicular regeneration potential in premature cockerels. *J. Reprod. Dev.* **63**, 563–570. doi:10.1262/jrd.2017-090

Cheng I.-F., Kaiser D., Huebscher D., Hasenfuss G., Guan K., and Schäfer K. (2012). Differentiation of multipotent adult germline stem cells derived from mouse testis into functional endothelial cells. *J. Vasc. Res.* **49**, 207–220.

Cheung A. M. Y., Brown A. S., Hastie L. A., Cucevic V., Roy M., Lacefield J. C., Fenster A., and Foster F. S. (2005). Three-dimensional ultrasound biomicroscopy for xenograft growth analysis. *Ultrasound Med. Biol.* **31**, 865–870. doi:10.1016/j.ultrasmedbio.2005.03.003

Chiarini-Garcia H., and Russell L. D. (2001). High-resolution light microscopic characterization of mouse spermatogonia. *Biol. Reprod.* **65**, 1170–1178.

Chikhovskaya J. V., van Daleen S. K. M., Korver C. M., Repping S., and van Pelt A. M. M. (2014). Mesenchymal origin of multipotent human testis-derived stem cells in human testicular cell cultures. *Mol. Hum. Reprod.* **20**, 155–167. doi:10.1093/molehr/gat076

Chinta S. J., Kumar M. J., Hsu M., Rajagopalan S., Kaur D., Rane A., Nicholls D. G., Choi J., and Andersen J. K. (2007). Inducible alterations of glutathione levels in adult dopaminergic midbrain neurons result in nigrostriatal degeneration. *J. Neurosci.* **27**, 13997–14006.

Choi K. H., Lee D. K., Kim S. W., Woo S. H., Kim D. Y., and Lee C. K. (2019). Chemically Defined Media Can Maintain Pig Pluripotency Network In Vitro. *Stem Cell Reports* **13**, 221–234. doi:10.1016/j.stemcr.2019.05.028

Chuma S., Kanatsu-Shinohara M., Inoue K., Ogonuki N., Miki H., Toyokuni S., Hosokawa M., Nakatsuji N., Ogura A., and Shinohara T. (2005). Spermatogenesis from epiblast and primordial germ cells following transplantation into postnatal mouse testis. *Development* **132**, 117–122.

Clark A. M., Garland K. K., and Russell L. D. (2000). Desert hedgehog (Dhh) gene is required in the mouse testis for formation of adult-type Leydig cells and normal development of peritubular cells and seminiferous tubules. *Biol. Reprod.* **63**, 1825–1838. doi:10.1095/biolreprod63.6.1825

Clark B. J., Soo S.-C., Caron K. M., Ikeda Y., Parker K. L., and Stocco D. M. (1995). Hormonal and developmental regulation of the steroidogenic acute regulatory protein. *Mol. Endocrinol.* **9**, 1346–1355.

Clermont Y. (1969). Two classes of spermatogonial stem cells in the monkey (Cercopithecus aethiops). *Am. J. Anat.* **126**, 57–71.

Clermont Y., and Perey B. (1957). Quantitative study of the cell population of the seminiferous tubules in immature rats. *Am. J. Anat.* **100**, 241–267.

Clouthier D. E., Avarbock M. R., Maika S. D., Hammer R. E., and Brinster R. L. (1996). Rat spermatogenesis in mouse testis. *Nature* **381**, 418–421.

Coelho M. J., Cabral A. T., and Fernandes M. H. (2000). Human bone cell cultures in biocompatibility testing. Part I: osteoblastic differentiation of serially passaged human bone marrow cells cultured in α-MEM and in DMEM. *Biomaterials* **21**, 1087–1094.

Colvin J. S., Green R. P., Schmahl J., Capel B., and Ornitz D. M. (2001). Male-to-female sex reversal in mice lacking fibroblast growth factor 9. *Cell* **104**, 875–889. doi:10.1016/S0092-8674(01)00284-7

Combes A. N., Wilhelm D., Davidson T., Dejana E., Harley V., Sinclair A., and Koopman P. (2009). Endothelial cell migration directs testis cord formation. *Dev. Biol.* **326**, 112–120. doi:10.1016/j.ydbio.2008.10.040

Conrad S., Azizi H., Hatami M., Kubista M., Bonin M., Hennenlotter J., Sievert K.-D., and Skutella T. (2016). Expression of genes related to germ cell lineage and pluripotency in single cells and colonies of human adult germ stem cells. *Stem Cells Int.* **2016**, 1–17.

Cool J., DeFalco T. J., and Capel B. (2011). Vascular-mesenchymal cross-talk through Vegf and Pdgf drives organ patterning. *Proc. Natl. Acad. Sci. U. S. A.* **108**, 167–172. doi:10.1073/pnas.1010299108

Corbier P., Edwards D. A., and Roffi J. (1992). The neonatal testosterone surge: a comparative study. *Arch. Int. Physiol. Biochim. Biophys.* **100**, 127–131.

Costoya J. A., Hobbs R. M., Barna M., Cattoretti G., Manova K., Sukhwani M., Orwig K. E., Wolgemuth D. J., and Pandolfi P. P. (2004). Essential role of Plzf in maintenance of spermatogonial stem cells. *Nat. Genet.* **36**, 653–659.

Coveney D., Cool J., Oliver T., and Capel B. (2008). Four-dimensional analysis of vascularization during primary development of an organ, the gonad. *Proc. Natl. Acad. Sci. U. S. A.* **105**, 7212–7217. doi:10.1073/pnas.0707674105

Creasy D. M., and Chapin R. E. (2013). Chapter 59 - Male Reproductive System. 'Haschek and Rousseaux's Handbook of Toxicologic Pathology (Third Edition)'. (Eds WM Haschek, CG Rousseaux and MA Wallig) pp. 2493–2598. (Academic Press: Boston) doi:https://doi.org/10.1016/B978-0-12-415759-0.00059-5

Culty M. (2009). Gonocytes, the forgotten cells of the germ cell lineage. *Birth Defects Res. Part C - Embryo Today Rev.* **87**, 1–26. doi:10.1002/bdrc.20142

Culty M. (2013). Gonocytes, from the fifties to the present: is there a reason to change the name? *Biol. Reprod.* **89**, 41–46.

Curley M., Milne L., Smith S., Atanassova N., Rebourcet D., Darbey A., Hadoke P. W. F., Wells S., and Smith L. B. (2018). Leukemia inhibitory factor-receptor is dispensable for prenatal testis development but is required in sertoli cells for normal spermatogenesis in mice. *Sci. Rep.* **8**, 1–13. doi:10.1038/s41598-018-30011-w

D'Souza R., Pathak S., Upadhyay R., Gaonkar R., D'Souza S., Sonawane S., Gill-Sharma M., and Balasinor N. H. (2009). Disruption of tubulobulbar complex by high intratesticular estrogens leading to failed spermiation. *Endocrinology* **150**, 1861–1869.

Dada T., Gadia R., Sharma A., Ichhpujani P., Bali S. J., Bhartiya S., and Panda A. (2011). Ultrasound biomicroscopy in glaucoma. *Surv. Ophthalmol.* **56**, 433–450.

Davidoff M. S., Breucker H., Holstein A. F., and Seidl K. (1990). Cellular architecture of the lamina propria of human seminiferous tubules. *Cell Tissue Res.* **262**, 253–261. doi:10.1007/BF00309880

Davidoff M. S., Middendorff R., Köfüncü E., Müller D., Ježek D., and Holstein A.-F. (2002). Leydig cells of the human testis possess astrocyte and oligodendrocyte marker molecules. *Acta Histochem.* **104**, 39–49.

Dawson E. P., Lanza D. G., Webster N. J., Benton S. M., Suetake I., and Heaney J. D. (2018). Delayed male germ cell sex-specification permits transition into embryonal carcinoma cells with features of primed pluripotency. *Development* **145**, 1–12.

Devi L., Pothana L., and Goel S. (2017). Dysregulation of angiogenesis-specific signalling in adult testis results in xenograft degeneration. *Sci. Rep.* **7**, 1–15. doi:10.1038/s41598-017-02604-4

Diekmann U., Wolling H., Dettmer R., Niwolik I., Naujok O., and Buettner F. F. R. (2019). Chemically defined and xenogeneic-free differentiation of human pluripotent stem cells into definitive endoderm in 3D culture. *Sci. Rep.* **9**, 1–14.

Dirami G., Ravindranath N., Pursel V., and Dym M. (1999). Effects of stem cell factor and

granulocyte macrophage-colony stimulating factor on survival of porcine type A spermatogonia cultured in KSOM. *Biol. Reprod.* **61**, 225–230.
Dissanayake D. (2018). In vitro spermatogenesis; past, present, and future. *Spermatozoa facts Perspect. London United kingdom* 25–51.
van Dissel-emiliani F. M. F., De Boer-brouwer M., and de Rooij D. G. (1996). Effect of fibroblast growth factor-2 on Sertoli cells and gonocytes in coculture during the perinatal period. *Endocrinology*. **137**, 647–654. doi:10.1210/endo.137.2.8593814
van Dissel-Emiliani F. M. F., de Boer-Brouwer M., Spek E. R., van Der Donk J. A., and de Rooij D. G. (1993). Survival and proliferation of rat gonocytes in vitro. *Cell Tissue Res.* **273**, 141–147.
van Dissel-Emiliani F. M. F., Grootenhuis A. J., de Jong F. H., and de Rooij D. G. (1989). Inhibin reduces spermatogonial numbers in testes of adult mice and Chinese hamsters. *Endocrinology* **125**, 1899–1903. doi:10.1210/endo-125-4-1898
van Dissel-Emiliani F. M. F., de Rooji D. G., and Meistrich M. L. (1989). Isolation of rat gonocytes by velocity sedimentation at unit gravity. *Reproduction* **86**, 759–766.
Dobrinski I. (2005). Germ cell transplantation and testis tissue xenografting in domestic animals. *Anim. Reprod. Sci.* **89**, 137–145. doi:10.1016/j.anireprosci.2005.06.020
Dobrinski I. (2007). De novo morphogenesis of functional testis tissue after ectopic transplantation of isolated cells. *Organogenesis* **3**, 79–82. doi:10.4161/org.3.2.4944
Dobrinski I. (2008). Male germ cell transplantation. *Reprod. Domest. Anim.* **43**, 288–294. doi:10.1111/j.1439-0531.2008.01176.x
Dobrinski I., Avarbock M. R., and Brinster R. L. (1999). Transplantation of germ cells from rabbits and dogs into mouse testes. *Biol. Reprod.* **61**, 1331–1339. doi:10.1095/biolreprod61.5.1331
Dobrinski I., Avarbock M. R., and Brinster R. L. (2000). Germ cell transplantation from large domestic animals into mouse testes. *Mol. Reprod. Dev.* **57**, 270–279.
Dobrinski I., and Travis A. J. (2007). Germ cell transplantation for the propagation of companion animals, non-domestic and endangered species. *Reproduction, Fertility and Development* **19**, 732–739. doi:10.1071/RD07036
Donovan P. J., Stott D., Cairns L. A., Heasman J., and Wylie C. C. (1986). Migratory and postmigratory mouse primordial germ cells behave differently in culture. *Cell* **44**, 831–838.
Dores C., Alpaugh W., and Dobrinski I. (2012). From in vitro culture to in vivo models to study testis development and spermatogenesis. *Cell Tissue Res.* **349**, 691–702. doi:10.1007/s00441-012-1457-x
Dores C., and Dobrinski I. (2014). De novo morphogenesis of testis tissue: an improved bioassay to investigate the role of VEGF165 during testis formation. *Reproduction* **148**, 109–117.
Dorval-Coiffec I., Delcros J.-G., Hakovirta H., Toppari J., Jégou B., and Piquet-Pellorce C. (2005). Identification of the leukemia inhibitory factor cell targets within the rat testis. *Biol. Reprod.* **72**, 602–611.
Dovere L., Fera S., Grasso M., Lamberti D., Gargioli C., Muciaccia B., Lustri A. M., Stefanini M., and Vicini E. (2013). The niche-derived glial cell line-derived neurotrophic factor (GDNF) induces migration of mouse spermatogonial stem/progenitor cells. *PLoS One* **8**, e59431.
Drumond A. L., Meistrich M. L., and Chiarini-Garcia H. (2011). Spermatogonial morphology and kinetics during testis development in mice: a high-resolution light microscopy approach. *Reproduction* **142**, 145–155.
Dufour J. M., Rajotte R. V., and Korbutt G. S. (2002). Development of an in vivo model to study testicular morphogenesis. *J. Androl.* **23**, 635–644. doi:10.1002/j.1939-4640.2002.tb02305.x

Dym M. (1994). Basement membrane regulation of sertoli cells. *Endocr. Rev.* **15**, 102–115. doi:10.1210/edrv-15-1-102

Edmonds M. E., and Woodruff T. K. (2020). Testicular organoid formation is a property of immature somatic cells, which self-assemble and exhibit long-term hormone-responsive endocrine function. *Biofabrication* **12**, 1–16. doi:10.1088/1758-5090/ab9907

Ehmcke J., Gassei K., and Schlatt S. (2008). Ectopic testicular xenografts from newborn hamsters (Phodopus sungorus) show better spermatogenic activity in aged compared with young recipients. *J. Exp. Zool. Part A Ecol. Genet. Physiol.* **309**, 278–287.

Elliot T. L., Downey D. B., Tong S., McLean C. A., and Fenster A. (1996). Accuracy of prostate volume measurements in vitro using three-dimensional ultrasound. *Acad. Radiol.* **3**, 401–406. doi:10.1016/S1076-6332(05)80673-7

Elzawam A. Z. (2013). Establishment of spermatogenesis following testicular tissue ectopic xenografting in alpaca. Washington State University.

Emmen J. M. A., McLuskey A., Adham I. M., Engel W., Grootegoed J. A., and Brinkmann A. O. (2000). Hormonal control of gubernaculum development during testis descent: Gubernaculum outgrowth in vitro requires both insulin-like factor and androgen. *Endocrinology* **141**, 4720–4727. doi:10.1210/endo.141.12.7830

Enders G. C., and May J. J. (1994). Developmentally regulated expression of a mouse germ cell nuclear antigen examined from embryonic day 11 to adult in male and female mice. *Dev. Biol.* **163**, 331–340.

Eng L. F. (1985). Glial fibrillary acidic protein (GFAP): the major protein of glial intermediate filaments in differentiated astrocytes. *J. Neuroimmunol.* **8**, 203–214.

Escalante-Alcalde D., and Merchant-Larios H. (1992). Somatic and germ cell interactions during histogenetic aggregation of mouse fetal testes. *Exp. Cell Res.* **198**, 150–158. doi:10.1016/0014-4827(92)90161-Z

Escalier D. (2006). Knockout mouse models of sperm flagellum anomalies. *Hum. Reprod. Update* **12**, 449–461.

Evans M. J., and Kaufman M. H. (1981). Establishment in culture of pluripotential cells from mouse embryos. *Nature* **292**, 154–156.

Fagoonee S., Pellicano R., Silengo L., and Altruda F. (2011). Potential applications of germline cell-derived pluripotent stem cells in organ regeneration. *Organogenesis* **7**, 116–122.

Fang F., Li Z., Zhao Q., Xiong C., and Ni K. (2020). Analysis of multi-lineage gene expression dynamics during primordial germ cell induction from human induced pluripotent stem cells. *Stem Cell Res. Ther.* **11**, 1–9.

Fayaz M. A., Awang-Junaidi A. H., Singh J., and Honaramooz A. (2020a). Long-term monitoring of donor xenogeneic testis tissue grafts and cell implants in recipient mice using ultrasound biomicroscopy. *Ultrasound Med. Biol.* **46**, 3088–3103. doi:10.1016/j.ultrasmedbio.2020.07.010

Fayaz M. A., Awang-Junaidi A. H., Singh J., and Honaramooz A. (2020b). Validation of ultrasound biomicroscopy for the assessment of xenogeneic testis tissue grafts and cell implants in recipient mice. *Andrology* **8**, 1332–1346. doi:10.1111/andr.12771

Fayomi A. P., and Orwig K. E. (2018). Spermatogonial stem cells and spermatogenesis in mice, monkeys and men. *Stem Cell Res.* **29**, 207–214. doi:10.1016/j.scr.2018.04.009

De Felici M. (2016). The formation and migration of primordial germ cells in mouse and man. *Results Probl. Cell Differ.* **58**, 23–46. doi:10.1007/978-3-319-31973-5_2

De Felici M., Scaldaferri M. L., Lobascio M., Iona S., Nazzicone V., Klinger F. G., and Farini D.

(2004). Experimental approaches to the study of primordial germ cell lineage and proliferation. *Hum. Reprod. Update* **10**, 197–206. doi:10.1093/humupd/dmh020

Fenster, A, Downey D. (2000). Three-dimensional ultrasound imaging. *AnN Rev Biomed Eng* **2**, 457–475.

Ferranti F., Muciaccia B., Ricci G., Dovere L., Canipari R., Magliocca F., Stefanini M., Catizone A., and Vicini E. (2012). Glial cell line–derived neurotrophic factor promotes invasive behaviour in testicular seminoma cells. *Int. J. Androl.* **35**, 758–768.

Filipponi D., Hobbs R. M., Ottolenghi S., Rossi P., Jannini E. A., Pandolfi P. P., and Dolci S. (2007). Repression of kit expression by Plzf in germ cells. *Mol. Cell. Biol.* **27**, 6770–6781.

Flanagan C. A., and Manilall A. (2017). Gonadotropin-releasing hormone (GnRH) receptor structure and GnRH binding. *Front. Endocrinol. (Lausanne).* **8**, 1–14. doi:10.3389/fendo.2017.00274

Flück C. E., Miller W. L., and Auchus R. J. (2003). The 17, 20-lyase activity of cytochrome P450c17 from human fetal testis favors the Δ5 steroidogenic pathway. *J. Clin. Endocrinol. Metab.* **88**, 3762–3766.

Flück C. E., and Pandey A. V (2017). Testicular Steroidogenesis. 'Endocrinology of the Testis and Male Reproduction'. (Eds M Simoni and IT Huhtaniemi) pp. 343–371. (Springer International Publishing: Cham) doi:10.1007/978-3-319-44441-3_10

Foster F. S., Zhang M. Y., Zhou Y. Q., Liu G., Mehi J., Cherin E., Harasiewicz K. A., Starkoski B. G., Zan L., Knapik D. A., and Adamson S. L. (2002). A new ultrasound instrument for in vivo microimaging of mice. *Ultrasound Med. Biol.* **28**, 1165–1172. doi:10.1016/S0301-5629(02)00567-7

França L. R., Silva Jr V. A., Chiarini-Garcia H., Garcia S. K., and Debeljuk L. (2000). Cell proliferation and hormonal changes during postnatal development of the testis in the pig. *Biol. Reprod.* **63**, 1629–1636.

Franz-Odendaal T. A., Hall B. K., and Witten P. E. (2006). Buried alive: how osteoblasts become osteocytes. *Dev. Dyn. an Off. Publ. Am. Assoc. Anat.* **235**, 176–190.

Fujihara M., Kim S. M., Minami N., Yamada M., and Imai H. (2011). Characterization and in vitro culture of male germ cells from developing bovine testis. *J. Reprod. Dev.* doi:10.1262/jrd.10-185M

Fukuda T., Hedinger C., and Groscurth P. (1975). Ultrastructure of developing germ cells in the fetal human testis. *Cell Tissue Res.* **161**, 55–70.

Gallagher S. J., Kofman A. E., Huszar J. M., Dannenberg J. H., DePinho R. A., Braun R. E., and Payne C. J. (2013). Distinct requirements for Sin3a in perinatal male gonocytes and differentiating spermatogonia. *Dev. Biol.* doi:10.1016/j.ydbio.2012.10.009

Garcia T. X., Farmaha J. K., Kow S., and Hofmann M.-C. (2014). RBPJ in mouse Sertoli cells is required for proper regulation of the testis stem cell niche. *Development* **141**, 4468–4478.

Gassei K., and Orwig K. E. (2013). SALL4 expression in gonocytes and spermatogonial clones of postnatal mouse testes. *PLoS One* **8**, e53976.

Gassei K., Schlatt S., and Ehmcke J. (2006). De novo morphogenesis of seminiferous tubules from dissociated immature rat testicular cells in xenografts. *J. Androl.* **27**, 611–618. doi:10.2164/jandrol.05207

Geens M., De Block G., Goossens E., Frederickx V., Van Steirteghem A., and Tournaye H. (2006). Spermatogonial survival after grafting human testicular tissue to immunodeficient mice. *Hum. Reprod.* **21**, 390–396.

Geens M., Goossens E., De Block G., Ning L., Van Saen D., and Tournaye H. (2008). Autologous

spermatogonial stem cell transplantation in man: current obstacles for a future clinical application. *Hum. Reprod. Update* **14**, 121–130.
Giavarina D. (2015). Understanding bland altman analysis. *Biochem. Medica* **25**, 141–151.
Gier H. T., and Marion G. B. (1969). Development of mammalian testes and genital ducts. *Biol. Reprod.* **1**, 1–23. doi:10.1095/biolreprod1.Supplement_1.1
Gill M. E., Hu Y.-C., Lin Y., and Page D. C. (2011). Licensing of gametogenesis, dependent on RNA binding protein DAZL, as a gateway to sexual differentiation of fetal germ cells. *Proc. Natl. Acad. Sci.* **108**, 7443–7448.
Glaser T., Opitz T., Kischlat T., Konang R., Sasse P., Fleischmann B. K., Engel W., Nayernia K., and Brüstle O. (2008). Adult germ line stem cells as a source of functional neurons and glia. *Stem Cells* **26**, 2434–2443.
Gnessi L., Basciani S., Mariani S., Arizzi M., Spera G., Wang C., Bondjers C., Karlsson L., and Betsholtz C. (2000). Leydig cell loss and spermatogenic arrest in platelet-derived growth factor (PDGF)-A-deficient mice. *J. Cell Biol.* **149**, 1019–1026. doi:10.1083/jcb.149.5.1019
Gnessi L., Fabbri A., and Spera G. (1997). Gonadal peptides as mediators of development and functional control of the testis: an integrated system with hormones and local environment. *Endocr. Rev.* **18**, 541–609.
Goel S., Fujihara M., Minami N., Yamada M., and Imai H. (2008). Expression of NANOG, but not POU5F1, points to the stem cell potential of primitive germ cells in neonatal pig testis. *Reproduction* **135**, 785–795. doi:10.1530/REP-07-0476
Goel S., Fujihara M., Tsuchiya K., Takagi Y., Minami N., Yamada M., and Imai H. (2009). Multipotential ability of primitive germ cells from neonatal pig testis cultured in vitro. *Reprod. Fertil. Dev.* **21**, 696–708. doi:10.1071/rd08176
Goel S., Sugimoto M., Minami N., Yamada M., Kume S., and Imai H. (2007). Identification, isolation, and in vitro culture of porcine gonocytes. *Biol. Reprod.* **77**, 127–137. doi:10.1095/biolreprod.106.056879
Goertz D. E., Yu J. L., Kerbel R. S., Burns P. N., and Foster F. S. (2002). High-frequency Doppler ultrasound monitors the effects of antivascular therapy on tumor blood flow. *Cancer Res.* **62**, 6371–6375. doi:10.1523/JNEUROSCI.1851-04.2004
Golden J. P., DeMaro J. A., Osborne P. A., Milbrandt J., and Johnson Jr E. M. (1999). Expression of neurturin, GDNF, and GDNF family-receptor mRNA in the developing and mature mouse. *Exp. Neurol.* **158**, 504–528.
Golestaneh N., Kokkinaki M., Pant D., Jiang J., DeStefano D., Fernandez-Bueno C., Rone J. D., Haddad B. R., Gallicano G. I., and Dym M. (2009). Pluripotent stem cells derived from adult human testes. *Stem Cells Dev.* **18**, 1115–1125.
Gonzalez A.-M., Buscaglia M., Ong M., and Baird A. (1990). Distribution of basic fibroblast growth factor in the 18-day rat fetus: localization in the basement membranes of diverse tissues. *J. Cell Biol.* **110**, 753–765.
González R., and Dobrinski I. (2015). Beyond the mouse monopoly: Studying the male germ line in domestic animal models. *ILAR J.* **56**, 83–98. doi:10.1093/ilar/ilv004
Grasso M., Fuso A., Dovere L., de Rooij D. G., Stefanini M., Boitani C., and Vicini E. (2012). Distribution of GFRA1-expressing spermatogonia in adult mouse testis. *Reproduction* **143**, 325–332.
Greco A., Mancini M., Gargiulo S., Gramanzini M., Claudio P. P., Brunetti A., and Salvatore M. (2012). Ultrasound biomicroscopy in small animal research: Applications in molecular and preclinical imaging. *J. Biomed. Biotechnol.* **2012**, 1–14. doi:10.1155/2012/519238

Greenfield A. (2015). Understanding sex determination in the mouse: genetics, epigenetics and the story of mutual antagonisms. *Journal of Genetics*. **94**, 585–590. doi:10.1007/s12041-015-0565-2

Grimaldi C., and Raz E. (2020). Germ cell migration—Evolutionary issues and current understanding. *Semin. Cell Dev. Biol.* **100**, 152–159. doi:https://doi.org/10.1016/j.semcdb.2019.11.015

Griswold M. D. (2016). Spermatogenesis: the commitment to meiosis. *Physiol. Rev.* **96**, 1–17.

Griswold S. L., and Behringer R. R. (2009). Fetal Leydig cell origin and development. *Sex. Dev.* **3**, 1–15. doi:10.1159/000200077

Griswold michael D., Bishop P. D., Kim K.-H., Ping R., Siiteri J. E., and Morales C. (1989). Function of Vitamin A in Normal and Synchronized Seminiferous Tubules. *Ann. N. Y. Acad. Sci.* **564**, 154–172. doi:10.1111/j.1749-6632.1989.tb25895.x

Gropp A., and Ohno S. (1966). The presence of a common embryonic blastema for ovarian and testicular parenchymal (follicular, interstitial and tubular) cells in cattle, Bos taurus. *Zeitschrift für Zellforsch. und mikroskopische Anat.* **74**, 505–528. doi:10.1007/BF00496841

Gu Y., Runyan C., Shoemaker A., Surani A., and Wylie C. (2009). Steel factor controls primordial germ cell survival and motility from the time of their specification in the allantois, and provides a continuous niche throughout their migration. **136**, 1295–1303.

Gu S., Wu Y.-M., Hong L., Zhang Z.-D., and Yin M.-Z. (2011). Glial fibrillary acidic protein expression is an indicator of teratoma maturation in children. *World J. Pediatr.* **7**, 262–265.

Guan K., Nayernia K., Maier L. S., Wagner S., Dressel R., Jae H. L., Nolte J., Wolf F., Li M., Engel W., and Hasenfuss G. (2006). Pluripotency of spermatogonial stem cells from adult mouse testis. *Nature* **440**, 1199–1203. doi:10.1038/nature04697

Gubbay J., Collignon J., Koopman P., Capel B., Economou A., Münsterberg A., Vivian N., Goodfellow P., and Lovell-Badge R. (1990). A gene mapping to the sex-determining region of the mouse Y chromosome is a member of a novel family of embryonically expressed genes. *Nature* **346**, 245–250. doi:10.1038/346245a0

Hadziselimovic F., and Herzog B. (1993). The development and descent of the epididymis. *Eur. J. Pediatr.* **152**, S6-9. doi:10.1007/BF02125424

Hadziselimovic F., and Zivkovic D. (2007). Is the prohibition of hormonal treatment for cryptorchidism, as suggested by the Nordic consensus group, justifiable? *Acta Paediatr.* **96**, 1368–1369.

van Den Ham R., van Pelt A. M. M., de Miguel M. P., van Kooten P. J. S., Walther N., and van Dissel-Emilani F. M. F. (1997). Immunomagnetic isolation of fetal rat gonocytes. *Am. J. Reprod. Immunol.* **38**, 39–45.

Hamilton W. B., Mosesson Y., Monteiro R. S., Emdal K. B., Knudsen T. E., Francavilla C., Barkai N., Olsen J. V., and Brickman J. M. (2019). Dynamic lineage priming is driven via direct enhancer regulation by ERK. *Nature* **575**, 355–360. doi:10.1038/s41586-019-1732-z

Hammes A., Guo J.-K., Lutsch G., Leheste J.-R., Landrock D., Ziegler U., Gubler M.-C., and Schedl A. (2001). Two splice variants of the Wilms' tumor 1 gene have distinct functions during sex determination and nephron formation. *Cell* **106**, 319–329.

Hamra F. K., Chapman K. M., Nguyen D. M., Williams-Stephens A. A., Hammer R. E., and Garbers D. L. (2005). Self renewal, expansion, and transfection of rat spermatogonial stem cells in culture. *Proc. Natl. Acad. Sci. U. S. A.* **102**, 17430–17435. doi:10.1073/pnas.0508780102

Hamra F. K., Chapman K. M., Wu Z., and Garbers D. L. (2008). Isolating highly pure rat

spermatogonial stem cells in culture. In Hou S. X., Singh S. R. (eds) Germline Stem Cells. Methods in Molecular Biology pp. 163–179. (Springer)

Hamra F. K., Gatlin J., Chapman K. M., Grellhesl D. M., Garcia J. V., Hammer R. E., and Garbers D. L. (2002). Production of transgenic rats by lentiviral transduction of male germ-line stem cells. *Proc. Natl. Acad. Sci. U. S. A.* **99**, 14931–14936. doi:10.1073/pnas.222561399

Hamra F. K., Richie C. T., and Harvey B. K. (2017) Long Evans rat spermatogonial lines are effective germline vectors for transgenic rat production. *Transgenic Res.* **26**, 477–489.

Han S., Gupta M. K., Sang J., and Lee H. T. (2009). Isolation and in vitro culture of pig spermatogonial stem cell. *Asian-Australas J Anim Sci* **22**, 187–193. doi:10.5713/ajas.2009.80324

Han I. S., Sylvester S. R., Kim K. H., Schelling M. E., Venkateswaran S., Blanckaert V. D., McGuinness M. P., and Griswold M. D. (1993). Basic fibroblast growth factor is a testicular germ cell product which may regulate Sertoli cell function. *Mol. Endocrinol.* **7**, 889–897.

Hanna H., Mir L. M., and Andre F. M. (2018). In vitro osteoblastic differentiation of mesenchymal stem cells generates cell layers with distinct properties. *Stem Cell Res. Ther.* **9**, 1–11.

Hannema S. E., and Hughes I. A. (2007). Regulation of Wolffian duct development. *Horm. Res.* **67**, 142–151. doi:10.1159/000096644

Hansson V., Calandra R., Purvis K., Ritzen M., and French F. S. (1976). Hormonal Regulation of Spermatogenesis. *Vitam. Horm.* **34**, 187–214. doi:https://doi.org/10.1016/S0083-6729(08)60076-X

Hao J., Yamamoto M., Richardson T. E., Chapman K. M., Denard B. S., Hammer R. E., Zhao G. Q., and Hamra F. K. (2008). Sohlh2 knockout mice are male-sterile because of degeneration of differentiating type A spermatogonia. *Stem Cells* **26**, 1587–1597.

Hasthorpe S., Barbie S., Farmer P. J., and Hutson J. M. (1999). Neonatal mouse gonocyte proliferation assayed by an in vitro clonogenic method. *J. Reprod. Fertil.* **116**, 335–344. doi:10.1530/jrf.0.1160335

Hatano O., Takakusu A., Nomura M., and Morohashi K. (1996). Identical origin of adrenal cortex and gonad revealed by expression profiles of Ad4BP/SF-1. *Genes to Cells* **1**, 663–671.

He Y., Chen X., Zhu H., and Wang D. (2015). Developments in techniques for the isolation, enrichment, main culture conditions and identification of spermatogonial stem cells. *Cytotechnology* **67**, 921–930. doi:10.1007/s10616-015-9850-4

He M., Friedman D. S., Ge J., Huang W., Jin C., Cai X., Khaw P. T., and Foster P. J. (2007). Laser peripheral iridotomy in eyes with narrow drainage angles: ultrasound biomicroscopy outcomes. The Liwan Eye Study. *Ophthalmology* **114**, 1513–1519. doi:10.1016/j.ophtha.2006.11.032

He M., Wang D., and Jiang Y. (2012). Overview of ultrasound biomicroscopy. *J. Curr. Glaucoma Pract.* **6**, 25–53.

Hermann B. P., Sukhwani M., Winkler F., Pascarella J. N., Peters K. A., Sheng Y., Valli H., Rodriguez M., Ezzelarab M., and Dargo G. (2012). Spermatogonial stem cell transplantation into rhesus testes regenerates spermatogenesis producing functional sperm. *Cell Stem Cell* **11**, 715–726.

Hermo L., Pelletier R., Cyr D. G., and Smith C. E. (2010). Surfing the wave, cycle, life history, and genes/proteins expressed by testicular germ cells. Part 3: developmental changes in spermatid flagellum and cytoplasmic droplet and interaction of sperm with the zona pellucida and egg plasma membrane. *Microsc. Res. Tech.* **73**, 320–363.

Herrid M., Davey R. J., Hutton K., Colditz I. G., and Hill J. R. (2009). A comparison of methods

for preparing enriched populations of bovine spermatogonia. *Reprod. Fertil. Dev.* **21**, 393–399.

Hess R. A., and Hermo L. (2018). Rete testis: structure, cell biology and site for stem cell transplantation. 'Encyclopedia of Reproduction (Second Edition)'. (Ed MK Skinner) pp. 263–269. (Academic Press: Oxford) doi:https://doi.org/10.1016/B978-0-12-801238-3.64592-0

Hess R. A., and Moore B. J. (1993). Histological methods for evaluation of the testis. *Methods Toxicol.* **3**, 86–94.

Hibino N., Yi T., Duncan D. R., Rathore A., Dean E., Naito Y., Dardik A., Kyriakides T., Madri J., Pober J. S., Shinoka T., and Breuer C. K. (2011). A critical role for macrophages in neovessel formation and the development of stenosis in tissue-engineered vascular grafts. *FASEB J.* **25**, 4253–4263. doi:10.1096/fj.11-186585

Hill J. R., Brownlee A., Davey R., Herrid M., Hutton K., Vignarajan S., and Dobrinski I. (2005). Initial results from male germ cell transfer between cattle breeds. *Reprod. Fertil. Dev.* **17**, 204.

Hill J. R., and Dobrinski I. (2005). Male germ cell transplantation in livestock. *Reprod. Fertil. Dev.* **18**, 13–18.

Hilscher W. (1991). The genetic control and germ cell kinetics of the female and male germ line in mammals including man. *Hum. Reprod.* **6**, 1416–1425.

Hilscher B., Hilscher W., Bülthoff-Ohnolz B., Krämer U., Birke A., Pelzer H., and Gauss G. (1974). Kinetics of gametogenesis. *Cell Tissue Res.* **154**, 443–470.

Hilton D. J., and Gough N. M. (1991). Leukemia inhibitory factor: a biological perspective. *J. Cell. Biochem.* **46**, 21–26.

Hiramatsu R., Harikae K., Tsunekawa N., Kurohmaru M., Matsuo I., and Kanai Y. (2010). FGF signaling directs a center-to-pole expansion of tubulogenesis in mouse testis differentiation. *Development* **137**, 303–312. doi:10.1242/dev.040519

Hirenallur-Shanthappa D. K., Ramírez J. A., and Iritani B. M. (2017). Chapter 5 - Immunodeficient Mice: The Backbone of Patient-Derived Tumor Xenograft Models. (Eds R Uthamanthil and PBT-PDTXM Tinkey) pp. 57–73. (Academic Press) doi:https://doi.org/10.1016/B978-0-12-804010-2.00005-9

Hoei-Hansen C. E., Almstrup K., Nielsen J. E., Brask Sonne S., Graem N., Skakkebaek N. E., Leffers H., Rajpert-De Meyts E., Hoei-Hansen C. E., Almstrup K., Nielsen J. E., Brask Sonne S., Graem N., Skakkebaek N. E., Leffers H., and Rajpert-De Meyts E. (2005). Stem cell pluripotency factor NANOG is expressed in human fetal gonocytes, testicular carcinoma in situ and germ cell tumours. *Histopathology* **47**, 48–56. doi:10.1111/j.1365-2559.2005.02182.x

Hofmann M. C. (2008). Gdnf signaling pathways within the mammalian spermatogonial stem cell niche. *Mol. Cell. Endocrinol.* **288**, 95–103. doi:10.1016/j.mce.2008.04.012

Hofmann M. C., Braydich-Stolle L., and Dym M. (2005). Isolation of male germ-line stem cells; Influence of GDNF. *Dev. Biol.* **279**, 95–103. doi:10.1016/j.ydbio.2004.12.006

Hofmann M., Braydich-Stolle L., Dettin L., Johnson E., and Dym M. (2005). Immortalization of mouse germ line stem cells. *Stem Cells* **23**, 200–210.

Hogg K., and Western P. S. (2015). Differentiation of fetal male germline and gonadal progenitor cells is disrupted in organ cultures containing knockout serum replacement. *Stem Cells Dev.* **24**, 2899–2911.

Holstein A. F., Maekawa M., Nagano T., and Davidoff M. S. (1996). Myofibroblasts in the lamina

propria of human seminiferous tubules are dynamic structures of heterogeneous phenotype. *Arch. Histol. Cytol.* **59**, 109–125. doi:10.1679/aohc.59.109

Honaramooz A. (2012). Cryopreservation of testicular tissue. *Curr. Front. Cryobiol. Rijeka INTECH* 209–228.

Honaramooz A. (2014). Reproduction in domestic ruminants VIII : proceedings of the Ninth International Symposium on Reproduction in Domestic Ruminants, Obihiro, Hokkaido, Japan, August 2014. In 'International Symposium on Reproduction in Domestic Ruminants', pp. 257–275

Honaramooz A., Behboodi E., Blash S., Megee S. O., and Dobrinski I. (2003). Germ cell transplantation in goats. *Mol. Reprod. Dev.* **64**, 422–428. doi:10.1002/mrd.10205

Honaramooz A., Behboodi E., Hausler C. L., Blash S., Ayres S., Azuma C., Echelard Y., and Dobrinski I. (2005). Depletion of endogenous germ cells in male pigs and goats in preparation for germ cell transplantation. *J. Androl.* **26**, 698–705. doi:10.2164/jandrol.05032

Honaramooz A., Behboodi E., Megee S. O., Overton S. A., Galantino-Homer H., Echelard Y., and Dobrinski I. (2003). Fertility and germline transmission of donor haplotype following germ cell transplantation in immunocompetent goats. *Biol. Reprod.* doi:10.1095/biolreprod.103.018788

Honaramooz A., Li M.-W., Penedo M. C. T., Meyers S., and Dobrinski I. (2004). Accelerated maturation of primate testis by xenografting into mice. *Biol. Reprod.* **70**, 1500–1503.

Honaramooz A., Megee S. O., and Dobrinski I. (2002). Germ cell transplantation in pigs. *Biol. Reprod.* **66**, 21–28. doi:10.1095/biolreprod66.1.21

Honaramooz A., Megee S., Rathi R., and Dobrinski I. (2007). Building a Testis: Formation of Functional Testis Tissue after Transplantation of Isolated Porcine (Sus scrofa) Testis Cells. *Biol. Reprod.* **76**, 43–47. doi:10.1095/biolreprod.106.054999

Honaramooz A., Megee S., Zeng W., Destrempes M. M., Overton S. A., Luo J., Galantino-Homer H., Modelski M., Chen F., and Blash S. (2008). Adeno-associated virus (AAV)-mediated transduction of male germ line stem cells results in transgene transmission after germ cell transplantation. *FASEB J.* **22**, 374–382.

Honaramooz A., Snedaker A., Boiani M., Schöler H., Dobrinski I., and Schlatt S. (2002). Sperm from neonatal mammalian testes grafted in mice. *Nature* **418**, 778–781. doi:10.1038/nature00918

Honaramooz A., and Yang Y. (2011). Recent advances in application of male germ cell transplantation in farm animals. *Vet. Med. Int.* **2011**, 1–9. doi:10.4061/2011/657860

Honaramooz A., Zeng W., Rathi R., Koster J., Ryder O., and Dobrinski I. (2004). 193 Testis tissue xenografting to preserve germ cells from a cloned banteng calf. *Reprod. Fertil. Dev.* **17**, 247.

Horton J. D., Goldstein J. L., and Brown M. S. (2002). SREBPs: activators of the complete program of cholesterol and fatty acid synthesis in the liver. *J. Clin. Invest.* **109**, 1125–1131.

Hu Y.-C., Nicholls P. K., Soh Y. Q. S., Daniele J. R., Junker J. P., van Oudenaarden A., and Page D. C. (2015). Licensing of primordial germ cells for gametogenesis depends on genital ridge signaling. *PLoS Genet.* **11**, e1005019.

Hu Y.-C., Okumura L. M., and Page D. C. (2013). Gata4 is required for formation of the genital ridge in mice. *PLoS Genet.* **9**, e1003629.

Hua J., Yu H., Liu S., Dou Z., Jing X., Yang C., Lei A., Wang H., and Gao Z. (2009). Derivation and characterization of human embryonic germ cells: serum-free culture and differentiation potential. *Reprod. Biomed. Online* **19**, 238–249.

Huang W., Ding L., Yao J., Hu H., Gao Y., Xie X., Lu M., Deng C., Xie Y., and Wang Z. (2021).

Testicular quantitative ultrasound: A noninvasive monitoring method for evaluating spermatogenic function in busulfan-induced testicular injury mouse models. *Andrologia* **53**, e13927.

Huang S., Sartini B. L., and Parks J. E. (2008). Spermatogenesis in testis xenografts grafted from pre-pubertal Holstein bulls is re-established by stem cell or early spermatogonia. *Anim. Reprod. Sci.* **103**, 1–12. doi:10.1016/j.anireprosci.2006.11.018

Huckins C. (1971). The spermatogonial stem cell population in adult rats. I. Their morphology, proliferation and maturation. *Anat. Rec.* **169**, 533–557. doi:10.1002/ar.1091690306

Huff D. S., Snyder III H. M., Rusnack S. L., Zderic S. A., Carr M. C., and Canning D. A. (2001). Hormonal therapy for the subfertility of cryptorchidism. *Horm. Res. Paediatr.* **55**, 38–40.

Huhtaniemi I. (1989). Endocrine function and regulation of the fetal and neonatal testis. *Int. J. Dev. Biol.* doi:10.1387/ijdb.2485691

Huleihel M., Nourashrafeddin S., and Plant T. M. (2015). Application of three-dimensional culture systems to study mammalian spermatogenesis, with an emphasis on the rhesus monkey (Macaca mulatta). *Asian J. Androl.* **17**, 972–980.

Hutson J. M., Balic A., Nation T., and Southwell B. (2010). Cryptorchidism. *Semin. Pediatr. Surg.* **19**, 215–224. doi:10.1053/j.sempedsurg.2010.04.001

Hutson J. M., and Hasthorpe S. (2005). Abnormalities of testicular descent. *Cell Tissue Res.* **322**, 155–158.

Hutson J. M., Li R., Southwell B. R., Petersen B. L., Thorup J., and Cortes D. (2013). Germ cell development in the postnatal testis: The key to prevent malignancy in cryptorchidism? *Front. Endocrinol. (Lausanne).* **3**, 1–11. doi:10.3389/fendo.2012.00176

Hutson J. M., Southwell B. R., Li R., Lie G., Ismail K., Harisis G., and Chen N. (2013). The regulation of testicular descent and the effects of cryptorchidism. *Endocr. Rev.* **34**, 725–752.

Hwang K., and Lamb D. J. (2010). New advances on the expansion and storage of human spermatogonial stem cells. *Curr. Opin. Urol.* **20**, 510–514. doi:10.1097/MOU.0b013e32833f1b71

Ibtisham F., Awang-Junaidi A. H., and Honaramooz A. (2020). The study and manipulation of spermatogonial stem cells using animal models. *Cell Tissue Res.* **380**, 393–414.

Ibtisham F., and Honaramooz A. (2020). Spermatogonial Stem Cells for In Vitro Spermatogenesis and In Vivo Restoration of Fertility. *Cells* **9**, 1–30.

Iczkowski K. A., Sun E. L., and Gondos B. (1991). Morphometric study of the prepubertal rabbit testis: germ cell numbers and seminiferous tubule dimensions. *Am. J. Anat.* **190**, 266–272.

Ingraham H. A., Lala D. S., Ikeda Y., Luo X., Shen W.-H., Nachtigal M. W., Abbud R., Nilson J. H., and Parker K. L. (1994). The nuclear receptor steroidogenic factor 1 acts at multiple levels of the reproductive axis. *Genes Dev.* **8**, 2302–2312.

Inoue K., Ishizawa M., and Kubota T. (2020). Monoclonal anti-dsDNA antibody 2C10 escorts DNA to intracellular DNA sensors in normal mononuclear cells and stimulates secretion of multiple cytokines implicated in lupus pathogenesis. *Clin. Exp. Immunol.* doi:10.1111/cei.13382

Irie N., Weinberger L., Tang W. W. C., Kobayashi T., Viukov S., Manor Y. S., Dietmann S., Hanna J. H., and Surani M. A. (2015). SOX17 is a critical specifier of human primordial germ cell fate. *Cell* **160**, 253–268.

Ishikawa H., and Schuman J. S. (2004). Anterior segment imaging: Ultrasound biomicroscopy. *Ophthalmol. Clin. North Am.* **17**, 7–20. doi:10.1016/j.ohc.2003.12.001

Ito M., Yokouchi K., Yoshida K., Kano K., Naito K., Miyazaki J., and Tojo H. (2006).

Investigation of the fate of Sry-expressing cells using an in vivo Cre/loxP system. *Dev. Growth Differ.* **48**, 41–47.
Izadpanah R., Trygg C., Patel B., Kriedt C., Dufour J., Gimble J. M., and Bunnell B. A. (2006). Biologic properties of mesenchymal stem cells derived from bone marrow and adipose tissue. *J. Cell. Biochem.* **99**, 1285–1297.
Izadyar F., Den Ouden K., Creemers L. B., Posthuma G., Parvinen M., and de Rooij D. G. (2003). Proliferation and differentiation of bovine type A spermatogonia during long-term culture. *Biol. Reprod.* **68**, 272–281.
Izadyar F., Pau F., Marh J., Slepko N., Wang T., Gonzalez R., Ramos T., Howerton K., Sayre C., and Silva F. (2008). Generation of multipotent cell lines from a distinct population of male germ line stem cells. *Reproduction* **135**, 771–784.
Izadyar F., Spierenberg G. T., Creemers L. B., Ouden K. den, and De Rooij D. G. (2002). Isolation and purification of type A spermatogonia from the bovine testis. *Reproduction* **124**, 85–94.
Jacobsen G. K. (1983). Alpha-fetoprotein (AFP) and human chorionic gonadotropin (HCG) in testicular germ cell tumours: a comparison of histologic and serologic occurrence of tumour markers. *Acta Pathol. Microbiol. Scand. Ser. A Pathol.* **91**, 183–190.
Jaffré F., Friedman A. E., Hu Z., MacKman N., and Blaxall B. C. (2012). β-Adrenergic receptor stimulation transactivates protease-activated receptor 1 via matrix metalloproteinase 13 in cardiac cells. *Circulation* **125**, 2993–3003. doi:10.1161/CIRCULATIONAHA.111.066787
Jahnukainen K., Ehmcke J., Hergenrother S. D., and Schlatt S. (2007). Effect of cold storage and cryopreservation of immature non-human primate testicular tissue on spermatogonial stem cell potential in xenografts. *Hum. Reprod.* **22**, 1060–1067.
Jaillard C., Chatelain P. G., and Saez J. M. (1987). In Vitro Regulation of Pig Sertoli Cell Growth and Function: Effects of Fibroblast Growth Factor and Somatomedin-C1. *Biol. Reprod.* **37**, 665–675. doi:10.1095/biolreprod37.3.665
Jaiswal R. S., Singh J., and Adams G. P. (2009). High-resolution ultrasound biomicroscopy for monitoring ovarian structures in mice. *Reprod. Biol. Endocrinol.* **7**, 1–7. doi:10.1186/1477-7827-7-69
Jameson S. A., Lin Y. T., and Capel B. (2012). Testis development requires the repression of Wnt4 by Fgf signaling. *Dev. Biol.* **370**, 24–32. doi:10.1016/j.ydbio.2012.06.009
Jan S. Z., Hamer G., Repping S., de Rooij D. G., van Pelt A. M. M., and Vormer T. L. (2012). Molecular control of rodent spermatogenesis. *Biochim. Biophys. Acta (BBA)-Molecular Basis Dis.* **1822**, 1838–1850.
Des Jardins C. (1993). 'Cell and molecular biology of the testis.' (C Des Jardins and LL Ewing, Eds.). (University Press, New York)
Javanmardy S., Asadi Mh., Movahedin M., Moradpour F., and Bahadoran H. (2016). Derivation of motor neuron-like cells from neonatal mouse testis in a simple culture condition. *Andrologia* **48**, 1100–1107.
Jenab S., and Morris P. L. (1998). Testicular leukemia inhibitory factor (LIF) and LIF receptor mediate phosphorylation of signal transducers and activators of transcription (STAT)-3 and STAT-1 and induce c-fos transcription and activator protein-1 activation in rat Sertoli but not germ ce. *Endocrinology* **139**, 1883–1890. doi:10.1210/endo.139.4.5871
Jeong D., McLean D. J., and Griswold M. D. (2003). Long-term culture and transplantation of murine testicular germ cells. *J. Androl.* **24**, 661–669.
Jiang F. X. (2001). Male germ cell transplantation: Promise and problems. *Reprod. Fertil. Dev.* **13**, 609–614. doi:10.1071/rd01059

Jiang F.-X., and Short R. V (1995). Male germ cell transplantation in rats: apparent synchronization of spermatogenesis between host and donor seminiferous epithelia. *Int. J. Androl.* **18**, 326–330. doi:https://doi.org/10.1111/j.1365-2605.1995.tb00570.x

Jiang F. X., and Short R. V. (1998a). Male germ cell transplantation: Present achievements and future prospects. *Int. J. Dev. Biol.* **42**, 1067–1073. doi:10.1387/ijdb.9853838

Jiang F. X., and Short R. V. (1998b). Different fate of primordial germ cells and gonocytes following transplantation. *APMIS* **106**, 58–62. doi:10.1111/j.1699-0463.1998.tb01319.x

Jiang X., Skibba M., Zhang C., Tan Y., Xin Y., and Qu Y. (2013). The roles of fibroblast growth factors in the testicular development and tumor. *J. Diabetes Res.* **2013**, 1–8.

Jing S., Wen D., Yu Y., Holst P. L., Luo Y., Fang M., Tamir R., Antonio L., Hu Z., Cupples R., Louis J.-C., Hu S., Altrock B. W., and Fox G. M. (1996). GDNF–Induced Activation of the Ret Protein Tyrosine Kinase Is Mediated by GDNFR-α, a Novel Receptor for GDNF. *Cell* **85**, 1113–1124. doi:https://doi.org/10.1016/S0092-8674(00)81311-2

Job J.-C., Toublanc J.-E., Chaussain J.-L., Gendrel D., Garnier P., and Roger M. (1988). Endocrine and immunological findings in cryptorchid infants. *Hormones* **30**, 167–172.

Johnston D. S., Olivas E., DiCandeloro P., and Wright W. W. (2011). Stage-specific changes in GDNF expression by rat Sertoli cells: a possible regulator of the replication and differentiation of stem spermatogonia. *Biol. Reprod.* **85**, 763–769.

Jones D. L., and Fuller M. T. (2009). Chapter 7 - Stem Cell Niches. 'Essentials of Stem Cell Biology (Second Edition)'. (Eds R Lanza, J Gearhart, B Hogan, D Melton, R Pedersen, ED Thomas, J Thomson and I Wilmut) pp. 61–72. (Academic Press: San Diego) doi:https://doi.org/10.1016/B978-0-12-374729-7.00007-X

de Jong J., Stoop H., Gillis A. J. M., Van Gurp R., van de Geijn G., Boer M. de, Hersmus R., Saunders P. T. K., Anderson R. A., and Oosterhuis J. W. (2008). Differential expression of SOX17 and SOX2 in germ cells and stem cells has biological and clinical implications. *J. Pathol. A J. Pathol. Soc. Gt. Britain Irel.* **215**, 21–30.

Kakiuchi K., Taniguchi K., and Kubota H. (2018). Conserved and non-conserved characteristics of porcine glial cell line-derived neurotrophic factor expressed in the testis. *Sci. Rep.* **8**, 1–14. doi:10.1038/s41598-018-25924-5

Kalds P., Zhou S., Cai B., Liu J., Wang Y., Petersen B., Sonstegard T., Wang X., and Chen Y. (2019). Sheep and goat genome engineering: From random transgenesis to the CRISPR era. *Front. Genet.* **10**, 1–27. doi:10.3389/fgene.2019.00750

Kanamori M., Oikawa K., Tanemura K., and Hara K. (2019). Mammalian germ cell migration during development, growth, and homeostasis. *Reprod. Med. Biol.* **18**, 247–255.

Kanatsu-Shinohara M. (2005). Genetic and epigenetic properties of mouse male germline stem cells during long-term culture. *Development* **29**, 1001–1012. doi:10.1242/dev.02004

Kanatsu-Shinohara M., Inoue K., Lee J., Yoshimoto M., Ogonuki N., Miki H., Baba S., Kato T., Kazuki Y., Toyokuni S., Toyoshima M., Niwa O., Oshimura M., Heike T., Nakahata T., Ishino F., Ogura A., and Shinohara T. (2004). Generation of pluripotent stem cells from neonatal mouse testis. *Cell*. doi:10.1016/j.cell.2004.11.011

Kanatsu-Shinohara M., Inoue K., Ogonuki N., Miki H., Yoshida S., Toyokuni S., Lee J., Ogura A., and Shinohara T. (2007). Leukemia inhibitory factor enhances formation of germ cell colonies in neonatal mouse testis culture. *Biol. Reprod.* **76**, 55–62. doi:10.1095/biolreprod.106.055863

Kanatsu-Shinohara M., Inoue K., Ogonuki N., Morimoto H., Ogura A., and Shinohara T. (2011). Serum- and feeder-free culture of mouse germline stem cells. *Biol. Reprod.* **84**, 97–105.

doi:10.1095/biolreprod.110.086462
Kanatsu-Shinohara M., Inoue K., Takashima S., Takehashi M., Ogonuki N., Morimoto H., Nagasawa T., Ogura A., and Shinohara T. (2012). Reconstitution of mouse spermatogonial stem cell niches in culture. *Cell Stem Cell* **11**, 567–578. doi:10.1016/j.stem.2012.06.011
Kanatsu-Shinohara M., Muneto T., Lee J., Takenaka M., Chuma S., Nakatsuji N., Horiuchi T., and Shinohara T. (2008). Long-term culture of male germline stem cells from hamster testes. *Biol. Reprod.* **78**, 611–617. doi:10.1095/biolreprod.107.065615
Kanatsu-Shinohara M., Ogonuki N., Inoue K., Miki H., Ogura A., Toyokuni S., and Shinohara T. (2003). Long-term proliferation in culture and germline transmission of mouse male germline stem cells. *Biol. Reprod.* **69**, 612–616. doi:10.1095/biolreprod.103.017012
Kanatsu-Shinohara M., Ogonuki N., Matoba S., Morimoto H., Ogura A., and Shinohara T. (2014). Improved serum- and feeder-free culture of mouse germline stem cells. *Biol. Reprod.* **91**, 1–11. doi:10.1095/biolreprod.114.122317
Kanatsu-Shinohara M., and Shinohara T. (2013). Spermatogonial Stem Cell Self-Renewal and Development. *Annu. Rev. Cell Dev. Biol.* **29**, 163–187. doi:10.1146/annurev-cellbio-101512-122353
Kanatsu-Shinohara M., Toyokuni S., Morimoto T., Matsui S., Honjo T., and Shinohara T. (2003). Functional assessment of self-renewal activity of male germline stem cells following cytotoxic damage and serial transplantation. *Biol. Reprod.* **68**, 1801–1807.
Kanatsu-Shinohara M., Toyokuni S., and Shinohara T. (2004a). Transgenic mice produced by retroviral transduction of male germ line stem cells in vivo. *Biol. Reprod.* **71**, 1202–1207. doi:10.1095/biolreprod.104.031294
Kanatsu-Shinohara M., Toyokuni S., and Shinohara T. (2004b). CD9 is a surface marker on mouse and rat male germline stem cells. *Biol. Reprod.* doi:10.1095/biolreprod.103.020867
Kanatsu-Shinohara M., Avarbock M. R., and Brinster R. L. (1999). Beta1- and alpha6-integrin are surface markers on mouse spermatogonial stem cells. *Proc. Natl. Acad. Sci.* **96**, 5504–5509.
Kaneko H., Kikuchi K., Nakai M., Tanihara F., Noguchi J., Noguchi M., Ito J., and Kashiwazaki N. (2012). Normal reproductive development of offspring derived by intracytoplasmic injection of porcine sperm grown in host mice. *Theriogenology* **78**, 898–906.
Kang J. W., Koo H. C., Hwang S. Y., Kang S. K., Ra J. C., Lee M. H., and Park Y. H. (2012). Immunomodulatory effects of human amniotic membrane-derived mesenchymal stem cells. *J. Vet. Sci.* **13**, 23–31.
Kanoh M., Ye P., Zhu W., Wiggins R. C., and Konat G. (1991). Effect of culture conditions on PLP and MAG gene expression in rat glioma C6 cells. *Metab. Brain Dis.* **6**, 133–143.
Kapałczyńska M., Kolenda T., Przybyła W., Zajączkowska M., Teresiak A., Filas V., Ibbs M., Bliźniak R., Łuczewski Ł., and Lamperska K. (2018). 2D and 3D cell cultures–a comparison of different types of cancer cell cultures. *Arch. Med. Sci. AMS* **14**, 910–919.
Karl J., and Capel B. (1998). Sertoli cells of the mouse testis originate from the coelomic epithelium. *Dev. Biol.* **203**, 323–333. doi:10.1006/dbio.1998.9068
Kawamura M., Miyagawa S., Miki K., Saito A., Fukushima S., Higuchi T., Kawamura T., Kuratani T., Daimon T., and Shimizu T. (2012). Feasibility, safety, and therapeutic efficacy of human induced pluripotent stem cell-derived cardiomyocyte sheets in a porcine ischemic cardiomyopathy model. *Circulation* **126**, S29–S37.
Kawasaki T., Imura F., Nakada A., Kubota H., Sakamaki K., Abe S., and Takamune K. (2006). Functional demonstration of the ability of a primary spermatogonium as a stem cell by tracing a single cell destiny in Xenopus laevis. *Dev. Growth Differ.* **48**, 525–535.

Kawasaki T., Saito K., Shinya M., Olsen L. C., and Sakai N. (2010). Regeneration of spermatogenesis and production of functional sperm by grafting of testicular cell aggregates in Zebrafish (Danio rerio). *Biol. Reprod.* **83**, 533–539.

Kayalioglu G., Altay B., Uyaroglu F. G., Bademkiran F., Uludag B., and Ertekin C. (2008). Morphology and innervation of the human cremaster muscle in relation to its function. *Anat. Rec. Adv. Integr. Anat. Evol. Biol. Adv. Integr. Anat. Evol. Biol.* **291**, 790–796.

Kerr C. L., Hill C. M., Blumenthal P. D., and Gearhart J. D. (2008). Expression of pluripotent stem cell markers in the human fetal ovary. *Hum. Reprod.* **23**, 589–599.

Ketelslegers J.-M., Hetzel W. D., Sherins Rj., and Catt K. J. (1978). Developmental changes in testicular gonadotropin receptors: plasma gonadotropins and plasma testosterone in the rat. *Endocrinology* **103**, 212–222.

Khaira H., McLean D., Ohl D. A., and Smith G. D. (2005). Spermatogonial stem cell isolation, storage, and transplantation. *J. Androl.* **26**, 442–450.

Khan S. A., Ndjountche L., Pratchard L., Spicer L. J., and Davis J. S. (2002). Follicle-stimulating hormone amplifies insulin-like growth factor I-mediated activation of AKT/protein kinase B signaling in immature rat Sertoli cells. *Endocrinology* **143**, 2259–2267.

Kim S., and Belmonte J. C. I. (2011). Pluripotency of male germline stem cells. *Mol. Cells* **32**, 113–121. doi:10.1007/s10059-011-1024-4

Kim Y., Bingham N., Sekido R., Parker K. L., Lovell-Badge R., and Capel B. (2007). Fibroblast growth factor receptor 2 regulates proliferation and Sertoli differentiation during male sex determination. *Proc. Natl. Acad. Sci. U. S. A.* **104**, 16558–16563. doi:10.1073/pnas.0702581104

Kim B.-G., Cho C. M., Lee Y.-A., Kim B.-J., Kim K.-J., Kim Y.-H., Min K.-S., Kim C. G., and Ryu B.-Y. (2010). Enrichment of testicular gonocytes and genetic modification using lentiviral transduction in pigs. *Biol. Reprod.* **82**, 1162–1169. doi:10.1095/biolreprod.109.079558

Kim S. M., Fujihara M., Sahare M., Minami N., Yamada M., and Imai H. (2014). Effects of extracellular matrices and lectin Dolichos biflorus agglutinin on cell adhesion and self-renewal of bovine gonocytes cultured in vitro. *Reprod. Fertil. Dev.* **26**, 268–281. doi:10.1071/RD12214

Kim Y. H., Kim B. J., Kim B. G., Lee Y. A., Kim K. J., Chung H. J., Hwang S., Woo J. S., Park J. K., Schmidt J. A., Pang M. G., and Ryu B. Y. (2013). Stage-specific embryonic antigen-1 expression by undifferentiated spermatogonia in the prepubertal boar testis. *J. Anim. Sci.* **91**, 3143–3154. doi:10.2527/jas.2012-6139

Kim B.-J., Lee Y.-A., Kim K.-J., Kim Y.-H., Jung M.-S., Ha S.-J., Kang H.-G., Jung S.-E., Kim B.-G., and Choi Y.-R. (2015). Effects of paracrine factors on CD24 expression and neural differentiation of male germline stem cells. *Int. J. Mol. Med.* **36**, 255–262.

Kim Y., Selvaraj V., Dobrinski I., Lee H., Mcentee M. C., and Travis A. J. (2006). Recipient preparation and mixed germ cell isolation for spermatogonial stem cell transplantation in domestic cats. *J. Androl.* **27**, 248–256. doi:10.2164/jandrol.05034

Kim Y., Selvaraj V., Pukazhenthi B., and Travis A. J. (2007). Effect of donor age on success of spermatogenesis in feline testis xenografts. *Reprod. Fertil. Dev.* **19**, 869–876.

Kim Y., Turner D., Nelson J., Dobrinski I., McEntee M., and Travis A. J. (2008). Production of donor-derived sperm after spermatogonial stem cell transplantation in the dog. *Reproduction* **136**, 823–831. doi:10.1530/REP-08-0226

Kim J. B., Zaehres H., Wu G., Gentile L., Ko K., Sebastiano V., Araúzo-Bravo M. J., Ruau D.,

Han D. W., and Zenke M. (2008). Pluripotent stem cells induced from adult neural stem cells by reprogramming with two factors. *Nature* **454**, 646–650.
Kispert A., and Gossler A. (2004). Chapter 11 - Introduction to Early Mouse Development. 'The Laboratory Mouse'. (Eds HJ Hedrich and G Bullock) pp. 175–191. (Academic Press: London) doi:https://doi.org/10.1016/B978-012336425-8/50064-9
Kita K., Watanabe T., Ohsaka K., Hayashi H., Kubota Y., Nagashima Y., Aoki I., Taniguchi H., Noce T., Inoue K., Miki H., Ogonuki N., Tanaka H., Ogura A., and Ogawa T. (2007). Production of Functional Spermatids from Mouse Germline Stem Cells in Ectopically Reconstituted Seminiferous Tubules. *Biol. Reprod.* **76**, 211–217. doi:10.1095/biolreprod.106.056895
Klamt B., Koziell A., Poulat F., Wieacker P., Scambler P., Berta P., and Gessler M. (1998). Frasier syndrome is caused by defective alternative splicing of WT1 leading to an altered ratio of WT1+/− KTS splice isoforms. *Hum. Mol. Genet.* **7**, 709–714.
Klonisch T., Fowler P. A., and Hombach-Klonisch S. (2004). Molecular and genetic regulation of testis descent and external genitalia development. *Dev. Biol.* **270**, 1–18. doi:10.1016/j.ydbio.2004.02.018
Kluin P. M., and de Rooij D. G. (1981). A comparison between the morphology and cell kinetics of gonocytes and adult type undifferentiated spermatogonia in the mouse. *Int. J. Androl.* **4**, 475–493.
Ko K., Tapia N., Wu G., Kim J. B., Bravo M. J. A., Sasse P., Glaser T., Ruau D., Han D. W., Greber B., Hausdörfer K., Sebastiano V., Stehling M., Fleischmann B. K., Brüstle O., Zenke M., and Schöler H. R. (2009). Induction of Pluripotency in Adult Unipotent Germline Stem Cells. *Cell Stem Cell* **5**, 87–96. doi:10.1016/j.stem.2009.05.025
Komeya M., Kimura H., Nakamura H., Yokonishi T., Sato T., Kojima K., Hayashi K., Katagiri K., Yamanaka H., and Sanjo H. (2016). Long-term ex vivo maintenance of testis tissues producing fertile sperm in a microfluidic device. *Sci. Rep.* **6**, 1–10.
Koopman P., Gubbay J., Vivian N., Goodfellow P., and Lovell-Badge R. (1991). Male development of chromosomally female mice transgenic for Sry. *Nature* **351**, 117–121. doi:10.1038/351117a0
Koopman P., Münsterberg A., Capel B., Vivian N., and Lovell-Badge R. (1990). Expression of a candidate sex-determining gene during mouse testis differentiation. *Nature* **348**, 450–452. doi:10.1038/348450a0
Koshimizu U., Watanabe D., Tajima Y., and Nishimune Y. (1992). Effects of W (c-kit) gene mutation on gametogenesis in male mice: agametic tubular segments in Wf/Wf testes. *Development* **114**, 861–867.
Koskenniemi J. J., Virtanen H. E., and Toppari J. (2017). Testicular growth and development in puberty. *Curr. Opin. Endocrinol. Diabetes Obes.* **24**, 215–224.
Kossack N., Meneses J., Shefi S., Nguyen H. N., Chavez S., Nicholas C., Gromoll J., Turek P. J., and Reijo-Pera R. A. (2009). Isolation and characterization of pluripotent human spermatogonial stem cell-derived cells. *Stem Cells* **27**, 138–149.
Koubova J., Menke D. B., Zhou Q., Cape B., Griswold M. D., and Page D. C. (2006). Retinoic acid regulates sex-specific timing of meiotic initiation in mice. *Proc. Natl. Acad. Sci. U. S. A.* **103**, 2474–2479. doi:10.1073/pnas.0510813103
Kreidberg J. A., Sariola H., Loring J. M., Maeda M., Pelletier J., Housman D., and Jaenisch R. (1993). WT-1 is required for early kidney development. *Cell* **74**, 679–691.
Kriks S., Shim J.-W., Piao J., Ganat Y. M., Wakeman D. R., Xie Z., Carrillo-Reid L., Auyeung

G., Antonacci C., and Buch A. (2011). Dopamine neurons derived from human ES cells efficiently engraft in animal models of Parkinson's disease. *Nature* **480**, 547–551.

Kubota H., Avarbock M. R., and Brinster R. L. (2003). Spermatogonial stem cells share some, but not all, phenotypic and functional characteristics with other stem cells. *Proc. Natl. Acad. Sci.* **100**, 6487–6492.

Kubota H., Avarbock M. R., and Brinster R. L. (2004a). Culture conditions and single growth factors affect fate determination of mouse spermatogonial stem cells. *Biol. Reprod.* **71**, 722–731. doi:10.1095/biolreprod.104.029207

Kubota H., Avarbock M. R., and Brinster R. L. (2004b). Growth factors essential for self-renewal and expansion of mouse spermatogonial stem cells. *Proc. Natl. Acad. Sci.* **101**, 16489–16494. doi:10.1073/pnas.0407063101

Kubota H., and Brinster R. L. (2006). Technology insight: In vitro culture of spermatogonial stem cells and their potential therapeutic uses. *Nat. Clin. Pract. Endocrinol. Metab.* **2**, 99–108. doi:10.1038/ncpendmet0098

Kubota H., and Brinster R. L. (2018). Spermatogonial stem cells. *Biol. Reprod.* **99**, 52–74. doi:10.1093/biolre/ioy077

Kubota H., Wu X., Goodyear S. M., Avarbock M. R., and Brinster R. L. (2011). Glial cell line-derived neurotrophic factor and endothelial cells promote self-renewal of rabbit germ cells with spermatogonial stem cell properties. *FASEB J.* **25**, 2604–2614. doi:10.1096/fj.10-175802

Kuijk E. W., Colenbrander B., and Roelen B. A. J. (2009). The effects of growth factors on in vitro-cultured porcine testicular cells. *Reproduction* **138**, 721–731. doi:10.1530/rep-09-0138

Kuijk E. W., de Gier J., Chuva de Sousa Lopes S. M., Chambers I., van Pelt A. M. M., Colenbrander B., and Roelen B. A. J. (2010). A distinct expression pattern in mammalian testes indicates a conserved role for NANOG in spermatogenesis. *PLoS One* **5**, e10957. doi:10.1371/journal.pone.0010987

Kumar R. S., Sudhakaran S., and Aung T. (2016). Angle-closure glaucoma: Imaging. 'Pearls of Glaucoma Management: Second Edition'. pp. 517–531 doi:10.1007/978-3-662-49042-6_56

Kumar D., Talluri T. R., Selokar N. L., Hyder I., and Kues W. A. (2021). Perspectives of pluripotent stem cells in livestock. *World J. Stem Cells* **13**, 1–29.

Kusaka M., Katoh-Fukui Y., Ogawa H., Miyabayashi K., Baba T., Shima Y., Sugiyama N., Sugimoto Y., Okuno Y., Kodama R., Iizuka-Kogo A., Senda T., Sasaoka T., Kitamura K., Aizawa S., and Morohashi K. I. (2010). Abnormal epithelial cell polarity and ectopic Epidermal Growth Factor Receptor (EGFR) expression induced in Emx2 KO Embryonic Gonads. *Endocrinology* **151**, 5893–5904. doi:10.1210/en.2010-0915

Lamb D. J. (1993). Growth factors and testicular development. *J. Urol.* **150**, 583–592. doi:10.1016/S0022-5347(17)35557-X

Lange U. C., Adams D. J., Lee C., Barton S., Schneider R., Bradley A., and Surani M. A. (2008). Normal germ line establishment in mice carrying a deletion of the Ifitm/Fragilis gene family cluster. *Mol. Cell. Biol.* **28**, 4688–4696.

Langenstroth D., Kossack N., Westernströer B., Wistuba J., Behr R., Gromoll J., and Schlatt S. (2014). Separation of somatic and germ cells is required to establish primate spermatogonial cultures. *Hum. Reprod.* **29**, 2018–2031.

Lara N. L. M., Costa G. M. J., Avelar G. F., Lacerda S. M. S. N., Hess R. A., and de França L. R. (2018). Testis Physiology–Overview and Histology. 'Encyclopedia of Reproduction (Second Edition)'. (Ed MK Skinner) pp. 105–116. (Academic Press: Oxford)

doi:https://doi.org/10.1016/B978-0-12-801238-3.64567-1
Larney C., Bailey T. L., and Koopman P. (2014). Switching on sex: Transcriptional regulation of the testis-determining gene Sry. *Development* **141**, 2195–2205. doi:10.1242/dev.107052
Larue L., Ohsugi M., Hirchenhain J., and Kemler R. (1994). E-cadherin null mutant embryos fail to form a trophectoderm epithelium. *Proc. Natl. Acad. Sci. U. S. A.* **91**, 8263–8267. doi:10.1073/pnas.91.17.8263
Laufer E., Kesper D., Vortkamp A., and King P. (2012). Sonic hedgehog signaling during adrenal development. *Mol. Cell. Endocrinol.* **351**, 19–27.
Lawson K. A., Dunn N. R., Roelen B. A. J., Zeinstra L. M., Davis A. M., Wright C. V. E., Korving J. P. W. F. M., and Hogan B. L. M. (1999). Bmp4 is required for the generation of primordial germ cells in the mouse embryo. *Genes Dev.* **13**, 434–436. doi:10.1101/gad.13.4.424
Lawson K. A., and Hage W. J. (1994). Clonal analysis of the origin of primordial germ cells in the mouse. *Ciba Found. Symp.* **182**, 68–84. doi:10.1002/9780470514573.ch5
Lee J., Kanatsu-Shinohara M., Inoue K., Ogonuki N., Miki H., Toyokuni S., Kimura T., Nakano T., Ogura A., and Shinohara T. (2007). Akt mediates self-renewal division of mouse spermatogonial stem cells. *Development* **134**, 1853–1859.
Lee J. H., Kim H. J., Kim H., Lee S. J., and Gye M. C. (2006). In vitro spermatogenesis by three-dimensional culture of rat testicular cells in collagen gel matrix. *Biomaterials* **27**, 2845–2853.
Lee W. Y., Park H. J., Lee R., Lee K. H., Kim Y. H., Ryu B. Y., Kim N. H., Kim J. H., Kim J. H., Moon S. H., Park J. K., Chung H. J., Kim D. H., and Song H. (2013). Establishment and in vitro culture of porcine spermatogonial germ cells in low temperature culture conditions. *Stem Cell Res.* **11**, 1234–249. doi:10.1016/j.scr.2013.08.008
Lefebvre V., Huang W., Harley V. R., Goodfellow P. N., and de Crombrugghe B. (1997). SOX9 is a potent activator of the chondrocyte-specific enhancer of the pro alpha1(II) collagen gene. *Mol. Cell. Biol.* **17**, 2336–2346. doi:10.1128/mcb.17.4.2336
Lehmann R. (2012). Germline stem cells: origin and destiny. *Cell Stem Cell* **10**, 729–739.
Leitch H. G., Tang W. W. C., and Surani M. A. (2013). Chapter 5 - Primordial Germ-Cell Development and Epigenetic Reprogramming in Mammals. 'Epigenetics and Development'. (Ed E Heard) Current Topics in Developmental Biology. pp. 149–187. (Academic Press) doi:https://doi.org/10.1016/B978-0-12-416027-9.00005-X
Lempiäinen A., Sankila A., Hotakainen K., Haglund C., Blomqvist C., and Stenman U.-H. (2014). Expression of human chorionic gonadotropin in testicular germ cell tumors. *Urol. Oncol. Semin. Orig. Investig.* **32**, 727–734.
Li J. Y. H., and Joyner A. L. (2001). Otx2 and Gbx2 are required for refinement and not induction of mid-hindbrain gene expression. *Development* **128**, 4979–4991.
Li H., MacLean G., Cameron D., Clagett-Dame M., and Petkovich M. (2009). Cyp26b1 expression in murine Sertoli cells is required to maintain male germ cells in an undifferentiated state during embryogenesis. *PLoS One* **4**, e7501.
Li H., Papadopoulos V., Vidic B., Dym M., and Culty M. (1997). Regulation of rat testis gonocyte proliferation by platelet-derived growth factor and estradiol: identification of signaling mechanisms involved. *Endocrinology* **138**, 1289–1298. doi:10.1210/endo.138.3.5021
Li B. C., Tian Z. Q., Sun M., Xu Q., Wang X. Y., Qin Y. R., Xu F., Gao B., Wang K. H., and Sun H. C. (2010). Directional differentiation of chicken primordial germ cells into adipocytes, neuron-like cells, and osteoblasts. *Mol. Reprod. Dev.* **77**, 795–801.
Li B., Wang X.-Y., Tian Z., Xiao X.-J., Xu Q., Wei C.-X., Sun H.-C., and Chen G.-H. (2010). Directional differentiation of chicken spermatogonial stem cells in vitro. *Cytotherapy* **12**,

326–331.
Li X., Wang C., Xiao J., McKeehan W. L., and Wang F. (2016). Fibroblast Growth Factors, old kids on the new block. *Semin. Cell Dev. Biol.* **53**, 155–1667.
de Lima e Martins Lara N., Costa G. M. J., Avelar G. F., Guimarães D. A., and França L. R. (2019). Postnatal testis development in the collared peccary (Tayassu tajacu), with emphasis on spermatogonial stem cells markers and niche. *Gen. Comp. Endocrinol.* **273**, 98–107. doi:https://doi.org/10.1016/j.ygcen.2018.05.013
Ling V., and Neben S. (1997). In vitro differentiation of embryonic stem cells: immunophenotypic analysis of cultured embryoid bodies. *J. Cell. Physiol.* **171**, 104–115.
Liu F., Cai C., Wu X., Cheng Y., Lin T., Wei G., and He D. (2016). Effect of Knock-out serum replacement on germ cell development of immature testis tissue culture. *Theriogenology* **85**, 193–199. doi:10.1016/j.theriogenology.2015.09.012
Liu A., Joyner A. L., and Turnbull D. H. (1998). Alteration of limb and brain patterning in early mouse embryos by ultrasound-guided injection of Shh-expressing cells. *Mech. Dev.* **75**, 107–115. doi:10.1016/S0925-4773(98)00090-2
Livera G., Rouiller-Fabre V., Durand P., and Habert R. (2000). Multiple effects of retinoids on the development of Sertoli, germ, and Leydig cells of fetal and neonatal rat testis in culture. *Biol. Reprod.* **62**, 1303–1314.
Lo K. C., Brugh III V. M., Parker M., and Lamb D. J. (2005). Isolation and enrichment of murine spermatogonial stem cells using rhodamine 123 mitochondrial dye. *Biol. Reprod.* **72**, 767–771.
Lording D. W., and De Kretser D. M. (1972). Comparative ultrastructural and histochemical studies of the interstitial cells of the rat testis during fetal and postnatal development. *J. Reprod. Fertil.* **29**, 261–269. doi:10.1530/jrf.0.0290261
Luan N. T., Sharma N., Kim S.-W., Ha P. T. H., Hong Y.-H., Oh S.-J., and Jeong D.-K. (2014). Characterization and cardiac differentiation of chicken spermatogonial stem cells. *Anim. Reprod. Sci.* **151**, 244–255.
Luckenbach A., and Yamamoto Y. (2018). Genetic & Environmental Sex Determination in Cold-blooded Vertebrates: Fishes, Amphibians, and Reptiles. 'Encyclopedia of Reproduction (Second Edition)'. (Ed MK Skinner) pp. 176–183. (Academic Press: Oxford) doi:https://doi.org/10.1016/B978-0-12-809633-8.20553-0
Lund R. D., Wang S., Klimanskaya I., Holmes T., Ramos-Kelsey R., Lu B., Girman S., Bischoff N., Sauvé Y., and Lanza R. (2006). Human embryonic stem cell–derived cells rescue visual function in dystrophic RCS rats. *Cloning Stem Cells* **8**, 189–199.
Luo J., Megee S., Rathi R., and Dobrinski I. (2006). Protein gene product 9.5 is a spermatogonia-specific marker in the pig testis: Application to enrichment and culture of porcine spermatogonia. *Mol. Reprod. Dev.* **73**, 1531–1540. doi:10.1002/mrd.20529
Mackay S., and Smith R. A. (2007). Effects of growth factors on testicular morphogenesis. *Int. Rev. Cytol.* **260**, 113–173.
Mackie E. J. (2003). Osteoblasts: novel roles in orchestration of skeletal architecture. *Int. J. Biochem. Cell Biol.* **35**, 1301–1305.
MacLean G., Li H., Metzger D., Chambon P., and Petkovich M. (2007). Apoptotic extinction of germ cells in testes of Cyp26b1 knockout mice. *Endocrinology* **148**, 4560–4567.
Maekawa M., Kamimura K., and Nagano T. (1996). Peritubular myoid cells in the testis : Their structure and function. *Archives of Histology and Cytology*. doi:10.1679/aohc.59.1
Mäkelä J. A., Koskenniemi J. J., Virtanen H. E., and Toppari J. Testis development. *Endocr. Rev.*

40, 857–905.
Mäkelä J. A., Koskenniemi J. J., Virtanen H. E., and Toppari J. (2019). Testis Development. *Endocrine Reviews*. doi:10.1210/er.2018-00140
Manku G., and Culty M. (2015). Mammalian gonocyte and spermatogonia differentiation: recent advances and remaining challenges. *Reproduction* **149**, R139–R157.
Manku G., Wang Y., Merkbaoui V., Boisvert A., Ye X., Blonder J., and Culty M. (2015). Role of retinoic acid and platelet-derived growth factor receptor cross talk in the regulation of neonatal gonocyte and embryonal carcinoma cell differentiation. *Endocrinology* **156**, 346–359.
Marh J., Tres L. L., Yamazaki Y., Yanagimachi R., and Kierszenbaum A. L. (2003). Mouse round spermatids developed in vitro from preexisting spermatocytes can produce normal offspring by nuclear injection into in vivo-developed mature oocytes. *Biol. Reprod.* **69**, 169–176.
Markert C. L. (1979). Gametogenesis, fertilization and early development. In 'Mead Johnson Symposium on Perinatal and Developmental Medicine', pp. 3–6
Marret C., and Durand P. (2000). Culture of porcine spermatogonia: effects of purification of the germ cells, extracellular matrix and fetal calf serum on their survival and multiplication. *Reprod. Nutr. Dev.* **40**, 305–319. doi:10.1051/rnd:2000127
Marshall G. R., and Plant T. M. (1996). Puberty occurring either spontaneously or induced precociously in rhesus monkey (Macaca mulatta) is associated with a marked proliferation of Sertoli cells. *Biol. Reprod.* **54**, 1192–1199.
Marziali G., Lazzaro D., and Sorrentino V. (1993). Binding of germ cells to mutant SId Sertoli cells is defective and is rescued by expression of the transmembrane form of the c-kit ligand. *Dev. Biol.* **157**, 182–190.
Masaki K., Sakai M., Kuroki S., Jo J.-I., Hoshina K., Fujimori Y., Oka K., Amano T., Yamanaka T., and Tachibana M. (2018). FGF2 has distinct molecular functions from GDNF in the mouse germline niche. *Stem Cell Reports* **10**, 1782–1792.
Matsui Y., Zsebo K., and Hogan B. L. M. (1992). Derivation of pluripotential embryonic stem cells from murine primordial germ cells in culture. *Cell* **70**, 841–847. doi:10.1016/0092-8674(92)90317-6
Matthiesson K. L., Stanton P. G., O'Donnell L., Meachem S. J., Amory J. K., Berger R., Bremner W. J., and McLachlan R. I. (2005). Effects of testosterone and levonorgestrel combined with a 5α-reductase inhibitor or gonadotropin-releasing hormone antagonist on spermatogenesis and intratesticular steroid levels in normal men. *J. Clin. Endocrinol. Metab.* **90**, 5647–5655.
McCarrey J. R. (2013). Toward a more precise and informative nomenclature describing fetal and neonatal male germ cells in rodents. *Biol. Reprod.* **89**, 41–47.
McCoshen J. A. (1982). In vivo sex differentiation of congeneic germinal cell aplastic gonads. *Am. J. Obstet. Gynecol.* **142**, 83–88. doi:10.1016/S0002-9378(16)32288-8
McCoshen J. A. (1983). Quantitation of sex chromosomal influence(s) on the somatic growth of fetal gonads in vivo. *Am. J. Obstet. Gynecol.* **145**, 469–473. doi:10.1016/0002-9378(83)90319-8
McGuinness M. P., and Orth J. M. (1992). Reinitiation of gonocyte mitosis and movement of gonocytes to the basement membrane in testes of newborn rats in vivo and in vitro. *Anat. Rec.* **233**, 527–537.
McLachlan R. I., Wreford N. G., De Kretser D. M., and Robertson D. M. (1995). The effects of recombinant follicle-stimulating hormone on the restoration of spermatogenesis in the gonadotropin-releasing hormone-immunized adult rat. *Endocrinology* **136**, 4035–4043.

McLaren A. (2003). Primordial germ cells in the mouse. *Dev. Biol.* **262**, 1–15.
McLaren A., Simpson E., Tomonari K., Chandler P., and Hogg H. (1984). Male sexual differentiation in mice lacking H–Y antigen. *Nature* **312**, 552–555.
McLaren A., and Southee D. (1997). Entry of mouse embryonic germ cells into meiosis. *Dev. Biol.* **187**, 107–113.
McLean D. J., Friel P. J., Johnston D. S., and Griswold M. D. (2003). Characterization of spermatogonial stem cell maturation and differentiation in neonatal mice. *Biol. Reprod.* **69**, 2085–2091.
Meachem S. J., Nieschlag E., and Simoni M. (2001). Inhibin B in male reproduction: pathophysiology and clinical relevance. *Eur. J. Endocrinol.* **145**, 561–571.
Mendis S. H. S., Meachem S. J., Sarraj M. A., and Loveland K. L. (2011). Activin A balances Sertoli and germ cell proliferation in the fetal mouse testis. *Biol. Reprod.* **84**, 379–391. doi:10.1095/biolreprod.110.086231
Meng X., Lindahl M., Hyvönen M. E., Parvinen M., de Rooij D. G., Hess M. W., Raatikainen-Ahokas A., Sainio K., Rauvala H., Lakso M., Pichel J. G., Westphal H., Saarma M., and Sariola H. (2000a). Regulation of cell fate decision of undifferentiated spermatogonia by GDNF. *Science* **287**, 1489–93. doi:10.1126/science.287.5457.1489
Meng X., Lindahl M., Hyvönen M. E., Parvinen M., de Rooij D. G., Hess M. W., Raatikainen-Ahokas A., Sainio K., Rauvala H., Lakso M., Pichel J. G., Westphal H., Saarma M., and Sariola H. (2000b). Regulation of cell fate decision of undifferentiated spermatogonia by GDNF. *Science* **287**, 1489–93.
Meng X., de Rooij D. G., Westerdahl K., Saarma M., and Sariola H. (2001). Promotion of seminomatous tumors by targeted overexpression of glial cell line-derived neurotrophic factor in mouse testis. *Cancer Res.* **61**, 3267–3271.
Merchant-Larios H., Moreno-Mendoza N., and Buehr M. (1993). The role of the mesonephros in cell differentiation and morphogenesis of the mouse fetal testis. *Int. J. Dev. Biol.* **37**, 407–415. doi:10.1387/ijdb.8292535
Merchant H. (1975). Rat gonadal and ovarian organogenesis with and without germ cells. An ultrastructural study. *Dev. Biol.* **44**, 1–21. doi:10.1016/0012-1606(75)90372-3
Meroni S. B., Galardo M. N., Rindone G., Gorga A., Riera M. F., and Cigorraga S. B. (2019). Molecular mechanisms and signaling pathways involved in sertoli cell proliferation. *Front. Endocrinol. (Lausanne).* **10**, 1–22.
Meuleman N., Tondreau T., Delforge A., Dejeneffe M., Massy M., Libertalis M., Bron D., and Lagneaux L. (2006). Human marrow mesenchymal stem cell culture: serum-free medium allows better expansion than classical α-MEM medium. *Eur. J. Haematol.* **76**, 309–316.
Miething A. (1993). Multinucleated spermatocytes in the aging human testis: formation, morphology, and degenerative fate. *Andrologia* **25**, 317–323. doi:10.1111/j.1439-0272.1993.tb02733.x
Miething A. (1995). Multinuclearity of germ cells in the senescent human testis originates from a process of cell-cell fusion. *J. Submicrosc. Cytol. Pathol.* **27**, 105–113.
de Miguel M. P., de Boer-Brouwer M., Paniagua R., van den Hurk R., de Rooij D. G., and van Dissel-Emiliani F. M. (1996). Leukemia inhibitory factor and ciliary neurotropic factor promote the survival of Sertoli cells and gonocytes in coculture system. *Endocrinology* **137**, 1885–1893.
Millar R. P. (2005). GnRHs and GnRH receptors. *Anim. Reprod. Sci.* **88**, 5–28.
Miller W. L., and Auchus R. J. (2011). The molecular biology, biochemistry, and physiology of

human steroidogenesis and its disorders. *Endocr. Rev.* **32**, 81–151.
Miller W. L., Flück C. E., Breault D. T., and Feldman B. J. (2021). The adrenal cortex and its disorders. 'Sperling Pediatric Endocrinology'. pp. 425–490. (Elsevier)
Milose J. C., Filson C. P., Weizer A. Z., Hafez K. S., and Montgomery J. S. (2012). Role of biochemical markers in testicular cancer: diagnosis, staging, and surveillance. *Open access J. Urol.* **4**, 1–8.
Mircea C. N., Lujan M. E., Jaiswal R. S., Singh J., Adams G. P., and Pierson R. A. (2009). Ovarian imaging in the mouse using ultrasound biomicroscopy (UBM): A validation study. *Reprod. Fertil. Dev.* **21**, 579–586. doi:10.1071/RD08295
Mirzapour T., Movahedin M., Tengku Ibrahim T. A., Koruji M., Haron A. W., Nowroozi M. R., and Rafieian S. H. (2012). Effects of basic fibroblast growth factor and leukaemia inhibitory factor on proliferation and short-term culture of human spermatogonial stem cells. *Andrologia* **44**, 41–55. doi:10.1111/j.1439-0272.2010.01135.x
Miyamoto N., Yoshida M., Kuratani S., Matsuo I., and Aizawa S. (1997). Defects of urogenital development in mice lacking Emx2. *Development* **124**, 1653–1664.
Mizuno M., Fujisawa R., and Kuboki Y. (2000). Type I collagen-induced osteoblastic differentiation of bone-marrow cells mediated by collagen-α2β1 integrin interaction. *J. Cell. Physiol.* **184**, 207–213.
Molyneaux K. A., Schaible K., and Wylie C. (2003). GP130, the shared receptor for the LIF/IL6 cytokine family in the mouse, is not required for early germ cell differentiation, but is required cell-autonomously in oocytes for ovulation. **130**, 4287–4294.
Molyneaux K. A., Stallock J., Schaible K., and Wylie C. (2001). Time-lapse analysis of living mouse germ cell migration. *Dev. Biol.* **240**, 488–498.
Molyneaux K. A., Zinszner H., Kunwar P. S., Schaible K., Stebler J., Sunshine M. J., O'Brien W., Raz E., Littman D., and Wylie C. (2003). The chemokine SDF1/CXCL12 and its receptor CXCR4 regulate mouse germ cell migration and survival. **130**, 4279–4286.
Montoto L. G., Arregui L., Sánchez N. M., Gomendio M., and Roldan E. R. S. (2012). Postnatal testicular development in mouse species with different levels of sperm competition. *Reproduction* **143**, 333–346.
Moore T. J., de Boer-Brouwer M., and van Dissel-Emiliani F. M. F. (2002). Purified gonocytes from the neonatal rat form foci of proliferating germ cells in vitro. *Endocrinology* **143,** 3171–3174. doi:10.1210/en.143.8.3171
Moreno S. G., Attali M., Allemand I., Messiaen S., Fouchet P., Coffigny H., Romeo P. H., and Habert R. (2010). TGFβ signaling in male germ cells regulates gonocyte quiescence and fertility in mice. *Dev. Biol.* **342**, 74–84. doi:10.1016/j.ydbio.2010.03.007
Mork L., Maatouk D. M., McMahon J. A., Guo J. J., Zhang P., McMahon A. P., and Capel B. (2012). Temporal differences in granulosa cell specification in the ovary reflect distinct follicle fates in mice. *Biol. Reprod.* **86**, 31–37.
Mortensen A. H., Schade V., Lamonerie T., and Camper S. A. (2015). Deletion of OTX2 in neural ectoderm delays anterior pituitary development. *Hum. Mol. Genet.* **24**, 939–953.
Mosbech C. H., Svingen T., Nielsen J. E., Toft B. G., Rechnitzer C., Petersen B. L., Rajpert-De Meyts E., and Hoei-Hansen C. E. (2014). Expression pattern of clinically relevant markers in paediatric germ cell-and sex-cord stromal tumours is similar to adult testicular tumours. *Virchows Arch.* **465**, 567–577.
Moudgal N. R., Sairam M. R., Krishnamurthy H. N., Sridhar S., Krishnamurthy H., and Khan H. (1997). Immunization of male bonnet monkeys (M. radiata) with a recombinant FSH receptor

preparation affects testicular function and fertility. *Endocrinology* **138**, 3065–3068.
Mullaney B. P., and Skinner M. K. (1992). Basic fibroblast growth factor (bFGF) gene expression and protein production during pubertal development of the seminiferous tubule: Follicle-stimulating hormone-induced sertoli cell bFGF expression. *Endocrinology*. doi:10.1210/endo.131.6.1446630
Nagai R., Shinomura M., Kishi K., Aiyama Y., Harikae K., Sato T., Kanai-Azuma M., Kurohmaru M., Tsunekawa N., and Kanai Y. (2012). Dynamics of GFRα1-positive spermatogonia at the early stages of colonization in the recipient testes of W/Wv male mice. *Dev. Dyn.* **241**, 1374–1384.
Nagano M., Avarbock M. R., and Brinster R. L. (1999). Pattern and Kinetics of Mouse Donor Spermatogonial Stem Cell Colonization in Recipient Testes1. *Biol. Reprod.* **60**, 1429–1436. doi:10.1095/biolreprod60.6.1429
Nagano M., Avarbock M. R., Leonida E. B., Brinster C. J., and Brinster R. L. (1998). Culture of mouse spermatogonial stem cells. *Tissue Cell* **30**, 389–397. doi:10.1016/S0040-8166(98)80053-0
Nagano M., Brinster C. J., Orwig K. E., Ryu B. Y., Avarbock M. R., and Brinster R. L. (2001). Transgenic mice produced by retroviral transduction of male germ-line stem cells. *Proc. Natl. Acad. Sci. U. S. A.* **98**, 13090–13095. doi:10.1073/pnas.231473498
Nagano M., McCarrey J. R., and Brinster R. L. (2001). Primate spermatogonial stem cells colonize mouse testes. *Biol. Reprod.* **64**, 1409–1416. doi:10.1095/biolreprod64.5.1409
Nagano M., Ryu B.-Y., Brinster C. J., Avarbock M. R., and Brinster R. L. (2003). Maintenance of mouse male germ line stem cells in vitro. *Biol. Reprod.* **68**, 2207–214. doi:10.1095/biolreprod.102.014050
Nagano R., Tabata S., Nakanishi Y., Ohsako S., Kurohmaru M., and Hayashi Y. (2000). Reproliferation and relocation of mouse male germ cells (gonocytes) during prespermatogenesis. *Anat. Rec. An Off. Publ. Am. Assoc. Anat.* **258**, 210–220.
Nagano M. C., and Yeh J. R. (2013). The identity and fate decision control of spermatogonial stem cells: where is the point of no return? *Curr. Top. Dev. Biol.* **102**, 61–95.
Nakai M., Kaneko H., Somfai T., Maedomari N., Ozawa M., Noguchi J., Ito J., Kashiwazaki N., and Kikuchi K. (2010). Production of viable piglets for the first time using sperm derived from ectopic testicular xenografts. *Reproduction* **139**, 331–335.
Nakajima K., and Wall R. (1991). Interleukin-6 signals activating junB and TIS11 gene transcription in a B-cell hybridoma. *Mol. Cell. Biol.* **11**, 1409–1418.
Nasiri Z., Hosseini S. M., Hajian M., Abedi P., Bahadorani M., Baharvand H., and Nasr-Esfahani M. H. (2012). Effects of different feeder layers on short-term culture of prepubertal bovine testicular germ cells In-vitro. *Theriogenology* **77**, 1519–1528. doi:https://doi.org/10.1016/j.theriogenology.2011.11.019
Naughton C. K., Jain S., Strickland A. M., Gupta A., and Milbrandt J. (2006). Glial cell-line derived neurotrophic factor-mediated ret signaling regulates spermatogonial stem cell fate. *Biol. Reprod.* **74**, 314–321. doi:10.1095/biolreprod.105.047365
Nef S., and Parada L. F. (1999). Cryptorchidism in mice mutant for Insl3. *Nat. Genet.* **22**, 295–299.
Nel-Themaat L., Jang C. W., Stewart M. D., Akiyama H., Viger R. S., and Behringer R. R. (2011). Sertoli cell behaviors in developing testis cords and postnatal seminiferous tubules of the mouse. *Biol. Reprod.* **84**, 342–350. doi:10.1095/biolreprod.110.086900
Nichols J., Zevnik B., Anastassiadis K., Niwa H., Klewe-Nebenius D., Chambers I., Schöler H.,

and Smith A. (1998). Formation of pluripotent stem cells in the mammalian embryo depends on the POU transcription factor Oct4. *Cell* **95**, 379–391. doi:10.1016/S0092-8674(00)81769-9

Nicola N. A., and Babon J. J. (2015). Leukemia inhibitory factor (LIF). *Cytokine Growth Factor Rev.* **26**, 533–544.

Niemann H., and Kues W. A. (2003). Application of transgenesis in livestock for agriculture and biomedicine. *Anim. Reprod. Sci.* **79**, 291–317.

Niu Z., Goodyear S. M., Avarbock M. R., and Brinster R. L. (2016). Chemokine (CXC) ligand 12 facilitates trafficking of donor spermatogonial stem cells. *Stem Cells Int.* **2016**, 1–8.

Niu Z., Wu S., Wu C., Li N., Zhu H., Liu W., and Hua J. (2016). Multipotent male germline stem cells (mGSCs) from neonate porcine testis. *Brazilian Arch. Biol. Technol.* **59**, 1–14. doi:10.1590/1678-4324-2016150449

Ntemou E., Kadam P., Van Saen D., Wistuba J., Mitchell R. T., Schlatt S., and Goossens E. (2019). Complete spermatogenesis in intratesticular testis tissue xenotransplants from immature non-human primate. *Hum. Reprod.* **34**, 403–13. doi:10.1093/humrep/dey373

Nuccitelli R., Pliquett U., Chen X., Ford W., James Swanson R., Beebe S. J., Kolb J. F., and Schoenbach K. H. (2006). Nanosecond pulsed electric fields cause melanomas to self-destruct. *Biochem. Biophys. Res. Commun.* **343**, 351–360. doi:10.1016/j.bbrc.2006.02.181

Nurmio M., Kallio J., Adam M., Mayerhofer A., Toppari J., and Jahnukainen K. (2012). Peritubular myoid cells have a role in postnatal testicular growth. *Spermatogenesis* **2**, 79–87.

O'Donnell L. (2014). Mechanisms of spermiogenesis and spermiation and how they are disturbed. *Spermatogenesis* **4**, e979623.

O'Donnell L., Nicholls P. K., O'Bryan M. K., McLachlan R. I., and Stanton P. G. (2011). Spermiation: the process of sperm release. *Spermatogenesis* **1**, 14–35.

O'Donnell L., Stanton P., and de Kretser D. M. (2015). Endocrinology of the male reproductive system and spermatogenesis. **141**, 37–46.

O'Shaughnessy P. J., Baker P. J., Heikkila M., Vainio S., and McMahon A. P. (2000). Localization of 17β-hydroxysteroid dehydrogenase/17-ketosteroid reductase isoform expression in the developing mouse testis—androstenedione is the major androgen secreted by fetal/neonatal Leydig cells. *Endocrinology* **141**, 2631–2637.

O'Shaughnessy P. J., and Fowler P. A. (2011). Endocrinology of the mammalian fetal testis. *Reproduction*. doi:10.1530/REP-10-0365

O'shaughnessy P. J., Monteiro A., and Abel M. (2012). Testicular development in mice lacking receptors for follicle stimulating hormone and androgen. *PLoS One* **7**, e35136.

Oakberg E. F. (1956). Duration of spermatogenesis in the mouse and timing of stages of the cycle of the seminiferous epithelium. *Am. J. Anat.* **99**, 507–516.

Oatley J. M., de Avila D. M., Reeves J. J., and McLean D. J. (2004). Spermatogenesis and germ cell transgene expression in xenografted bovine testicular tissue. *Biol. Reprod.* **71**, 494–501. doi:10.1095/biolreprod.104.027953

Oatley J. M., and Brinster R. L. (2008). Regulation of spermatogonial stem cell self-renewal in mammals. *Annu. Rev. Cell Dev. Biol.* **24**, 263–286.

Oatley J. M., Reeves J. J., and McLean D. J. (2005). Establishment of spermatogenesis in neonatal bovine testicular tissue following ectopic xenografting varies with donor age. *Biol. Reprod.* **72**, 358–364.

Oatley J. M., Reeves J. J., McLean D. J., Oatley J. M., and Reeves J. J. (2005). Establishment of spermatogenesis in neonatal bovine testicular tissue following ectopic xenografting varies

with donor age bovine testis tissue from 8-wk calves produces more spermatids after xenografting than other age donors. *Biol. Reprod. Off. J. Soc. Study Reprod.* **72**, 358–364.
Ogawa T., Dobrinski I., Avarbock M. R., and Brinster R. L. (2000). Transplantation of male germ line stem cells restores fertility in infertile mice. *Nat. Med.* **6**, 29–34.
Ogawa T., Ohmura M., Tamura Y., Kita K., Ohbo K., Suda T., and Kubota Y. (2004). Derivation and morphological characterization of mouse spermatogonial stem cell lines. *Arch. Histol. Cytol.* **67**, 297–306.
Ohbo K., Yoshida S., Ohmura M., Ohneda O., Ogawa T., Tsuchiya H., Kuwana T., Kehler J., Abe K., and Schöler H. R. (2003). Identification and characterization of stem cells in prepubertal spermatogenesis in mice. *Dev. Biol.* **258**, 209–225.
Ohmura M., Naka K., Hoshii T., Muraguchi T., Shugo H., Tamase A., Uema N., Ooshio T., Arai F., and Takubo K. (2008). Identification of stem cells during prepubertal spermatogenesis via monitoring of nucleostemin promoter activity. *Stem Cells* **26**, 3237–3246.
Ohmura M., Yoshida S., Ide Y., Nagamatsu G., Suda T., and Ohbo K. (2004). Spatial analysis of germ stem cell development in Oct-4/EGFP transgenic mice. *Arch. Histol. Cytol.* **67**, 285–296.
Ohta H., Wakayama T., and Nishimune Y. (2004). Commitment of fetal male germ cells to spermatogonial stem cells during mouse embryonic development. *Biol. Reprod.* **70**, 1286–1291. doi:10.1095/biolreprod.103.024612
Ohta H., Yomogida K., Yamada S., Okabe M., and Nishimune Y. (2000). Real-time observation of transplanted 'green germ cells': proliferation and differentiation of stem cells. *Dev. Growth Differ.* **42**, 105–112.
Ornitz D. M., and Itoh N. (2015). The fibroblast growth factor signaling pathway. *Wiley Interdiscip. Rev. Dev. Biol.* **4**, 215–266.
Orriss I. R., Taylor S. E. B., and Arnett T. R. (2012). Rat osteoblast cultures. *Bone Res. Protoc.* **816**, 31–41.
Orth J. M. (1982). Proliferation of Sertoli cells in fetal and postnatal rats: a quantitative autoradiographic study. *Anat. Rec.* **203**, 485–492.
Orth J. M., Qiu J., Jester W. F., and Pilder S. (1997). Expression of the c-kit gene is critical for migration of neonatal rat gonocytes in vitro. *Biol. Reprod.* **57**, 676–683. doi:10.1095/biolreprod57.3.676
Orth J. M., and Rosemarie B. (1990). Functional coupling of neonatal rat Sertoli cells and gonocytes in coculture. *Endocrinology* **127**, 2812–2820.
Orwig K. E., Ryu B. Y., Avarbock M. R., and Brinster R. L. (2002). Male germ-line stem cell potential is predicted by morphology of cells in neonatal rat testes. *Proc. Natl. Acad. Sci. U. S. A.* **99**, 11706–11711. doi:10.1073/pnas.182412099
Ostrer H., Huang H. Y., Masch R. J., and Shapiro E. (2007). A cellular study of human testis development. *Sex. Dev.* **41**, 1316–1324. doi:10.1159/000108930
Pan G. J., Chang Z. Y., Schöler H. R., and Duanqing P. E. I. (2002). Stem cell pluripotency and transcription factor Oct4. *Cell Res.* **12**, 321–329.
Parikka V., Väänänen A., Risteli J., Salo T., Sorsa T., Väänänen H. K., and Lehenkari P. (2005). Human mesenchymal stem cell derived osteoblasts degrade organic bone matrix in vitro by matrix metalloproteinases. *Matrix Biol.* **24**, 438–447.
Paris M. C. J., and Schlatt S. (2007). Ovarian and testicular tissue xenografting: its potential for germline preservation of companion animals, non-domestic and endangered species. *Reprod. Fertil. Dev.* **19**, 771–782.

Park J. E., Park M. H., Kim M. S., Park Y. R., Yun J. I., Cheong H. T., Kim M., Choi J. H., Lee E., and Lee S. T. (2017). Porcine spermatogonial stem cells self-renew effectively in a three dimensional culture microenvironment. *Cell Biol. Int.* doi:10.1002/cbin.10844

Patni P., Mohanty S. K., and Singh R. (2017). Embryonic Development of the Testis. 'Male Infertility: Understanding, Causes and Treatment'. (Eds R Singh and K Singh) pp. 13–24. (Springer Singapore: Singapore) doi:10.1007/978-981-10-4017-7_2

Pauls K., Schorle H., Jeske W., Brehm R., Steger K., Wernert N., Büttner R., and Zhou H. (2006). Spatial expression of germ cell markers during maturation of human fetal male gonads: an immunohistochemical study. *Hum. Reprod.* **21**, 397–404.

Pavlin C., and Foster S. (2012). Ultrasound biomicroscopy of the eye. *Springer Sci. Bus. Media* 3–5.

Pavlin C. J., Ritch R., and Foster F. S. (1992). Ultrasound biomicroscopy in plateau iris syndrome. *Am. J. Ophthalmol*. **113**, 390–395. doi:10.1016/S0002-9394(14)76160-4

Pavlin C. J., Sherar M. D., and Foster F. S. (1990). Subsurface ultrasound microscopic imaging of the intact eye. *Ophthalmology* **97**, 244–250.

Pelliniemi L. J. (1974). Ultrastructure of gonadal ridge in male and female pig embryos. *Anat. Embryol. (Berl).* **147**, 2–34. doi:10.1007/BF00317961

van Pelt A. M. M., Morena A. R., van Dissel-Emiliani F. M. F., Boitani C., Gaemers I. C., de Rooij D. G., and Stefanini M. (1996). Isolation of the synchronized A spermatogonia from adult vitamin A-deficient rat testes. *Biol. Reprod.* **55**, 439–444.

Pesce M., Farrace M. G., Piacentini M., Dolci S., and De Felici M. (1993). Stem cell factor and leukemia inhibitory factor promote primordial germ cell survival by suppressing programmed cell death (apoptosis). *Development* **118**, 1089–1094.

Petersen B., Carnwath J. W., and Niemann H. (2009). The perspectives for porcine-to-human xenografts. *Comp. Immunol. Microbiol. Infect. Dis.* **32**, 91–105. doi:10.1016/j.cimid.2007.11.014

Pfeifer L. F. M., Adams G. P., Pierson R. A., and Singh J. (2014). Ultrasound biomicroscopy: A non-invasive approach for in vivo evaluation of oocytes and small antral follicles in mammals. *Reprod. Fertil. Dev.* **26**, 48–54. doi:10.1071/RD13305

Pfeifer L. F. M., Siqueira L. G. B., Adams G. P., Pierson R. A., and Singh J. (2012). In vivo imaging of cumulus-oocyte-complexes and small ovarian follicles in cattle using ultrasonic biomicroscopy. *Anim. Reprod. Sci.* **131**, 88–94. doi:10.1016/j.anireprosci.2012.02.014

Phillips B. T., Gassei K., and Orwig K. E. (2010). Spermatogonial stem cell regulation and spermatogenesis. *Philos. Trans. R. Soc. B Biol. Sci.* **365**, 1663–1678. doi:10.1098/rstb.2010.0026

Piquet-Pellorce C., Dorval-Coiffec I., Pham M. D., and Jégou B. (2000). Leukemia inhibitory factor expression and regulation within the testis. *Endocrinology* **141**, 1136–1141. doi:10.1210/endo.141.3.7399

Povlsen C. O., Skakkebaek N. E., Rygaard J., and Jensen G. (1974). Heterotransplantation of human foetal organs to the mouse mutant nude. *Nature* **248**, 247–249. doi:10.1038/248247a0

Puri P. (1986). A biphasic model for the hormonal control of testicular descent. *J. Pediatr. Surg.* **2**, 419–421. doi:10.1016/s0022-3468(86)80163-4

Qasemi-Panahi B., Tajik P., Movahedin M., Moghaddam G., Barzgar Y., and Heidari-Vala H. (2011). Differentiation of bovine spermatogonial stem cells into osteoblasts. *Avicenna J. Med. Biotechnol.* **3**, 149–153.

Qu S., Yan L., Fang B., Ye S., Li P., Ge S., Wu J., Qu D., and Song H. (2017). Generation of

enhanced definitive endoderm from human embryonic stem cells under an albumin/insulin-free and chemically defined condition. *Life Sci.* **175**, 37–46.
Rajpert-De Meyts E. (2006). Developmental model for the pathogenesis of testicular carcinoma in situ: genetic and environmental aspects. *Hum. Reprod. Update* **12**, 303–323.
Rajpert-De Meyts E., Hanstein R., Jørgensen N., Græm N., Vogt P. H., and Skakkebaek N. E. (2004). Developmental expression of POU5F1 (OCT-3/4) in normal and dysgenetic human gonads. *Hum. Reprod.* **19**, 1338–1344.
El Ramy R., Verot A., Mazaud S., Odet F., Magre S., and Le Magueresse-Battistoni B. (2005). Fibroblast growth factor (FGF) 2 and FGF9 mediate mesenchymal–epithelial interactions of peritubular and Sertoli cells in the rat testis. *J. Endocrinol.* **187**, 135–147.
Rathi R., Honaramooz A., Zeng W., Schlatt S., and Dobrinski I. (2005). Germ cell fate and seminiferous tubule development in bovine testis xenografts. *Reproduction* **130**, 923–929. doi:10.1530/rep.1.00912
Rathi R., Honaramooz A., Zeng W., Turner R., and Dobrinski I. (2006). Germ cell development in equine testis tissue xenografted into mice. *Reproduction* **131**, 1091–1098.
Rathi R., Zeng W., Megee S., Conley A., Meyers S., and Dobrinski I. (2008). Maturation of testicular tissue from infant monkeys after xenografting into mice. *Endocrinology* **149**, 5288–5296. doi:10.1210/en.2008-0311
Reddy N., Mahla R. S., Thathi R., Suman S. K., Jose J., and Goel S. (2011). Gonadal status of male recipient mice influences germ cell development in immature buffalo testis tissue xenograft. *Reproduction* **143**, 59–69.
Redmer T., Diecke S., Grigoryan T., Quiroga-Negreira A., Birchmeier W., and Besser D. (2011). E-cadherin is crucial for embryonic stem cell pluripotency and can replace OCT4 during somatic cell reprogramming. *EMBO Rep.* **12**, 720–726. doi:10.1038/embor.2011.88
Reijo R. A., Dorfman D. M., Slee R., Renshaw A. A., Loughlin K. R., Cooke H., and Page D. C. (2000). DAZ family proteins exist throughout male germ cell development and transit from nucleus to cytoplasm at meiosis in humans and mice. *Biol. Reprod.* **63**, 1490–1496. doi:10.1095/biolreprod63.5.1490
Rey R. (1999). Invited Reviews-The prepubertal testis: A quiescent or a silently active organ? *Histol. Histopathol.* **14**, 991–1000.
Rey R. A. (2014). Mini-puberty and true puberty: differences in testicular function. In 'Annales d'endocrinologie', pp. 58–63. (Elsevier)
Rey R. A., Campo S. M., Bedecarrás P., Nagle C. A., and Chemes H. E. (1993). Is infancy a quiescent period of testicular development? Histological, morphometric, and functional study of the seminiferous tubules of the cebus monkey from birth to the end of puberty. *J. Clin. Endocrinol. Metab.* **76**, 1325–1331.
Rey R. A., Musse M., Venara M., and Chemes H. E. (2009). Ontogeny of the androgen receptor expression in the fetal and postnatal testis: its relevance on Sertoli cell maturation and the onset of adult spermatogenesis. *Microsc. Res. Tech.* **72**, 787–795.
Riboldi M., Rubio C., Pellicer A., Gil-Salom M., and Simón C. (2012). In vitro production of haploid cells after coculture of CD49f+ with Sertoli cells from testicular sperm extraction in nonobstructive azoospermic patients. *Fertil. Steril.* **98**, 580–590.
Richards A. J., Enders G. C., and Resnick J. L. (1999). Differentiation of murine premigratory primordial germ cells in culture. *Biol. Reprod.* **61**, 1146–1151.
Robaire B., and Hinton B. T. (2015). Chapter 17 - The Epididymis. 'Knobil and Neill's Physiology of Reproduction (Fourth Edition)'. (Eds TM Plant and AJ Zeleznik) pp. 691–771. (Academic

Press: San Diego) doi:https://doi.org/10.1016/B978-0-12-397175-3.00017-X
Robaire B., Hinton B. T., and Orgebin-Crist M.-C. (2006). The epididymis. 'Knobil and Neill's physiology of reproduction'. pp. 1071–1148. (Elsevier)
Robb R. (1995). 'Three-dimensional biomedical imaging: Principles and practice.' (VCH Publications: Ney York)
Robinson J. (2006). Prenatal programming of the female reproductive neuroendocrine system by androgens. *Reproduction* **132**, 539–547. doi:10.1530/rep.1.00064
Rodriguez-Sosa J. R., Costa G. M. J., Rathi R., França L. R., and Dobrinski I. (2012). Endocrine modulation of the recipient environment affects development of bovine testis tissue ectopically grafted in mice. *Reproduction* **144**, 37–51.
Rodriguez-Sosa J. R., and Dobrinski I. (2009). Recent developments in testis tissue xenografting. *Reproduction* **138**, 187–194.
Rodriguez-Sosa J. R., Dobson H., and Hahnel A. (2006). Isolation and transplantation of spermatogonia in sheep. *Theriogenology* **66**, 2091–2103. doi:10.1016/j.theriogenology.2006.03.039
Rodriguez-Sosa J. R., Silvertown J. D., Foster R. A., Medin J. A., and Hahnel A. (2009). Transduction and Transplantation of Spermatogonia into the Testis of Ram Lambs through the Extra-testicular Rete. *Reprod. Domest. Anim.* **44**, 612–620. doi:https://doi.org/10.1111/j.1439-0531.2007.01030.x
Rolland A. D., Lehmann K. P., Johnson K. J., Gaido K. W., and Koopman P. (2011). Uncovering gene regulatory networks during mouse fetal germ cell development. *Biol. Reprod.* **84**, 790–800.
Romito A., and Cobellis G. (2016). Pluripotent stem cells: current understanding and future directions. *Stem Cells Int.* **2016**, 1–20.
de Rooij D. G. (1998). Stem cells in the testis. *Int. J. Exp. Pathol.* **79**, 67–80.
de Rooij D. G. (2001). Proliferation and differentiation of spermatogonial stem cells. *Reproduction* **121**, 347–354.
de Rooij D. G., and van Dissel-Emiliani F. M. F. (1997). Regulation of proliferation and differentiation of stem cells in the male germ line. 'Stem Cells'. (Ed CS Potten) pp. 283–313. (Academic Press: London) doi:https://doi.org/10.1016/B978-012563455-7/50010-6
de Rooij D. G., and Mizrak S. C. (2008). Deriving multipotent stem cells from mouse spermatogonial stem cells: a new tool for developmental and clinical research. **135**, 2207–2213.
de Rooij D. G., and Russell L. D. (2000). All you wanted to know about spermatogonia but were afraid to ask. *J. Androl.* **21**, 776–798. doi:10.1002/j.1939-4640.2000.tb03408.x
de Rooji D. G. (1998). Stem cells in the testis. *Int. J. Exp. Pathol.* **79**, 67–80.
Roosen-Runge E. C., and Anderson D. (1959). The development of the interstitial cells in the testis of the albino rat. *Cells Tissues Organs* **37**, 125–137. doi:10.1159/000141460
Roosen-Runge E. C., and Giesel Jr L. O. (1950). Quantitative studies on spermatogenesis in the albino rat. *Am. J. Anat.* **87**, 1–30.
Roosen-Runge E. C., and Leik J. (1968). Gonocyte degeneration in the postnatal male rat. *Am. J. Anat.* **122**, 275–299.
Rosselot C., Kierszenbaum A. L., Rivkin E., and Tres L. L. (2003). Chronological gene expression of ADAMs during testicular development: Prespermatogonia (gonocytes) express fertilin β (ADAM2). *Dev. Dyn. an Off. Publ. Am. Assoc. Anat.* **227**, 458–467.
Roudebush W. E., Often N. L., and Butler W. J. (1994). Alpha-minimum essential medium (MEM)

enhances in vitro hatched blastocyst development and cell number per embryo over Ham's F-10. *J. Assist. Reprod. Genet.* **11**, 203–207.
Roulet V., Denis H., Staub C., Le Tortorec A., Delaleu B., Satie A.-P., Patard J.-J., Jégou B., and Dejucq-Rainsford N. (2006). Human testis in organotypic culture: application for basic or clinical research. *Hum. Reprod.* **21**, 1564–1575.
Runyan C., Schaible K., Molyneaux K., Wang Z., Levin L., and Wylie C. (2006). Steel factor controls midline cell death of primordial germ cells and is essential for their normal proliferation and migration. *Development* **133**, 4861–4869.
Russell L. D. (1979). Observations on the inter-relationships of Sertoli cells at the level of the blood-testis barrier: Evidence for formation and resorption of Sertoli-Sertoli tubulobulbar complexes during the spermatogenic cycle of the rat. *Am. J. Anat.* **155**, 259–279.
Russell L. D. (1980). Sertoli-germ cell interrelations: A review. *Gamete Res.* **3**, 179–202.
Russell L., and Clermont Y. (1976). Anchoring device between Sertoli cells and late spermatids in rat seminiferous tubules. *Anat. Rec.* **185**, 259–277.
Russell L. D., and de França L. R. (1995). Building a testis. *Tissue Cell* **27**, 129–147.
Russell L. D., and Griswold M. D. (1993). 'The sertoli cell.' (Cache River Press: Clearwater, FL)
Ryu B.-Y., Kubota H., Avarbock M. R., and Brinster R. L. (2005). Conservation of spermatogonial stem cell self-renewal signaling between mouse and rat. *Proc. Natl. Acad. Sci.* **102**, 14302–143071. doi:10.1073/pnas.0506970102
Ryu B. Y., Orwig K. E., Kubota H., Avarbock M. R., and Brinster R. L. (2004). Phenotypic and functional characteristics of spermatogonial stem cells in rats. *Dev. Biol.* **274**, 158–170. doi:10.1016/j.ydbio.2004.07.004
Sadri-Ardekani H. et al. (2009). Propagation of Human Spermatogonial Stem Cells in Vitro. *Am. Med. Assoc.* doi:10.1001/jama.2009.1689
Sadri-Ardekani H., Akhondi M. A., Van Der Veen F., Repping S., and Van Pelt A. M. M. (2011). In vitro propagation of human prepubertal spermatogonial stem cells. *JAMA - J. Am. Med. Assoc.* doi:10.1001/jama.2011.791
Saez J. M., Chatelain P. G., Perrard-Sapori M.-H., Jaillard C., and Naville D. (1988). Differentiating effects of somatomedin-C/insulin-like growth factor I and insulin on Leydig and Sertoli cell functions. *Reprod. Nutr. Développement* **28**, 989–1008.
Sahare M., Kim S. M., Otomo A., Komatsu K., Minami N., Yamada M., and Imai H. (2016). Factors supporting long-term culture of bovine male germ cells. *Reprod. Fertil. Dev.* **28**, 989–1008. doi:10.1071/RD15003
Sahare M. G., Suyatno, and Imai H. (2018). Recent advances of in vitro culture systems for spermatogonial stem cells in mammals. *Reprod. Med. Biol.* **17**, 134–142. doi:10.1002/rmb2.12087
Saito K., O'Donnell L., McLachlan R. I., and Robertson D. M. (2000). Spermiation failure is a major contributor to early spermatogenic suppression caused by hormone withdrawal in adult rats. *Endocrinology* **141**, 2779–2785.
Saitou M., and Yamaji M. (2012). Primordial germ cells in mice. *Cold Spring Harb. Perspect. Biol.* **4**, a008375.
Sakib S., Voigt A., Goldsmith T., and Dobrinski I. (2019). Three-dimensional testicular organoids as novel in vitro models of testicular biology and toxicology. *Environ. Epigenetics* **5,** dvz011. doi:10.1093/eep/dvz011
Sasaki K., Nakamura T., Okamoto I., Yabuta Y., Iwatani C., Tsuchiya H., Seita Y., Nakamura S., Shiraki N., and Takakuwa T. (2016). The germ cell fate of cynomolgus monkeys is specified

in the nascent amnion. *Dev. Cell* **39**, 169–185.
Sato T., Aiyama Y., Ishii-Inagaki M., Hara K., Tsunekawa N., Harikae K., Uemura-Kamata M., Shinomura M., Zhu X. B., and Maeda S. (2011). Cyclical and patch-like GDNF distribution along the basal surface of Sertoli cells in mouse and hamster testes. *PLoS One* **6**, e28367.
Sato T., Katagiri K., Gohbara A., Inoue K., Ogonuki N., Ogura A., Kubota Y., and Ogawa T. (2011). In vitro production of functional sperm in cultured neonatal mouse testes. *Nature*. doi:10.1038/nature09850
Sato T., Katagiri K., Kojima K., Komeya M., Yao M., and Ogawa T. (2015). In vitro spermatogenesis in explanted adult mouse testis tissues. *PLoS One* **10**, e0130171.
Sato Y., Nozawa S., Yoshiike M., Arai M., Sasaki C., and Iwamoto T. (2010). Xenografting of testicular tissue from an infant human donor results in accelerated testicular maturation. *Hum. Reprod.* **25**, 1113–1122.
Savvulidi F., Ptacek M., Savvulidi Vargova K., and Stadnik L. (2019). Manipulation of spermatogonial stem cells in livestock species. *J. Anim. Sci. Biotechnol.* **10**, 1–18. doi:10.1186/s40104-019-0355-4
Schlatt S., Honaramooz A., Boiani M., Schöler H. R., and Dobrinski I. (2002). Progeny from Sperm Obtained after Ectopic Grafting of Neonatal Mouse Testes. *Biol. Reprod.* **68**, 2331–2335. doi:10.1095/biolreprod.102.014894
Schlatt S., Honaramooz A., Ehmcke J., Goebell P. J., Rübben H., Dhir R., Dobrinski I., and Patrizio P. (2006). Limited survival of adult human testicular tissue as ectopic xenograft. *Hum. Reprod.* **21**, 384–389. doi:10.1093/humrep/dei352
Schlatt S., Kim S. S., and Gosden R. (2002). Spermatogenesis and steroidogenesis in mouse, hamster and monkey testicular tissue after cryopreservation and heterotopic grafting to castrated hosts. *Reproduction* **124**, 339–346. doi:10.1530/rep.0.1240339
Schlatt S., Westernströer B., Gassei K., and Ehmcke J. (2010a). Donor-host involvement in immature rat testis xenografting into nude mouse hosts. *Biol. Reprod.* **82**, 888–895.
Schlatt S., Westernströer B., Gassei K., and Ehmcke J. (2010b). Donor-Host Involvement in Immature Rat Testis Xenografting into Nude Mouse Hosts1. *Biol. Reprod.* 888–895. doi:10.1095/biolreprod.109.082073
Schlesser H. N., Simon L., Hofmann M. C., Murphy K. M., Murphy T., Hess R. A., and Cooke P. S. (2008). Effects of ETV5 (Ets variant gene 5) on testis and body growth, time course of spermatogonial stem cell loss, and fertility in mice. *Biol. Reprod.* **78**, 483–489. doi:10.1095/biolreprod.107.062935
Schmahl J., Eicher E. M., Washburn L. L., and Capel B. (2000). Sry induces cell proliferation in the mouse gonad. *Development* **127**, 65–73.
Schmidt J. A., de Avila J. M., and McLean D. J. (2006). Effect of vascular endothelial growth factor and testis tissue culture on spermatogenesis in bovine ectopic testis tissue xenografts. *Biol. Reprod.* **75**, 167–175. doi:10.1095/biolreprod.105.049817
Schöne M., Männicke N., Somerson J. S., Marquass B., Henkelmann R., Aigner T., Raum K., and Schulz R. M. (2016). 3D ultrasound biomicroscopy for assessment of cartilage repair tissue: volumetric characterisation and correlation to established classification systems. *Eur. Cells Mater.* **31**, 119–135.
Schultheiss M., Januschowski K., Ruschenburg H., Schramm C., Schnichels S., Szurman P., Bartz-Schmidt K. U., and Spitzer M. S. (2013). Dulbecco's Modified Eagle Medium is neuroprotective when compared to standard vitrectomy irrigation solution. *Graefe's Arch. Clin. Exp. Ophthalmol.* **251**, 1613–1619. doi:10.1007/s00417-012-2255-6

Schumacher J. (2012). Chapter 59 - Testis. 'Equine Surgery (Fourth Edition)'. (Eds JA Auer and JA Stick) pp. 804–840. (W.B. Saunders: Saint Louis) doi:https://doi.org/10.1016/B978-1-4377-0867-7.00059-4

Seandel M., James D., Shmelkov S. V., Falciatori I., Kim J., Chavala S., Scherr D. S., Zhang F., Torres R., Gale N. W., Yancopoulos G. D., Murphy A., Valenzuela D. M., Hobbs R. M., Pandolfi P. P., and Rafii S. (2007). Generation of functional multipotent adult stem cells from GPR125 + germline progenitors. *Nature* **449**, 346–350. doi:10.1038/nature06129

Seisenberger S., Andrews S., Krueger F., Arand J., Walter J., Santos F., Popp C., Thienpont B., Dean W., and Reik W. (2012). The dynamics of genome-wide DNA methylation reprogramming in mouse primordial germ cells. *Mol. Cell* **48**, 849–862.

Setchell B. P. (1990). The testis and tissue transplantation: historical aspects. *J. Reprod. Immunol.* **18**, 1–8.

Sharma M., and Braun R. E. (2018). Cyclical expression of GDNF is required for spermatogonial stem cell homeostasis. *Development* **145**, dev151555.

Sharma S., Sandhowe-Klaverkamp R., and Schlatt S. (2018). Differentiation of testis xenografts in the prepubertal marmoset depends on the sex and status of the mouse host. *Front. Endocrinol. (Lausanne).* **9**, 2–12. doi:10.3389/fendo.2018.00467

Sharma S., Schlatt S., Van Pelt A., and Neuhaus N. (2019). Characterization and population dynamics of germ cells in adult macaque testicular cultures. *PLoS One* **14**, e0218194.

Sharpe R. M. (1994). 'Regulation of spermatogenesis. In: Knobil E, Neill JD, eds.'

Sharpe R. M., McKinnell C., Kivlin C., and Fisher J. S. (2003). Proliferation and functional maturation of Sertoli cells, and their relevance to disorders of testis function in adulthood. *Reproduction* **125**, 769–784.

Shaw G., and Renfree M. B. (2014). Wolffian duct development. *Sex. Dev.* **8**, 273–280.

Shen M. M., Skoda R. C., Cardiff R. D., Campos-Torres J., Leder P., and Ornitz D. M. (1994). Expression of LIF in transgenic mice results in altered thymic epithelium and apparent interconversion of thymic and lymph node morphologies. *EMBO J.* **13**, 1375–1385.

Sherar M. D., Starkoski B. G., Taylor W. B., and Foster F. S. (1989). A 100 MHz B-Scan ultrasound backscatter microscope. *Ultrason. Imaging* **21**, 95–105. doi:10.1177/016173468901100202

Shetty G., Mitchell J. M., Lam T. N. A., Wu Z., Zhang J., Hill L., Tailor R. C., Peters K. A., Penedo M. C., and Orwig K. E. (2018). Donor spermatogenesis in de n ovo formed seminiferous tubules from transplanted testicular cells in rhesus monkey testis. *Hum. Reprod.* **33**, 2249–2255.

Shi G., and Jin Y. (2010). Role of Oct4 in maintaining and regaining stem cell pluripotency. *Stem Cell Res. Ther.* **1**, 1–9. doi:10.1186/scrt39

Shikina S., and Yoshizaki G. (2010). Improved in vitro culture conditions to enhance the survival, mitotic activity, and transplantability of rainbow trout type a spermatogonia. *Biol. Reprod.* **83**, 268–276.

Shima Y. (2019). Development of fetal and adult Leydig cells. *Reprod. Med. Biol.* **18**, 323–330.

Shima Y., Matsuzaki S., Miyabayashi K., Otake H., Baba T., Kato S., Huhtaniemi I., and Morohashi K. I. (2015). Fetal leydig cells persist as an androgen-independent subpopulation in the postnatal testis. *Mol. Endocrinol.* **29**, 1581–1593. doi:10.1210/me.2015-1200

Shima Y., Miyabayashi K., Haraguchi S., Arakawa T., Otake H., Baba T., Matsuzaki S., Shishido Y., Akiyama H., Tachibana T., Tsutsui K., and Morohashi K. I. (2013). Contribution of Leydig and Sertoli cells to testosterone production in mouse fetal testes. *Mol. Endocrinol.* **27**,

63–73. doi:10.1210/me.2012-1256
Shinohara T. (2002). Birth of offspring following transplantation of cryopreserved immature testicular pieces and in-vitro microinsemination. *Hum. Reprod.* doi:10.1093/humrep/17.12.3039
Shinohara T., and Brinster R. L. (2000). Enrichment and transplantation of spermatogonial stem cells. *Int. J. Androl.* **23**, 89–91. doi:https://doi.org/10.1046/j.1365-2605.2000.00025.x
Shinohara T., Orwig K. E., Avarbock M. R., and Brinster R. L. (2000). Spermatogonial stem cell enrichment by multiparameter selection of mouse testis cells. *Proc. Natl. Acad. Sci.* **97**, 8346–8351.
Shubhada S., Glinz M., and Lamb D. J. (1993). Sertoli Cell Secreted Growth Factor Cellular Origin, Paracrine and Endocrine Regulation of Secretion. *J. Androl.* doi:10.1002/j.1939-4640.1993.tb01659.x
Sikka S. C., and Gurbuz N. (2006). Chapter 32 - Reproductive Toxicity of Organophosphate and Carbamate Pesticides. 'Toxicology of Organophosphate & Carbamate Compounds'. (Ed RC Gupta) pp. 447–462. (Academic Press: Burlington) doi:https://doi.org/10.1016/B978-012088523-7/50033-8
Silva M. J., Brodt M. D., Ko M., and Abu-Amer Y. (2005). Impaired marrow osteogenesis is associated with reduced endocortical bone formation but does not impair periosteal bone formation in long bones of SAMP6 mice. *J. Bone Miner. Res.* **20**, 419–427.
Simon L., Ekman G. C., Kostereva N., Zhang Z., Hess R. A., Hofmann M., and Cooke P. S. (2009). Direct transdifferentiation of stem/progenitor spermatogonia into reproductive and nonreproductive tissues of all germ layers. *Stem Cells* **27**, 1666–1675.
Simon L., Ekman G. C., Tyagi G., Hess R. A., Murphy K. M., and Cooke P. S. (2007). Common and distinct factors regulate expression of mRNA for ETV5 and GDNF, Sertoli cell proteins essential for spermatogonial stem cell maintenance. *Exp. Cell Res.* **313**, 3090–3099. doi:10.1016/j.yexcr.2007.05.002
Simon L., Hess R. A., and Cooke P. S. (2010). Spermatogonial stem cells, in vivo transdifferentiation and human regenerative medicine. *Expert Opin. Biol. Ther.* **10**, 519–530.
Sinclair A. H., Berta P., Palmer M. S., Hawkins J. R., Griffiths B. L., Smith M. J., Foster J. W., Frischauf A. M., Lovell-Badge R., and Goodfellow P. N. (1990). A gene from the human sex-determining region encodes a protein with homology to a conserved DNA-binding motif. *Nature* **346**, 240–244. doi:10.1038/346240a0
Singh V. K., Saini A., Kalsan M., Kumar N., and Chandra R. (2016). Describing the stem cell potency: the various methods of functional assessment and in silico diagnostics. *Front. cell Dev. Biol.* **4**, 134.
Sivasubramaniyan K., Harichandan A., Schilbach K., Mack A. F., Bedke J., Stenzl A., Kanz L., Niederfellner G., and Bühring H.-J. (2015). Expression of stage-specific embryonic antigen-4 (SSEA-4) defines spontaneous loss of epithelial phenotype in human solid tumor cells. *Glycobiology* **25**, 902–917.
Skakkebaek N. E., Berthelsen J. G., Giwercman A., and Müller J. (1987). Carcinoma-in-situ of the testis: possible origin from gonocytes and precursor of all types of germ cell tumours except spermatocytoma. *Int. J. Androl.* **10**, 19–28.
Skakkebaek N. E., Jensen G., Povlsen C. O., and Rygaard J. (1974). Heterotransplantation of human foetal testicular and ovarian tissue to the mouse mutant nude: a preliminary stud. *Acta Obstet. Gynecol. Scand.* **29**, 73–75. doi:10.3109/00016347409157196
Skinner M. K. (2005). Sertoli Cell Secreted Regulatory Factors. 'Sertoli Cell Biology'.

doi:10.1016/B978-012647751-1/50009-X
Smith E. P., Hall S. H., Monaco L., French F. S., Wilson E. M., and Conti M. (1989). A rat Sertoli cell factor similar to basic fibroblast growth factor increases c-fos messenger ribonucleic acid in cultured Sertoli cells. *Mol. Endocrinol.* **3**, 954–961.
Smith L. B., and Walker W. H. (2014). The regulation of spermatogenesis by androgens. *Semin. Cell Dev. Biol.* **30**, 2–13.
Snedaker A. K., Honaramooz A., and Dobrinski I. (2004). A game of cat and mouse: xenografting of testis tissue from domestic kittens results in complete cat spermatogenesis in a mouse host. *J. Androl.* **25**, 926–930.
Snyder C. S., Kaushal S., Kono Y., Cao H. S. T., Hoffman R. M., and Bouvet M. (2009). Complementarity of ultrasound and fluorescence imaging in an orthotopic mouse model of pancreatic cancer. *BMC Cancer* 1–10. doi:10.1186/1471-2407-9-106
Solter D., and Knowles B. B. (1978). Monoclonal antibody defining a stage-specific mouse embryonic antigen (SSEA-1). *Proc. Natl. Acad. Sci. U. S. A.* doi:10.1073/pnas.75.11.5565
Song H.-W., and Wilkinson M. F. (2012). In vitro spermatogenesis: A long journey to get tails. *Spermatogenesis* **2**, 238–244.
Sonne S. B., Almstrup K., Dalgaard M., Juncker A. S., Edsgard D., Ruban L., Harrison N. J., Schwager C., Abdollahi A., and Huber P. E. (2009). Analysis of gene expression profiles of microdissected cell populations indicates that testicular carcinoma in situ is an arrested gonocyte. *Cancer Res.* **69**, 5241–5250.
Sordoillet C., Savona C., Chauvin M. A., De Peretti E., Feige J. J., Morera A. M., and Benahmed M. (1992). Basic fibroblast growth factor enhances testosterone secretion in cultured porcine Leydig cells: site (s) of action. *Mol. Cell. Endocrinol.* **89**, 163–171.
Spiller C. M., Feng C. W., Jackson A., Gillis A. J. M., Rolland A. D., Looijenga L. H. J., Koopman P., and Bowles J. (2012). Endogenous Nodal signaling regulates germ cell potency during mammalian testis development. *Dev.* **139**, 4123–4132. doi:10.1242/dev.083006
Sprengel R., Braun T., Nikolics K., Segaloff D. L., and Seeburg P. H. (1990). The testicular receptor for follicle stimulating hormone: structure and functional expression of cloned cDNA. *Mol. Endocrinol.* **4**, 525–530.
Spurney C. F., Lo C. W., and Leatherbury L. (2006). Fetal mouse imaging using echocardiography: A review of current technology. *Echocardiography* **23**, 891–899. doi:10.1111/j.1540-8175.2006.00335.x
Stebler J., Spieler D., Slanchev K., Molyneaux K. A., Richter U., Cojocaru V., Tarabykin V., Wylie C., Kessel M., and Raz E. (2004). Primordial germ cell migration in the chick and mouse embryo: the role of the chemokine SDF-1/CXCL12. *Dev. Biol.* **272**, 351–361.
Stokvis A., van Neck J. W., van Dijke C. F., van Wamel A., and Coert J. H. (2009). High-resolution ultrasonography of the cutaneous nerve branches in the hand and wrist. *J. Hand Surg. Eur. Vol.* **34**, 766–771. doi:10.1177/1753193409102268
Van Straaten H. W. M., and Wensing C. J. G. (1977). Histomorphometric aspects of testicular morphogenesis in the pig. *Biol. Reprod.* **17**, 467–472.
Streckfuss-Bömeke K., Vlasov A., Hülsmann S., Yin D., Nayernia K., Engel W., Hasenfuss G., and Guan K. (2009). Generation of functional neurons and glia from multipotent adult mouse germ-line stem cells. *Stem Cell Res.* **2**, 139–154.
Struijk R. B., Mulder C. L., van der Veen F., van Pelt A. M. M., and Repping S. (2013). Restoring fertility in sterile childhood cancer survivors by autotransplanting spermatogonial stem cells: are we there yet? (I Virant-Klun, Ed.). *Biomed Res. Int.* **2013**, 903142.

doi:10.1155/2013/903142
Stukenborg J.-B., Schlatt S., Simoni M., Yeung C.-H., Elhija M. A., Luetjens C. M., Huleihel M., and Wistuba J. (2009). New horizons for in vitro spermatogenesis? An update on novel three-dimensional culture systems as tools for meiotic and post-meiotic differentiation of testicular germ cells. *Mol. Hum. Reprod.* **15**, 521–529.
Stukenborg J., Wistuba J., Luetjens C. M., Elhija M. A., Huleihel M., Lunenfeld E., Gromoll J., Nieschlag E., and Schlatt S. (2008). Coculture of spermatogonia with somatic cells in a novel three-dimensional soft-agar-culture-system. *J. Androl.* **29**, 312–329.
Su S., Szarek M., Vooght A., Hutson J., and Li R. (2014). Gonocyte transformation to spermatogonial stem cells occurs earlier in patients with undervirilisation syndromes. *J. Pediatr. Surg.* **49**, 323–327.
Sundström J., Pelliniemi L. J., Kuopio T., Veräjänkorva E., Fröjdman K., Harley V., Salminen E., and Pöllänen P. (1999). Characterization of the model for experimental testicular teratoma in 129/SvJ-mice. *Br. J. Cancer* **80**, 149–160.
Suyatno, Kitamura Y., Ikeda S., Minami N., Yamada M., and Imai H. (2018). Long-term culture of undifferentiated spermatogonia isolated from immature and adult bovine testes. *Mol. Reprod. Dev.* **85**, 236–249. doi:10.1002/mrd.22958
Suzuki S., and Sato K. (2003). The fertilising ability of spermatogenic cells derived from cultured mouse immature testicular tissue. *Zygote* **11**, 307–316.
Svingen T., and Koopman P. (2013). Building the mammalian testis: Origins, differentiation, and assembly of the component cell populations. *Genes Dev.* **27**, 2409–2426. doi:10.1101/gad.228080.113
Swindle M. M., Makin A., Herron A. J., Clubb F. J., and Frazier K. S. (2012). Swine as models in biomedical research and toxicology testin. *Vet. Pathol.* **49**, 344–356. doi:10.1177/0300985811402846
Tadokoro Y., Yomogida K., Ohta H., Tohda A., and Nishimune Y. (2002). Homeostatic regulation of germinal stem cell proliferation by the GDNF/FSH pathway. *Mech. Dev.* **113**, 29–39. doi:10.1016/S0925-4773(02)00004-7
Tagelenbosch R. A. J., and de Rooij D. G. (1993). A quantitative study of spermatogonial multiplication and stem cell renewal in the C3H/101 F1 hybrid mouse. *Mutat. Res. - Fundam. Mol. Mech. Mutagen.* **290**, 193–200. doi:10.1016/0027-5107(93)90159-D
Takahashi M. (2001). The GDNF/RET signaling pathway and human diseases. *Cytokine and Growth Factor Reviews*. doi:10.1016/S1359-6101(01)00012-0
Takahashi K., Tanabe K., Ohnuki M., Narita M., Ichisaka T., Tomoda K., and Yamanaka S. (2007). Induction of pluripotent stem cells from adult human fibroblasts by defined factors. *Cell* **131**, 861–872.
Takahashi K., and Yamanaka S. (2006). Induction of pluripotent stem cells from mouse embryonic and adult fibroblast cultures by defined factors. *Cell* **126**, 663–676.
Takashima S., Kanatsu-Shinohara M., Tanaka T., Morimoto H., Inoue K., Ogonuki N., Jijiwa M., Takahashi M., Ogura A., and Shinohara T. (2015). Functional differences between GDNF-dependent and FGF2-dependent mouse spermatogonial stem cell self-renewal. *Stem Cell Reports* **4**, 489–502. doi:10.1016/j.stemcr.2015.01.010
Tanaka S. S., Yamaguchi Y. L., Tsoi B., Lickert H., and Tam P. P. L. (2005). IFITM/Mil/fragilis family proteins IFITM1 and IFITM3 play distinct roles in mouse primordial germ cell homing and repulsion. *Dev. Cell* **9**, 745–756.
Tevosian S. G., Jiménez E., Hatch H. M., Jiang T., Morse D. A., Fox S. C., and Padua M. B.

(2015). Adrenal development in mice requires GATA4 and GATA6 transcription factors. *Endocrinology* **156**, 2503–2517.

Tharmalingam M. D., Jorgensen A., and Mitchell R. T. (2018). Experimental models of testicular development and function using human tissue and cells. *Mol. Cell. Endocrinol.* **468**, 95–110. doi:10.1016/j.mce.2017.12.011

Thomson J. A., Itskovitz-Eldor J., Shapiro S. S., Waknitz M. A., Swiergiel J. J., Marshall V. S., and Jones J. M. (1998). Embryonic stem cell lines derived from human blastocysts. *Science* **282**, 1145–1147.

Tilgner K., Atkinson S. P., Golebiewska A., Stojković M., Lako M., and Armstrong L. (2008). Isolation of primordial germ cells from differentiating human embryonic stem cells. *Stem Cells* **26**, 3075–3085.

Tiptanavattana N., Radtanakatikanon A., Hyttel P., Holm H., Buranapraditkun S., Setthawong P., Techakumphu M., and Tharasanit T. (2015). Determination phase at transition of gonocytes to spermatogonial stem cells improves establishment efficiency of spermatogonial stem cells in domestic cats. *J. Reprod. Dev.* **61**, 581–588.

Tiwana M. S., and Leslie S. W. (2017). 'Anatomy, Abdomen and Pelvis, Testicle.'

Tomiyama H., Hutson J. M., Truong A., and Agoulnik A. I. (2003). Transabdominal testicular descent is disrupted in mice with deletion of insulinlike factor 3 receptor. *J. Pediatr. Surg.* **38**, 1793–1798. doi:10.1016/j.jpedsurg.2003.08.047

Toor J. S., and Sikka S. C. (2017). Chapter 59 - Developmental and Reproductive Disorders–Role of Endocrine Disruptors in Testicular Toxicity. 'Reproductive and Developmental Toxicology (Second Edition)'. (Ed RC Gupta) pp. 1111–1121. (Academic Press) doi:https://doi.org/10.1016/B978-0-12-804239-7.00059-7

Trowell O. A. (1959). The culture of mature organs in a synthetic medium. *Exp. Cell Res.* **16**, 118–147.

Tu J., Fan L., Tao K., Zhu W., Li J., and Lu G. Stem cell factor affects fate determination of human gonocytes in vitro. *Reproduction* **134**, 757–765. doi:10.1530/REP-07-0161

Turnbull D., Bloomfield T., Baldwin S., Foster S., and Joyner A. (1995). Ultrasound backscatter microscope analysis of early mouse embryonic brain development. *Proc. Natl. Acad. Sci.* **92**, 2239–2243.

Turner R. M., Rathi R., Honaramooz A., Zeng W., and Dobrinski I. (2010). Xenografting restores spermatogenesis to cryptorchid testicular tissue but does not rescue the phenotype of idiopathic testicular degeneration in the horse (Equus caballus). *Reprod. Fertil. Dev.* **22**, 673–683.

Uchida A., and Dobrinski I. (2018). Germ cell transplantation and neospermatogenesis. 'The Complete Guide to Male Fertility Preservation'. (Eds A Majzoub and W Agrawal) pp. 361–375. (Springer)

Ueno N., Baird A., Esch F., Ling N., and Guillemin R. (1987). Isolation and partial characterization of basic fibroblast growth factor from bovine testis. *Mol. Cell. Endocrinol.* **49**, 189–194.

Upadhyay S., and Zamboni L. (1982). Ectopic germ cells: natural model for the study of germ cell sexual differentiation. *Proc. Natl. Acad. Sci.* **79**, 6584–6588.

Vergouwen R. P. F. A., Jacobs S. G. P. M., Huiskamp R., Davids J. A. G., and de Rooij D. G. (1991). Proliferative activity of gonocytes, Sertoli cells and interstitial cells during testicular development in mice. *J. Reprod. Fertil.* **93**, 233–243. doi:10.1530/jrf.0.0930233

Vidal V. P. I., Chaboissier M. C., de Rooij D. G., and Schedl A. (2001). Sox9 induces testis development in XX transgenic mice. *Nat. Genet.* **28**, 216–217. doi:10.1038/90046

Vilain E., and McCabe E. R. B. (1998). Mammalian sex determination: From gonads to brain. *Mol. Genet. Metab.* **65**, 74–84. doi:10.1006/mgme.1998.2749

Viotti M., Niu L., Shi S.-H., and Hadjantonakis A.-K. (2012). Role of the gut endoderm in relaying left-right patterning in mice. *PLoS Biol* **10**, e1001276.

Virtanen P., and Isotupa K. (1980). Staining properties of alizarin red S for growing bone in vitro. *Cells Tissues Organs* **108**, 202–207.

Volarevic V., Markovic B. S., Gazdic M., Volarevic A., Jovicic N., Arsenijevic N., Armstrong L., Djonov V., Lako M., and Stojkovic M. (2018). Ethical and safety issues of stem cell-based therapy. *Int. J. Med. Sci.* **15**, 36–45.

Wagner T., Scandura G., Roe A., Beltran L., Shamash J., Alfrangis C., Daugaard G., Grantham M., and Berney D. (2020). Prospective molecular and morphological assessment of testicular prepubertal-type teratomas in postpubertal men. *Mod. Pathol.* **33**, 713–721.

Wakao S., Kitada M., Kuroda Y., Ogura F., Murakami T., Niwa A., and Dezawa M. (2012). Morphologic and gene expression criteria for identifying human induced pluripotent stem cells. *PLoS One* **7**, e48677.

Wang X., Chen T., Zhang Y., Li B., Xu Q., and Song C. (2015). Isolation and culture of pig spermatogonial stem cells and their in vitro differentiation into neuron-like cells and adipocytes. *Int. J. Mol. Sci.* **16**, 26333–26346. doi:10.3390/ijms161125958

Wang Y., and Culty M. (2007). Identification and distribution of a novel platelet-derived growth factor receptor β variant: Effect of retinoic acid and involvement in cell differentiation. *Endocrinology*. doi:10.1210/en.2006-1206

Wang Q. Z., and Hna C. S. (2008). Serum-free knockout SR medium supports the short-time viability of mouse spermatogonial stem cells. *Fen zi xi bao sheng wu xue bao= J. Mol. cell Biol.* **41**, 162–166.

Wang S., Wang X., Ma L., Lin X., Zhang D., Li Z., Wu Y., Zheng C., Feng X., and Liao S. (2016). Retinoic acid is sufficient for the in vitro induction of mouse spermatocytes. *Stem Cell Reports* **7**, 80–94.

Wang N., Wang Y., Xie Y., and Wang H. (2016). OTX2 impedes self–renewal of porcine iPS cells through downregulation of NANOG expression. *Cell death Discov.* **2**, 1–10.

Wang J., Zohar R., and McCulloch C. A. (2006). Multiple roles of α-smooth muscle actin in mechanotransduction. *Exp. Cell Res.* **312**, 205–214.

Warr N., and Greenfield A. (2012). The molecular and cellular basis of gonadal sex reversal in mice and humans. *Wiley Interdiscip. Rev. Dev. Biol.* **1**, 559–577. doi:10.1002/wdev.42

Wartenberg H., Kinsky I., Viebahn C., and Schmolke C. (1991). Fine structural characteristics of testicular cord formation in the developing rabbit gonad. *J. Electron Microsc. Tech.* **19**, 133–157. doi:10.1002/jemt.1060190203

Watanabe T., Hayashi H., Kita K., Kubota Y., and Ogawa T. (2009). Ectopic porcine spermatogenesis in murine subcutis: tissue grafting versus cell-injection methods. *Asian J. Androl.* **11**, 317–323. doi:10.1038/aja.2008.5

Wei X., Jia Y., Xue Y., Geng L., Wang M., Li L., Wang M., Zhang X., and Wu X. (2016). GDNF-expressing STO feeder layer supports the long-term propagation of undifferentiated mouse spermatogonia with stem cell properties. *Sci. Rep.* doi:10.1038/srep36779

Wernig M., Meissner A., Foreman R., Brambrink T., Ku M., Hochedlinger K., Bernstein B. E., and Jaenisch R. (2007). In vitro reprogramming of fibroblasts into a pluripotent ES-cell-like state. *Nature* **448**, 318–324.

Widenfalk J., Parvinen M., Lindqvist E., and Olson L. (2000). Neurturin, RET, GFRα-1 and

GFRα-2, but not GFRα-3, mRNA are expressed in mice gonads. *Cell Tissue Res.* **299**, 409–415. doi:10.1007/s004419900068

Wilhelm D., Palmer S., and Koopman P. (2007). Sex determination and gonadal development in mammals. *Physiol. Rev.* **87**, 1–28. doi:10.1152/physrev.00009.2006

Wobus A. M., and Boheler K. R. (2005). Embryonic stem cells: prospects for developmental biology and cell therapy. *Physiol. Rev.* **85**, 635–678.

Wolf X. A., Serup P., and Hyttel P. (2011). Three-dimensional localisation of NANOG, OCT4, and E-cadherin in porcine pre- and peri-implantation embryos. *Dev. Dyn.* **240**, 204–210. doi:10.1002/dvdy.22491

Wong E. W. P., Mruk D. D., and Cheng C. Y. (2008). Biology and regulation of ectoplasmic specialization, an atypical adherens junction type, in the testis. *Biochim. Biophys. Acta (BBA)-Biomembranes* **1778**, 692–708.

Wu X., Goodyear S. M., Abramowitz L. K., Bartolomei M. S., Tobias J. W., Avarbock M. R., and Brinster R. L. (2012). Fertile offspring derived from mouse spermatogonial stem cells cryopreserved for more than 14 years. *Hum. Reprod.* **27**, 1249–1259.

Wu X., Goodyear S. M., Tobias J. W., Avarbock M. R., and Brinster R. L. (2011). Spermatogonial stem cell self-renewal requires ETV5-mediated downstream activation of Brachyury in mice. *Biol. Reprod.* **85**, 1114–1123. doi:10.1095/biolreprod.111.091793

Wu X., Schmidt J. A., Avarbock M. R., Tobias J. W., Carlson C. A., Kolon T. F., Ginsberg J. P., and Brinster R. L. (2009). Prepubertal human spermatogonia and mouse gonocytes share conserved gene expression of germline stem cell regulatory molecules. *Proc. Natl. Acad. Sci.* **106**, 21672–21677.

Wu Z., Templeman J. L., Smith R. A., and Mackay S. (2005). Effects of glial cell line-derived neurotrophic factor on isolated developing mouse Sertoli cells in vitro. *J. Anat.* **206**, 175–184.

Xu X., Browning V. L., and Odorico J. S. (2011). Activin, BMP and FGF pathways cooperate to promote endoderm and pancreatic lineage cell differentiation from human embryonic stem cells. *Mech. Dev.* **128**, 412–427.

Xu J., Wan P., Wang M., Zhang J., Gao X., Hu B., Han J., Chen L., Sun K., and Wu J. (2015). AIP1-mediated actin disassembly is required for postnatal germ cell migration and spermatogonial stem cell niche establishment. *Cell Death Dis.* **6**, e1818–e1818.

Yang H., Hao D., Liu C., Huang D., Chen B., Fan H., Liu C., Zhang L., Zhang Q., and An J. (2019). Generation of functional dopaminergic neurons from human spermatogonial stem cells to rescue parkinsonian phenotypes. *Stem Cell Res. Ther.* **10**, 1–19.

Yang Y., and Honaramooz A. (2011). Efficient purification of neonatal porcine gonocytes with Nycodenz and differential plating. *Reprod. Fertil. Dev.* **23**, 496–505. doi:10.1071/rd10042

Yang H., Liu C., Chen B., An J., Zhang R., Zhang Q., Zhao J., He B., and Hao D.-J. (2017). Efficient generation of functionally active spinal cord neurons from spermatogonial stem cells. *Mol. Neurobiol.* **54**, 788–803.

Yang H., Liu Y., Hai Y., Guo Y., Yang S., Li Z., Gao W.-Q., and He Z. (2015). Efficient conversion of spermatogonial stem cells to phenotypic and functional dopaminergic neurons via the PI3K/Akt and P21/Smurf2/Nolz1 pathway. *Mol. Neurobiol.* **52**, 1654–1669.

Yang Q.-E., and Oatley J. M. (2014). Spermatogonial stem cell functions in physiological and pathological conditions. *Curr. Top. Dev. Biol.* **107**, 235–267.

Yang Y., Workman S., and Wilson M. J. (2019). The molecular pathways underlying early gonadal development. *J. Mol. Endocrinol.* **62**, R47–R64.

Yang Y., Yarahmadi M., and Honaramooz A. (2010). Development of novel strategies for the isolation of piglet testis cells with a high proportion of gonocytes. *Reprod. Fertil. Dev.* **22**, 1057–1065. doi:10.1071/RD09316

Yang F., Zhang J., Liu Y., Cheng D., and Wang H. (2015). Structure and functional evaluation of porcine NANOG that is a single-exon gene and has two pseudogenes. *Int. J. Biochem. Cell Biol.* **59**, 142–152. doi:10.1016/j.biocel.2014.12.009

Yano H., Readhead C., Nakashima M., Ren S.-G., and Melmed S. (1998). Pituitary-directed leukemia inhibitory factor transgene causes Cushing's syndrome: neuro-immune-endocrine modulation of pituitary development. *Mol. Endocrinol.* **12**, 1708–1720.

Yao T., and Asayama Y. (2017). Animal-cell culture media: History, characteristics, and current issues. *Reprod. Med. Biol.* **16**, 99–117. doi:10.1002/rmb2.12024

Yao S., Chen S., Clark J., Hao E., Beattie G. M., Hayek A., and Ding S. (2006). Long-term self-renewal and directed differentiation of human embryonic stem cells in chemically defined conditions. *Proc. Natl. Acad. Sci.* **103**, 6907–6912.

Yao H. H.-C., Whoriskey W., and Capel B. (2002). Desert Hedgehog/Patched 1 signaling specifies fetal Leydig cell fate in testis organogenesis. *Genes Dev.* **16**, 1433–1440.

Yin X., Chen Z., Liu Z., and Dang G. (2007). Icariine stimulates proliferation and differentiation of human osteoblasts by increasing production of bone morphogenetic protein 2. *Chin. Med. J. (Engl).* **120**, 204–210.

Ying Y., Liu X.-M., Marble A., Lawson K. A., and Zhao G.-Q. (2000). Requirement of Bmp8b for the generation of primordial germ cells in the mouse. *Mol. Endocrinol.* **14**, 1053–1063.

Ying Y., and Zhao G.-Q. (2001). Cooperation of endoderm-derived BMP2 and extraembryonic ectoderm-derived BMP4 in primordial germ cell generation in the mouse. *Dev. Biol.* **232**, 484–492.

Yokonishi T., Sato T., Komeya M., Katagiri K., Kubota Y., Nakabayashi K., Hata K., Inoue K., Ogonuki N., and Ogura A. (2014). Offspring production with sperm grown in vitro from cryopreserved testis tissues. *Nat. Commun.* **5**, 1–6.

Yoshida K., Chambers I., Nichols J., Smith A., Saito M., Yasukawa K., Shoyab M., Taga T., and Kishimoto T. (1994). Maintenance of the pluripotential phenotype of embryonic stem cells through direct activation of gp130 signalling pathways. *Mech. Dev.* **45**, 163–171.

Yoshida S., Sukeno M., and Nabeshima Y. (2007). A vasculature-associated niche for undifferentiated spermatogonia in the mouse testis. *Science* **317**, 1722–1726.

Yoshida S., Sukeno M., Nakagawa T., Ohbo K., Nagamatsu G., Suda T., and Nabeshima Y. (2006). The first round of mouse spermatogenesis is a distinctive program that lacks the self-renewing spermatogonia stage. **1495**–**1505**, 133.

Younan G., Suber F., Xing W., Shi T., Kunori Y., Åbrink M., Pejler G., Schlenner S. M., Rodewald H.-R., Moore F. D., Stevens R. L., Adachi R., Austen K. F., and Gurish M. F. (2010). The inflammatory response after an epidermal burn depends on the activities of mouse mast cell proteases 4 and 5. *J. Immunol.* **185**, 17681–7690. doi:10.4049/jimmunol.1002803

Young J. S., Guttman J. A., Vaid K. S., Shahinian H., and Vogl A. W. (2009). Cortactin (CTTN), N-WASP (WASL), and clathrin (CLTC) are present at podosome-like tubulobulbar complexes in the rat testis. *Biol. Reprod.* **80**, 153–161.

Youssefi R., Tajik P., Movahedin M., and Akbarinejad V. (2016). Enhancement in colonization of bovine spermatogonial stem cells following addition of knock-out serum replacement to culture medium. *Vet. Res. forum an Int. Q. J.* **7**, 275–280.

Yu J., Cai Z., Wan H., Zhang F., Ye J., Fang J., Gui Y., and Ye J. (2006). Development of neonatal

mouse and fetal human testicular tissue as ectopic grafts in immunodeficient mice. *Asian J. Androl.* **8**, 393–403.

Yuan J., Wegenka U. M., Lütticken C., Buschmann J., Decker T., Schindler C., Heinrich P. C., and Horn F. (1994). The signalling pathways of interleukin-6 and gamma interferon converge by the activation of different transcription factors which bind to common responsive DNA elements. *Mol. Cell. Biol.* **14**, 1657–1668.

Zeineddine D., Abou Hammoud A., Mortada M., and Boeuf H. (2014). The Oct4 protein: more than a magic stemness marker. *Am. J. Stem Cells* **3**, 74–82.

Zeng W., Alpaugh W., Stefanovski D., Schlingmann K., Dobrinski I., and Turner R. M. (2017). Xenografting of isolated equine (Equus caballus) testis cells results in de novo morphogenesis of seminiferous tubules but not spermatogenesis. *Andrology* **5**, 336–346.

Zeng W., Avelar G. F., Rathi R., Franca L. R., and Dobrinski I. (2006). The length of the spermatogenic cycle is conserved in porcine and ovine testis xenografts. *J. Androl.* **27**, 527–533.

Zeng W., Snedaker A. K., Megee S., Rathi R., Chen F., Honaramooz A., and Dobrinski I. (2009). Preservation and transplantation of porcine testis tissue. *Reprod. Fertil. Dev.* **21**, 489–497.

Zeng W., Tang L., Bondareva A., Honaramooz A., Tanco V., Dores C., Megee S., Modelski M., Rodriguez-Sosa J. R., Paczkowski M., Silva E., Wheeler M., Krisher R. L., and Dobrinski I. (2013). Viral transduction of male germline stem cells results in transgene transmission after germ cell transplantation in pigs. *Biol. Reprod.* **27**, 1–9. doi:10.1095/biolreprod.112.104422

Zeng W., Tang L., Bondareva A., Luo J., Megee S. O., Modelski M., Blash S., Melican D. T., Destrempes M. M., Overton S. A., Gavin W. G., Ayres S., Echelard Y., and Dobrinski I. (2012). Non-viral transfection of goat germline stem cells by nucleofection results in production of transgenic sperm after germ cell transplantation. *Mol. Reprod. Dev.* **79**, 255–261. doi:10.1002/mrd.22014

Zhang P., Chen X., Zheng Y., Zhu J., Qin Y., Lv Y., and Zeng W. (2017). Long-term propagation of porcine undifferentiated spermatogonia. *Stem Cells Dev.* **26**, 1121–1131. doi:10.1089/scd.2017.0018

Zhang Z., Gong Y., Guo Y., Hai Y., Yang H., Yang S., Liu Y., Ma M., Liu L., and Li Z. (2013). Direct transdifferentiation of spermatogonial stem cells to morphological, phenotypic and functional hepatocyte-like cells via the ERK1/2 and Smad2/3 signaling pathways and the inactivation of cyclin A, cyclin B and cyclin E. *Cell Commun. Signal.* **11**, 1–15.

Zhang Z., Hill J., Holland M., Kurihara Y., and Loveland K. L. (2008). Bovine Sertoli cells colonize and form tubules in murine hosts following transplantation and grafting procedures. *J. Androl.* **29**, 418–430. doi:10.2164/jandrol.107.004465

Zhang Y., Wang S., Wang X., Liao S., Wu Y., and Han C. (2012). Endogenously produced FGF2 is essential for the survival and proliferation of cultured mouse spermatogonial stem cells. *Cell Res.* **22**, 773–776.

Zhao G.-Q., and Garbers D. L. (2002). Male germ cell specification and differentiation. *Dev. Cell* **2**, 537–547.

Zheng Y., He Y., An J., Qin J., Wang Y., Zhang Y., Tian X., and Zeng W. (2014). THY1 is a surface marker of porcine gonocytes. *Reprod. Fertil. Dev.* **26**, 533–539. doi:10.1071/RD13075

Zheng Y., Thomas A., Schmidt C. M., and Dann C. T. (2014). Quantitative detection of human spermatogonia for optimization of spermatogonial stem cell culture. *Hum. Reprod.* **29**, 2497–2511. doi:10.1093/humrep/deu232

Zheng Y., Tian X., Zhang Y., Qin J., An J., and Zeng W. (2013). In vitro propagation of male germline stem cells from piglets. *J. Assist. Reprod. Genet.* **30**, 945–952. doi:10.1007/s10815-013-0031-0

Zhou Y.-Q., Foster F. S., Parkes R., and Adamson S. L. (2003). Developmental changes in left and right ventricular diastolic filling patterns in mice. *Am. J. Physiol. - Hear. Circ. Physiol.* **285**, 1563–1575. doi:10.1152/ajpheart.00384.2003

Zhou R., Wu J., Liu B., Jiang Y., Chen W., Li J., He Q., and He Z. (2019). The roles and mechanisms of Leydig cells and myoid cells in regulating spermatogenesis. *Cell. Mol. Life Sci.* **76**, 2681–2695.

Zimmermann S., Steding G., Emmen J. M. A., Brinkmann A. O., Nayernia K., Holstein A. F., Engel W., and Adham I. M. (1999). Targeted disruption of the Insl3 gene causes bilateral cryptorchidism. *Mol. Endocrinol.* **13**, 681–691. doi:10.1210/mend.13.5.0272

Zirkin B. R., and Goldberg E. (2018). Spermatids. 'Encyclopedia of Reproduction (Second Edition)'. (Ed MK Skinner) pp. 42–46. (Academic Press: Oxford) doi:https://doi.org/10.1016/B978-0-12-801238-3.64426-4

Zogbi C., Tesser R. B., Encinas G., Miraglia S. M., and Stumpp T. (2012). Gonocyte development in rats: proliferation, distribution and death revisited. *Histochem. Cell Biol.* **138**, 305–322.

APPENDIX A

A PRELIMINARY STUDY FOR THE DEVELOPMENT OF A GONADOTROPIN- AND IMMUNODEFICIENT MOUSE MODEL FOR SUBSEQUENT STUDY OF TESTIS TISSUE XENOGRAFTING AND *DE NOVO* TESTIS TISSUE FORMATION

Background and rationale:

Performing hypophysectomy on most mouse strains is challenging and is further complicated in immunodeficient mice, which is why the mouse suppliers do not offer this procedure for such strains. Development of a hypophysectomized immunocompromised mouse model would provide a new window of opportunity for various prospective studies on these animals without the interference of endogenous gonadotropins. This model would have applications in various research areas including endocrinology, developmental biology, and stem cell biology as well as reproduction physiology.

Objectives and hypotheses:

The ultimate objective of this study was to develop a gonadotropin- and immunodeficient mouse model for the subsequent endocrinology studies.

Our specific objectives included: 1) to compare the feasibility of trans-auricular and para-pharyngeal approaches to hypophysectomy using mouse cadavers; and 2) to develop and validate the surgical competency to perform survival hypophysectomy to create a gonadotropin-deficient immunodeficient mouse model.

Our specific hypotheses included: 1) the trans-auricular approach to hypophysectomy would be a more feasible approach (less invasive and time consuming) than the para-pharyngeal approach; 2) the hypophysectomized mice would be able to survive for at least one month post-operation; and 3) compared to the sham-operated mice, hypophysectomized mice will have significantly reduced testis size, vesicular glands, body weight, and germ cell layers in their seminiferous tubules.

Results:

Feasibility of the two approaches of hypophysectomy (trans-auricular and para-pharyngeal) were investigated using mouse cadavers. Para-pharyngeal approach was found to be a more practical

method due to better visualization of the gland and hence reducing the risk of damage to the surrounding tissues. This approach was adopted for use on live mice; however, it has not yet provided satisfactory results because the animals only survived until the completion of the operation. Therefore, the para-pharyngeal method of pituitary removal appeared to be more achievable and reliable, which does not support our first hypothesis. Our second and third hypotheses have not been achieved due to complications associated with the recovery of animals post-operatively.

APPENDIX A.1

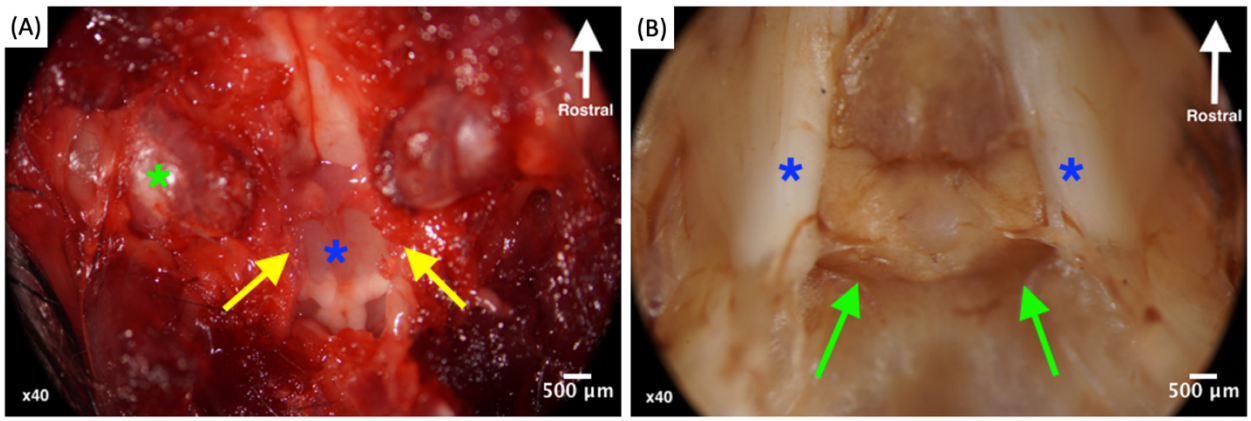

Ventral and dorsal approaches to removing the pituitary gland in mouse cadavers aimed at locating this gland in mice. (A) In the ventral approach, using a freshly euthanized mouse, the structures covering the base of the skull were completely removed. The occipital bone located between the two tympanic bullae (one tympanic bulla is shown with a green asterisk) was cut out (yellow arrows) to access the cranium structures, including the pituitary gland, through the window created in the cranial floor (blue asterisk). (B) Using a dorsal approach and after removing the brain, the pituitary gland (green arrows) is readily visible located between the two trigeminal nerves (blue asterisks). The sample was fixed in Bouin's solution prior to dissection to maintain the structures in their original location.

APPENDIX A.2

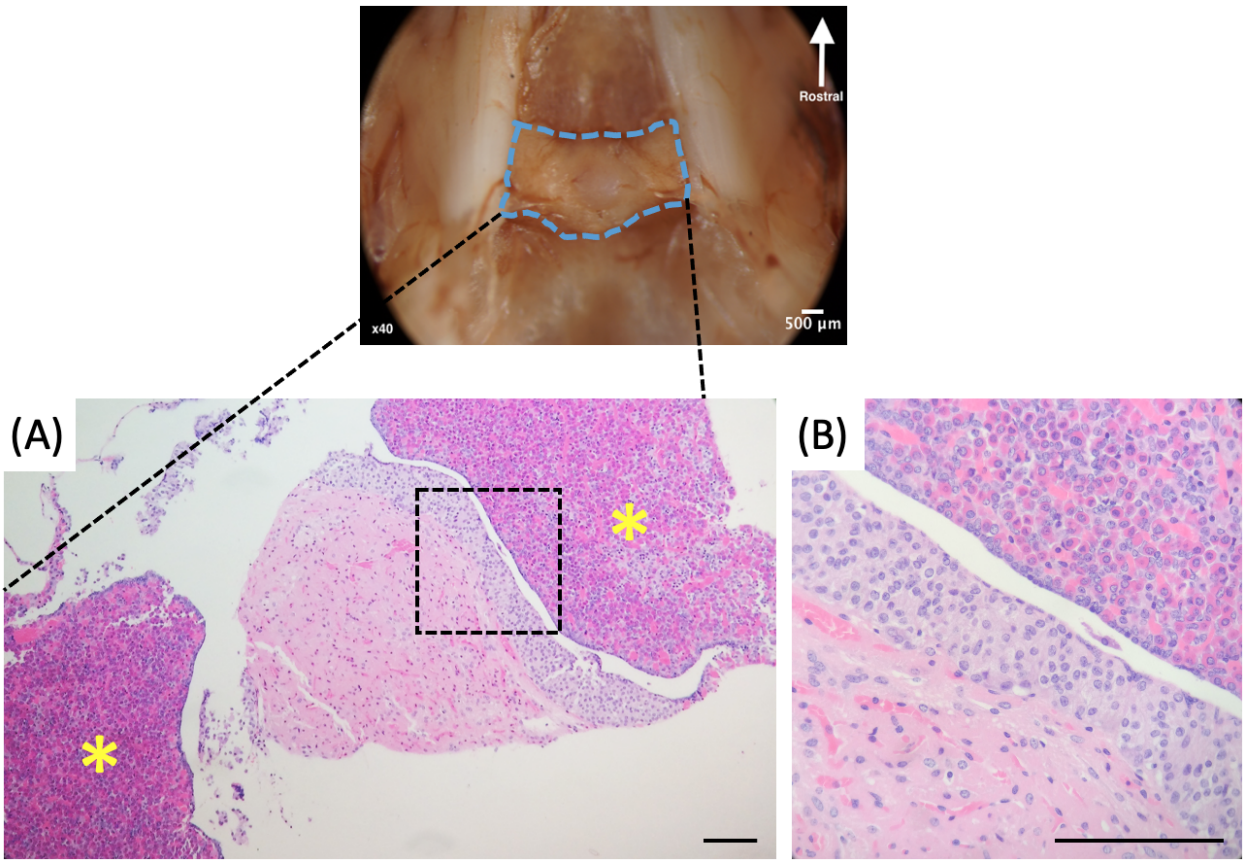

Histological appearance of the collected pituitary gland in mice. (A) Low magnification of the complete pituitary gland stained with H&E. Two purple structures (yellow asterisks) surrounding the middle lightly stained structure are pars distalis region of the adenohypophysis (anterior pituitary gland). (B) Higher magnification of the pituitary gland reveals the typical histological attributes including the presence of both acidophil cells (pink in color) and basophil cells (purple) on the upper parts of the image indicating the adenohypophysis, presence of the Rathke's pouch as a gap in the middle of the image, presence of basophil cells indicating the pars intermedia (intermediate lobe), and the nervous tissue of the pars nervosa (posterior pituitary or neurohypophysis) with the typical pituicytes and Herring bodies. (Scale bars = 100 µm)

APPENDIX A.3

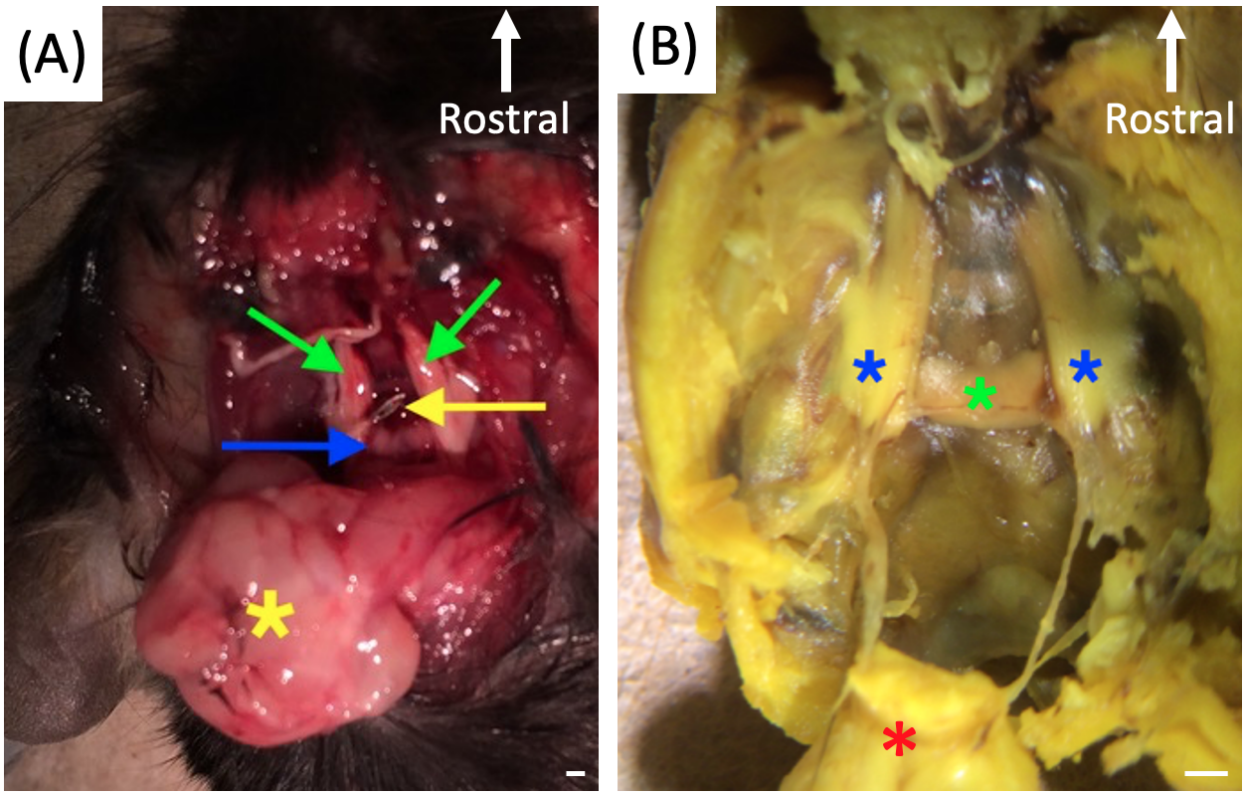

Investigating the feasibility of two standard approaches of hypophysectomy on euthanized mice. Position of the inserted needle tip shown after necropsy of a mouse undergoing trans-auricular approach to hypophysectomy (A) and the location of the pituitary gland in a fixed sample for comparison (B). Even after the needle was successfully passed through the external and internal auditory canals, the sharp needle tip and lack of visual control pose too great a risk to the animal for the approach to be practical because the pituitary gland is in close proximity to the trigeminal nerves and other nervous structures including the hypothalamus. In the left panel (A), the proximity of the trigeminal nerves (green arrows), to the pituitary gland (blue arrow) is shown along with the position of the inserted needle tip (yellow arrow). The yellow asterisk indicates the rolled over brain. In the right panel (B), the pituitary gland (green asterisk) is shown in between the two trigeminal nerves (blue asterisks); the red asterisk indicates the displaced brain. (Scale bars = 1 mm)

APPENDIX A.4

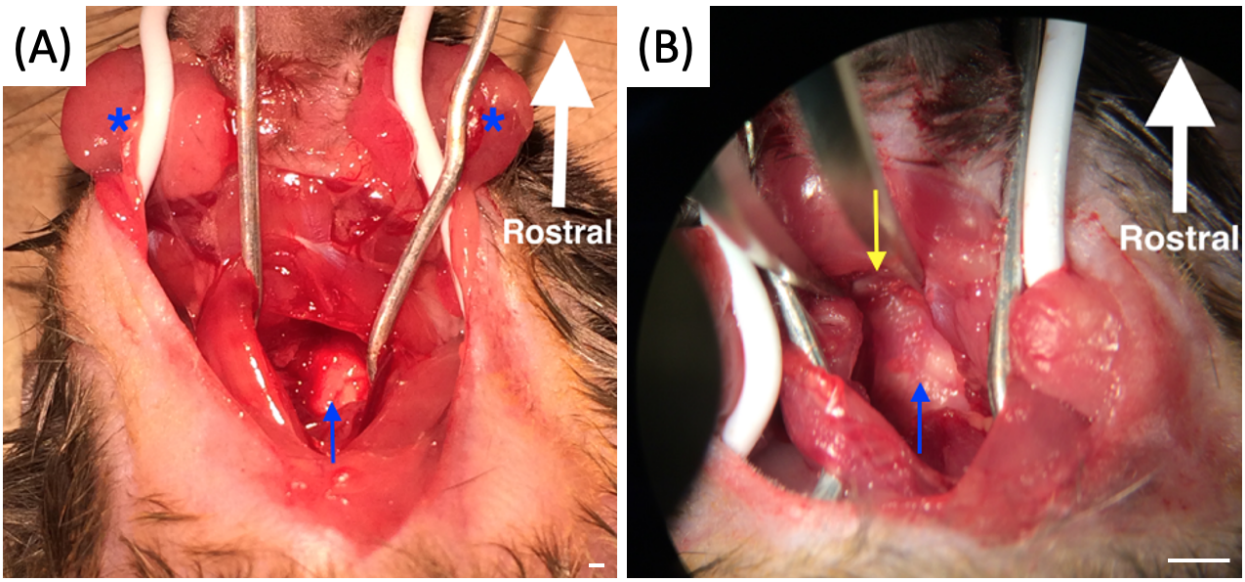

The para-pharyngeal approach to hypophysectomy in mouse cadavers. (A) The skin is incised, the soft tissues including the salivary glands (blue asterisks), trachea and muscles are retracted using a paper clip as a retractor. The pharyngeal mucosa is removed to make the base of the cranium visible (blue arrow). (B) The sagittal crest along with the blue line representing the spheno-occipital synchondrosis (yellow arrow) can be observed. (Scale bars = 1 mm)

APPENDIX A.5

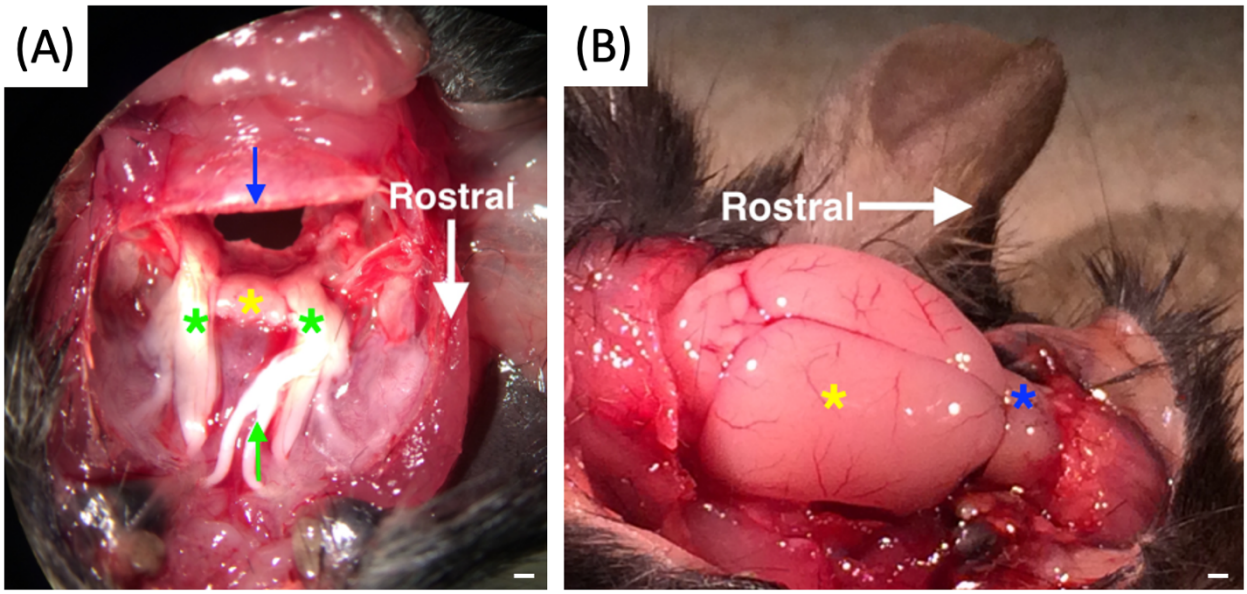

Pituitary removal in euthanized mice. (A) After performing para-pharyngeal hypophysectomy in mouse cadavers, the cranium was opened to observe the location of the hole. In this case, the point of the burr was placed caudal to the synchondrosis making a perforation behind the pituitary gland (blue arrow). The pituitary (yellow asterisk), the optic chiasma (green arrow) and trigeminal nerves (green asterisks) can be identified in this image. (B) The brain case is removed to investigate the extent of damage and the exact location of the perforation. Yellow asterisk in this figure shows the brain and the blue asterisk represents the olfactory lobe. (Scale bars = 1 mm)

APPENDIX A.6

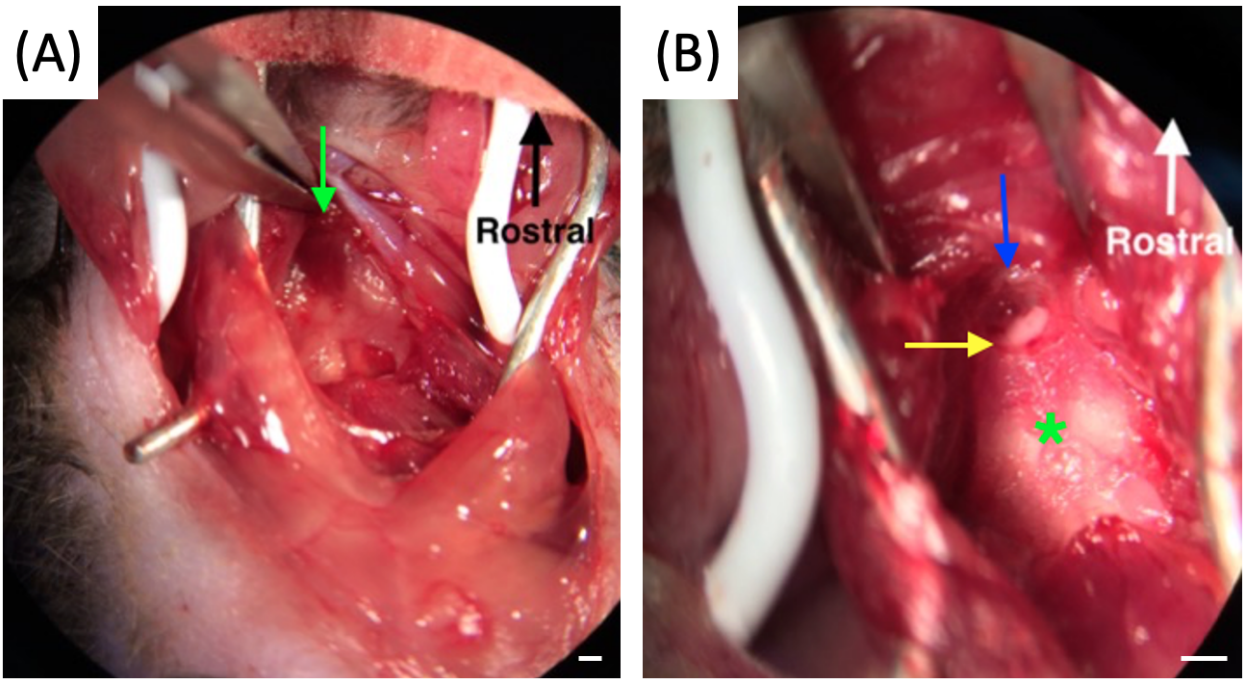

Practicing removal of the pituitary gland from anesthetized survival mice. (A) Soft tissues are retracted and the muscles are dissected to provide visualization of the spheno-occipital synchondrosis (green arrow). (B) The synchondrosis is known as the hallmark of location of the pituitary gland located directly dorsal to the suture between the occipital and sphenoid bones. Using a fine burr attached to a rotor and utilizing the lowest rotation speed, the base of the skull (green asterisk) is perforated to gain access to the pituitary gland (blue arrow). The white color structure located dorsal to the bone represents the gland (yellow arrow). Using a blunt 16G needle attached to a suction pump set to 15 in-Hg (inch mercury) pressure, the gland was removed from its place and the soft tissues were returned to their original location. The skin was closed using wound clips and the mouse was monitored for any abnormal signs. (Scale bars = 1 mm)